UNCLASSIFIED

AD NUMBER
ADC034018

CLASSIFICATION CHANGES

TO: unclassified

FROM: confidential

LIMITATION CHANGES

TO:

Approved for public release, distribution unlimited

FROM:

Distribution limited to U.S. Gov't. agencies and their Contractors; Specific authority; 11 Apr 84. Other requests must be referred to the Commanding Officer, NORDA, NSTL Station, MS 39529.

AUTHORITY

ONR ltr., Ser 93/160, 10 Mar 1999; SAME

THIS PAGE IS UNCLASSIFIED

AD-E001569

CONFIDENTIAL

NORDA Report 35
Book 1 of 3

The Acoustic Model Evaluation Committee (AMEC) Reports

Volume II

The Evaluation of the FACT PL9D Transmission Loss Model (U)

Prepared by Richard B. Lauer

Environmental Requirements and Program Analysis Group
Ocean Science and Technology Laboratory

AD C034018

September 198[illegible]

Distribution limited to U.S. Government agencies only. TBE 11 APR 1984
Other requests for this document must be referred to the Commanding Officer, Naval Ocean Research and Development Activity, NSTL Station, Mississippi 39529

Classified by OPNAVINST 5513.5 (3)
Declassify on: Originating Agency's Determination Required

Including the Physics of the Fact PL9D Model
prepared by Charles L. Bartberger
Naval Air Development Center

Naval Ocean Research and Development Activity
NSTL Station, Mississippi 39529

84 04 06 507

CONFIDENTIAL

Foreword (U)

(U) The Acoustic Model Evaluation Committee (AMEC) has been chartered to serve as an advisory group to the Director, Naval Oceanography Division (OP-952), on matters dealing with model evaluation. In fulfillment of its charter AMEC will produce a series of reports detailing the results of model evaluations. Volume I described the evaluation methodology selected and the manner in which it has been implemented. Volume IA describes propagation loss data sets suitable for the evaluation of models in a range independent environment. This report, Volume II, presents the results of evaluating the FACT PL9D propagation loss model.

G. T. Phelps

G.T. Phelps, Captain, USN
Commanding Officer, NORDA

Executive Summary (U)

(U) The Acoustic Model Evaluation Committee (AMEC) has applied the methodology described in Volume I of this series of reports to evaluate the FACT PL9D model. The accuracy of FACT PL9D has been assessed by quantitative comparisons with eight sets of experimental data covering a broad spectrum of environmental acoustic scenarios. The physics of FACT PL9D has been examined by C. Bartberger of the Naval Air Development Center with abundant use of test cases. FACT PL9D is found to run extremely fast, typically 3-6 seconds on the UNIVAC 1108 computer. The model is well documented, including comments within the computer code. Many serious deficiencies and errors in the physics of FACT PL9D were discovered in the surface direct module, "axis-to-axis" computations, curve fitting in range-angle space, caustic correction application, decisions regarding coherence and amplitude reduction factors, and number of rays calculated in the outermost source angle sector. Other deficiencies are lack of eigenray information, dependence of initial range and range increment for propagation loss calculations, and the lack of vertical beampatterns and external bottom loss capabilities. This evaluation was completed in September 1980.

Preface (U)

(U) This report was prepared under the joint sponsorship of the Naval Sea Systems Command, Program Manager, P. R. Tiedeman (SEA 63D3), PE 63708N; the Surveillance Environmental Acoustic Support Project, Program Manager, Dr. Robert A. Gardner (NORDA Code 520), PE 63795N; the Tactical ASW Environmental Acoustic Support Project, Program Manager, E. D. Chaika (NORDA Code 530), PE 63795N; via the auspices o. OP-952D (Capt. J. Harlett).

Acknowledgments (U)

(U) The author wishes to acknowledge the valuable contributions of Dr. F. R. DiNapoli of the Naval Underwater Systems Center, New London, Conn., while he was chairman of the Panel on Sonar System Models (POSSM) for his support of the development of the model evaluation methodology adopted by AMEC on an interim basis. The stimulating discussions with Dr. A. L. Anderson, formerly of the Naval Ocean Research and Development Activity, resulted in many refinements of the model evaluation methodology and the concept of having a portable test package for model evaluation. This volume and its successors, giving the results of specific model evaluations, would not have been possible without the support and direction given by Mr. R. Winokur during his tenure in OP-095E and 952D. Dr. M. C. Karamargin of the Naval Underwater Systems Center, New London, is well deserving of praise for editing and organizing a vast amount of environmental and acoustic data, running the acoustic models, and producing all the figures and quantitative accuracy assessment results by the "difference technique." Finally, my thanks to the members of AMEC for valuable insight and for recommendations that have substantially increased the quality and the practicality of the model evaluation effort.

Contents (U)

1.0	(U)	Introduction	1
1.1	(U)	The AMEC Methodology	2
1.2	(U)	Modifications to FACT PL9D for AMEC Evaluation	4
2.0	(U)	FACT PL9D Description	5
2.1	(U)	Applications	11
2.2	(U)	Assumptions, Approximations and Limitations of the FACT Model	12
2.3a	(U)	Problems, Deficiencies and Needed Alterations Compiled from a Survey of FACT Users	15
2.3b	(U)	Additional Problems and Deficiencies of the FACT Model	19
3.0	(U)	Running Time	24
4.0	(U)	Core Storage	25
5.0	(U)	The Physics of FACT Model	25
5.1	(U)	Discussion of the Specific Features of the FACT Model	27
6.0	(U)	FACT PL9D Program Flow	119
7.0	(U)	FACT PL9D Inputs	121
7.1	(U)	FACT PL9D Outputs	123
8.0	(U)	Organizational Responsibility for FACT PL9D	130
9.0	(U)	Test Cases for Implementation on a New Computer	130
9.1	(U)	Computer Systems on Which FACT Versions are Running	130

Contents (U)

10.0 (U) FACT Versions	131
10.1 (U) SHALFACT: A Shallow Water Transmission Loss Model	131
10.2 (U) Minifact	132
10.3 (U) ICAPS Version of FACT	133
10.4 (U) Generic FACT	143
10.5 (U) Interactive FACT PL9D	145
10.6 (U) PLRAY	146
11.0 (U) Test Cases Used in AMEC Evaluation	149
11.1 (U) Results of Test Cases Used in AMEC Evaluation	151
12.0 (U) Summary and Recommendations	160
13.0 (U) References	165

THIS PAGE

INTENTIONALLY

LEFT BLANK

The Acoustic Model Evaluation Committee (AMEC) Reports

Volume II: The Evaluation of the FACT PL9D Transmission Loss Model (U)

1.0 (U) Introduction

(U) This volume is the second in a series of Acoustic Model Evaluation Committee (AMEC) reports. Volume I deals in detail with the model evaluation methodology and its implementation in fulfillment of AMEC's charter. This volume details the application of that methodology for the evaluation of the Fast Asymptotic Coherent Transmission (FACT) model, version PL9D, as run on a UNIVAC 1108 computer at the Naval Underwater Systems Center, New London Laboratory. To perform the accuracy assessment portion of the evaluation, several modifications to FACT PL9D were required and are described in section 1.2.

(U) The model evaluation methodology is described in section 1.1 and in greater detail in Volume I of this series. The primary issues for which we seek to provide model evaluation information are (1) model description, (2) physics and mathematics, (3) run time, (4) core storage, (5) complexity of program execution, (6) ease of effecting program alterations, (7) ease of implementation (on a different computer), (8) cognizant individual(s) or organizational element(s), (9) by-products, (10) special features, (11) references, and (12) accuracy assessment.

(U) In April 1973, the FACT model was designated as the Navy Interim Standard Model for the prediction of transmission loss in an environment which can be characterized by a flat bottom and a single sound speed profile. Largely due to this designation, the FACT model has become the Navy's workhorse, finding its most frequent usage at Fleet Numerical Ocean Central (FNOC), Monterey, Calif., where programs are run 450-500 times per day, and as the primary propagation loss module of the Integrated Command ASW Prediction System (ICAPS), which is being widely distributed to land-based and fleet units. FACT is also used at numerous naval activities (U.S. and allies) throughout the world and by companies under U.S. Navy contract for a broad spectrum of applications, as detailed in section 2.2.

(U) Four classes of models are described by Hersey (1977): Research Model, Candidate Model, Navy Evaluated Model, and Navy Operational Model. With the publication of this report, FACT PL9D has fulfilled the requirements for status as a Navy Evaluated Model. The FACT model has, as indicated above, been a Navy Operational Model for many years due to its prior designation as Navy Interim Standard Model.

(U) As we shall see, one of FACT's most attractive features is its fast run time, typically 2-8 seconds on the UNIVAC 1108 computer with the EXEC VIII operating system. The requirements for rapid run time had a great effect on the approach taken and algorithms chosen. FACT is also attractive in terms of core storage required (21855 decimal words on the UNIVAC 1108). FACT is a rather well-documented model and the availability of test cases facilitates implementation on a new computer.

(U) The version of FACT which is under evaluation here is FACT PL9D. Although not evaluated, other versions of FACT are described in section 10.0, and references to these versions are provided, if available.

1.1 (U) The AMEC Methodology

(U) Volume I of this series of reports presents the AMEC model evaluation methodology in detail. The following list is a synopsis of this methodology; these items are taken from an information request form sent to those persons responsible (usually the developer) for a model which is to undergo evaluation, and, taken together with the physics review and accuracy assessment, constitute the evaluation.

(U) Range Independent Propagation Loss Information requested for AMEC:

1. (U) Model Description

- Purpose(s) of the model.

- List of input variables and their units (inputs obtained from associated data bases, internal routines, functions or tables should be so identified).

- List of output options. Examples of tabular and graphical results.

- A list of systems (e.g., sonar prediction, engagement model, etc.) supported by the model, including the role of the model in the system and the stated purpose of the systems.

- Limitations designed into the model, through inherent limits of the physics, mathematics, environmental description, computer implementation, etc. These limitations, taken together, define the model's domain of applicability and include frequency, bandwidth, range, etc. Also included are limitations involving choice of computer, graphics, and telemetry links. Outline the extent to which the limitations result from design decisions based upon the basic purpose of the model development effort or tradeoffs required by time (run time or product delivery), cost and computer assets.

- A list of extant model versions. Note differences between versions including computer, changes in inputs and outputs, assignments of default values, graphics, program language, use of overlays, etc.

2. (U) Run Time

- Provide run time as function of computer, number of points and input/output selections, and model version. Divide run time into computation time and time required for printing and plotting. Describe tradeoffs between accuracy and run time as affected by input options.

3. (U) Core Storage

- Provide information on core storage requirements on a version basis. Identify techniques used to reduce core requirements including use of overlays, memory mapping, disk memory swap and the use of techniques such as interpolation in place of calculation.

4. (U) Complexity of Execution

- Provide a program listing.

- Define all input and output parameters under user control.

- What default values or conditions are assigned with the program?

- Identify restrictions on parameter values.

- Identify unusual parameters and provide guidance for their selection.

- Does a user's guide exist? If so, please forward.

5. (U) Ease of Effecting Programs Alterations

- Supply a program flow chart.

- A list of program variables and their definition.

- Extent to which a model is tied into a specific computer executive system or special equipments or programs, library routines, etc.

6. (U) Ease of Implementation on a Different Computer

• List of computers (and executive systems) on which model is presently running.

• List of military and civilian activities using the model.

• Computer language(s) used by the model (all versions).

• Special codes (e.g.,plotting routines, library functions).

• Extent of program dependence on a given computer executive system system.

• Identify test cases to assure proper running on a new computer (including scenarios treated); are all subroutines and lines of code exercised?

• List of all errors returned and the situations that caused them.

7. (U) Cognizant Individual(s) or Organizational Elements, Names and Addresses of Those Responsible for

• Theory upon which model is based.

• Model development.

• Computer implementation.

• Model maintenance and configuration management.

8. (U) References

• A list of references, including those that discuss theories upon which model is based and numerical methods employed. References worthy of special mention follow: a user's guide; a response to SECNAVINST 3560.1, Tactical Digital Systems Documentation Standards of 8 August 1974, or a response to DOD Standard 7935.1-S, Automated Data Systems Documentation Standards of 13 September 1977.

9. (U) By-Products

• A list of output by-products (e.g., eigenray information, arrival angle vs. range, ray diagram).

• A list of by-products not available externally but which are internally calculated.

10. (U) Special Features

• A list of special features (e.g., provision for beampatterns, multi-frequency results through interpolation, etc.).

(U) The review of the physics and mathematics and computer implementation of a given model is undertaken by an independent expert in the appropriate field of modeling. In particular, the physics and mathematics are examined to define the model's domain of applicability through assumptions, approximations, and the assignment of "nominal values" to various parameters.

(U) The reporting of the model's physics includes the basic foundations and approach, any unusual techniques and, especially, any extensions to theory or unique capabilities otherwise unavailable. Examination of the model's physics and mathematics is to include consideration of environmental inputs, including theories and the appropriateness of data base selection. The computer implementation is examined to assure that the calculations required by the theory are correctly performed. The efficiency or other aspects of the program code are not addressed.

(U) Two accuracy assessment procedures are employed in AMEC evaluation. Both yield quantitative results and involve comparison of model outputs with experimental data or the output of a reference model. The steps of the first procedure, called the Difference technique, follow:

• Smooth the reference data set (only if CW or exhibiting large fluctuations) and

the output of the model (only if coherent phase addition was used) by applying a 2 km moving window.

• Subtract the model output from the reference data set (after appropriate smoothing).

• If possible, divide the difference curve into range intervals corresponding to direct path, bottom interaction and convergence zone modes. If not possible, either (a) do not subdivide into range intervals; (b) use quasi-arbitrary intervals, which may be tactically useful; or (c) subdivide on the basis of any features evident in the measured data.

• In each range interval calculate the mean μ and the standard deviation σ of the differences.

• Analyze results, attempting to identify causes of discrepancies. The above steps are supported by figures as follows: measured data, smoothed measured data, model output, smoothed model output, and difference between smoothed curves. These curves are drawn to the same scale and may be overlaid on a light table, facilitating comparison and diagnosis.

(U) As useful as this technique is in identifying significant differences and facilitating diagnosis, it has a number of shortcomings: (a) misleading in convergence zones where range errors are as significant as errors in level; (b) it is conceivable that large errors occur at dB levels of no consequence for operational systems; and (c) the difference approach leads to answers which are not particularly useful to fleet purposes, especially in the context of specific sonar systems.

(U) These shortcomings are eliminated in the second accuracy assessment technique, called the FOM (Figure of Merit) technique. In this technique the data is once again smoothed as in the first step. FOM are then selected in 5 dB steps. For each FOM, detection range information is tabulated: range of continuous coverage, ranges of convergence zone starts and ends, and in range intervals over which detection coverage is zonal in nature--the percentage of the interval over which detection can be made. This FOM vs. detection range analysis is performed for model and reference data set, the results compared, and reasons sought for significant disparities.

(U) Taken together, the two accuracy assessment techniques--the Difference and FOM techniques--lead to results useful to scientific analysis and for system performance estimation.

1.2 (U) Modifications to FACT PL9D for AMEC Evaluation

(U) The version of FACT run at the Naval Underwater Systems Center, New London Laboratory, for AMEC evaluation is essentially FACT PL9D but with some alterations; most were necessary to meet requirements of the AMEC evaluation. The changes follow:

(1) Provision made to write propagation loss vs. range results to external files for further processing by MCPROG (Model Comparison Program) used for accuracy assessment by quantitatively comparing model results with experimental data and for plotting.

(2) Double precision updates contained in the NAVOCEANO FACT code were transferred to the NUSC version.

(3) Code was inserted to prevent the processing of more than one frequency in any single FACT execution.

(4) For an input frequency of less than 1000 Hz, bottom class 2 is treated the same as bottom class 1 and bottom class 5 is treated as class 4. This modification was effected by inserting a code that changed user inputted bottom class values 2 and 5 to 1 and 4, respectively,

when and only when the input frequency is less than 1000 Hz. When such change is performed by the program, a message is written in the FACT printed output indicating the new bottom class value.

(U) The FNOC bottom loss tables are to be used in determining bottom loss values when the user-specified input frequency is below 1000 Hz. For frequencies at or above 1000 Hz, the analytic equations corresponding to NAVOCEANO bottom loss types 1 through 9 are used.

(5a) An option has been added to the FACT card input that permits the user to specify whether an external bottom loss table is to be read and processed in place of the normally used internal FACT bottom loss functions. This user-provided bottom loss table is in the form of a formatted card image external file containing 91 floating point values representing the bottom loss (dB) for each of the bottom reflection angles from 0° to 90°, inclusive, in 1° steps. Each record in this file must have the format 10F8.4.

(U) This option resulted from a requirement to use measured bottom loss values in some cases and values from MGS curves (taken from the RAYMODE X model) in some cases, in addition to FACT's internal values.

(5b) Code has been added to FACT to determine the critical angle whenever a bottom loss function is provided by the user. This determination is performed as follows:

• If the slope of the bottom loss curve is constant (i.e., if $(B_I - B_{I-1}) = (B_{I+1})$, for all I, where B_I is the Ith bottom loss values), then the critical angle will be set to 15°.

• If the slope is not constant, then the critical angle will be set to the first angle at which there is a change in the slope. That is, the critical angle will be set to the first $B_{I+1} - B_I$. However, if I is greater than 15, the critical angle will be set to 15°.

(5c) Code has been added to permit user specification of a critical angle that will override the internally computed value (as determined in 5b. above) in the case where the user has provided an external bottom loss function. This override feature will be implemented as follows:

• The second FACT input data card (i.e., the card after the title card) contains a new entry in columns 51-60 with variable name USERCR (which stands for "user critical angle"). USERCR will be used only if column 45 on the same card is a "1", indicating that user-specified bottom loss values are to be processed. USERCR will be a floating point number (i.e., a number with an expressed decimal point) with the following values:

• USERCR = 0.(or blank) means that the internally computed critical angle is to be used. > 0. means that the value of USERCR (deg.) will override the internally computed value. < 0. means that a critical angle of Ø is to be used. (This apparent artificiality of requiring that a negative USERCR value indicate a critical angle of 0. is made necessary by the fact that, in floating point input processing, a "blank" is the same as a "0"., and it is "nice"to have the default case, namely a a blank, indicate that the internally determined critical angle is to be used.)

(U) The separation of critical angle THETCR from bottom loss choice is expected to have a negligible (and beneficial) effect on FACT's accuracy, especially when the 15° default is chosen. This is because values less than 5° and greater than 20° have been found to result in poor range-angle curve fitting.

2.0 (U) FACT PL9D Description

(U) The following description is extracted from the FACT Model Vol. II (Baker and Spofford, 1974), followed by a description contained in the FACT Handout (included as section 5), which is provided at the front of the FACT PL9 program listing:

(U) "The objective of FACT is to estimate, by using raytracing techniques, the acoustic transmission loss in a single-profile, flat-bottom ocean environment, as a function of range and frequency. Additionally, if requested, FACT will produce the arrival angles (at the receiver) of individual ray paths, again as a function of range. Transmission loss (dB re 1 yard) is tabulated in a single array of dimension 250 x 6 at up to 250 equally spaced range points for each of one to six frequencies. Arrival information is written to an auxiliary (tape or disk) file as individual records containing fields for range, angle, and intensities at up to six frequencies."

(U) As indicated in the documentation included as part of the FACT Handout, the primary component of the FACT Package is a single subroutine FACTTL, which may be incorporated into any of a number of complete programs requiring an estimation of transmission loss versus range and frequency. One example of a standalone program is included: TLOSS, a program which reads input parameters from cards, calls on FACTTL for losses, and prints or plots the results. This program is primarily useful to analysts requiring a small number of runs as part of a design program on a demand basis.

(U) Two additional transmission loss models may be used to supplement FACT in those cases where a full FACT solution is liable to result in excessive running times. These models, SHALTL and HFCHTL, are designed specifically to approximate the results of a complete FACT solution in shallow-water transmission and half-channel transmission, respectively. Subroutine HFCHTL is an integral component of FACTTL in that the output of HFCHTL is supplemented by the output of FACTTL for the direct and bottom-reflected paths. On the other hand, in order to employ subroutine SHALTL a modification to TLOSS is required (e.g., replacing the call to FACTTL by a call to SHALTL). Care should be exercised in using both of these models, as both serve only as quick-running alternatives to the normal FACT processing. Additionally, the HFCHTL model requires further care in use, in that it is valid for only the specific frequencies and source/receiver combinations contained within the listing.

(U) In the following list, only the most significant steps in determining transmission loss are outlined; many computational steps, such as the calculation of constants and other factors essential to the calculation are covered in detail in the sections in Baker and Spofford (1974) dealing with individual subroutines. Some liberties have been taken in describing the sequences of calculations, but it is essentially:

Profile correction: The profile points are corrected to take account of spherical earth geometry.

Axis location: The deep sound channel axis, if any, of the profile is located, and, under certain conditions, the source and receiver depths are altered to allow simulation of axis-to-axis transmission.

Profile augmentation: The source and receiver depths are inserted in the profile as explicit points, altered slightly, if necessary, to avoid equal velocities at the two depths.

Geometry factors: A number of flags are set (at various points throughout the program) to indicate various geometrical relationships between source and receiver.

Low frequency effects: The WKB phase factors for low frequency cutoff are calculated.

Ray selection: The angles of the rays to be traced are selected, and grouped into one or more families. The selection is based on the velocity profile, source, and receiver depths. Rays are chosen so that within each family, an analytical fit of Range vs. Angle can be made, thus smoothing and retaining legitimate caustics while removing false caustics; the functional form of the fit will vary with family type. If the profile and associated source and receiver

depths lead either to more than 20 families or 100 rays, processing is terminated and the transmission loss array is returned with zero values for all entries.

Ray tracing notes: Because the environment is single profile, flat bottom, any ray which is traced exhibits a periodicity over the range of interest and is actually traced for only a single such cycle.

Path combinations: Depending upon the geometries involved, either two or four paths from the source to the receiver may be combined into a single path of doubled or quadrupled intensity.

Half-channel note: When a half-channel case has been flagged on input, only the direct and bottom and surface-reflected arrivals are processed. In these cases, the non-direct path, non-bottom and surface reflected contribution to intensities are approximated and added by a separate half-channel model.

Final processing: When all families have been processed, surface-duct contributions, if present, are added to those intensities already calculated, and are then converted to transmission losses (re one yard).

(U) Processing of an arrival order of a family of rays consists of the following steps:

- The arrival ranges for each of the (one to four) paths with this order are calculated.
- For each path, the coefficients and parameters required to express range as a function of ray angle are calculated. Any one of four possible functional forms is used, according to family characteristics.
- If the range intervals for all four paths exceed the maximum range of interest, processing of arrival orders for the family is terminated.
- Subroutine INSTOR (or CUSP, if applicable) is called to calculate and add the intensity arising from each (smoothed and fitted) path to the transmission loss array at each range point for each frequency.
- If the intensities from all four paths drop below a specified minimum value, processing of arrival orders for the family is terminated.

(U) Processing of one path of an arrival order by INSTOR or CUSP consists of the following steps:

- The type of fit of range versus ray angle is examined to determine whether or not a caustic exists and to find the minimum and maximum ranges at which contributions to total intensity are made.
- If this range interval is beyond the range of interest, processing of the path is terminated.
- At each applicable range point, the number of arrivals (rays) is calculated: zero indicates the shadow of a caustic, one or two indicates an illuminated region.
- The intensity contribution from each ray is added to the transmission loss array for each frequency at the range being processed. The intensity is computed as an analytic function of range and frequency, and the values of ray angle and the derivations of range with ray angle at this range; the latter is obtained by examination of the range vs. ray angle fit.
- The calculated intensities are modified, if required, by factors reflecting coherent, semi-coherent, or incoherent path addition, shadow-zone fall-off, low-frequency cutoff effects, and bottom-bounce losses as applicable.
- If flagged, range, arrival angle. and the intensity information is written to an external file.
- When all range points have been processed, a flag is set to indicate if the minimum range of the path has exceeded the range of interest, or if the contribution to intensity has dropped below a specified minimum value.

From the FACT Handout (U)

FAST ASYMPTOTIC COHERENT TRANSMISSION (FACT) MODEL

DEVELOPED BY

ACOUSTIC ENVIRONMENTAL SUPPORT DETACHMENT

OFFICE OF NAVAL RESEARCH

1 APRIL 1973

THE FACT MODEL IS A RAY ACOUSTIC MODEL WHICH UTILIZES HIGHER ORDER THEORY FOR THE SOLUTION IN THOSE AREAS IN WHICH THE ASSUMPTIONS OF RAY ACOUSTICS ARE LIMITING. THE PRINCIPAL IMPROVEMENTS OF THE FACT PROGRAM ARE AS FOLLOWS--

THE GEOMETRIC INTENSITIES COMPUTED BY THE CLASSICAL EXPRESSIONS OF RAY ACOUSTICS ARE DISCARDED AT CAUSTICS WHERE THEY PREDICT INFINITE INTENSITY. RATHER, THE FIELD NEAR THE CAUSTIC IS EVALUATED USING THE APPROPRIATE ASYMPTOTIC EXPRESSIONS FOR THE PARTICULAR TYPE OF CAUSTIC-

1. SMOOTH CAUSTICS (2-RAY SYSTEMS) - BREKHOVSKIKH'S EXPRESSIONS.
2. CUSPED CAUSTICS (3-RAY SYSTEMS) FOR SOURCE AND RECEIVER AT THE SAME DEPTH - LUDWIG'S EXPRESSIONS.
3. COMBINED SMOOTH AND CUSPED CAUSTICS (4-RAY SYSTEMS). THE RMS SUM OF THE SMOOTH AND CUSPED-CAUSTIC FIELDS.

CAUSTIC FIELDS ARE EXTENDED INTO THE SHADOW ZONE TO THE RANGE OF THE CUSP WHERE THE SMOOTH CAUSTIC ORIGINATED.

THE TOTAL INTENSITY AT ANY ONE RANGE POINT IS COMPUTED BY A "SEMI-COHERENT" ADDITION OF ARRIVALS. FOR SHALLOW SOURCES AND/OR RECEIVERS THE PATHS WITHIN AN ARRIVAL ORDER WHICH DIFFER ONLY BY A SURFACE REFLECTION AT THE SOURCE (AND RECEIVER) HAVE PREDICTABLE PHASES RELATIVE TO ONE ANOTHER. PHASE DIFFERENCES BETWEEN DIFFERENT FAMILIES OR ARRIVAL ORDERS ARE LESS PREDICTABLE. THE "SEMI-COHERENT" SUMMATION REFERS TO THE COHERENT OR PHASED SUMMATION OF THE FIRST SET OF PATHS FOLLOWED BY THE INCOHERENT OR POWER SUMMATION OF THE RESULTING SETS. AS THE RATE IN THE OSCILLATIONS OF A PARTICULAR COHERENT SUMMATION INCREASES THE RANGE GRID MAY BECOME TOO COARSE TO ADEQUATELY SAMPLE THE OSCILLATIONS. WHEN THIS OCCURS THE SUMMATION IS PERFORMED WITH AN EFFECTIVELY REDUCED COHERENCE UNTIL FOR VERY COARSE GRIDS ALL PATHS ARE SUMMED INCOHERENTLY.

AXIS-TO-AXIS TRANSMISSION IS TREATED IN THE FOLLOWING WAY. THE PERIOD OF THE AXIAL RAY IS COMPUTED FOR THE SMOOTH PROFILE CORRESPONDING TO THE LINEARLY SEGMENTED PROFILE. THE RAY WITH THE SAME PERIOD WHEN TRACED IN THE LINEARLY SEGMENTED PROFILE IS FOUND AND THE DEPTHS OF ITS HORIZONTAL TURNING POINTS ARE DETERMINED. IF THE SOURCE AND RECEIVER ARE BETWEEN THESE DEPTHS, THEY ARE BOTH MOVED TO THE NEARER DEPTH. THE NET EFFECT OF THIS MOVE IS TO PRODUCE A CUSPED CAUSTIC AT THE RANGE OF THE CUSP WHICH WOULD OCCUR FOR THE AXIAL-RAY FAMILY IN THE EQUIVALENT SMOOTH PROFILE.

UNCLASSIFIED

A WKB PHASE-INTEGRAL TECHNIQUE IS USED TO REDUCE THE INTENSITY (ON A FREQUENCY DEPENDENT BASIS) OF THE RAYS SHALLOWER THAN THE RAY-EQUIVALENT OF THE FIRST NORMAL MODE. THIS SIMULATES LOW-FREQUENCY CUT-OFF EFFECTS ON RAYS WHICH CYCLE WITH VERTICAL AMPLITUDES WHICH ARE SMALL IN TERMS OF WAVELENGTHS.

A SHALLOW WATER MODEL IS INCLUDED WHICH MAY BE EXERCISED FOR WATER DEPTHS OF LESS THAN 1000 FEET, AND FREQUENCY/BOTTOM CLASS COMBINATIONS WHERE RAYS STRIKING THE BOTTOM AT LESS THAN CRITICAL SUFFER NO REFLECTION LOSS. THE RESULTING TRANSMISSION LOSS CURVE IS A SMOOTHED APPROXIMATION TO THE CURVE GENERATED IN THE FACT MODEL AND REQUIRES CONSIDERABLY LESS COMPUTATION TIME. FOR ASRAP PURPOSES THE SHALLOW WATER MODEL IS ALWAYS USED WHERE APPROPRIATE. FOR THE GENERAL USER IT IS OPTIONAL.

A HALF CHANNEL MODEL HAS ALSO BEEN INCLUDED SPECIFICALLY FOR ASRAP PURPOSES. FOR THE PARTICULAR SOURCE DEPTHS AND FREQUENCIES USED IN ASRAP HALF-CHANNEL CASES THE INTENSITY DUE TO RSR PATHS IS APPROXIMATED BY A CURVE OF THE FORM OF

TL = A + 10 * LOG (R)

WHERE A IS A FUNCTION OF THE SOURCE AND RECEIVER DEPTHS, THE FREQUENCY, AND THE BOTTOM DEPTH. AGAIN THIS CURVE APPROXIMATES THE NORMAL FACT RESULT, HOWEVER, TAKES CONSIDERABLY LESS COMPUTER TIME. FOR ASRAP THIS IS ALWAYS USED WHERE APPROPRIATE. FOR GENERAL USERS IT WILL BE INVOKED WHEN THE MIXED LAYER DEPTH IS SET TO THE BOTTOM, HOWEVER UNLESS THE SOURCE AND RECEIVER DEPTHS AND FREQUENCIES CORRESPOND TO ASRAP CASES IT SHOULD BE AVOIDED. FINALLY,THE BASIC TRANSMISION LOSS PROGRAM (EXCLUDING THE SHALLOW-WATER AND HALF CHANNEL APPROXIMATIONS) MAY BE USED TO OBTAIN ARRIVAL STRUCTURE AS FOLLOWS. FOR EACH RAY THROUGH EACH RANGE POINT A RECORD IS WRITTEN ON DISC (OR TAPE) CONTAINING -

RANGE,ANGLE,(TL(I),I=1,NFREQ) (FORMAT 8F10.3)

WHICH MAY BE USED FOR LATER COMPUTATIONS. THE ANGLE (RANGE) CURVE IS ALSO PLOTTED (ON THE LINE PRINTER).

Critical Angle Usage (U)

(U) Some important aspects of the FACT PL9D model are not discussed in the aforementioned documentation. The first aspect involves the FACT usage and specification of critical angles. As reported by Jacobs (1980):

(U) "The table of FACT 'critical angle' values (contained in the array THETCR in subroutine FACTTL) was derived from the FNOC bottom loss curves and is stored as a function of bottom class. That is, the critical angle that will be used in a particular FACT execution is dependent only on the user specified bottom class. This critical angle is used by FACT in two ways, both of which are not related to the computation of bottom loss. These two ways are as follows:

Let A = maximum {
- initial angle of the ray that strikes the bottom at the critical angle
- 5° more than the initial angle of the first ray in the last ray family (i.e., the SRBR family).
}

"1. Rays with initial angles steeper than A are terminated after 4 bottom bounces while rays with initial angles shallower than A are not terminated after a particular no. of bounces.

"2. Rays with initial angles steeper than A are fit with an R-θ (range-arrival angle) curve that differs in form from the fit used for shallower rays (see Section 3.2 of the document "THE FACT MODEL," Volume I, November 1974, by C. Spofford).

(U) "Note that as a consequence of this critical angle determination and usage, special care must be taken when FACT bottom loss processing is in any way modified. In particular, modification of FACT to accept and process user specified bottom loss values should be accompanied by the appropriate modification of critical angle values."

Source/Receiver Depth Alterations (U)

(U) A second topic which has been reported (Stephens, 1979) to augment the basic FACT documentation is concerned with the manner in which FACT modifies source and receiver depths and sound speed values in subroutine INSERT and AXIS. These are investigated in section 5.0, The Physics of FACT PL9D, by C. L. Bartberger. The alterations are too numerous to be detailed here. It is significant, however, that the depths of source and receiver can be altered within FACT PL9D and the sound speed profile altered, and that these alterations are not included at present in the FACT output.

Multi-Frequency Runs (U)

(U) In the course of running 77 FACT PL9D test cases (Jacobs, 1979) it was found that, in some cases, the FACT output for a particular frequency depended on whether the frequency was processed with other frequencies (a maximum of six frequencies may be processed in a single run) in the same FACT execution or whether the frequency was processed alone.

(U) Initial investigations indicate that the cause of this phenomenon may be the use of the <u>minimum</u> frequency being processed to compute the range at which the shadow zone near a caustic tapers off (in subroutine INSTOR), or the WKB phase factors for low-frequency cutoff effects (in subroutine CRITA).

(U) The discrepancies observed were a 33 dB difference in the 150-180 dB range and a 5.7 dB difference in the 122-128 dB range. It is not known what discrepancies are possible for losses less than 100 dB. Caution would indicate, however, that FACT should be run in a single frequency basis whenever possible.

2.1 (U) Applications (as compiled from a survey of FACT users)

1. Ocean acoustic propagation loss computation in real time (FACT model converted to real time use by rearranging depth and range dependent computations) in the following U.S. Navy training devices: 21A37, 21A38, 21A39, 21A41, 21A42. [Singer Co., Simulation Products Division]

2. Environmental inputs for ASW simulation models such as APSURF; performance predictions in specified environments for use in major analytical studies. [Center for Naval Analyses]

3. Acoustic sensor performance predictions and ASW operations analysis. [MAR, Incorporated]

4. Experiment planning performance modeling. [Bolt, Beranek, and Newman, Inc.]

5. Propagation loss data for active and passive sonar performance and evaluations in operating environments. [General Electric Company]

6. ASW/Russian Analysis. [Rohr Marine, Inc.]

7. Research and Teaching. [Naval Postgraduate School, Dept. of Oceanography]

8. Arctic Modeling. [Columbia University, Lamont-Doherty Geological Observatory]

9. Acoustic studies in support of U.S. Navy [Bell Telephone Laboratories]

10. Analysis/Modeling for Trainers. [IBM FSD Manassas]

11. ASW acoustic performance analysis. [Lockheed-California Company]

12. System evaluation and incorporated into PRISM. [Naval Ocean Systems Center]

13. ICAPS (Integrated Command ASW Prediction System) Tactical Analysis. [Naval Oceanographic Office]

14. Input into sonobuoy placement models. [Naval Air Development Center]

15. Performance evaluation, system simulation, experiment planning. [Tetra Tech]

16. Towed array modeling, buoy modeling, world-wide force survivability estimates, active sonar evolutions. [ORI, Inc.]

17. Used to generate propagation loss table for the Multi-Environment Trainer 14A11. [Cubic Corporation]

18. Support of P3-C/S34/LAMPS MKIII Acoustic Testing (T and E). [Naval Air Test Center (AT-410]

19. General purpose-transmission loss vs. frequency. [Naval Research Laboratory, Code 8160]

20. Performance prediction for acoustic surveillance systems. [Sanders Associates, Ocean Systems Division]

21. Routine predictions of propagation losses (including those along separate arrival paths) for comparison with experimental measurements, for comparison with the predictions of other models, and for use in simulations of system performance. [Defence Research Establishment Pacific]

22. Computation of torpedo acquisition range. [Naval Underwater Weapons Engineering Station]

23. Comparison of model results with data for model evaluation, incorporated into the Generic Sonar Model after modularization. [Naval Underwater Systems Center, New London Laboratory]

24. Passive sonar performance prediction on such systems as AN/BQQ-( ) ISPE. [Tracor, Inc.]

25. In response to requests for predictions of transmission loss vs. range and arrival structure for short-to-intermediate ranges and for frequencies between 50 Hz and 15 kHz. [Naval Ocean Systems Center, Code 724]

26. Provide range users estimates of acoustical conditions to aid test planning and/or evaluate test results. [Naval Underwater Systems Center, West Palm Beach Detachment]

27. Naval analysis programs for ONR, P3 and S3 programs for NAVAIR, and operational support for COMPATWINSPAC. [Santa Barbara Analysis and Planning Corporation]

28. Prediction of performance of airborne acoustic systems. [Naval Air Development Center]

29. Analysis of airborne ASW weapon systems (sensor performance)... required to supplement and better understand contractor and field station analysis inputs. [Naval Air Systems Command, Code AIR-526W3]

30. Propagation loss model for sonar trainers (applicable to trainers built several years ago and used extensively since then). [Honeywell, Inc., Training and Control Systems Center]

31. Transmission loss for surface ship applications. [DT NSRDC, Code 1926]

32. Sonar design and performance prediction. [EG&G, Washington Analytical Service Center, Inc.]

33. Ocean medium model for sonar trainers and simulators. Device 21440 "Advance Submarine Attach Trainer," San Diego, California. Device ATF "Acoustic Test Facility, Patuxent Naval Center, Maryland. This model is used to verify other ocean models being developed or used (e.g., AMOS, NISSM II). [AAI Corporation]

34. General analysis support and performance predictions supplied to PM-4, OPNAV, PAE, and NAVSEA. [TRW Inc., Defense and Space Systems Corp.]

35. Research into bottom interaction effects. [Applied Research Laboratories, University of Texas at Austin]

36. Passive ASRAP (Airborne Sensor Range Prediction) and Transmission Loss on a request basis; 400-500 FACT runs per day. [Fleet Numerical Ocean Center, Monterey, California.]

2.2 (U) Assumptions, Approximations and Limitations of the FACT Model *(As extracted from Spofford, 1974, with editing)*

1. ASRAP. FACT was originally designed for ASRAP (Airborne Sensor Range Prediction) program at FNWC (now Fleet Numerical Ocean Center) in Monterey, California.

2. Run Time. Minimization of program running time was crucial in the development of FACT.

3. Ray Acoustics. FACT is a ray acoustics model augmented with higher order asymptotic corrections in the vicinity of caustics, and the phased addition of selected paths experiencing significant, predictable coherence effects.

4. Sound Speed Profile. The sound speed profile c(z) is treated as a continuous piece-wise linear function of depth z (i.e., within each layer dc/dz is a constant and is discontinuous at layer boundaries).

5. Bottom Loss. Bottom loss is a function of a bottom type designator, frequency, and grazing angle. For frequencies less than 1 kHz and greater than 3.5 kHz, the bottom loss is given by the FNOC tables (Bassett and Wolff, 1970) and for frequencies between 1 and 3.5 kHz by Naval Oceanographic Office curves (Christensen, Frank and Kaufman, 1972).

6. Sea Surface. The ocean surface is treated as a perfect reflector (with a 180° phase shift) for all rays considered. For propagation in a surface duct, rays are not used and the surface duct module includes a rough surface loss which is dependent on frequency, sea state and mixed layer depth (i.e., duct thickness).

7. Surface-Range Interference. Long-term departures from the rms intensity sum are primarily due to long-range surface-image interference effects. The phase difference is estimated from the ray geometry in the immediate vicinity of the source, and detailed travel-time calculations are not used. Since the two ray amplitudes are essentially equal, a rapidly computed, local phased sum is obtained.

8. Semi-Coherence. The semi-coherent option provides an automated smooth transition from the fully coherent two-path sum to the incoherent sum as the number of range points per cycle of interference decreases from 6 to 8/3. This option is recommended for general use. Keep in mind, however, that it may yield range step-dependent transmission loss.

9. Caustic Corrections. Combined smooth and cusped caustics (4 ray systems) constitute a system for which the necessary asymptotic expressions are not available. For a well-separated system the smooth and cusped-caustic fields may be added on an rms basis. This technique is currently incorporated in FACT. For very tight geometries, a phased sum of the two fields has been required on occasion (Holford and Spofford, 1973); however, this computation is difficult to automate. The use of cusped caustic corrections and associated movements of source-receiver depth are discussed in section 5.0, The Physics of the FACT PL9D Model, by C.L. Bartberger.

10. Low Frequency Cut-Off Effects. In the FACT model the total transmission loss is computed by summing on an incoherent or rms basis the intensities of sets of rays which contribute to the field at each range/depth point of interest. Within each set certain coherent combinations of paths may have already been performed either explicitly (for surface-image interference) or implicitly (near caustics). The subsequent incoherent combination of these sets assumes that the relative phase differences between sets are both unpredictable and rapidly changing with range. For very low frequencies (geometries with dimensions of several wavelengths) both of these assumptions may be incorrect. Most importantly, as frequencies decrease to near cut-off for the first trapped mode, large-scale cancellations occur, resulting in significant uniform degradations in the rms intensity.

(U) In the FACT model this effect is approximated by reducing the amplitudes of rays which would experience uniform destructive interference. The rays expected to experience this interference are those with angles shallower than the ray equivalent of the first propagating mode as determined by the standard WKB approximations (Brekhovskikh, 1960). This approach is admittedly approximate and attempts to capture only the very gross features. The extension of ray theory to a situation so clearly in the domain of wave techniques is speculative at best--until a thoroughly substantiated technique is developed, wave programs should be used whenever possible for these cases.

11. Axis-to-Axis Propagation. A problem in ray tracing is modeling "axis-to-axis" transmission. The difficulty is that at any range on the axis, there exists an infinite number (as the ray angle approaches zero) of refracted rays (each of non-zero intensity) connecting the source and receiver. Hence, the rms summation of these paths yields an infinite intensity and the ray solution is invalid. This problem is an undesirable byproduct of the linearly segmented velocity profile. The linearly segmented profile is an approximation to a smooth profile which may be modeled by

segments (having a discontinuous second derivative across the axis). The motivation for this model is to capture the character of transmission associated with the near-axial rays. The prominent features of these rays is a strong focus F_0. The implementation of this approach in FACT is accomplished by:

a. Estimating the second derivatives of c(z) above and below the axis and establishing an equivalent smooth profile;

b. Computing the period (distance to F_0) for the axial ray in the smooth profile;

c. Finding the ray of minimum angle in the linearly segmented profile with this period;

d. If source and receiver are between the upper and lower turning points of this ray, moving both the source and receiver to the depth of either the upper or lower turning point.

(U) The resulting transmission loss for this set of near-axial rays will then exhibit the strong focusing of a cusped caustic (simulating the focusing of F_0) at the appropriate range. By moving the source and receiver to the same depth whenever they are both between the turning points, the gross features of the near-axial wave field are assumed to be essentially independent of depth for a near-axis source (Editor's underlining).

12. Surface Duct Module. The surface duct module was developed for FNOC by Clay and Patro (Clay, 1968). Intensity in the surface duct is found from conservation of energy modified by range dependent losses caused by duct leakage and rough surface scattering of energy from the duct (Marsh and Schulkin, 1967). For source and receiver both in the duct, intensity is independent of their depths; for cross-duct cases (only source or receiver in the duct) the intensity is reduced by 10 dB; for neither source nor receiver in the duct, no ducted contribution is computed. Although the user has the option of tracing rays in the duct, this procedure is not recommended because long-range computations require excessive computer time, no leakage or surface scattering effects are included, and cross-layer coupling is not computed. A preliminary analysis of the surface duct model (La Bianco, 1972) has shown that the leakage term does not correspond to the mechanism which dominates duct leakage and, in particular, has the wrong dependence on the below-layer (thermocline) gradient.

13. Special Purpose Shallow Water Model. When low-loss bottom classes are specified (i.e., zero loss up to critical angle) a large number of bottom bounce paths must be computed in shallow water with large impact on run time. An option allows approximation of the surface-reflected bottom-reflected computations by an analytical expression which includes surface-image interference effects. This option was motivated by FNOC ASRAP areas of less than 1 Kft depth.

14. Special Purpose Half-Channel Model. Again for ASRAP forecasts, excessive run time is required for shallow sources and receivers when the sound speed increases monotonically from surface to bottom. For the four frequencies and three source receiver depth combinations used in ASRAP the FACT RSR intensities (excluding volume attenuation) were fitted with functions from which a look-up table was generated. RSR intensities from this table are added to bottom-bounce and direct path intensities computed in the normal way. This routine should be used only for precise ASRAP geometric and frequencies.

15. Ray Selection. The extreme speed requirements imposed on the FACT program preclude the use of a curvilinear sound speed profile (because of the excessive time required to trace rays); instead, a linearly segmented profile corrected for earth-curvature effects is employed. Th

gradient discontinuities associated with boundaries between segments are known to introduce false caustics. The automatic elimination of these requires a careful preselection of the rays traced and an additional smoothing of the resulting angle vs. range (θR) curves. The ray selection process consists of identifying families of rays and specifying two or more rays per family while avoiding rays with horizontal turning points beyond a level where the gradient increases (i.e., a new layer is entered). [See The Physics of the FACT PL9D model by C.L. Bartberger in section 5.0 for problems in ray selection in the bottom bounce family.]

16. Smoothing θ vs. R Curves. After the rays are traced, the arrival ranges of all the rays within a family are grouped to form an arrival order. The range to the arrival as a function of the source angle, θ, is then fit with one of several functions depending upon the family. The purpose of this fitting is to remove false caustics, obtain the relevant parameters of true caustics, and provide continuous analytical functions for R(θ) which may subsequently be inverted and differentiated to obtain the intensities of all rays through all points of interest. [A further description of and problems associated with the smoothing of θ vs. R curves is found in section 5.0 describing the physics of the FACT PL9D model by C.L. Bartberger.]

17. Coherent Path Summation. If the two-path sum is written as

$$I_2 = 2I_1 \quad [1- \delta \cos \frac{(2\omega D \sin\theta)}{c}]$$

where I_1, is the single-path intensity assumed the same for both paths and D is the depth of interest, we see that $\delta=0$ yields the incoherent sum whereas $\delta=1$ yields the fully coherent sum

$$I_2 = 4I_1 \sin^2 (\frac{\omega D \sin\theta}{c})$$

thus δ plays the role of a coherence factor, and without inferring any physical significance, it is used to provide a smooth transition from a fully coherent to incoherent sum as the sampling interval becomes inadequate. The number of range points sampled per angle of interference for a given arrival order is N_p. The smoothing, or coherence, factor is then determined by

$$\delta = \begin{cases} 0 & Np \leq 8/3 \\ \dfrac{Np - 8/3}{6 - 8/3} & 8/3 < N < 6 \\ 1 & Np \geq 6 \end{cases}$$

[A discussion of coherence is found in section 5.0, The Physics of the FACT PL9D Model, by C.L. Bartberger.]

2.3.a (U) Problems, Deficiencies and Needed Alterations Compiled from a Survey of FACT Users

1. No travel time computation available. [Singer Co., Simulation Products Division]

2. Shifting range increments can change prediction (e.g., propagation loss at 2000 yards might change, depending on whether output is given every 500 yards or every 1000 yards. [Center for Naval Analyses]

3. Future program growth can be in "structuring" the code--[IBM.FSD Manassas]

4. A standard modification for using the arrival angle structure with vertical line arrays--would be useful. [Lockheed-California Co.]

5. Inability to run low (<1 kHz) and high frequencies in the same run stream on Univac 1108. [Naval Oceanographic Office]

6. Frequency range for "real" or "believable" propagation loss is unknown. [Naval Oceanographic Office]

7. (a) The surface duct module gives reresults that are not very believable (e.g., it produces propagation losses with no differences for f = 100 vs. 350 Hz).

(b) Too optimistic propagation loss in convergence zones (e. g., in CNA 1 area, propagation loss in the third convergence zone at approximately 90-100 mi was approximately 80 dB for frequencies from 40 to 400 Hz. This is hard to believe.)

(c) Straighten out the bottom loss mess.*

(d) Improve the treatment of absorption losses so that they are valid over a wide range of frequencies (30 to 80 kHz) and reflect the fact that deeper water is cooler and therefore should have less loss.

(e) Handle the "double channel" sound velocity profiles that occur in the North Atlantic.

(f) Allow the imposition of a vertical pattern weighting (e.g., from a VLA (Vertical Line Array)) on both the source, and independently on the receiver.

*Editor's Note: We couldn't resist the clarity and pain of this comment. Actually there are a number of bottom loss "messes": (1) the correctness of the FNOC low frequency bottom loss charts; (2) the correctness of the low-frequency bottom loss curves, especially the discontinuities of the curves in frequency; and (3) the connection between a bottom loss type selection which implies a critical angle selection which, in turn, determines the angle at which two curves fit to points in angle vs. range join, and the angle to which bottom loss computations are terminated cease after four bounces.

(g) Describe the limits of the model (e.g., where it should not be used; at what frequencies or other conditions it gives bad answers; whether the answers are likely to be over- or under-estimates, etc.) [ORI, Inc.]

8. (a) Due to the word length of the machine for which FACT was written, the PLOTTL cannot be used as it currently exists (on our SEL). A machine independent version of a line printer plot routine would be convenient.

(b) Increase FACT's ability to address problems relating to acoustic propagation in shallow water. [Cubic Corporation]

9. No active, ray trace, or VLAD (Vertical Line Array Difar) capability. [Naval Air Test Center (AT-41)]

10. A need for CALCOMP ray trajectory plot (however, since FACT would produce only a limited set of critical rays, this plot seems inappropriate for this program). [Naval Research Laboratory, Code 8160].

11. Is revised bottom loss model coming out? [Saunders Associates, Ocean Systems Division]

12. (a) Sensitivity of source/receiver positions with respect to both surface and subsurface ducts.

(b) Interpretation of arrival structure for low angle, fully refracted ray families, particularly for multi-duct profiles. The FACT wave-theory processing algorithms are limited in the above situations. Most inconsistent results were eliminated by using double precision arithmetic in all calculations. Even the extra 4 bits of a 36 bit UNIVAC was found to make a difference in some cases. The following points briefly summarize the DREP updates to the original FACT PL9D version (Editor's Note: These are included since they are DREP's reponses to perceived deficiencies in FACT PL9D):

(i) The overlay structure of the code has been changed to accommodate the use of double precision arithmetic in all computations. The change appears to have eliminated the apparent round-off problem noticed for certain source/receiver depth combinations associated with specific sound speed profiles.

(ii) A rapid CALCOMP plotting routine for displaying propagation losses versus range for up to six frequencies on one graph has replaced the earlier routines. The use of a minimal labelling convention has significantly reduced the Calcomp plotting time required for several source/receiver combinations.

(iii) Provision for storing the propagation loss results and arrival structure information on magnetic tape is available. Data for a maximum of 24 source/receiver combinations, each with 6 frequencies and 250 range points can be handled during one job submission.

(iv) A separate program has been developed to retrieve the FACT propagation loss and arrival angle information from the output magnetic tape and provide fully annotated graphical capability.

(v) Input/output units can be either English or metric.

(vi) A simple band-average option is available using 6 frequencies.

(vii) A ray-tracing package option can be used to display the ray paths which are automatically selected for processing by the FACT routines.

(viii) In addition to the internally provided FNOC bottom loss tables, a bottom loss versus grazing angle curve may be supplied by the user. Alternately, a frequency independent Rayleigh reflection curve can be generated from a user-supplied density ratio and sound speed ratio given at the ocean bottom interface.

(ix) A "quasi" eigenray summary can be listed. At each range point, the propagation loss for each frequency, the ray angle at the source, the ray angle at the receiver, and the corresponding transmit time along the ray path is provided. Since arrival angle information is obtained by interpolation (curve fitting) techniques, the angle at the source determined by Snell's Law is not exact. This is particularly true of low-angle rays. [Defence Research Establishment Pacific]

13. (a) Structure conversions (we use it as ping-to-ping path loss predictor in time-sequential data stream).

(b) Insufficent comment cards.

(c) No guards for out-of-range ALOG and COS. [Naval Underwater Weapons Engineering Station]

14. Future versions should offer (a) arrival angle vs. range plot option, and (b) listing of travel time or doppler shift of each ray, or (c) an option to dump this data into mass storage files or tape files. [Naval Ocean Systems Center, Code 724]

15. We have modified FACT PL9D to use the vertical line array response with the internal arrival structure. This was modeled after the work done by SAI (Bill Kirby) for Naval Ocean Research and Development Activity. [Santa Barbara Analysis and Planning Corporation]

16. The capability to include horizontal and vertical beampatterns. [Naval Air Systems Command, Code AIR 526W3]

17. We have modified our version of the FACT model to permit the user to read in his own set of bottom loss curves. To exercise this option, the user reads in a value of 10 for the parameter IB. In TLOSS a statement has been inserted which calls BTMLOS if IB = 10. In BTMLOS a card is read which indicates the number of bottom loss frequencies and their values (not necessarily the same as the

frequencies specified for the propagation loss). This routine is followed by the data for the loss curved. In view of the way the program is written, it is necessary to add an additional value to the THETCR array in FACTTL. Since it is not known in advance what the critical angles (if any) of the bottom loss curves will be, it is necessary to select some value of THETCR which will be used for all bottom loss curves. The value selected is the most conservative one appearing in the original array, namely, 0.087.

(U) Although we have not made any extensive investigation of the possible errors resulting from a mismatch between the value of THETCR and the bottom loss curves read in, it seems highly unlikely that such errors could be serious. We have never observed any unusual results which could be attributed to this modification. [Naval Air Development Center]

18. I would like the most up-to-date version of FACT to assess its applicability in the frequency and environmental domains of future trainers (sonar systems). Running a model in real time is highly desirable for trainers. [Honeywell, Inc., Training and Control Systems Center]

19. Uncertainty as to source model type (monopole; surface image included or not) and how to impose directivity on the source. [DT NSRDC, Code 1926]

20. (a) Bottom loss being a discontinuous function of frequency at low frequencies causes undesirable effects when processing "received" signal spectrums.

(b) The strength of the sum of all arrivals is provided, but the strength of each arrival is not available. This causes difficulties when FACT is used in conjunction with a directional array which only "sees" one or two arrivals and "filters"the rest.

(c) Model could be made generally more "user oriented." Documentation should be expanded. [EG&G, Washington Analytical Service Center, Inc.]

21. Output data format and Ray Grouping format. [AAI Corporation]

22. A FACT run was made using a 4-point profile, a 152 m source, a bottom depth of 3660 m, and with the receiver 30 m off the bottom. The maximum range was 888 km with 3.7 km range steps. With a bottom type 4, we get very sharp convergence zones out to a range of 600 km. Beyond this range, FACT no longer predicts any convergence zones.

(U) We looked into this problem and found that for these first 10 convergence zones the refracting rays do not form a caustic. For all successive orders, the rays do form caustics. FACT calculates a range (RCUT) at which the shadow zone created by the caustic is to be tapered off. An accompanying page describes how RCUT is calculated. FACT also calculates a range (RCM) at which point the caustic field extended into the shadow zone would be 40 dB below the caustic value:

$-3.5 = \alpha(\mathrm{RCM} - \mathrm{RC})_{\alpha}$, RC = range of caustic and

$$\alpha = \frac{2^{1/3}\sin^{2/3}}{\left(\frac{\partial^2 R}{\partial\theta 2}\right)^{1/3}_{y'}}\left(\frac{\omega}{c}\right)^{2/3}$$

(U) At the moment, FACT calculates the caustic field between RC and either RCUT or RCM. When the caustic occurs at the minimum range in the family, FACT chooses the larger of the two ranges. When the caustic occurs at the maximum range, FACT chooses the shorter of the two ranges.

(U) In our FACT run, when the caustic occurs, it is at the maximum range. The zero-degree ray is in a family which does not reach the receiver and has a

smaller period. This leads to a choice of RCUT which, in this case, is less than even the minimum range of the family of interest. This means that no calculations are performed for this family. When FACT is changed to choose the larger of these two ranges, the convergence zones beyond 600 km do appear. [Applied Research Laboratories, University of Texas at Austin].

2.3.b (U) Additional Problems and Deficiencies of the FACT Model

(U) FALSE CAUSTICS. While implementing and testing Generic FACT (Weinberg, 1977) a problem resulting in the generation of false caustics was found, the cause located and a correction implemented (however, not in FACT PL9D as yet). The problem was isolated due to the eigenray outputs of Generic FACT and the existence of other models in generic form. The error and its correction are described as follows (note: this same error is noted in section 5.0, The Physics of the FACT PL9D Model, by C.L. Bartberger):

(U) The Generic Sonar Model is structured so that individual contributions to the caustic pressure, eigenrays, can be examined individually. It was soon discovered that Generic FACT generated a family of eigenrays corresponding to a false caustic not generated by the Multi-path Expansion (another eigenray model resident in the Generic Sonar Model). This family of relatively high intensity masked the caustic phenomena.

(U) The reader may wish to pass over the remainder of this section which requires a detailed knowledge of FACT.

(U) According to the Naval Underwater Systems Center listing of FACT, the FORTRAN card:

```
15 IF ((THETC.LE.THMA).AND.(THETC.GE.
THMIN)) GO TO (30,35), IGTYP INSTOR 93
```

is responsible for the questionable eigenrays.

Here

THETC is the angle at which a caustic intersects depth Y(K2), THMIN, THMAX are angular bounds of a group of rays, and IGTYP equals 2, indicating that the range of the rays in the group is fit with the parabola,

```
R = A(1) + A(2)*DTHC + A(3)*DTHC**2
```

A necessary condition for caustics to occur is

```
DR/DDTHC = A(2) + 2.0*A(3)*DTHC = 0
```

so that

```
DTHC = -A(2)/(2,*A(3))          INSTOR96
```

and

```
THETC = THMIN + DTHC**2         INSTOR97
```

In order for the caustic to belong to the group, the inequality

```
0 < DTHC < (THMAX-THMIN)**0.5
```

must be satisfied. Instead, suppose that DTHC is small and negative. Then INSTOR 93 would incorrectly place the false caustic in the group. However, when the additional test that DTHC be positive was inserted in Generic FACT, the questionable eigenrays disappeared and the true caustic became visible.

(U) SUBSURFACE CHANNELS. A second problem discovered in the course of implementing and testing Generic FACT (Weinberg, 1977) involves the treatment of subsurface channels. As described in the reference:

(U) FACT incorporates asymptotic techniques in order to model low frequency diffraction effects not treated by classical ray theory. As this last example will demonstrate, this technique is inappropriate when the source and receiver lie within a weak sub-surface channel.

(U) Consider the sound speed profile in Figure 2.4-1. A weak sub-surface channel lies below the 100 ft (30.48 m) surface duct and extends to a depth of 1265 ft (385.572 m). Figures 2.4-2 and 2.4-3 are ray diagrams for the 640 ft (195.072 m) depth source and consists of source angles ranging from -20° to +20° in 1/2° steps. Bottom bounce rays were terminated at their second reflection in the ray diagram for illustrative purpose. One sees that the 0° ray is trapped in the sub-surface channel while the $\pm 1/2°$ rays escaped.

(U) By applying the eigenray printout option of the Generic Sonar Model to investigate the 45 kyd (41.148 km) region, we found that the Generic FACT was dominated by subsurface channel energy (Fig. 2.4-4) while the Multipath Expansion[1] was bottom bounce limited (Fig. 2.4-5). Analytic investigation supported by FFP[2] and RAYMODE[3] predictions shown in Figures 2.4-6 and 2.4-7, respectively, substantiate the Multipath Expansion.

(U) Possible improvement to Generic FACT predictions could be achieved by smoothing weak subsurface channels out of sound speed profiles or by adding specialized logic similar to the FACT surface duct model.

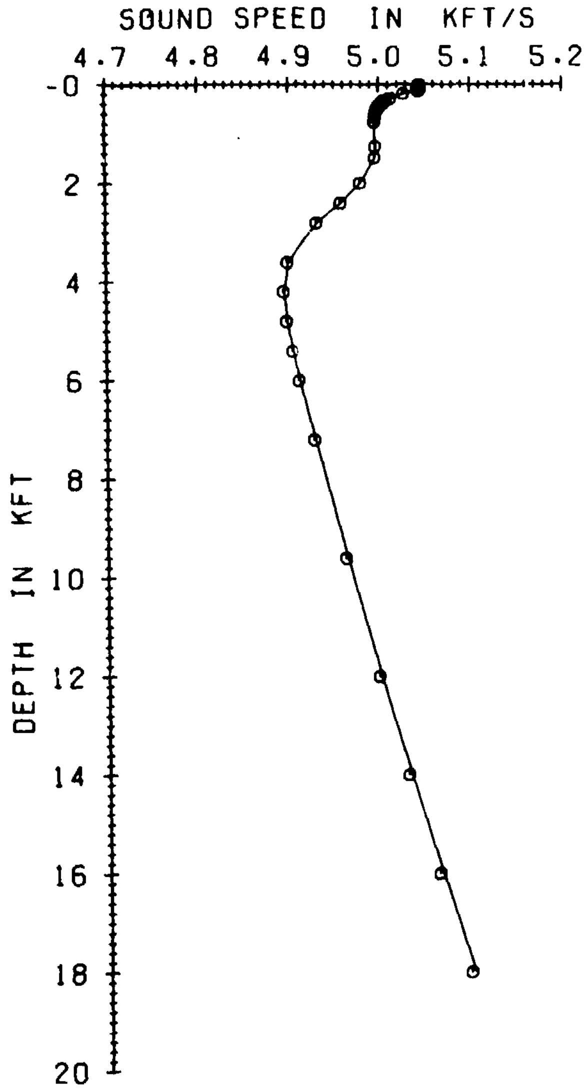

UNCLASSIFIED

Figure 2.4-1. (U) Sound speed versus depth

---

[1]The multipath Expansion model is another eigenray model resident in the Generic Sonar Model.

[2]FFP is the Fact Field Program, a fully coherent field theory program developed by Dr. F. DiNapoli of the Naval Underwater Systems Center, New London Laboratory.

[3]RAYMODE is a propagation loss program which utilizes ray and normal mode theory, developed by Dr. G. Leibiger of the Naval Underwater Systems Center, New London Laboratory. Since publication of (Weinberg, 1977), RAYMODE has been incorporated as one of the eigenray models available in the Generic Sonar Model.

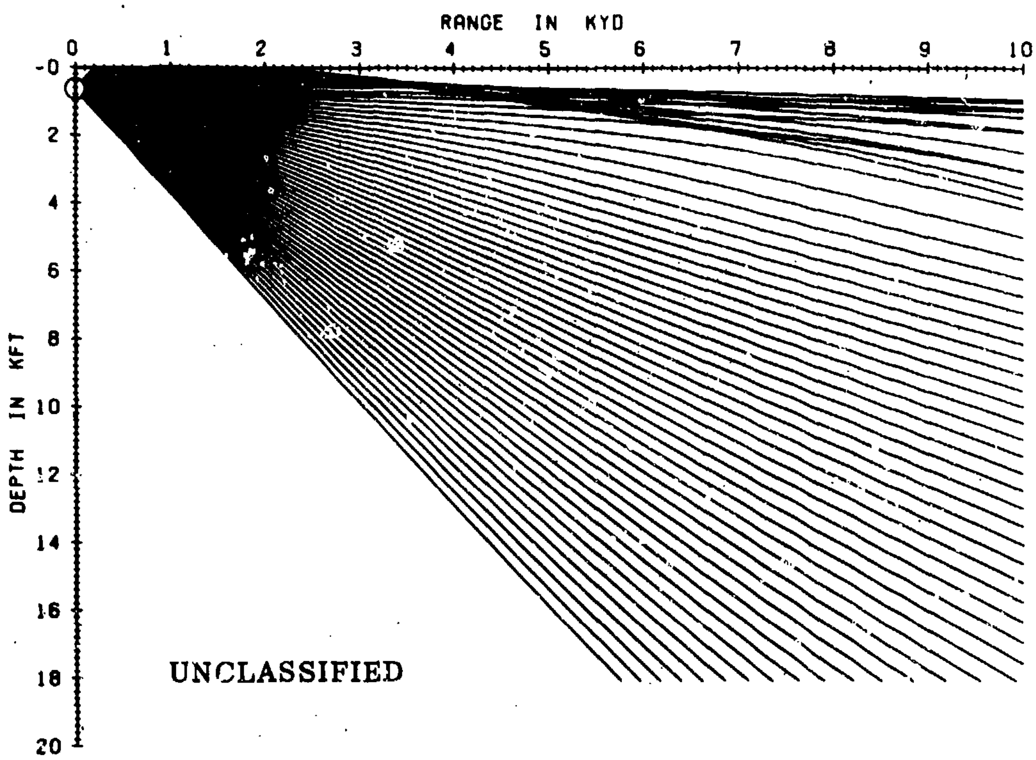

Figure 2.4-2. (U) Ray diagram for a 640 ft (195.072 m) source

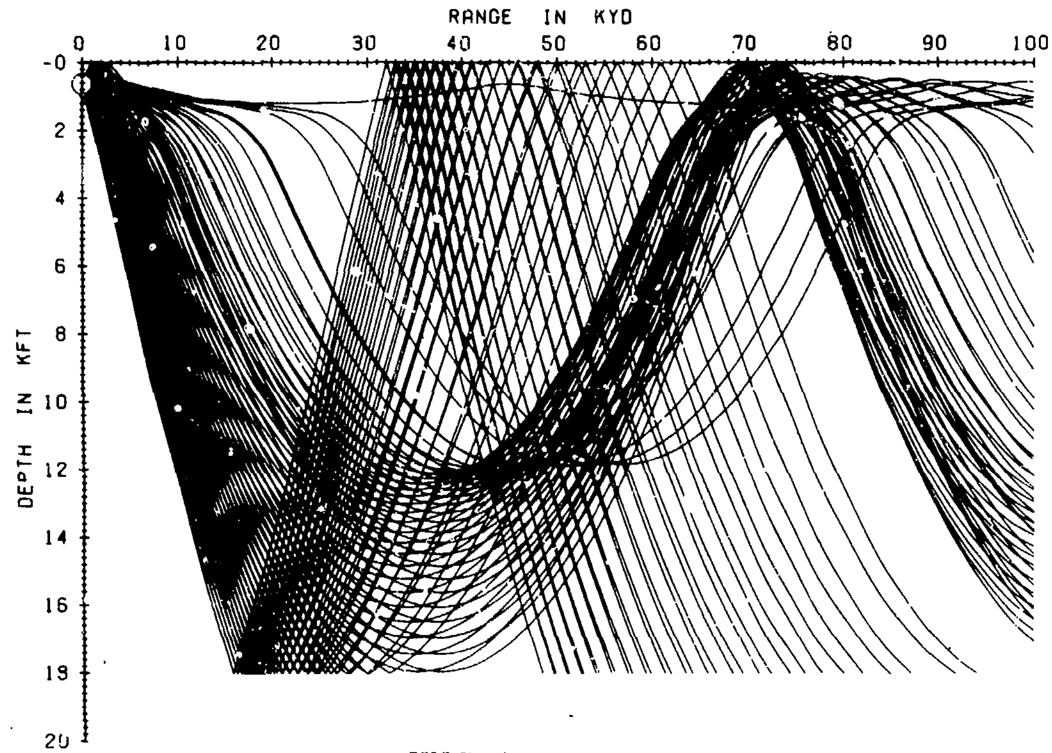

Figure 2.4-3. (U) Ray diagram for a 640 ft (195.072 m) source, including source angles from - 20° to +20° in ½° steps

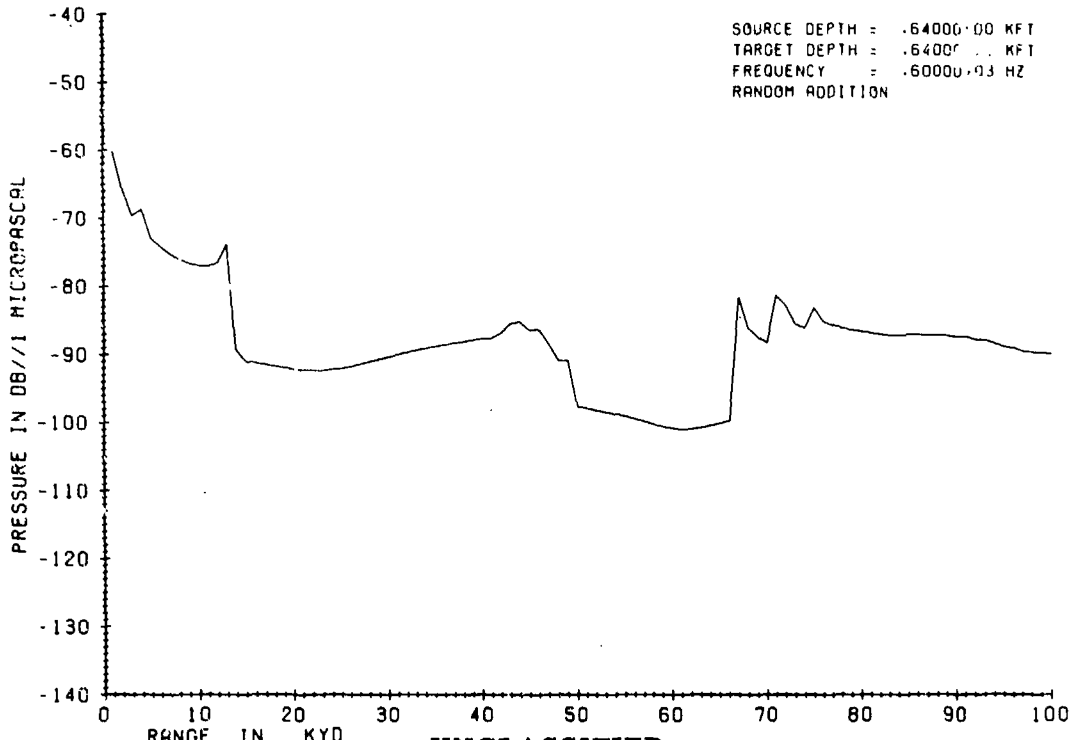

UNCLASSIFIED

Figure 2.4-4. (U) Propagation loss versus range computed by generic FACT

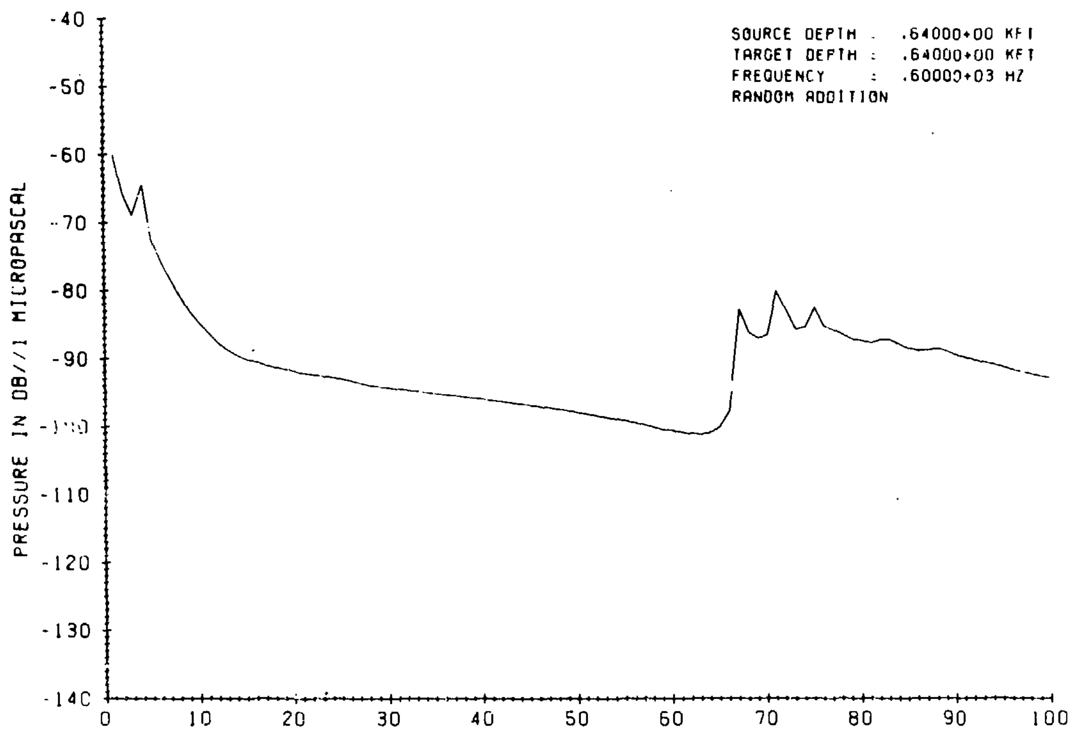

UNCLASSIFIED

Figure 2.4-5. (U) Propagation loss versus range computed by the multipath expansion

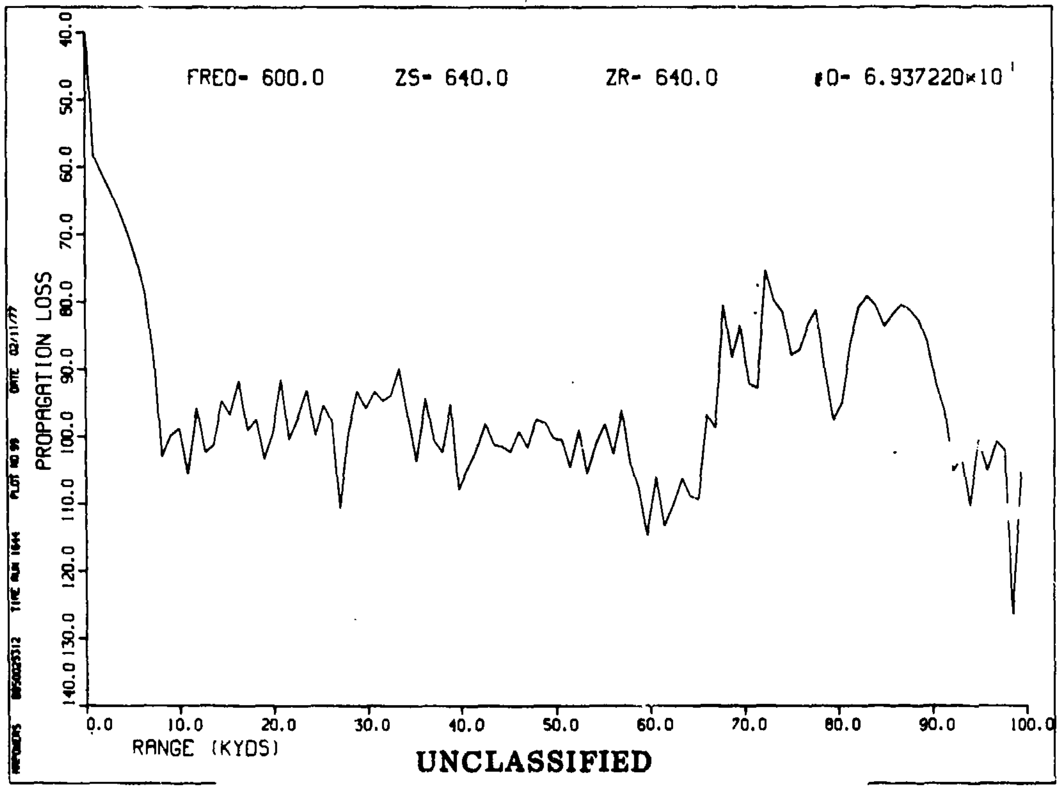

UNCLASSIFIED

Figure 2.4-6. (U) Propagation loss versus range computed by FFP

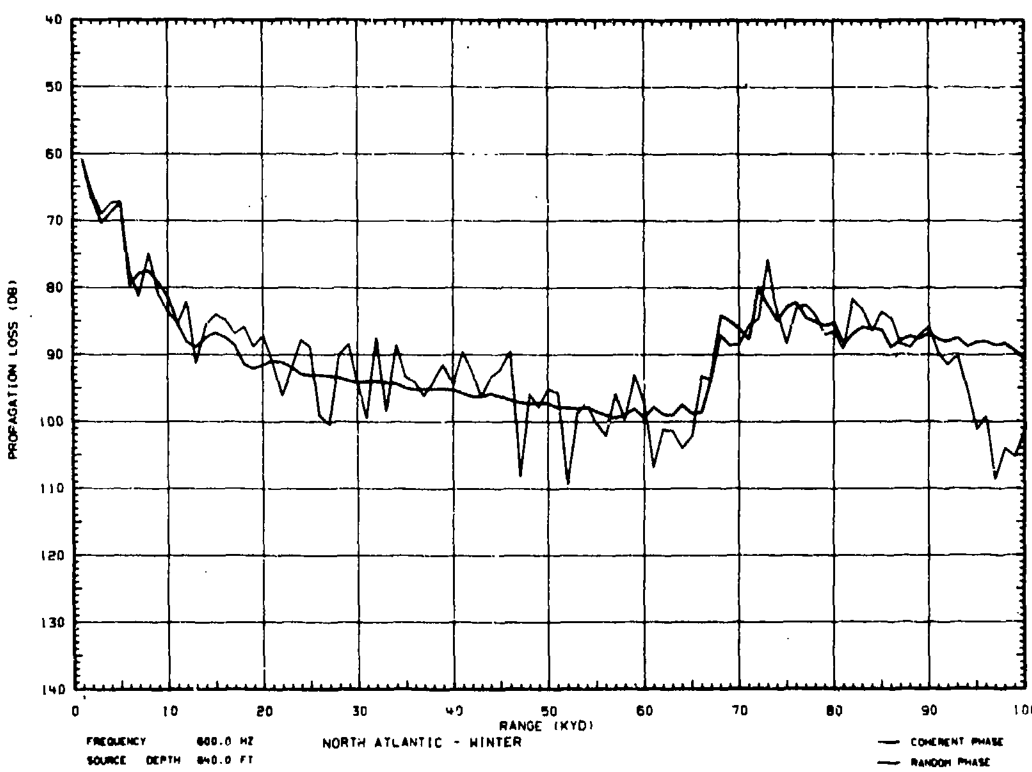

UNCLASSIFIED

Figure 2.4-7. (U) Propagation loss versus range computed by RAYMODE

3.0 (U) Running Time

(U) The running times for the cases examined in the FACT PL9D evaluation are given in Table 3.1. Except as noted, running times are the total of running the three coherence options. All running times were obtained on the Univac 1108 computer at the Naval Underwater Systems Center, New London Laboratory, in New London, Conn. The run time for a single coherence option is approximately 60% of the run time for all three coherence options.

Table 3.1

Data Set	Case	Coherence Option	Source Depth (m)	Receiver Depth (m)	Frequency (Hz)	Run Time (sec)	No. of Points
Hays-Murphy	I	C	24.4	137.2	35	4.67	200
	I	I	24.4	137.2	35	5.52	200
	II	I	24.4	137.2	67.5	4.58	200
	III	C	24.4	137.2	100	4.61	200
	III	S	24.4	137.2	100	5.27	200
	IV	C	24.4	137.2	200	3.66	200
	IV	S	24.4	137.2	200	3.94	200
PARKA	I	S	152.4	91.4	50	2.58	200
	II	S	152.4	91.4	400	2.52	200
Bearing Stake	I	S,C,I[1]	91	496	25	19.5	250
	II	S,C,I	91	1685	25	20.5	250
	III	S,C,I	91	3320	25	20.8	250
	IV	S,C,I	91	3350	25	19.9	250
	V	S,C,I	18	496	140	11.9	250
	VI	S,C,I	18	1685	140	11.8	250
	VII	S,C,I	18	3320	140	11.2	250
	VIII	S,C,I	18	3350	140	10.8	250
	IX	S,C,I	18	496	290	11.7	250
	X	S,C,I	18	1685	290	10.6	250
	XI	S,C,I	18	3320	290	10.3	250
	XII	S,C,I	18	3350	290	10.6	250
FASOR	I (FIG)	S,C,I	6.1	37	1500	4.5	200
	II (OAK)	S,C,I	23	37	1500	11.2	200
	III (THORN)	S,C,I	23	37	1500	6.0	200
	IV (REDWOOD)	S,C,I	6.1	37	1500	3.4	200
JOAST	I	S,C,I	6.1	18.3	3700	5.5	250
	II	S,C,I	6.1	79.2	3700	5.5	250
	III	S,C,I	6.1	163.1	3700	5.5	250
	IV	S,C,I	6.1	18.3	3700	5.4	250
	V	S,C,I	6.1	79.2	3700	5.3	250
	VI	S,C,I	6.1	163.1	3700	5.4	250
	VII	S,C,I	6.1	18.3	3700	6.3	250
	VIII	S,C,I	6.1	79.2	3700	5.1	250
	IX	S,C,I	6.1	163.1	3700	6.2	250
	X	S,C,I	6.1	18.3	3700	5.1	250
	XI	S,C,I	6.1	163.1	3700	5.2	250
	XII	S,C,I	6.1	18.3	3700	7.2	250
	XIII	S,C,I	6.1	79.2	3700	4.7	250
	XIV	S,C,I	6.1	304.8	3700	5.0	250
SUDS	I	S,C,I	45	17	400	4.5	200
	II	S,C,I	45	112	400	3.3	200
	III	S,C,I	42	43	1000	4.9	200
	IV	S,C,I	42	112	1000	3.3	200
	V	S,C,I	41	6	1500	3.2	200
	VI	S,C,I	41	59	1500	3.4	200
	VII	S,C,I	41	6	2500	3.1	200
	VIII	S,C,I	41	59	2500	3.3	200
	IX	S,C,I	45	17	3500	3.5	200

1. S = Semicoherent, C = Coherent, I = Incoherent

UNCLASSIFIED

Table 3.1 (continued)

Data Set	Case		Coherence Option	Source Depth (m)	Receiver Depth (m)	Frequency (Hz)	Run Time (sec)	No. of Points
	X		S,C,I	45	112	3500	3.2	200
	XI		S,C,I	42	17	5000	3.3	200
	XII		S,C,I	42	112	5000	3.6	200
Gulf of Alaska	I	140	S,C,I	30.5	30.5	1500	6.1	250
	II	140	S,C,I	30.5	304.8	1500	7.4	250
	III	143	S,C,I	30.5	30.5	1500	7.6	250
	IV	143	S,C,I	30.5	304.8	1500	8.8	250
	V	124	S,C,I	30.5	30.5	1500	5.7	250
	VI	124	S,C,I	30.5	304.8	1500	6.5	250
	VII	1124	S,C,I	1066.8	30.5	2500	7.3	250
	VIII	112A	S,C,I	1066.8	304.8	2500	7.7	250
	IX	112B	S,C,I	1066.8	30.5	2500	6.3	250
	X	112B	S,C,I	1066.8	304.8	2500	7.9	250
	XI	107	S,C,I	304.8	30.5	2500	5.6	250
	XII	107	S,C,I	304.8	304.8	2500	5.8	250
	XIII	108	S,C,I	304.8	30.5	2500	5.5	250
	XIV	108	S,C,I	304.8	304.8	2500	5.9	250
LORAD*	IA		I	15.2	30.5	530	6.9	300*
	IB		I	15.2	30.5	530	6.9	300
	IC		I	15.2	30.5	530	6.8	300
	ID		I	15.2	30.5	530	6.8	300
	IE		I	15.2	30.5	530	6.8	300
	IF		I	15.2	30.5	530	6.8	300
	IG		I	15.2	30.5	530	6.8	300
	IIA		I	15.2	304.8	530	5.3	300
	IIB		I	15.2	304.8	530	5.3	300
	IIC		I	15.2	304.8	530	5.1	300
	IID		I	15.2	304.8	530	5.1	300
	IIE		I	15.2	304.8	530	5.1	300
	IIF		I	15.2	304.8	530	5.1	300
	IIG		I	15.2	304.8	530	5.2	300

*The Generic FACT model was used for comparing with LORAD data. This version of the FACT model is not limited to 250 points as is the case with FACT PL9D.

UNCLASSIFIED

4.0 (U) Core Storage

(U) From page 4-3 of Baker and Spofford (1974):

"Core requirement, excluding input and output, but including all other FACT and system computational routines, is approximately 8,400 decimal (20,300 octal) cells on the CDC 6400/6600."

(U) From page 5-8 of the same document:

"To make an object program for the card input program TLOSS, all components with the exception of AUTOTL and SHALTL should be compiled. The resulting program occupies approximately 44000 (octal) words on the CDC 6600."

5.0 (U) The Physics of FACT Model
(by C.L. Bartberger)

(U) The physical principles upon which the FACT model is based and the implementation of those principles in the computer program are reasonably well documented in Volumes I and II of the FACT report.[1,2]. Furthermore, since the FACT model has been in wide use for a considerable period of time, and its major features are well known, there seemed to be little value in merely repeating information that is already available. It was therefore felt that a more fruitful approach to a study of the physics of the model would be to look for problem areas, to assemble a set of examples (test cases) for the purpose

of illustrating them, and to examine in detail the operation of the program as it executed the test runs. A few of the examples selected had previously been encountered accidentally in runs in which FACT had been found to yield peculiar results, and it was desired to ascertain why. Also, after a study of the FORTRAN coding a number of questions arose which led to the selection of other examples.

(U) The PL9D version of FACT currently resident at NADC had been previously modified to permit the insertion of external bottom loss curves and to provide the option of expressing ranges in kiloyards as well as in nautical miles. For the present investigation an extensive set of diagnostic print statements has been inserted, making it possible to follow in detail the progress of the computations and to observe the contribution of each arrival to the resultant intensity at every range point.

(U) This report consists of a brief description of the program, followed by a more extensive discussion of several of the major features illustrated by the examples. A description of the examples, an analysis of the behavior of the FACT model in executing them, and an interpretation of some of the results obtained are presented.

(U) It should be noted that although the examples presented in this report are heavily weighted to illustrate the errors and deficiencies of the FACT model and must not be considered to be a representative sample of all environmental i ts, they are nevertheless all based on real-world data, and most of them were encountered in the course of routine day-to-day work of the laboratory. The problems they present must be taken seriously.

(U) Finally, it is acknowledged that the scope of this investigation has of necessity been somewhat limited. No attempt has been made to examine all the details of the FACT model. Attention has been focused chiefly upon the more salient features considered most likely to be encountered in routine operations. Very little attention has been paid to the behavior of the model at high frequencies. To cite a few examples of special cases which have not been investigated, there are other occasions for moving source and receiver depths besides those mentioned in this report, there are situations in which the velocity profile itself is modified, and there are special provisions for cases in which the source or receiver is at the surface or on the bottom.

Brief Description of the Model (U)

(U) FACT is a computer program which calculates acoustic propagation loss as a function of receiver range for a pair of fixed source and receiver depths. Computations may be made simultaneously at up to 6 acoustic frequencies. The user has the option of specifying either incoherent or semi-coherent* summation of ray energies. FACT contains approximate wave corrections to overcome a number of deficiencies of basic ray theory. These include corrections for smooth caustics, cusped caustics, propagation of shallow-angle rays in the vicinity of the axis of a sound channel, and propagation in a surface duct. It also contains a simplified approximate routine to replace ray computations in a "half-channel", i.e., in an environment in which the sound speed increases monotonically from the surface to the bottom.

(U) FACT is a range-independent model which assumes a horizontally stratified ocean with a flat bottom, the structure of the ocean being specified by a single velocity profile. Linear interpolation is employed between input profile points (method of constant gradients). The effect of the bottom is represented by

*A third option referred to as "fully coherent" is also available, but it is not fully coherent and is considered to be of dubious value.

sets of curves of bottom loss vs. grazing angle, frequency, and bottom type. The surface is assumed to be a perfect reflector except that when the surface duct module is used, a loss term is incorporated which varies with wave height, frequency, and duct depth. The frequency-dependent volume attenuation is computed simply as a function of horizontal range instead of actual path length. This approximation is acceptable at low frequencies but becomes questionable at frequencies much above a few kilohertz.

(U) The following is a somewhat oversimplified summary of the flow of computations in a FACT run. Before computing any rays, FACT incorporates some logic which may under certain circumstances result in moving the source and receiver depths away from the values originally specified by the user. It then examines the resulting pair of depths and selects the depth with the lower sound speed to serve as the ray receiver. Depending upon existing conditions, therefore, the true source and true receiver may be interchanged.

(U) The program then divides the source angle space (0 to 90 degrees) into a number of sectors (NGRPS) whose boundaries are determined by limiting rays to the surface, bottom, local profile maxima, and certain other points on the profile. In each sector a set of nonuniformly spaced source angles is selected and the corresponding rays are computed. The rays are continued out to as many cycles (periods) s required for the maxima range specified by the user. At each cycle the computed ray ranges are smoothed by fitting the range-angle curves with parabolas or, for steep angles, with a formula which approaches the proper behavior at 90 degrees. These curves are used in place of the originally computed ranges to test for the presence of caustics and to compute ray intensities. If no caustic is present, the intensity is computed from ray theory, using the slope of the fitted curve as the range derivative. Special routines are provided for both smooth caustics and cusped caustics. The intensities at the various receiver ranges are summed in a two-dimensional range-frequency array. As conditions dictate, either the surface duct module or the half channel module may be invoked. At the completion of the above process the resultant intensities are converted to dB loss and the attenuation losses are added.

5.1 (U) Discussion of the Specific Features of the FACT Model

Alteration of Source and Receiver Depths (U)

(U) In the FACT model there are two conditions under which the source and receiver depths are moved. One has to do with the problem of cusped caustics and the other is concerned with the propagation of rays in the vicinity of the axis of a sound channel.

(U) Although cusped caustics can occur under other conditions, the FACT treatment is limited to the case where the source and receiver are at the same depth and is concerned only with the cusps which occur at that depth. If the source and receiver depths specified by the user differ by less than 10 ft, subroutine INSERT temporarily sets the source depth equal to the receiver depth. It then calls subroutine AXIS, where the problem of near-axial rays is treated. Upon the return to INSERT, if the two depths are equal, the source depth is moved. Although a number of special cases are considered which will be ignored in the present discussion, the normal procedure is to move the source downward if it occurs at a layer boundary, and upward otherwise. The amount of movement is the smallest of three values: (1) one half the layer thickness, (2) an amount sufficient to change the sound speed by 2 ft/sec, and (3) 10 ft. Except for the case of a very thin layer or a gradient whose magnitude exceeds 0.2 sec^{-1}, the normal shift is 10 ft.

(U) Although the cusped caustic correction is based on the assumption that the two depths are equal, the designers of the FACT model apparently felt that it was safer to avoid equal depths. It should be noted, however, that the 10-foot separation is capable of making significant changes in the character of the range-angle curves on which the caustic correction is based, as will be seen in several examples, and in critical environments can cause serious errors.

(U) The problem with near-axial rays arises from the use of straight-line segments in fitting the velocity profile. If the source and receiver are located on the axis of a sound channel, where the gradient changes discontinuously from a negative to a positive value, the period (cycle distance) of a ray approaches zero as the ray angle approaches zero. As a result there is an infinite number of rays which propagate to a receiver at any given range, resulting in infinite predicted intensity. Even when the source or receiver is moved somewhat away from the axis the predicted intensity is abnormally high. To avoid this inherent error of ray theory, FACT moves the source and receiver away from the axis to what it considers a safe distance.

(U) The procedure adopted is to examine the first layer boundary on either side of the axis, selecting the one which has the smaller sound speed. The point on the opposite segment which has the same sound speed is then located. A "smooth" profile is then generated by fitting two half-parabolas, one on either side of the axis. Each parabola is fitted to the point previously selected and goes through the axial point with zero gradient. Next, the period of the axial ray in the "smooth" profile is computed. Then, returning to the original profile, the ray is computed which has the same period as the previously computed axial ray. The upper and lower vertex depths of this ray are determined. If either the source depth or the receiver depth (or both) lie outside the interval between vertices, no shift is made. However, if both lie within the interval, both are moved to whichever vertex depth lies closer to the nearer of these two depths. In this way FACT guarantees that no rays will be computed which have very short periods.

(U) There are situations in which the above procedure is fraught with difficulties, as will be seen in the examples, especially Example 7. One problem is that it is possible to generate excessively large changes in the depths specified by the user. Another problem lies in the ad hoc method of generating the "smooth" profile. Simply interpolating a single point on one of the straight-line profile segments is capable of making major changes in the resulting propagation loss. It should also be pointed out that the user is given no warning that the results of his run may apply to significantly different depths from what he originally requested.

(U) The interchange of source and receiver in cases where the source has the higher sound speed is performed after the above procedure has been completed.

Sector and Ray Selection (U)

(U) Before computing any rays FACT divides the source angle quadrant into sectors such that within each sector all the rays have essentially the same type of trajectory. The concept of sector division is illustrated with a simplified example in Figures 5-1 and 5-2. At the left in Figure 5-1 is a tri-linear profile with the source and receiver depths labeled S and R. To the right of the profile are plots of limiting rays from the source. Ray A, with a source angle θ_A, is the tangent ray to the receiver depth. Ray B, with a source angle θ_B, is the limiting ray to the bottom of the surface duct. When it reaches this limiting depth it splits into two rays B_1 and B_2. Ray C, with a source angle θ_C, is the limiting

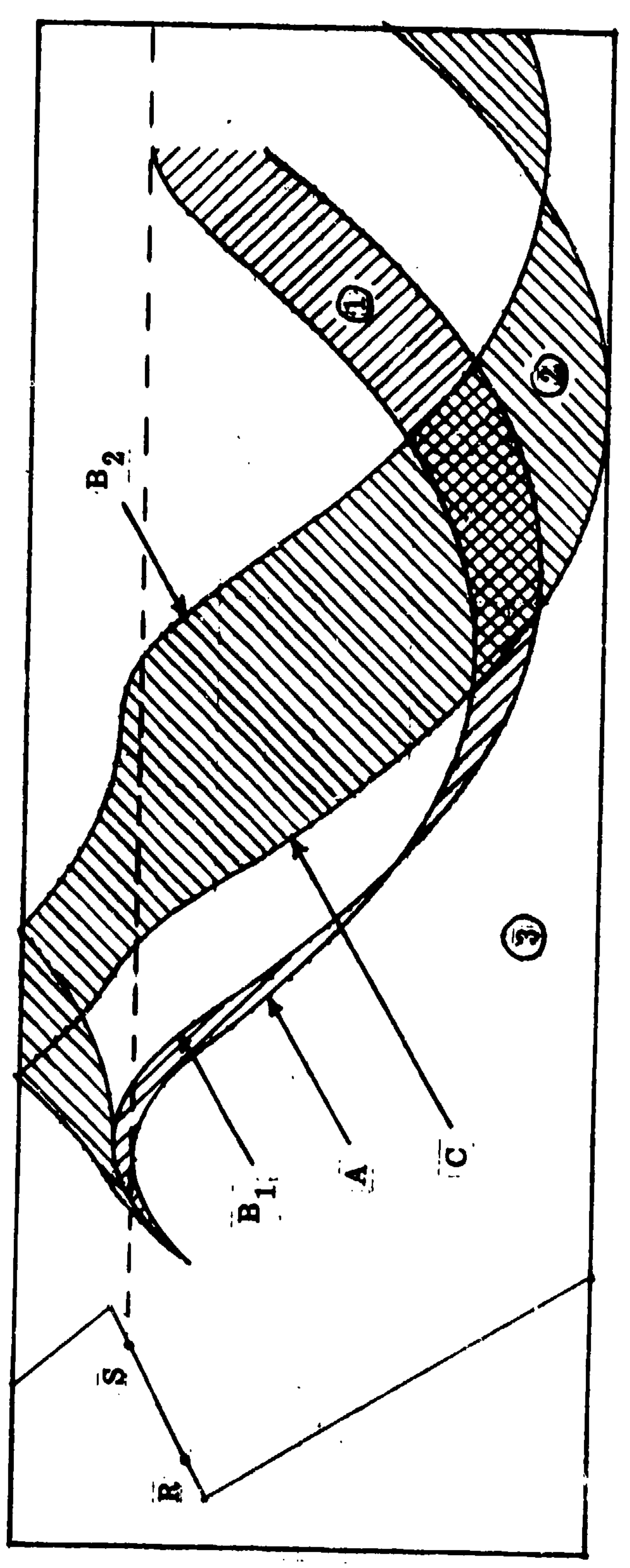

UNCLASSIFIED

(U) Figure 5-1. Families of Rays Classified According to Sectors.

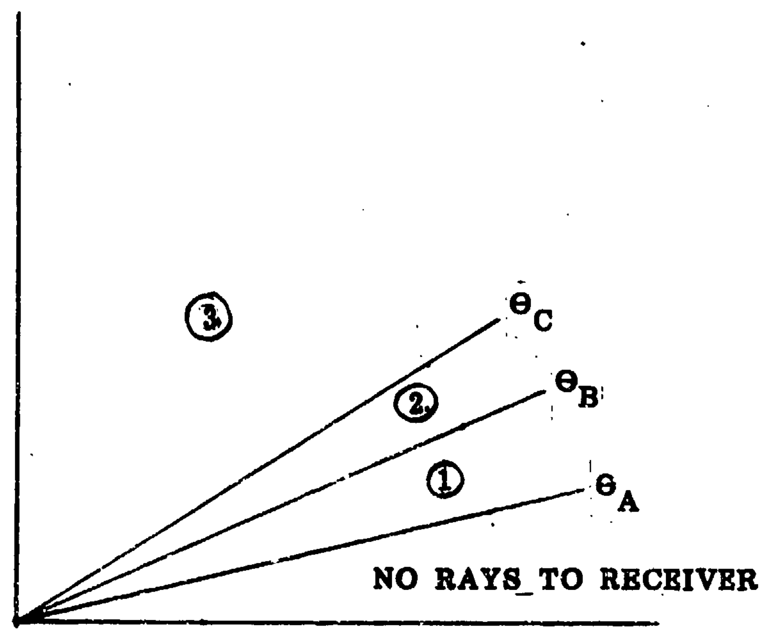

UNCLASSIFIED

(U) Figure 5-2. Source Angle Sectors.

ray to the bottom. The division of the source angle quadrant into sectors is shown in Figure 5-2. The sector corresponding to angles less than θ_A is not applicable since no rays in this sector can reach the receiver. Sector 1 extends from θ_A to θ_B and contains the family of RR rays included within the shaded area between rays A and B_1, labeled 1 in Figure 5-1. Sector 2 extends from θ_B to θ_C and contains the family of RSR rays included within the shaded area between rays B_2 and C, labeled 2. The outermost sector 3 extends from θ_C to 90 degrees and contains the family of bottom bounce rays included within the area below ray C in Figure 5-1.

(U) The sector division procedure employed by FACT is as follows. Beginning with the source depth, an examination is made simultaneously of the upper and lower portions of the profile (above and below the source). The layer boundaries are flagged in order of monotonically increasing sound speed as the search proceeds outward to the surface and bottom. Only those boundaries are flagged whose sound speed is larger than any of the values previously encountered. Whenever a flagged boundary is encountered where a local maximum exists or where the magnitude of the gradient on the far side is less than the magnitude of the gradient on the near side by an amount exceeding 0.0001 sec^{-1}, a new sector is formed. Limiting rays to the surface and bottom also determine sector boundaries. The final sector consists of bottom-bounce rays whose vertex velocity exceeds the maximum sound speed of the profile.

(U) In determining the ray source angles in each sector a small dead zone is reserved at each edge, so that the first ray angle is 0.00001 radian beyond the inner edge and the last is 0.00001 radian short of the outer edge. The second angle is 0.0001 radian beyond the first. If within the sector there are limiting rays to other layer boundaries where the gradient changes by more than 0.0001 sec^{-1} (the change in this case being an increase in magnitude as the profile search proceeds outward from the source depth), the sector is divided into subsectors. Within each subsector the rays are uniformly spaced by means of an algorithm which sets the spacing at the largest possible value not exceeding 0.008 radian.

(U) The last sector consists of only two rays. The first is the ray at the edge of the dead zone by the inner boundary. The second ray is tentatively selected to yield a bottom grazing angle equal to THETCR, which is presumably intended to represent the critical angle of the bottom loss curve.* However, this ray is required to be at least 5 degrees steeper in source angle than the first ray.

(U) It would appear that the decision to compute only two rays in the outer sector was made for the purpose of cutting down running time. However, as will be seen in Example 3, two rays are not always sufficient to yield acceptable results.

Arrival Orders and Numbers of "Paths" (U)

(U) The remainder of the computer program (except for the final computation of the propagation loss in dB) is contained in a sector DO loop (NG = 1, NGRPS). Within each sector the family of rays is processed according to arrival orders. The concept of arrival orders is most easily visualized in the case of a shallow source and shallow receiver in a deep ocean. The arrival order is the number of passages through the deep part of the ocean, or perhaps more precisely, the number of lower vertices experienced by the ray. The zero order arrivals are the direct arrivals. There are two of these, one which goes directly to the

*FACTTL supplies a single number for each bottom type, independent of frequency. (See paragraph on Bottom Loss, p. 55)

receiver without experiencing any vertices, and one which experiences one upper vertex. In the first and subsequent arrival orders there are four ray types, one with no upper vertices, a second with an upper vertex at the source end, a third with an upper vertex at the receiver end, and a fourth with upper vertices at both ends. Borrowing a term from the FORTRAN coding, we shall designate these ray types as "paths."

(U) Because of the coherence feature FACT makes a test (described later) before deciding how many paths to process in each sector. For zero order arrivals there are only two candidate rays for coherence. If, as a result of the test, these rays fail to meet the criterion for coherence, they are processed incoherently regardless of the coherence option requested by the user, and the number of paths is 2. On the other hand, if the criterion is met, only the shorter of the two rays is computed, regardless of the coherence option specified by the user. If semi-coherent (or "fully" coherent*) addition has been specified, the single ray intensity is later multiplied by a coherence factor in which the phase relationship between the rays is taken into account; otherwise it is multiplied by 2.

(U) For the first and subsequent order arrivals the test is made at both the source and receiver ends. If the criterion is not met at either end, all four rays are processed incoherently and the number of paths is 4. If the criterion is met at one end only, the four ray types are separated into pairs and only one ray type of each pair is calculated, the other being assumed to have equal intensity. The number of paths is then 2. If semi-coherent summation has been requested, the intensities of the two ray pairs are later multiplied by appropriate coherence factors; otherwise they are multiplied by 2. If the criterion is met at both ends, only one ray (the shortest) is computed and the number of paths is reduced to 1. The intensity of this ray is later multiplied by 4 for incoherent addition and by a joint coherence factor for semi-coherent addition.

* This is an essentially meaningless option, as will be discussed later.

Range-Angle Curves (U)

(U) Curves of horizontal range vs. ray source angle or receiver angle (or any monotonic function of these angles) are exceedingly useful in analyzing the behavior of the sound field. According to ray theory the intensity of a ray arrival is inversely proportional to the slope of the curve, i.e., the range derivative, and caustics occur at stationary points where the derivative is zero.

(U) The FACT model makes extensive use of this concept. It is well known that when the velocity profile is approximated by straight-line segments, discontinuities in slope between adjacent segments can lead to false caustics. In an attempt to avoid this problem FACT generates a smooth approximation to the actual curves by fitting curves of a simple mathematical form. This is done for each path of each arrival order in each sector. In all sectors except the outermost the fitted curves are parabolas of the form

$$r = a_1 + a_2x + a_3x^2$$

The independent variable x may be expressed in either of two forms

$$x = \tan \theta_R \text{ or } x = \sqrt{\theta_R - \theta_1}$$

where θ_R is the angle of the ray at the receiver depth and θ_1 is the angle of the first ray computed in the sector. The tangent form is the one normally used. However, when the sector is bounded on its inner edge by a limiting ray to the surface, bottom, or a

local profile maximum, the square root form is used.* The justification for using the square root formula is that it represents the actual behavior of the range-angle curve in the immediate vicinity of the limiting angle. There is no guarantee, however, that the approximation will be adequate throughout the remainder of the sector.

(U) The parabolas are fitted to three points (three rays computed in the sector). The logic for selecting the points is somewhat complicated. In cases where the inner edge of the sector is bounded by a ray which arrives horizontally at the receiver depth (IREFRZ = 1), there is a continuum of receiver angles from the maximum value (last ray) on the negative side to the same maximum value on the positive side. Normally the negative and positive sides correspond to different paths, but in this case the range-angle curves for the two paths are joined at zero degrees to form a single curve, and the parabola is fitted to the end points on either side and to the center point (actually the first ray computed, which is displaced slightly from the center because of the dead zone). In all other cases the first and last rays of the sector are selected for two of the three points of the fit. If a range extremum (maximum or minimum) occurs within the sector, this extremum serves as the third point of the fit. Otherwise the second ray of the sector is used.

(U) In the outermost sector the type of fit depends upon whether the rays cross a limiting depth at a local profile maximum in traveling from the source to the receiver. In all cases a formula of the form:

$$r = 1/(a_4 \tan \theta_R + a_5)$$

is used in the interval from θ_R to 90 degrees, where θ_R is the angle of the steeper of the two rays computed in the sector. This formula is selected because it approximates the behavior of the range-angle curves in the limit as θ_R approaches 90 degrees. The coefficient a_4 is simply the total vertical distance traversed by the ray between the source and receiver. The constant a_5 may be evaluated by fitting the formula to a single point. If no limiting depth is crossed by the ray, the above steep-angle formula is used throughout the sector and is fitted to the first of the two rays (range r_1, angle θ_1). It will be noted that in this case the second ray is not used, and the computed intensities at all ranges covered by the sector are based on the computation of a single ray. On the other hand, if a limiting depth is crossed, the steep-angle formula is fitted at θ_2 and is used only between θ_2 and 90 degrees. In the interval between θ_1 and θ_2 a parabola is fitted to these two points and is forced to join the steep-angle formula at θ_2 with continuous slope. Because of the limiting depth involved, the parabola is of the square root type.

(U) The curve fitting scheme used by FACT has a number of advantages. It smooths out the irregularities resulting from the discontinuities in slope of the linear segmented velocity profile. It speeds up the computations in two ways. First, it is easier to calculate the slope of a simple curve like a parabola than to calculate the actual range derivative, and second, the steep-angle formula reduces the number of rays which must be computed. Also the use of parabolas is well suited to the caustic corrections because the expansions on which they are based require a parabolic fit.

(U) However, there are also disadvantages. The true range-angle curves are

*This statement is somewhat oversimplified. For example, if the ray in traveling between the source and receiver does not actually reach the limiting depth, the tangent formula is used.

not always conducive to fitting with parabolas, and cases can be found where the curve fitting can lead to gross errors. Errors in slope cause errors in computing ray intensities. Errors in curvature in the vicinity of a maximum or minimum can cause errors in caustic corrections (See Examples 1 and 7). It is also possible for the parabola to exhibit a minimum or maximum range within the angular interval of the sector, even though no such extremum occurs in the actual computed ranges.* Furthermore, it appears that the decision to compute only two rays in the final sector--or, more precisely, not to compute any rays at angles steeper than the critical angle of the bottom loss curve--was ill-advised. Although the steep-angle formula is an excellent approximation for steep angles, there are serious problems in attempting to extend it down to angles of the order of 5 to 10 degrees, as may be seen in Example 3.

Coherence Computations (U)

(U) In the FACT model coherence is applied only to the rays of individual arrival orders. The resulting intensities of different arrival orders are added incoherently. This type of energy addition is properly designated as semi-coherent. It preserves the broad, sweeping oscillations associated with coherence within the individual arrival orders, which are frequently observed in real-world data. It ignores the rapid fluctuations resulting from interference between different arrival orders, which are meaningful only in a statistical sense. The type of computation which takes completely into account the interference among all orders (e.g., parabolic equation or normal modes) may properly be termed fully coherent.

*An example of this phenomenon was encountered shortly after the FACT model was first received at NADC. Unfortunately the details are no longer available.

(U) The concept of semi-coherent ray addition employed in the FACT model is based on the assumption that the only interference pattern of significance is that generated by surface reflections. If the depths of the source and receiver are very small in comparison with the depth of the ocean, then all four paths from the source to the receiver which involve one or more passages through the deep ocean will have essentially the same trajectory and will differ from each other essentially only by a surface reflection at the source and/or receiver end. Considering first the source end, the assumption made in FACT is that in the vicinity of the source the pair of interfering rays which differ only by a surface reflection are parallel straight lines and that the phase angle between them can be computed from the local difference in path length, plus the 180-degree phase reversal upon reflection. A similar consideration applies at the receiver end.

(U) For zero order arrivals coherence is considered only at the source end if the source is shallower than the receiver and only at the receiver end if it is deeper. Unless one of these two depths is quite shallow and the other quite deep, the parallel-line approximation is rather poor for zero order arrivals, and the resulting pattern cannot be expected to be very accurate. However, in most cases the direct propagation zone is quite short and the interference pattern plays an insignificant role.

(U) For the first and subsequent arrival orders, when coherence occurs only at the source end, the four paths are broken up into two pairs. The two paths of one pair arrive at the receiver from below, while the two paths of the other pair arrive at the receiver from above. Coherence is applied separately to each pair, and the resulting intensities are added incoherently. Likewise, if coherence occurs only at the receiver end, the four paths are broken up into two pairs such that the two paths of one

pair leave the source in a downward direction while the two paths of the other pair leave in an upward direction. As indicated previously, if coherence occurs at both ends, only one ray is computed and the resulting coherence factor is the product of the two individual factors.

(U) Since the type of coherence considered in FACT is a surface-imaging phenomenon, it is to be expected that the correlation between interfering paths should deteriorate progressively as the depth of the source or receiver is increased. However, the coherence treatment in the FACT model is apparrently not conducive to the incorporation of a progressive deterioration,* since an abrupt on-off technique is used instead. In considering coherence at the source (or receiver) end, FACT computes the horizontal distance traveled by the ray in propagating from the source (or receiver) depth to the surface and back. If this distance exceeds 2 nautical miles it is arbitrarily assumed that coherence does not exist, and the rays are added incoherently, regardless of the coherence option specified by the user.

(U) Before a decision is made, the horizontal separation is determined for the first and last rays of the sector. The decision is then based on the larger of the two separations. Such a procedure can frequently lead to undesirable results, as may be seen in Examples 3b and 4. In both cases the shallower ray gave the larger horizontal separation, which was in excess of the 2-mile limit. However, this condition occurred only over a small range interval at the far end of the region covered by the sector. Over the bulk of the region in each case the horizontal separation was well within the limit, yet the rays were combined incoherently.

(U) In the design of the coherence feature of the FACT model it was recognized that situations may arise where the oscillations of the interference pattern are so rapid in relation to the range increment specified by the user that a sampling problem exists; that is, a plot based on only the sampled points will not adequately represent the true curve. Clearly the only satisfactory way to solve this problem is to use a smaller range increment. However, this information is not available in advance to the user. In cases where a run is made with too large an increment it was decided to provide an ad hoc solution simply by cutting down the amplitude of the oscillations. It was decided that if there are 6 or more range points per cycle of the oscillations, the sampling is adequate and no reduction in amplitude is made. If the number of points per cycle is less than 2-2/3, the sampling is considered totally inadequate and the amplitude is cut to zero, yielding in effect incoherent addition. If the number of points per cycle is intermediate between these two values, the amplitude is multiplied by an attenuation factor which varies linearly from 1 to 0.

(U) In determining the number of points per cycle FACT computes an average value over the family of rays in the sector. It computes the total number of phase cycles and divides this by the total number of range points. However, in the first bottom-bounce region, where the interference pattern is of prime importance, the frequency of the oscillations varies drastically with range. As a result cases may arise, as illustrated in Example 2, where the use of an average value generates a partial reduction in amplitude and leads to poor results at both ends of the range interval. At short ranges, where the oscillations are

*In the development of the NADC ray model PLRAY [3], which approaches the coherence problem in essentially the same way as FACT, an attempt was made to introduce a type of progressive decorrelation, but the scheme was abandoned because of difficulties encountered.

rapid, the curve is poorly sampled, whereas at long ranges, where no reduction is necessary, the curve is represented by the wrong amplitude.

(U) It will be noted in the FACT propagation loss curve of Example 2 that the oscillations are quite well defined at ranges at least down to 25 kyd and are reasonably well defined at ranges even somewhat less than that. Now, at 25 kyd the number of points per cycle is only 4. This suggests that the FACT figure of 6 may be too conservative.

(U) It would appear desirable to investigate this matter further with a view to determining optimum values for the upper and lower limits of the transition region.

(U) The coherence terminology used in this report differs from that used in the FACT report. In the latter the type of energy summation used in the model exclusive of the amplitude reduction associated with the sampling problem is referred to as "fully coherent," and the application of the amplitude reduction renders it "semi-coherent." It is felt that these definitions are erroneous. A fully coherent model is one in which the mutual phase interference of all paths to the receiver is included. FACT does not have this capability. It is felt that the basic FACT approach should logically be termed semi-coherent and that the amplitude reduction feature is merely a modification of semi-coherence. Furthermore, the "fully coherent" mode provided to the user, whereby the amplitude reduction algorithm is bypassed, is considered to be an essentially meaningless option. If it was considered necessary to incorporate that feature in order to avoid distortions due to inadequate sampling, what is the value of bypassing it? (Incidentally, in view of the current observation that the distortions, at least in the vicinity of 4 points per cycle, are less severe than implied by the parameter values used in the model, there may be some value in using the "fully coherent" option after all.)

(U) In the past a considerable number of runs have been made on a variety of velocity profiles in which the semicoherent output of FACT has been compared with the NADC normal mode model AP2. In most of the runs the FACT interference pattern in the first bottom bounce region agreed surprisingly well with that generated by AP2. The poorest agreement tended to occur when the source and receiver were located in or below a strong thermocline. The source of disagreement is undoubtedly in the ray refraction due to the strong gradient, which violated the assumption of straight-line propagation. In addition, the agreement was observed to deteriorate with increasing frequency. This result is also to be expected, since the error in the phase angle is proportional to the frequency. It should be pointed out, however, that the quality of the interference pattern is dependent upon the quality of the curve fitting which is applied to the range-angle curves. Example 3 exhibits a case where a serious error in curve fitting results in a significant distortion in the interference pattern.

(U) Although the special cases associated with placing the source or receiver at the surface have not been analyzed in this investigation, one difficulty with the FACT treatment of coherence is obvious. If either the source or the receiver is at the surface, the coherent intensity, if properly computed, will be zero and the propagation loss will be infinite. Furthermore, if the computations are done incoherently, the resulting propagation loss will not correspond to physical reality. Hence either way the FACT predictions for this case are meaningless.

Types of Caustic Correction (U)

(U) FACT contains wave corrections for two types of caustics--smooth caustics and cusped caustics. Caustics are surfaces in three-dimensional space along which ray theory erroneously predicts infinite intensity. The trace of a caustic surface in the vertical plane in

which the ray paths of the FACT model are confined is a line formed as the locus of a family of tangent rays. A simple example of a caustic is shown in Figure 5-3. This is an example of a smooth caustic. Figure 5-4 shows a more complicated ray diagram generated by a bi-linear profile. At the extreme right of the plot two smooth caustics can be observed, one at the top of the family of rays and the other at the bottom. As the range decreases, the two caustic lines approach each other and finally join to form a cusp at the point C, which is located at the same depth as the source. This is a cusped caustic. Another feature of interest in Figure 5-4 is the additional smooth caustic which occurs in the vicinity of the cusp, at the inner edge of the ray paths. It will be noted that in addition to the cusp at C a second cusp C' is formed at the reciprocal depth.

(U) FACT contains wave corrections both for smooth caustics and for cusped caustics of the type which occur at the same depth as the receiver. Although it is understood that there may be coupling between a cusped caustic and a nearby smooth caustic, as illustrated in Figure 5-4, FACT performs the corrections independently.

(U) If the source and receiver depths were originally specified within 10 ft of each other, or if, as a result of the operations performed in subroutine AXIS they were moved together (and then separated again in INSERT), the cusped caustic correction procedure is automatically applied in CUSP. Otherwise the smooth caustic correction procedure of INSTOR is applied. Further, if associated with the cusp there is also a smooth caustic, subroutine CUSP, after completion of the cusped caustic correction, calls INSTOR for processing the additional smooth caustic.

Smooth Caustics (U)

(U) The smooth caustic correction is a relatively straightforward implementation of Brekhovskikh's theoretical development, replacing the standard ray intensity formula with an alternate formula involving the Airy function Ai(-x)*. The intensity of the field in the vicinity of the caustic is proportional to the square of the Airy function and inversely proportional to the 2/3 power of the second derivative of range with respect to ray angle (at the receiver, in the FACT model). The extent in range over which the correction is applied depends on the argument x of the Airy function, which is proportional to the distance in range from the caustic and to the 1/3 power of the second range derivative.

(U) In the FACT model the presence or absence of a smooth caustic is determined from an examination of the constants of the parabola fitted to the range-angle curve. The caustic is assumed to be located at the vertex of the parabola. Since every parabola has a vertex, the question at issue is whether the vertex lies in a physically realizable region. The location of the vertex is computed and a test is first made to determine if the angle lies within the sector. If not, there is no caustic. Otherwise the range of the caustic is tested. In order that a caustic be assumed present the range must be greater than zero.

(U) On the insonified side of the caustic ($x > 0$) the interval within which the correction is applied is normally terminated at a value of 1.77 which,

---

*The negative sign is used with the argument x to be consistent with the formulation in FACT.

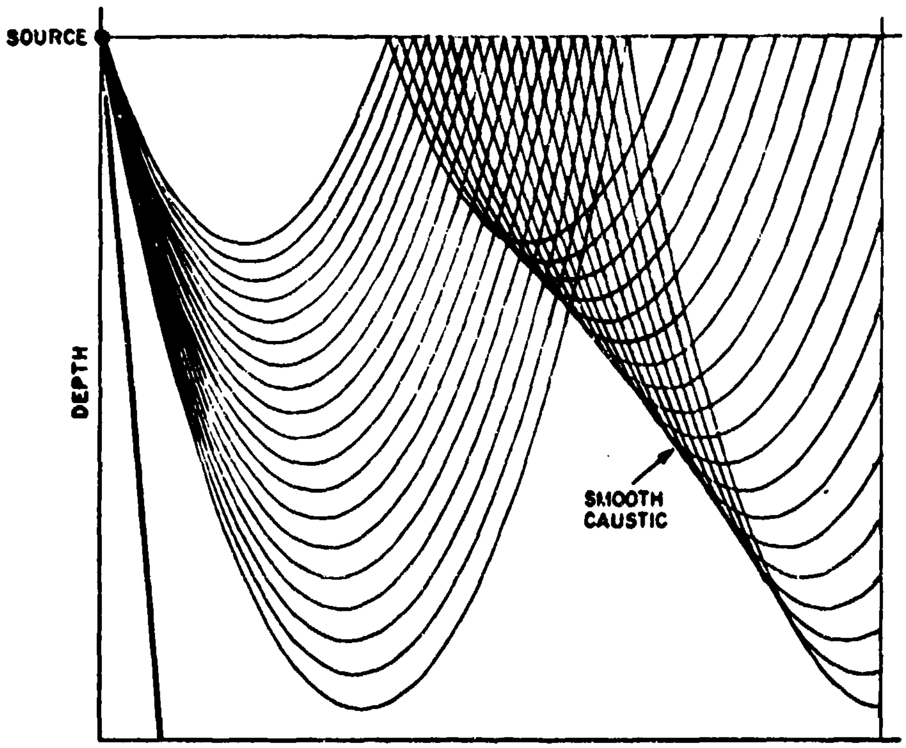

UNCLASSIFIED

(U) Figure 5-3. Development of a Smooth Caustic in a Pressure-Gradient Profile

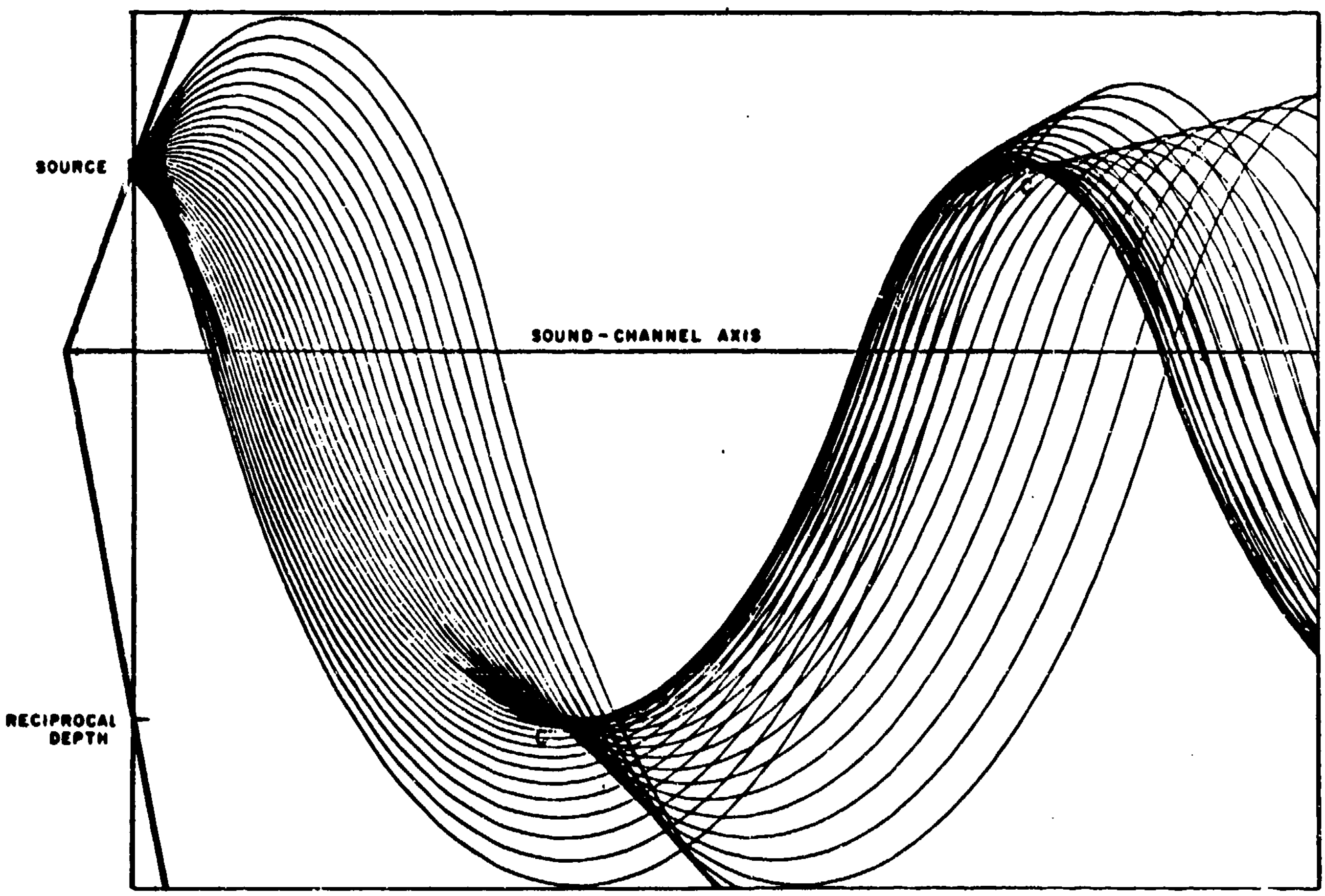

UNCLASSIFIED

(U) Figure 5-4. Development of a Four-Ray System (Smooth Caustic Near a Cusped Caustic)

according to theory, provides a smooth transition to the incoherent sum of the intensities of the two rays which form the caustic. An exception to this rule occurs when processing the smooth caustic associated with a cusp. On the near branch of the curve (between the caustic and the cusp) the intensity is computed from the Airy function formula without regard to the above limit and is compared with the intensity computed from the cusp formula; the larger of the two is selected.*

(U) On the shadow zone side of the caustic the intensity computed from the Airy function falls off exponentially. Ideally this procedure should be carried out to a point in range where the intensity contribution is negligible in comparison with the contributions from other paths. A good value of x to select for this limit is -3.5. However, in actual operation of the program it is possible that errors in estimating the second range derivative, which controls the scale of x in relation to the range, may cause the field to decay too slowly and thereby extend into a region where physically the intensity is expected to be negligible. To treat this situation FACT introduces a parameter RCUT which is intended to define the maximum distance to which the field is allowed to extend into the shadow zone. To accomplish the cut-off the argument of the Airy function is arbitrarily multiplied by a secant function whose angle is zero at the caustic and increases to 90 degrees when the range reaches RCUT. Thus, the argument x is forced to approach infinity and the intensity to approach zero at the defined limit.

(U) The logic by which RCUT is evaluated is not understood. In the examples studied one case was found (Example 5) in which an apparently erroneous value of RCUT was generated. This was a minimum range caustic and the value of RCUT was larger than the maximum range of all of the rays of the sector.

(U) Since the lower index of the DO loop in which the intensities are computed is determined by RCUT and the upper limit is determined by the largest ray range, the lower index turned out to be larger than the upper index. As a result the DO loop was bypassed and no intensities were computed. This error has been observed previously by Payne and Focke [4].

(U) Another error, previously reported by Weinburg [5], was encountered in Example 6. When a parabola is fitted to the square root of $\theta - \theta_1$, the portion of the parabola corresponding to negative values of the square root has no physical significance. Yet through an error in logic it is possible for a minimum or maximum on the negative side to be treated as a genuine caustic.

(U) The accuracy of the caustic correction is critically dependent upon the quality of the parabolic fit to the computed range-angle points. In the examples studied, several cases have been found in which erroneous caustic corrections have been generated. In Example 1 over-smoothing of the range-angle curves has yielded both erroneous range derivatives and erroneous ray angles which in turn have generated the peculiar-looking convergence zones which may be seen in the propagation loss curve. In Example 6 the distortion in the parabolas is so bad that the Airy functions are spread out over almost the entire range of the plot. The peaks of the Airy functions are so broad that they cannot be discerned in the propagation loss curve.

Cusped Caustics (U)

(U) The FACT model contains a wave correction for cusps which are formed at the common source/receiver depth when these two depths are equal. A typical set of range-angle curves, derived from a simple bi-linear profile with the

*Actually the reciprocals of the intensities are computed and the smaller of the two is selected.

source and receiver at 1000 ft, is shown in Figure 5-5. The branches marked 1, 2, 3, and 4 are the four paths designated by NP in the program. The cusp C, located at the common intersection point, is formed by the two branches 2 and 3 which, when the source and receiver are exactly at the same depth, form a continuous curve with an extremum (maximum or minimum) at the zero degree angle. In a manner typical of the FACT approach this curve is fitted with a parabola which forms the basis of the intensity correction procedure. The shape of the intensity curve is controlled by the square of the modulus of the Pearcey function Pe(O,Y), whose argument Y is proportional to the distance of the range point from the cusp. The constant of proportionality is a function of the coefficient of the ray angle in the parabolic formula. This coefficient also controls the magnitude of the intensity. Thus in a manner similar to that of the Airy function for smooth caustics the curvature of the parabola determines both the range scale and the magnitude of the caustic correction intensity.

(U) On the insonified side three rays are involved in the range interval from the cusp to the point where branches 2 and 3 end. Beyond that point there is only one ray. However, apart from the identification of these rays for the purpose of applying low-frequency cutoff effects (to be discussed later) and including the rays in the arrival structure output, it does not appear that this change in the ray structure is reflected in the intensity computations, since the intensity is determined by parameters which do not explicitly involve the number of rays.

(U) Depending on the situation there may or may not be a smooth caustic on the shadow side of the cusp. If there is no caustic, the intensity is computed in the normal manner in subroutine CUSP. However, if there is such a caustic, a different procedure is involved. The theory developed for the cusped caustic does not include the effect of an adjacent smooth caustic. When such a caustic is present, CUSP calls INSTOR for processing it. On the branch of the range-angle curve between the smooth caustic and the cusp, INSTOR computes the intensity from both formulas and selects the larger of the two.

(U) The cusped caustic correction incorporated in FACT, as described above, is based on the geometry of Figure 5-5 which assumes that the source and receiver are at the same depth. Unfortunately this geometry is not applicable because in subroutine INSERT the two depths are always moved apart. The separation is normally 10 ft although if the source and receiver are in a layer with a strong gradient it may be somewhat less. A very slight depth separation alters the shapes of the range-angle curves significantly. Figure 5-6 shows a portion of a family of curves, in the vicinity of the cusp, in which the receiver depth is moved upward through 5 ft in steps of one foot. It will be noted that although branches 2 and 3 appear to be two halves of the same curve when the two depths are exactly equal, they really belong to different curves. Actually branches 1 and 2 belong to one curve which (in Fig. 5-6) rapidly moves downward from the cusp as the depths begin to separate. Branches 3 and 4 belong to the other curve which rapidly moves upward. The effect of a 10-foot separation is shown in the curves marked with x's in Figure 5-7. The appearance of these curves is quite different from the classic picture of two intersecting lines.

(U) But this is not the only problem with the FACT cusped caustic correction. Apparently on the basis of the theoretical assumption that the source and receiver depths are supposed to be the same, FACT fits the cusp parabola to the source depth instead of the receiver depth. But elsewhere in the program a redefinition of the true source and receiver depths has been made on the basis that the ray source must have a lower sound speed than the ray receiver. As a

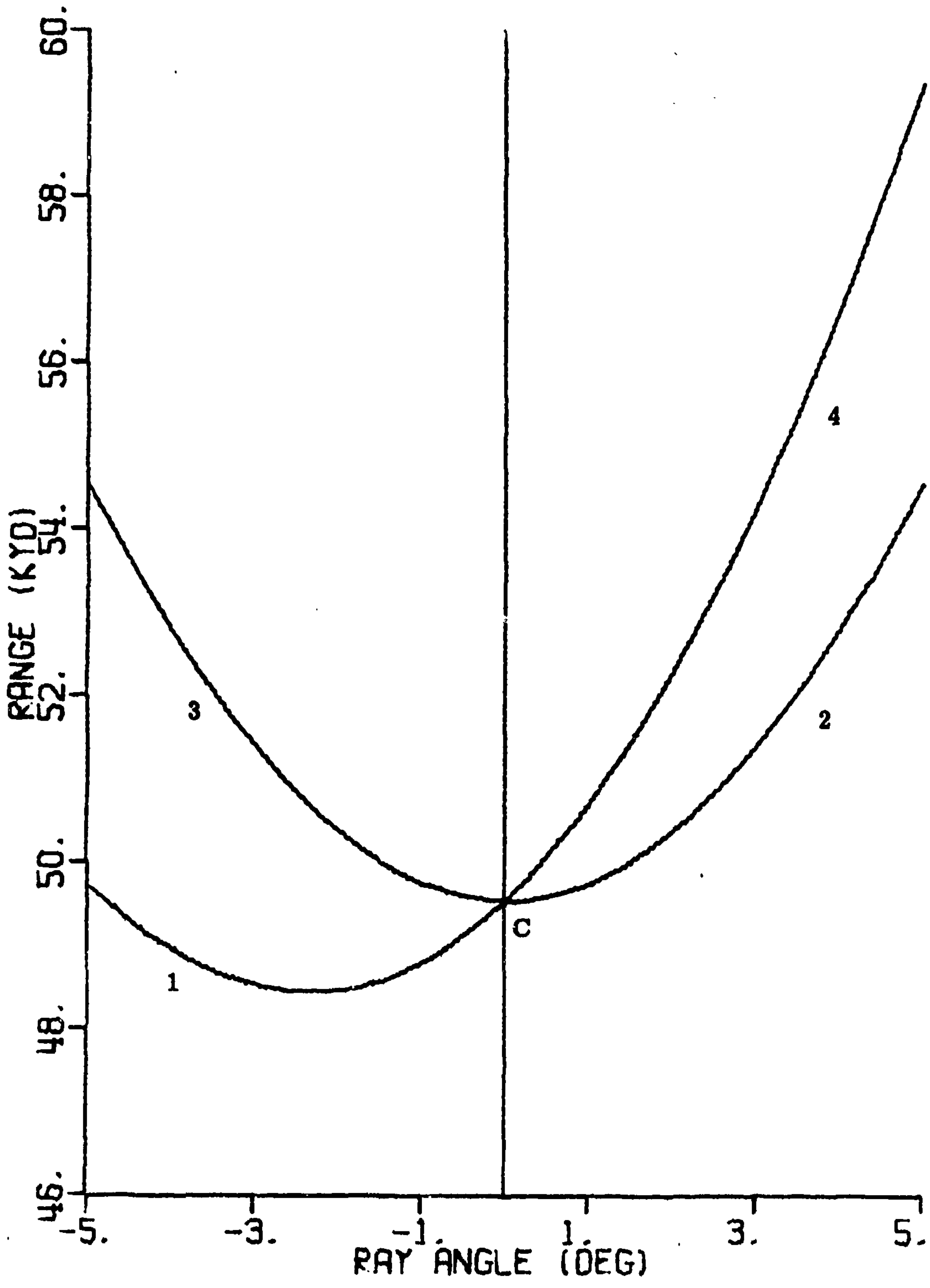

UNCLASSIFIED

(U) Figure 5-5. Range-angle Curves Showing Cusped Caustic and Associated Smooth Caustic For a Bi-linear Profile. Source and Receiver at Same Depth.

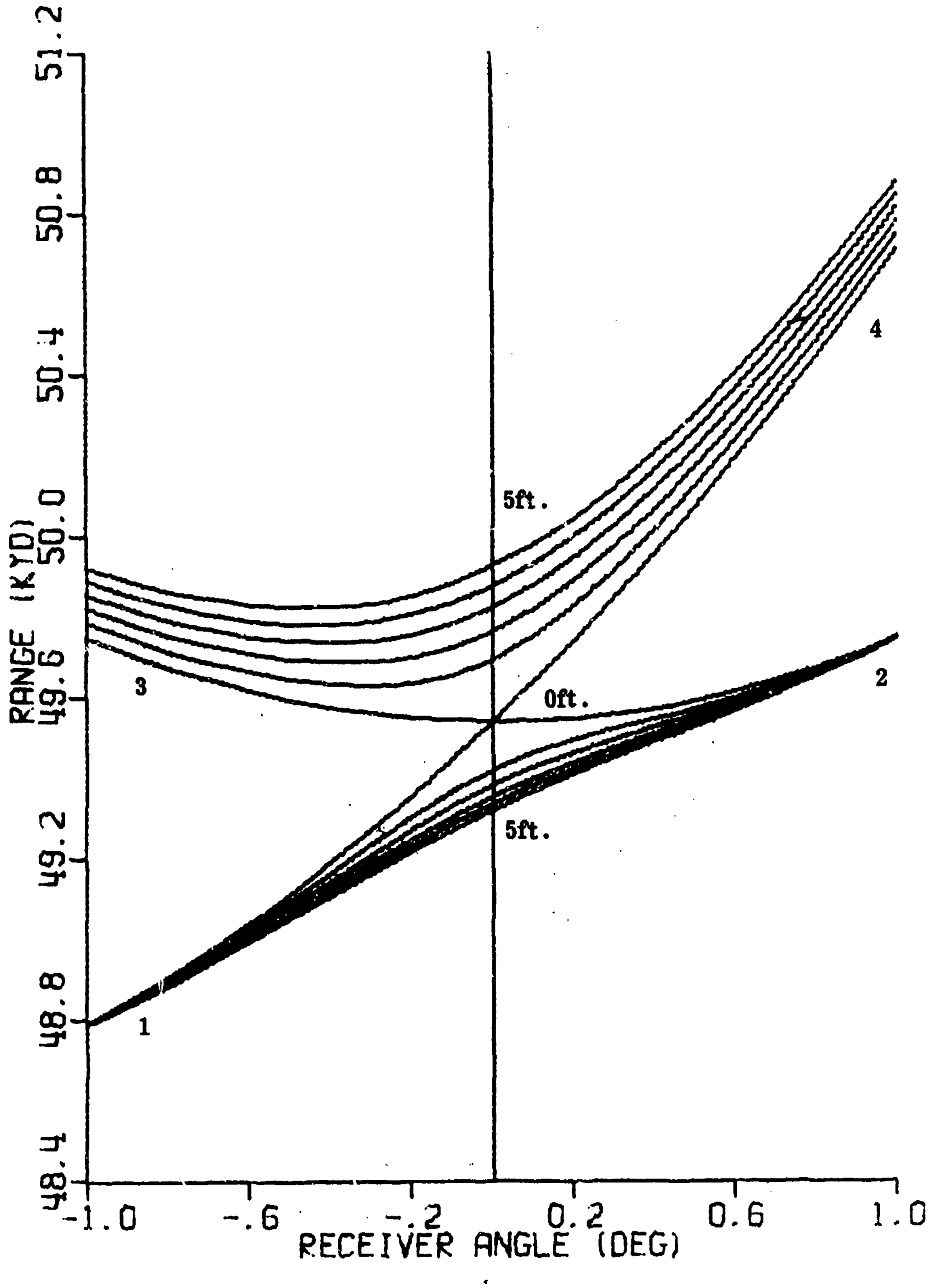

UNCLASSIFIED

(U) Figure 5-6. Effect on Range-angle Curves of Separating Source and Receiver by 5 Feet in Steps of 1 Foot; Bi-linear Profile.

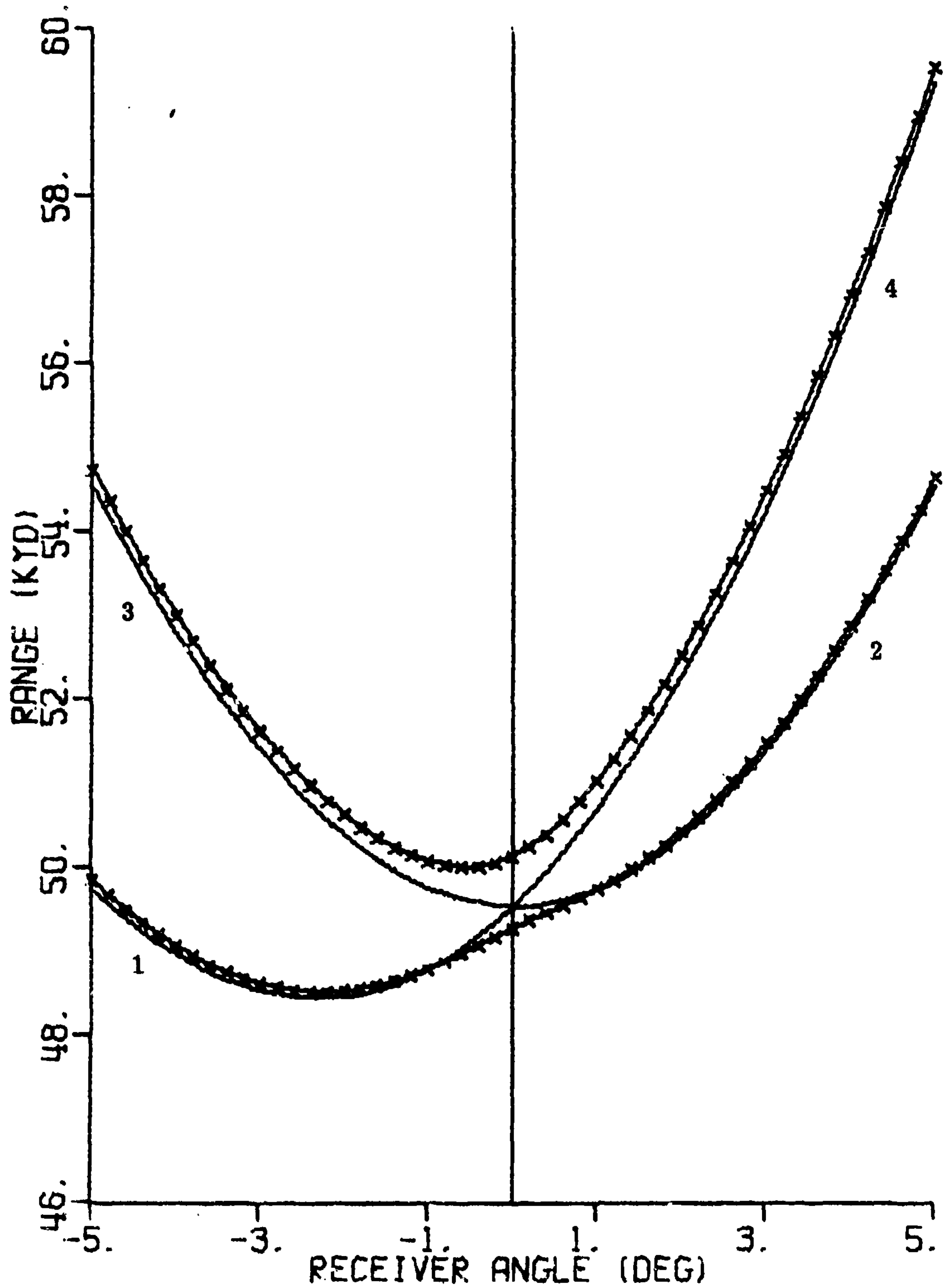

UNCLASSIFIED

(U) Figure 5-7. Range-angle Curves for Source and Receiver Separated by 0 Feet (———) and 10 Feet (***); Bi-linear Profile

result of this action there is a blank sector on either side of zero in source angle space, defined by the limiting ray to the receiver depth, within which no rays from the source can reach the receiver. If the data of Figure 5-7 are replotted as a function of source angle, the results appear as in Figure 5-8, which clearly shows the blank sector. If now a parabola is fitted to these curves, it covers a forbidden region. It is not obvious what effect this error has on the results, though clearly the effect must depend on the width of the forbidden sector. It will be seen, however, that an extreme case was found in Example 6 which led to a totally unreasonable propagation loss curve.

(U) A comment is in order at this point about the fitting of the parabola to the smooth caustic associated with a cusp when such a caustic is present. First of all it will be noted that while the cusp parabola is in source angle space, the smooth caustic parabola is in receiver angle space. Secondly, because the source and receiver are separated in depth, the actual position of the cusp does not lie on any of the range-angle curves computed from the rays. The cusp is assumed to be located midway between the points on branches 2 and 3 corresponding to the first ray of the sector, whose receiver angle is very close to zero. The smooth caustic lies on branch 1 or branch 4, depending upon whether it is a minimum- or maximum-range caustic. Consider a minimum range caustic such as that shown in Figure 5-7. If the minimum range occurs in one of the rays in the interior of the sector, there are three points to which the parabola can be fitted - the first and last rays of the sector and the ray with the minimum range. However, rather than using the first ray, FACT selects instead the cusp point (or, more exactly, its estimate of the cusp point). But note that because of the separation in depth of the source and receiver, the cusp does not lie on branch 1; it lies at a range intermediate between branches 2 and 3. This is an invitation to trouble. In cases where the minimum range occurs for the first ray of the sector, the first point and the minimum point are coincident and only two points are available for the fit. In this case the slope of the curve at zero degrees is used as the third condition. The slope is computed from a formula derived from the classic case where the source and receiver depths are identical. Use of the formula with the actual geometry where the source and receiver depths differ by 10 ft can result in a poor fit. Examples of both types of fit have been encountered in the current study and in virtually all cases the fit has been poor. In one instance the three-point fit was so bad that the minimum point of the parabola occurred at a negative range.

Why the Cusped Caustic Correction? (U)

(U) When the source and receiver depths are specified to be more than 10 ft apart, no cusped caustic correction is applied (unless as a result of the axial manipulations they are moved together, a feature with which the present discussion is not concerned). On the other hand, when the specified separation has <u>any value</u> less than 10 ft, the two depths are first moved together and then moved apart. As has been stated previously, the resulting separation is normally 10 ft, although in special cases it may be somewhat less. Let us ignore the special cases and assume the normal value of 10 ft.

(U) If we now imagine a set of runs to be made in which all inputs are held constant except the source depth and imagine that the depth separation between the source and receiver is initially, say, 20 ft and is then steadily reduced to zero, we see that there will be a continuous variation in the output until a separation of 10 ft is reached. At this point the cusped caustic correction takes over and some sort of discontinuity must occur. At all separations less than 10 ft there can be no change

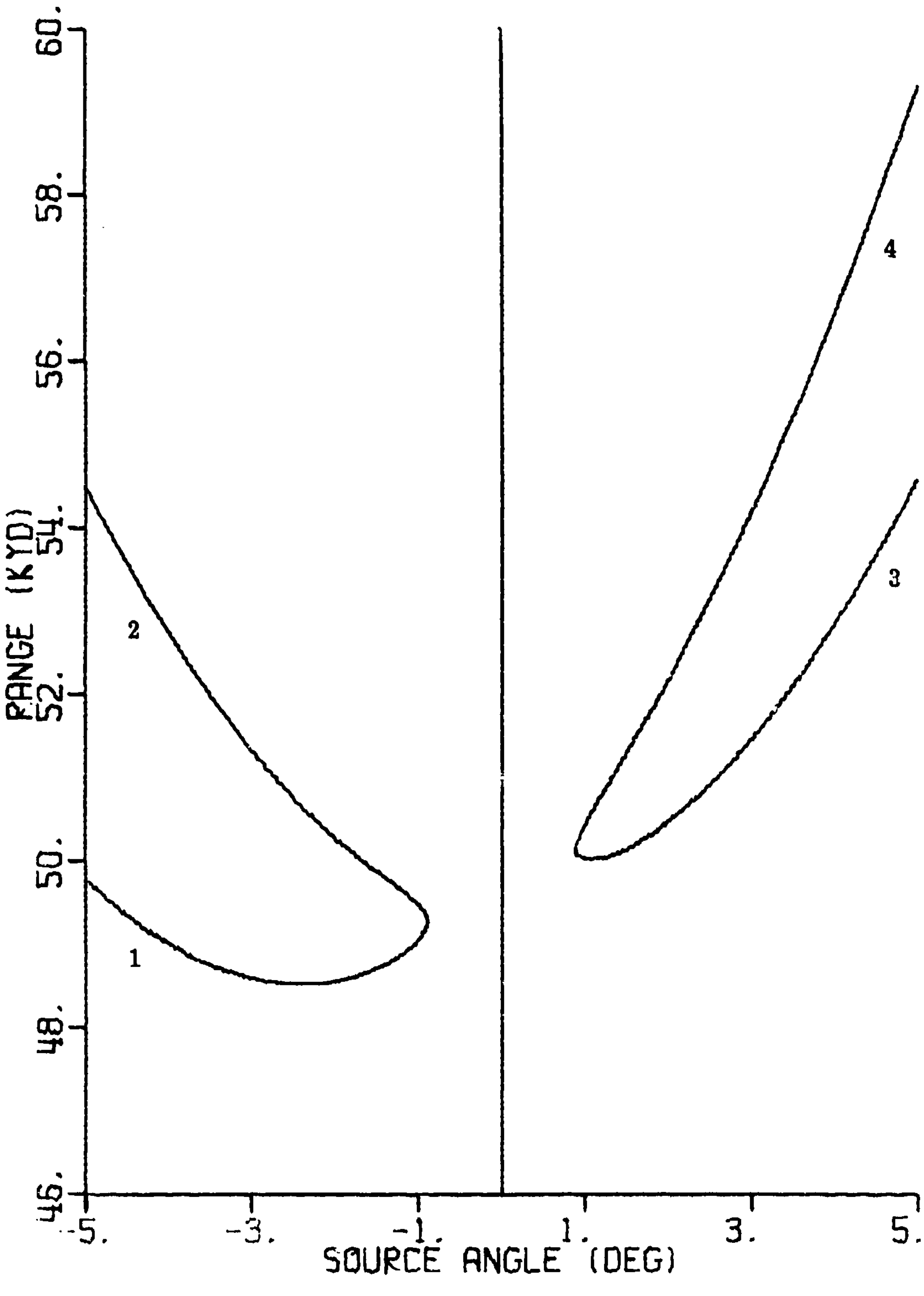

UNCLASSIFIED

(U) Figure 5-8. Range-angle Curves in Source Angle Space for Source and Receiver Separated by 10 Feet; Bi-linear Profile.

whatever in the output, since the altered source and receiver locations are constant, independent of the initially specified values. Hence the output is independent of the source depth.

(U) In Example 5 a test was made of the effect of the discontinuity by making two runs, one with a separation of 9.99 ft and the other with a separation of 10.01 ft. The effect of the discontinuity was quite noticeable but not drastic; whether it should be considered serious or not is probably a matter of judgment. However, the question at issue is the following. If the corrected and uncorrected results are considered to be equally valid at a separation of 10 ft and if no change in the corrected results occurs when the separation is less than 10 ft, what does the cusped caustic correction accomplish, other than a discontinuity at 10 ft? Would it not be just as valid to use the uncorrected 10-foot results as to use the corrected 10-foot results over this interval? Such an approach would simplify the computer program and avoid the difficulties discussed earlier in this section.

Low Frequency Cut-Off Effects (U)

(U) The subject of low-frequency cutoff effects is related to the problem of near-axial rays discussed previously. In subroutine AXIS a scheme is implemented whereby the source and receiver depths, if they are too close to the axis of a sound channel, are moved sufficiently far away to prevent the propagation of any rays with a period (cycle distance) less than a certain somewhat arbitrarily determined minimum value. This correction is independent of frequency. The low frequency cut-off feature is a further modification of ray theory involving frequency effects.

(U) Subroutine CRITA contains a procedure for estimating what is termed a frequency-dependent "critical angle". The critical angle is the angle (at the channel axis) of the ray equivalent to the first normal mode capable of propagating in the channel. The estimation is based on the WKB phase integral approximation, which states that the total phase change of the mode depth function in executing one complete cycle up and down between the mode during points must be one cycle (2 radians).

(U) The procedure for implementing this concept depends upon the extent in depth over which the ray travels, that is, upon the location of the ray vertex depths. If both vertex depths lie within the first profile layer on either side of the axis, the implementation is straightforward. However, if the ray path extends outward into other layers, the procedure is more complicated. The logic in the program proved difficult to understand.

(U) A careful check of the formulas involved in the critical angle computation (for the straightforward case) has revealed what appear to be several errors. First, for an internal sound channel the WKB phase integral condition for the first mode is expressed by FACT in the following form:

$$T - R/c_v = 3/4f,$$

where T and R are the ray travel time and horizontal range for one complete cycle, c_v is the ray vertex velocity, and f is the frequency. The correct formula appears to be

$$T - R/c_v = 1/2f.$$

The formula given for a surface channel appears to be correct.

(U) Secondly, the formula used by FACT for the critical angle of an internal channel (when the equivalent ray does not extend out into other layers) is

$$\theta_c = [f\ (1/g_1 + 1/g_2)]^{-1/3},$$

where g_1 and g_2 are the magnitudes of the gradients in the layers on either

side of the axis. The correct formula appears to be

$$\sin \theta_c = [(4/3)f\ (1/g_1 + 1/g_2)]^{-1/3}.$$

Since the critical angle is usually relatively small, the error in replacing the sine with the angle itself is probably negligible. A discrepancy was also found in the corresponding formula for the critical angle in a surface channel. Incidentally, the same surface channel formula is used for a bottom channel, implying a phase reversal there, as at the surface. No further investigation has been made of the low frequency cut-off effects at the surface or bottom.

(U) When the question arises about what to do about rays which propagate at angles shallower than the critical angle for the first normal mode, mode theory is of little help since no such phenomenon occurs there. The theory behind the FACT procedure is not understood. The procedure is as follows. After processing each ray arrival, INSTOR computes the angle θ_x of the ray at the channel axis and compares it with the critical angle θ_c. If θ_x exceeds the critical angle, no further action is necessary; otherwise a correction is applied to the intensity. If the critical ray does not extend beyond the boundaries of the layers adjacent to the channel axis, the correction factor can be written in simple closed form. It is

$$2 \sin^2 [0.75\,\pi(\theta_x/\theta_c)^3].$$

A plot of this function is shown in Figure 5-9. It will be noted that for value of the ratio θ_x/θ_c in excess of 1 the correction factor is 1. As the ratio drops below 1 the factor suddenly takes off in an increasing direction, reaching a value of 2 at a ratio of 0.874. Below this point it drops rapidly to zero. It is not clear why the intensity should climb to double its normal value when the ray falls into what should be a region of decay.

Bottom Loss (U)

(U) FACT contains internally two sets of bottom loss curves. One set applies to frequencies less than 1000 Hz and greater than 3500 Hz. The second set applies to frequencies in the range between these two values. The first set consists of 30 curves, broken down into 6 frequency bands with 5 FNOC bottom types for each frequency. The frequency bands are as follows:

0 - 150 Hz
150 - 300 Hz
300 - 700 Hz
700 - 1000 Hz
3500 - 4500 Hz
4500 - Hz

(U) The second set consists of 9 curves corresponding to 9 different bottom types.

(U) When the first set of bottom loss curves is used, no attempt is made to interpolate between frequencies. The bottom loss as a function of frequency is thus constant throughout each band and jumps discontinuously at the boundary between one band and the next. Discontinuities are undesirable in the model output.

(U) In the input data deck the bottom type is specified by a single parameter whose value is applicable to all the specified frequencies. This arrangement is satisfactory, providing the array of input frequencies is restricted to one set of curves or the other, but is unacceptable if both sets are involved; e.g., 900, 1000, 1100 Hz, since there is no correlation between, say, type 3 of one set and type 3 of the other.

(U) Associated with the bottom type numbers is an array of angles THETCR(I) which play a role in determining the source angle of the second (and last) ray computed in the outermost sector (NG = NGRPS). If the first set of bottom loss curves is examined, it is observed that most of them exhibit an interval of

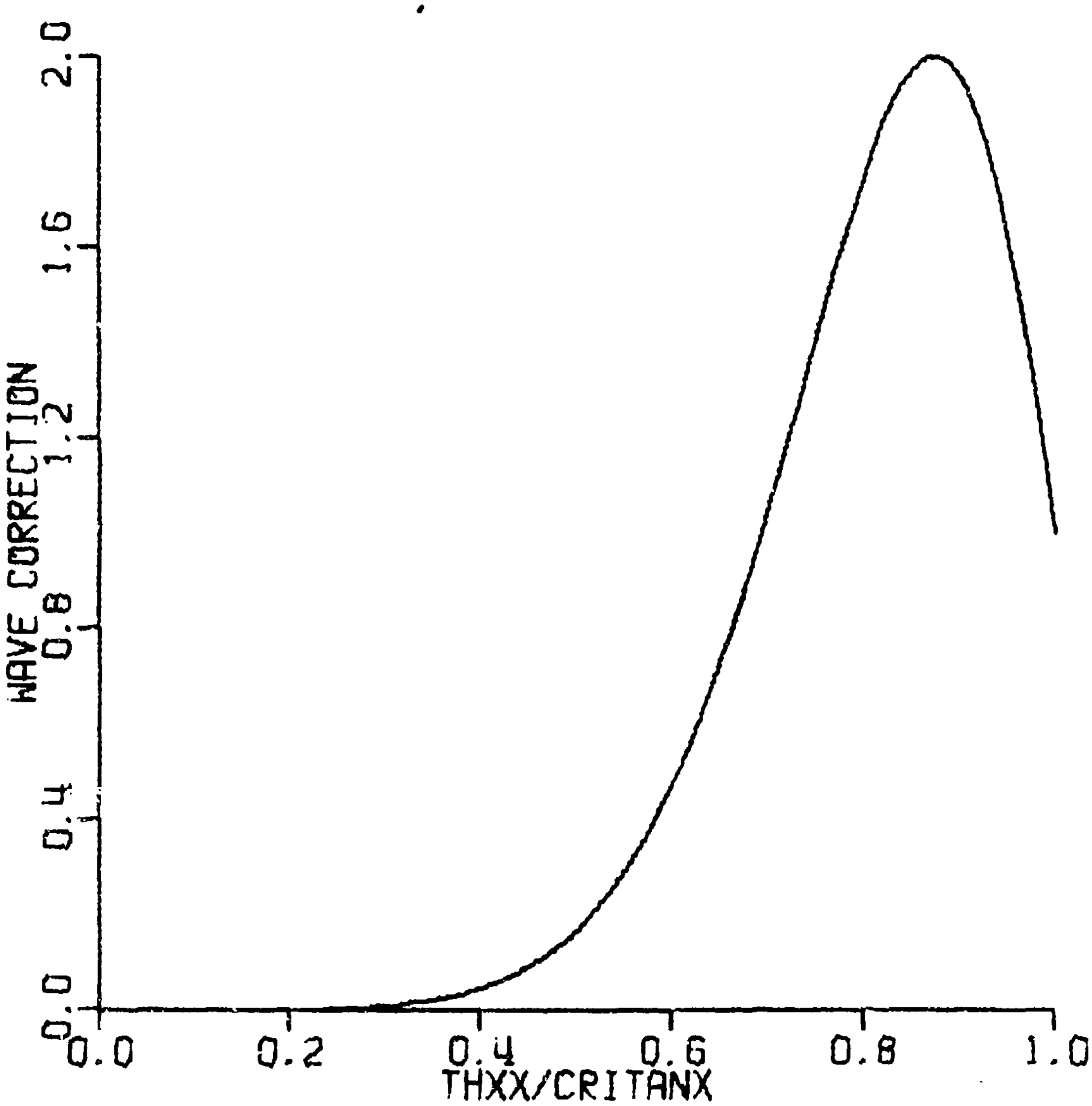

UNCLASSIFIED

(U) Figure 5-9. Low Frequency Wave Correction for Near-axial Rays.

low loss at small grazing angles, beyond which a rapid rise in loss takes place. The angle at which the rapid rise begins is suggestive of a critical angle. It is further observed that the critical angles of the curves corresponding to the lowest frequency band exactly match the first 5 values of THETCR. It is thus apparent that the THETCR array was set up to represent the critical angles of the bottom loss curves. It will be noted, however, that the correspondence is accurate only for the lowest frequency band of the first set of curves, and no obvious critical angles are apparent at all in the second set of curves.

(U) In view of the information gained from the examples, especially Example 3, it appears that more than two rays are required in the last sector. In lieu of the present arrangement in FACT it would be preferable to compute a family of a half dozen or so rays extending out in source angle to a fixed value of perhaps 20 or 30 degrees. Such a procedure would cost very little in running time, would significantly improve the accuracy of the results (avoiding the problem of Example 3), and would remove the dependence of the internal workings of the program on the characteristics of the bottom loss curves.

Ray Termination--Maximum Number of Cycles (U)

(U) The rules for breaking out of the arrival order loop, which processes one ray cycle after another, depend upon the sector. There is one basic rule, however, which is applicable to all sectors. If the maximum intensity of the arrivals at all of the range points covered by the rays of the sector falls below a value corresponding to a 150 dB loss, no further cycles are processed.

(U) In all sectors but the outermost the criterion for stopping is the minimum range of all the rays of the sector. As soon as this minimum exceeds the maximum range specified in the inputs, the processing is terminated.

(U) In the last sector the situation is different, since that sector includes all ray angles out to 90 degrees and hence all ranges down to the first. The rules call for at least 4 bottom bounces, unless, of course, the intensity criterion comes into play first. After 4 bottom bounces a flag is set and thereafter the steeper rays beyond the last ray computed are no longer included. This means that whenever the range of the last ray exceeds the maximum range specified by the user, the computations are terminated.

(U) The theory behind this logic appears to be based on the concept that the last ray computed strikes the bottom at the critical angle of the applicable bottom loss curve. The logic guarantees 4 bottom bounces at angles greater than this critical angle. There is some question whether 4 bounces are always enough. In an early version of the NADC ray model PLRAY the number of bottom bounces was limited to 4, but cases were found where more were needed. A brief investigation of this question was made in FACT by modifying the program to require a minimum of 8 instead of 4 bounces. A sample run with a low-loss bottom was made on both versions. Differences up to 1.7 dB were observed.

Surface Duct Model (U)

(U) Comments on the surface duct module will be limited, since this feature is not original with FACT and has been in use at FNOC, Monterey, for many years. One of its major limitations is that it does not include any depth dependence for the source and receiver other than a 10 dB reduction when the source and receiver are on opposite sides of the bottom boundary of the duct. A few comparisons have been made at relatively low frequencies among FACT, the AP2 normal mode model, and PLRAY, which contains a locally generated surface duct module with depth dependence included. Generally the surface duct modules of both ray models gave results which agreed reasonably well with each other

and with the normal mode output. In most real world environments, particularly at low frequencies, the effect of the surface duct is significant only at short ranges where it affects the rate of fall-off of intensity in the direct propagation zone. When the source and receiver are on opposite sides of the duct boundary the contribution of the ducted energy tends to be insignificant. (No runs were made in the kilohertz region.)

Half-Channel Module (U)

(U) This is a special purpose feature which can be used instead of ray computations whenever the sound speed increases monotonically from the surface to the bottom, i.e., the ocean is a half channel. It consists of a cylindrical spreading formula containing parameters which involve the frequency and the source, receiver, and ocean depths. No investigation has been made of it in the present study.

Arrival Structure Output (U)

(U) This feature has not been investigated except to note the following. (1) Because of the possible interchange of source and receiver, a flag (KRC) must be set to identify which end represents the true receiver. (2) When coherence is deemed possible, a single ray is computed in lieu of a pair of rays (ICOH = 1 or 2) or all four rays (ICOH = 3). Proper account of this fact must be taken in determining the arrival structure.

Examples (U)

Introduction (U)

(U) Inasmuch as the examples investigated in this study were for the most part encountered accidentally in the course of routine work on other projects, and since many of them illustrate not one but several features of the FACT model, it is impossible to fit them neatly into any coherent classification scheme. For this reason it may be well to begin with a concise summary, stating in brief the principal contributions of each to an understanding of the physics of the FACT Model.

Example 1. (U) Provides an example of poor curve-fitting of range-angle parabolas, leading to erroneous caustic corrections.

Example 2. (U) Illustrates the method by which the amplitude reduction technique is applied to the surface imaging interference pattern in cases of inadequate range sampling.

Example 3. (U) Illustrates the inadequacy of computing only two rays in the outermost source angle sector. Poor curve fitting results in erroneous ray intensities and in distortions of the coherent interference pattern. Provides an example of undesirable suppression of coherence computations.

Example 4. (U) Illustrates the deficiencies of the cusped caustic procedure and that of the associated smooth caustic. Provides another example of undesirable suppression of coherent interference pattern.

Example 5. (U) Examines two runs with receiver depths differing by 0.01 ft, showing effect of moving source and receiver depths. Provides an example of suppression of one set of arrivals due to error in parameter RCUT.

Example 6. (U) Generates excessive changes in source and receiver depths. Exceedingly poor range-angle curve fitting generates very bad caustic corrections. Provides an example of false caustic generated by parabola of square root type (vertex occurring in negative square root region).

Example 7. (U) Large changes in output result from interpolating one extra point in velocity profile. Provides

examples of gross errors in range-angle curve fitting.

Example 8. (U) Profile exhibits modified type of surface duct with negative gradient at surface and local minimum at bottom of first layer. Runs made with and without use of surface duct module yield widely different results. Runs made in each case with two receiver depths differing by 0.1 ft show drastic effects caused by shifting of source and receiver depths. Sawtooth pattern in propagation loss curves caused by insufficient number of bottom bounces. False caustic generated as in Example 6.

Example 9. (U) Investigates effect of subsurface channel as a function of frequency with source in channel and receiver (1) in channel and (2) above channel.

Example 10. (U) Investigates cause of previously reported discrepancies in propagation loss at 700 Hz between two runs, one made at 700 Hz only and the other at two frequencies, 700 and 300 Hz.

Example 1 (U)

(U) This example was accidentally encountered in the process of making a set of routine predictions for a number of different ocean areas. The velocity profile, shown in Figure 5-10, is from the North Pacific. The bottom loss was a constant 6 dB at all grazing angles. The source was located at a depth of 300 ft, the receiver at 1000 ft, and the frequency was 50 Hz. The predicted semicoherent propagation loss curve, shown at the top of Figure 5-11, looked so strange that runs were made on two NADC programs--PLRAY, a ray model similar in many respects to FACT, and AP2, a normal mode program capable of accepting the same environmental inputs. As may be seen in Figure 5-11, the results of both NADC programs are in fair agreement. In particular, both exhibit a pair of double convergence zones having a reasonably normal appearance. It is the shape of the FACT convergence zones which raised the suspicion of trouble.

(U) With the aid of the diagnostic print statements inserted for this purpose into the NADC version of FACT, the cause of the trouble has been identified. The convergence zones are formed by the rays of the first sector. These are RR rays confined to the depth interval extending from the layer boundary at 98.4 ft on the upper side to the corresponding image depth (approximately 7715 ft) on the lower side. Curves of range vs. receiver angle for the rays of the first sector are shown in Figure 5-12. These are the scallopy curves with peaks at ± 5.3 degrees and dips around ± 6 degrees. Incidentally, FACT does not compute enough rays to define these curves adequately for plotting. Fortunately the data for the curves could be obtained from the old NADC Ray-Tracing Program [6] which includes, among its numerous options, the fitting of the velocity profile with straight-line segments and the specification of families of rays by their source angles. The dips in the range-angle curves around 6 degrees are caustics generated by the kink in the profile at the layer boundary at 4921 ft. FACT smooths the irregularities in the curves by fitting parabolas with tan θ as the independent variable. From the coefficients tabulated in the diagnostic output the parabolas were calculated and are shown as the smooth curves in Figure 5-12. The caustics which form the FACT convergence zones are generated by the minima which occur in the parabolas near zero degrees. In this example it is seen that the parabolas are rather poor fits to the true curves. The caustic corrections are determined by the characteristics of the curves in the vicinity of their minima. The two characteristics of principal interest are the angle at which the minimum occurs and the second derivative of range with respect to angle. The intensity varies as $(r''^2/\sin\theta_R)^{1/3}$, while the scale factor which determines the extent in range of the Airy function varies as $(r''/\sin^2\theta_R)^{1/3}$, where r" is the

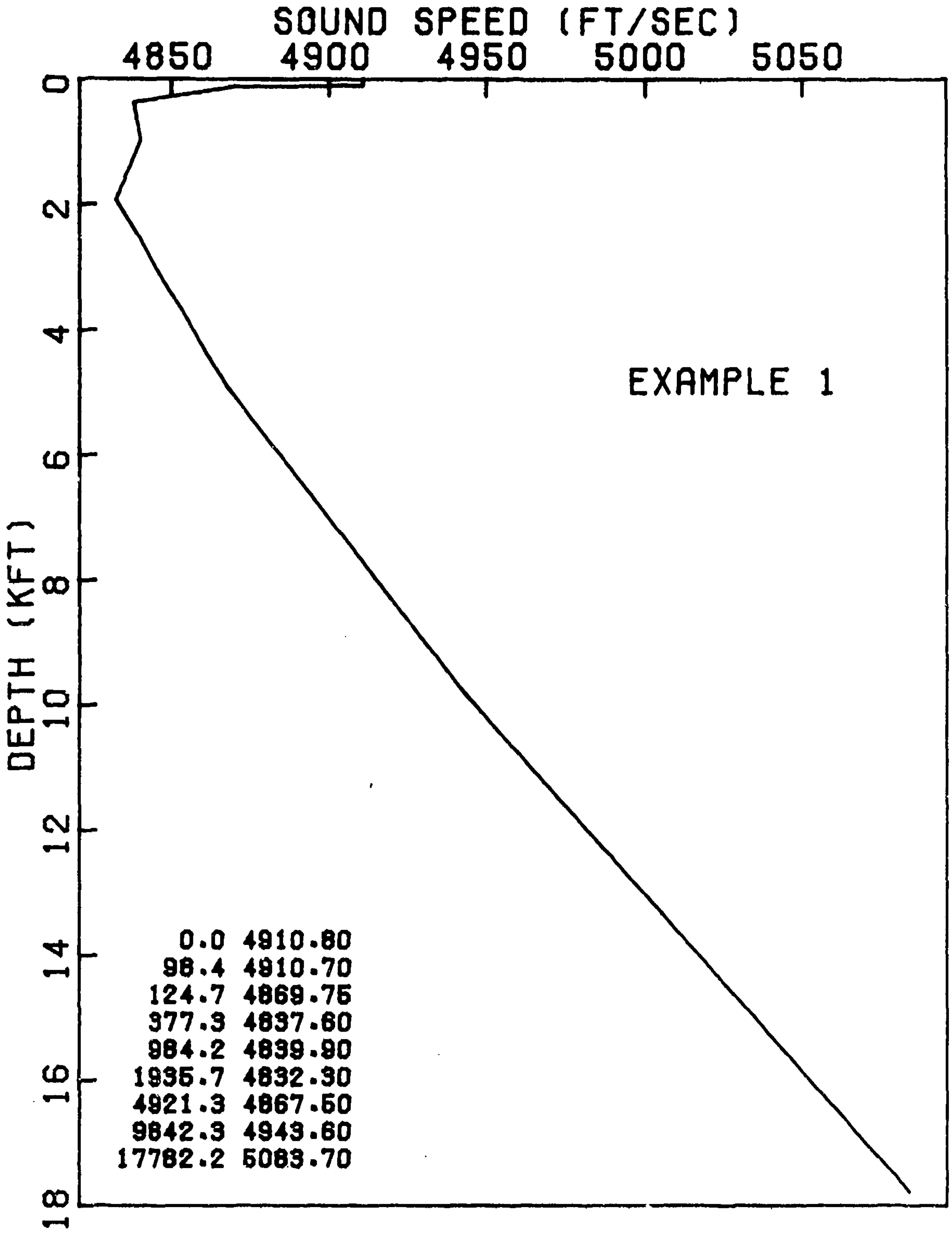

UNCLASSIFIED

(U) Figure 5-10. Sound Speed Versus Depth Profile, Example 1.

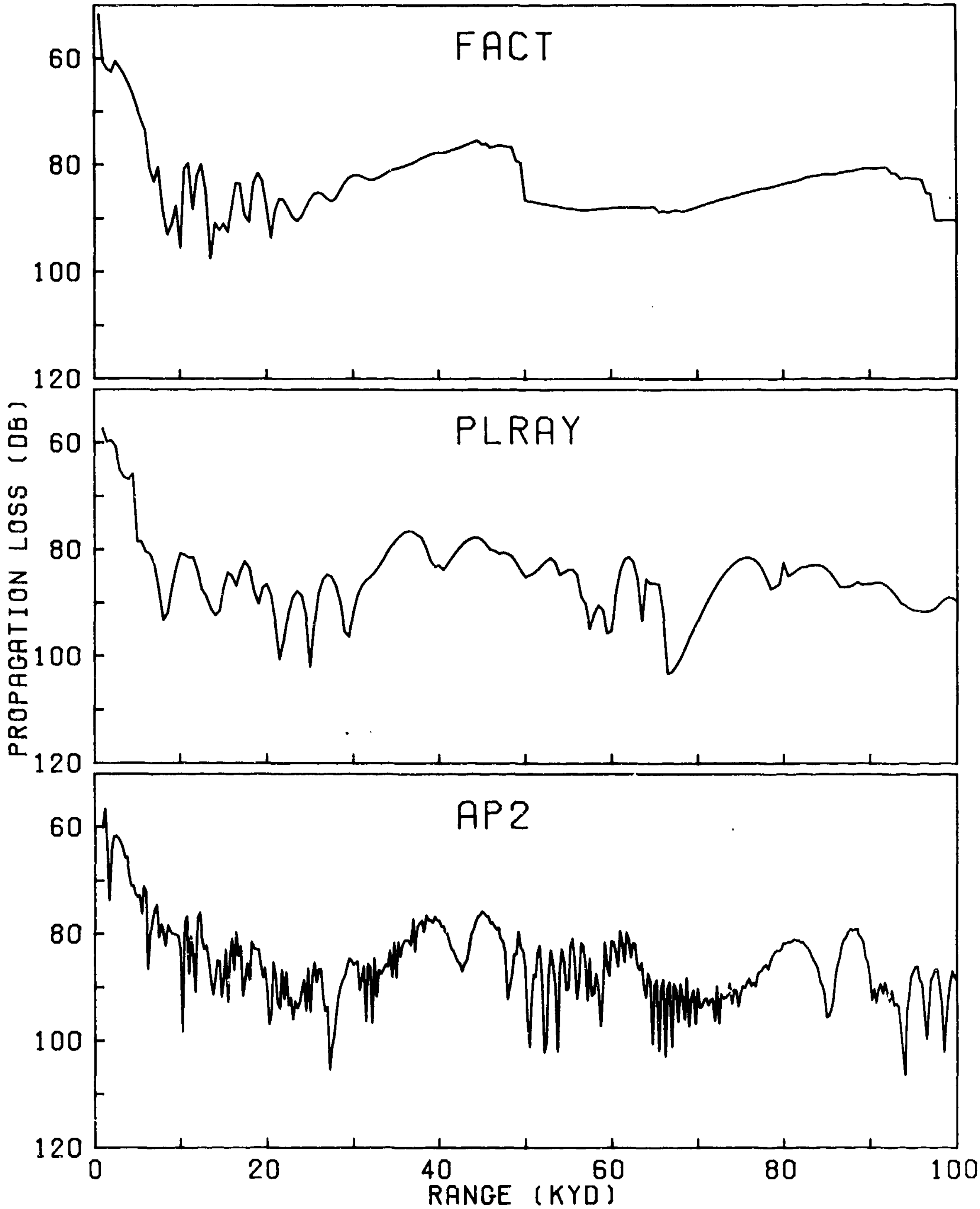

UNCLASSIFIED

(U) Figure 5-11. Propagation Loss, Example 1.

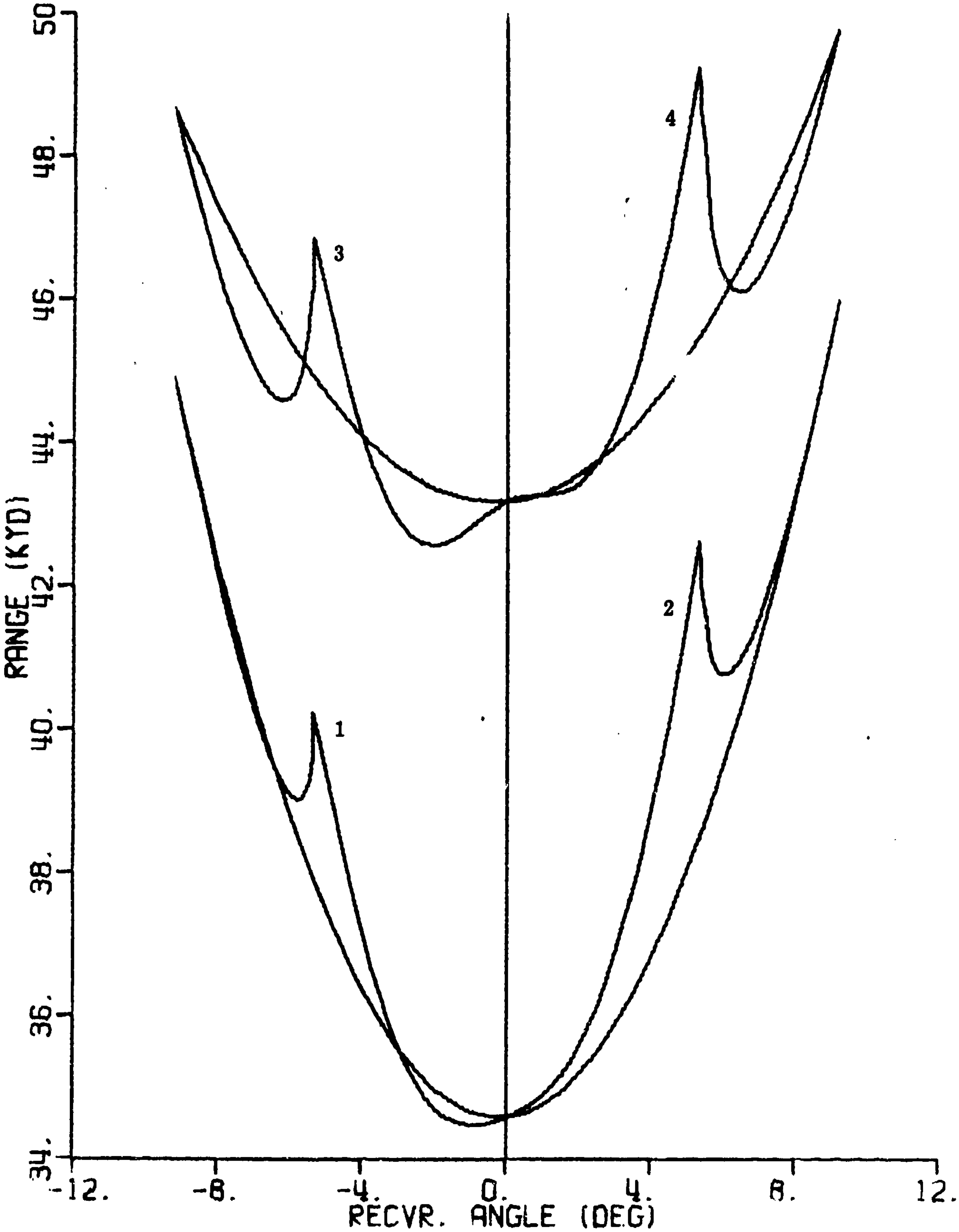

UNCLASSIFIED

(U) Figure 5-12. Range-angle Curves, Example 1.

second derivative of range with respect to angle and θ_R is the angle at the receiver. From Figure 5-12 it is clear that the values of both r" and θ_R derived from the parabolas are too small.

(U) To aid the interpretation of these errors the contributions of the caustic corrections for the first two convergence zones are superimposed on the FACT propagation loss curve in Figure 5-13. It is obvious that the strange shape of the curve is a direct result of the caustic corrections. Comparison with the results of the PLRAY and AP2 runs in Figure 5-11 shows that the intensity predicted by the FACT caustic corrections is about right but the range scale of the Airy function is much too large. From this observation it appears that the errors in r" and θ_R approximately compensate each other in the ratio $r''^2/\sin \theta_R$ but result in a gross error in the ratio $r''/\sin^2\theta_R$.

Example 2 (U)

(U) This example illustrates the effect of the algorithm employed in FACT to cut down the amplitude of the interference oscillations in semi-coherent runs when the range increment specified by the user is too large to provide adequate sampling of the true curve. This example was encountered accidentally when making comparison runs between FACT and PLRAY for the PLRAY report. This run was made at 300 Hz on the Pacific Ocean profile shown in Figure 5-14 with an FNOC Type 3 bottom. The source was located at a depth of 300 ft and the receiver at 1000 ft. The range increment was 500 yards.

(U) Plots of propagation loss vs. range are shown in Figure 5-15. It will be noted that FACT shows a constant amplitude of the interference oscillations throughout the bottom bounce region, whereas PLRAY shows oscillations whose amplitude is virtually zero at short ranges and builds up to large values at the longer ranges. The concept behind the FACT amplitude reduction is that when the number of specified range points per cycle of oscillations is greater than 6, the sampling is considered adequate and no reduction is effected. On the other hand, when the number of points per cycle is less than 2-2/3, the sampling is considered to be totally inadequate and the amplitude is cut to zero, yielding in effect incoherent addition. If the number of points per cycle is intermediate between these two limiting values, the amplitude is multiplied by a reduction factor which varies from 1 to 0.

(U) In the FACT model the number of points per cycle is computed as an average over the entire range interval covered by the rays of the particular sector under consideration. However, in the bottom bounce region of this example the number of points per cycle varies drastically with range. The interference pattern is associated almost totally with the 300-foot source depth since the oscillations associated with the 1000-foot receiver depth are too rapid for adequate sampling over almost the entire range interval. Since the diagnostic output available with PLRAY yields the actual phase angle at each range point, it is possible to obtain the number of points per cycle as a function of range.* Figure 5-16 shows a curve of this function over a range interval from 5 to 45 kyd. It will be seen that the number of points per cycle varies from a minimum of about 1.7 at short ranges to a huge value of over 11 at 45 kyd. FACT in this example computed an average value of 4.34 (shown by the tic mark) yielding a constant reduction factor of approximately 0.5 across the board. As a result, the propagation loss curve shows extremely choppy behavior at short ranges where the true curve is grossly undersampled and very smooth oscillations of reduced amplitude at long ranges where the true curve could have been adequately represented.

*The actual number of points per cycle is computed by PLRAY but is not available in the diagnostic print-out.

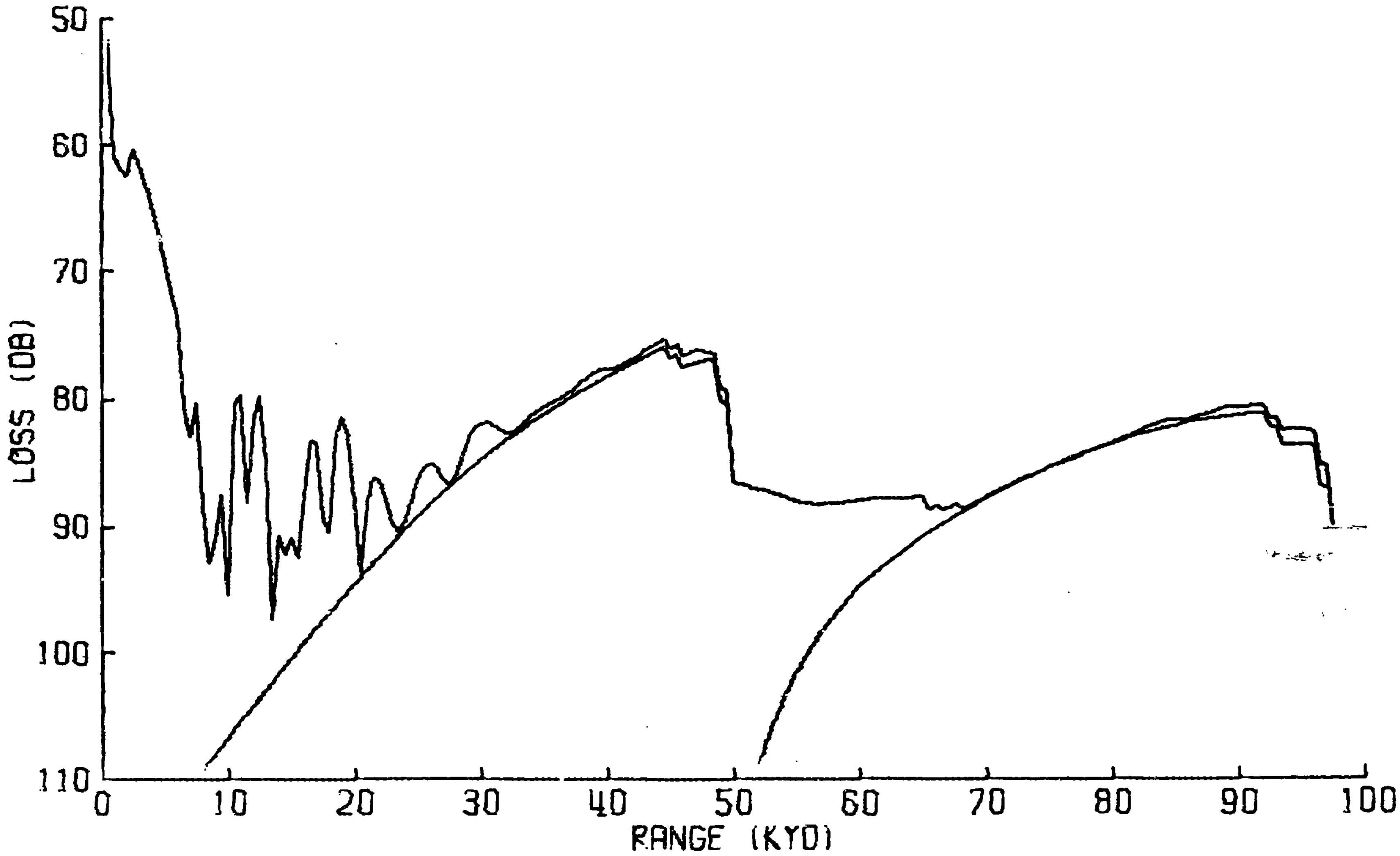

UNCLASSIFIED

(U) Figure 5-13. Contributions of Caustics, Example 1.

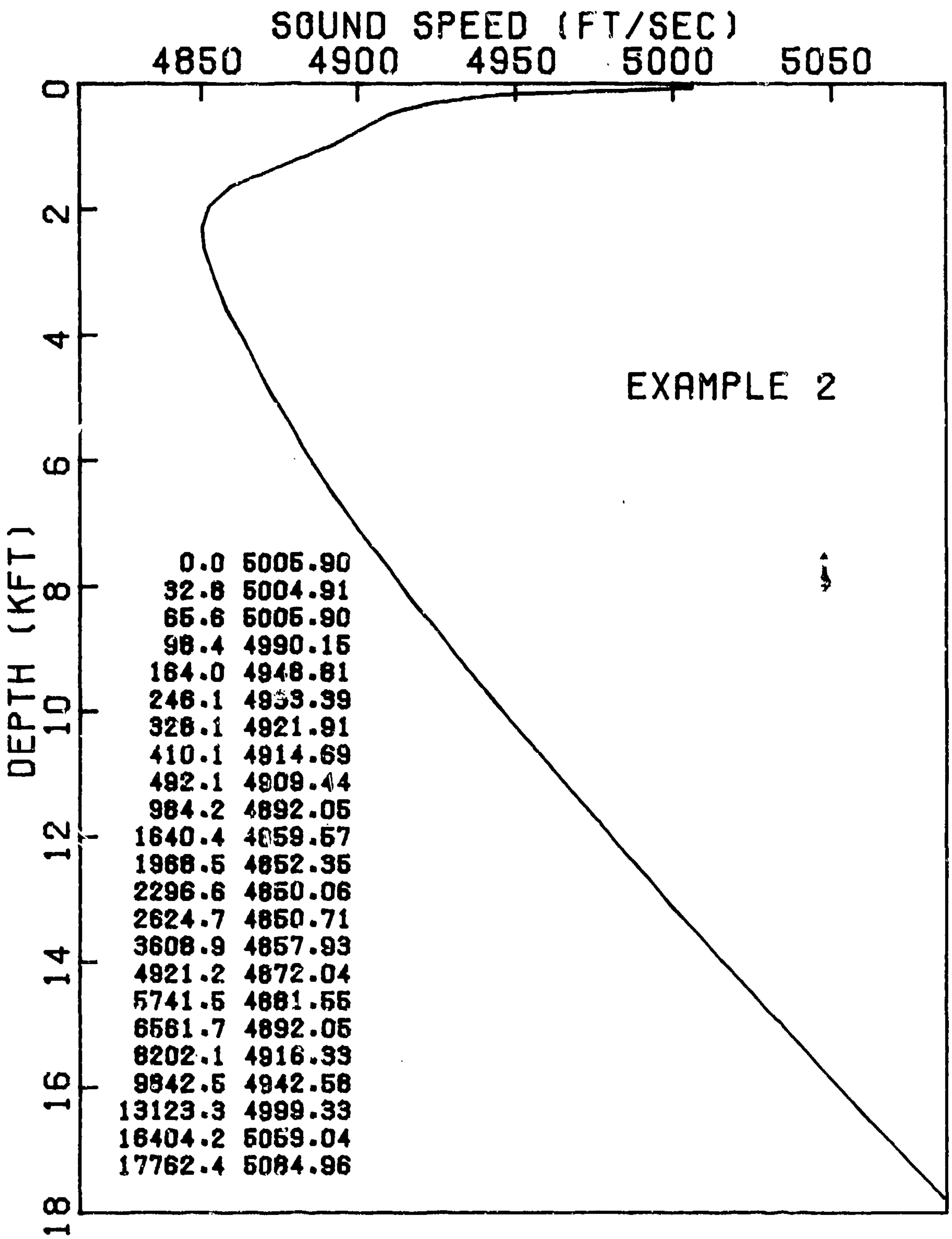

UNCLASSIFIED

(U) Figure 5-14. Sound Speed Versus Depth Profile, Example 2.

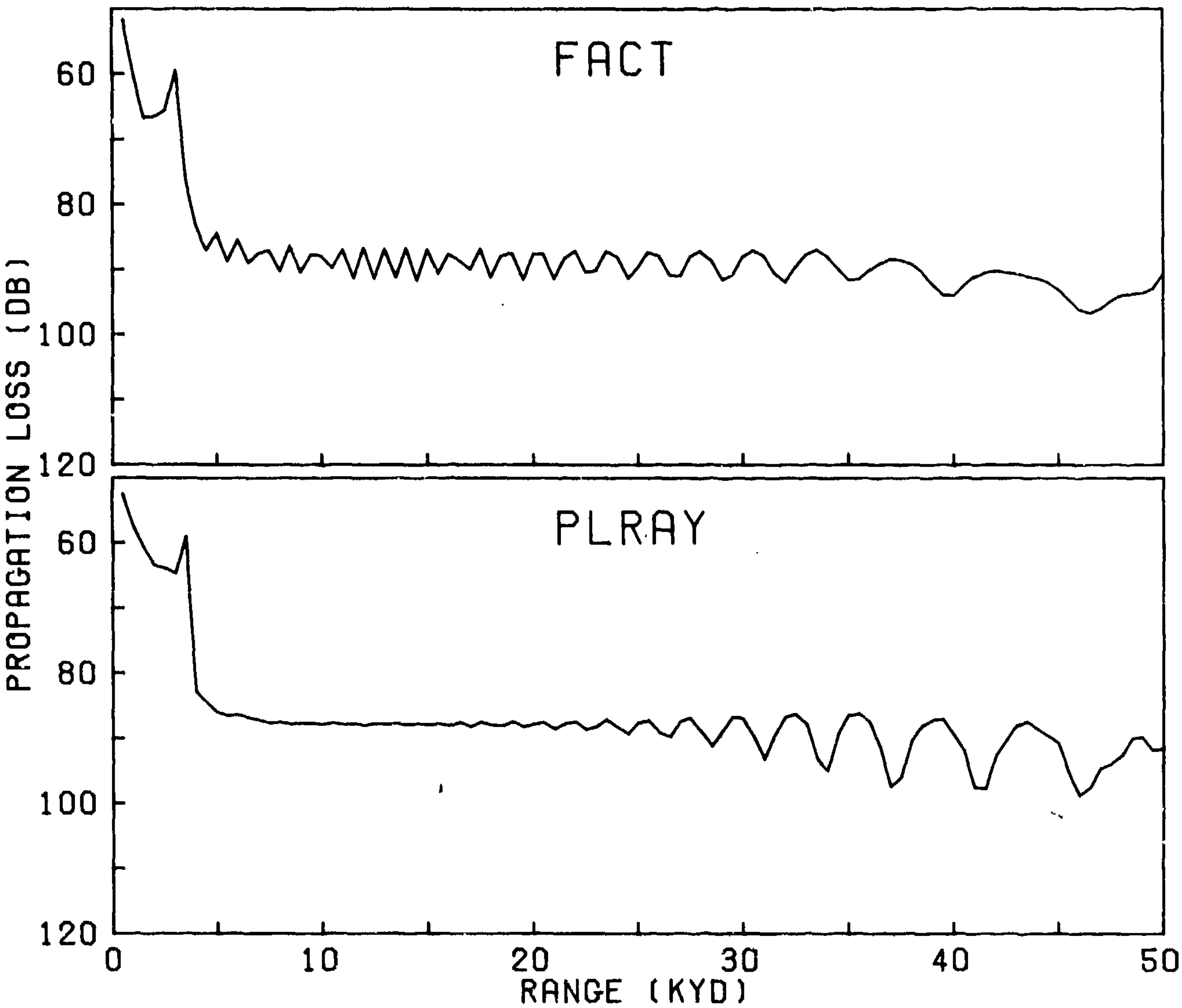

UNCLASSIFIED

(U) Figure 5-15. Propagation Loss, Example 2.

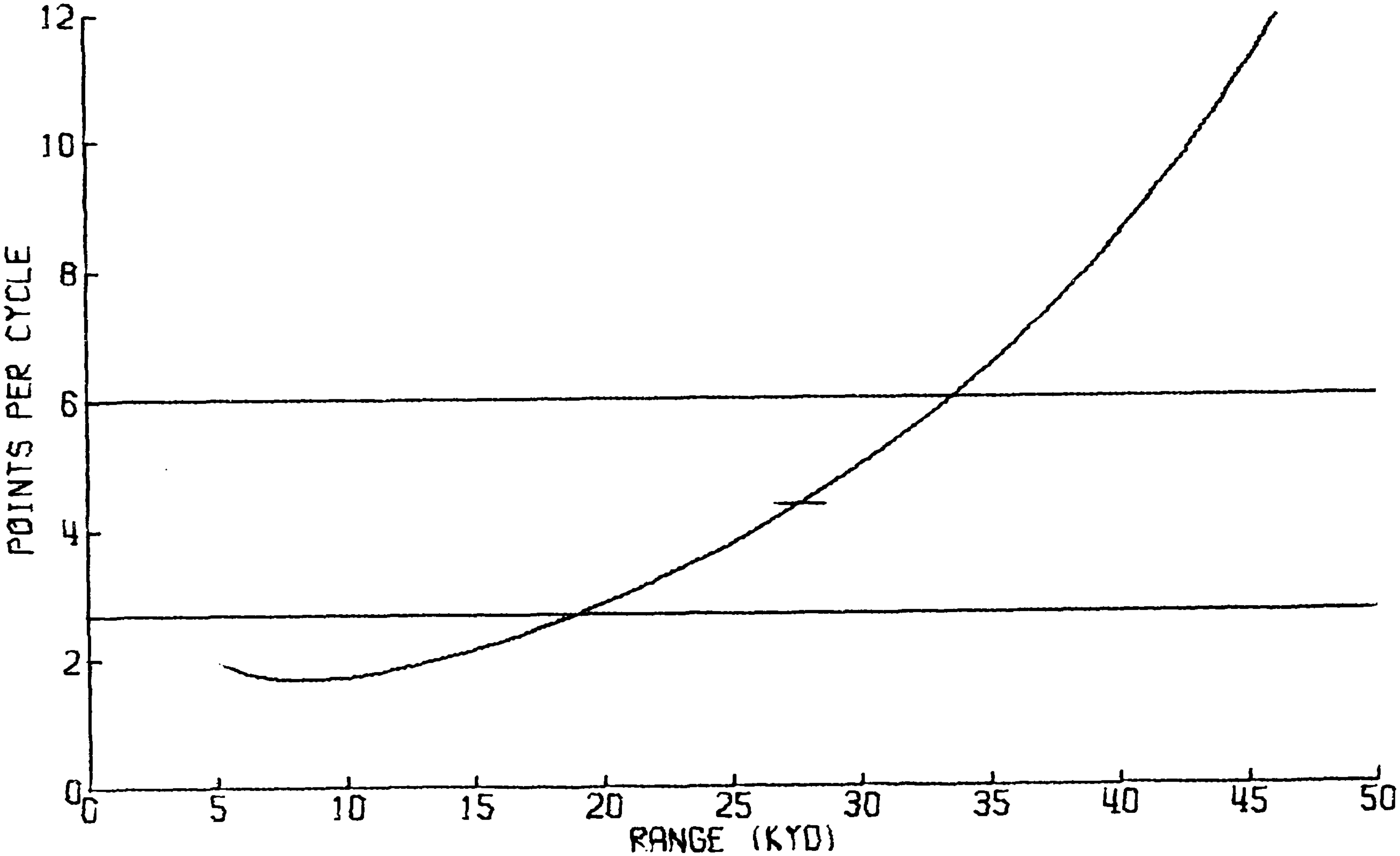

UNCLASSIFIED

(U) Figure 5-16. Number of Range Points per Phase Cycle of Interference Pattern, Example 2.

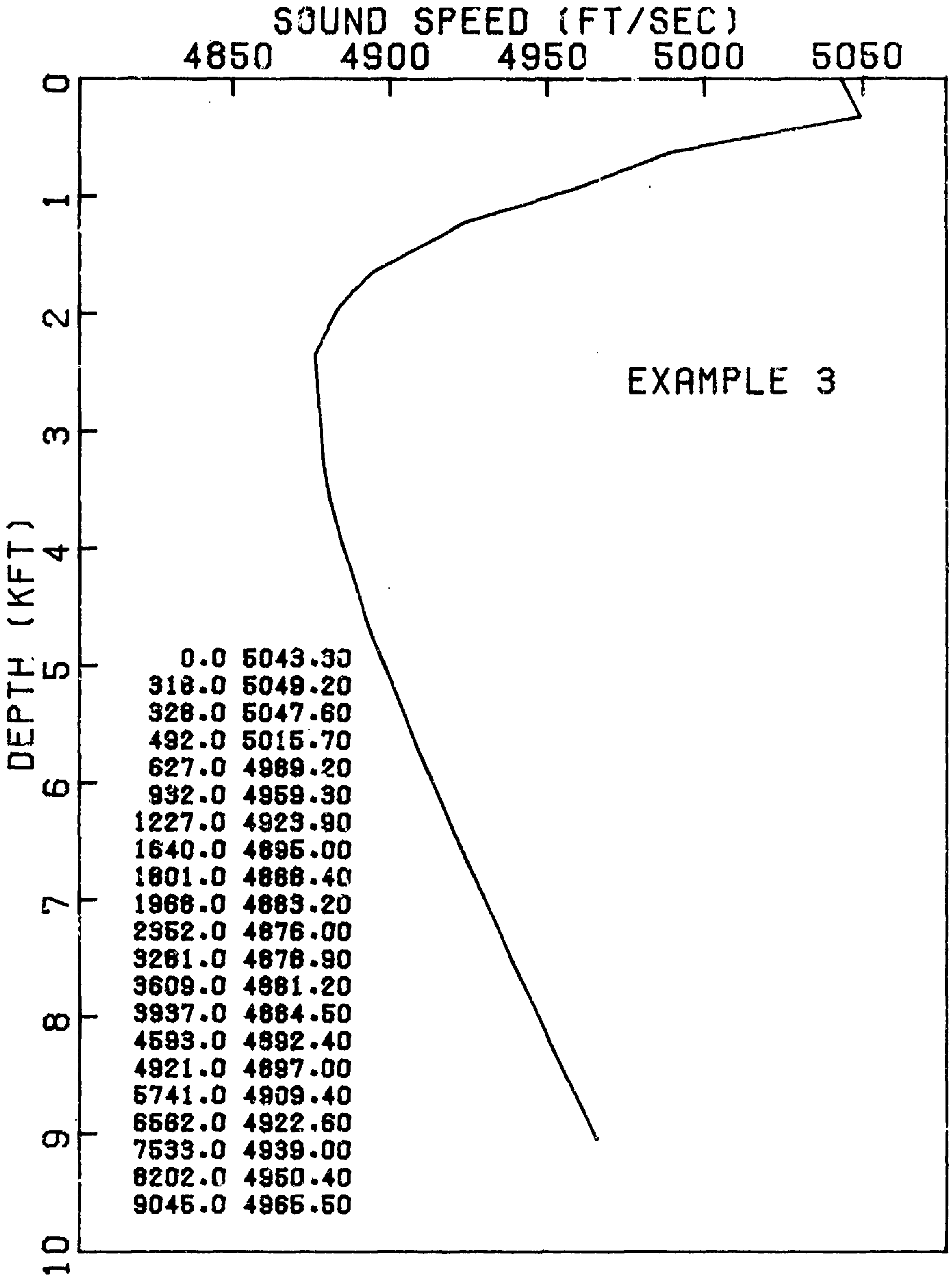

UNCLASSIFIED

(U) Figure 5-17. Sound Speed Versus Depth Profile, Example 3.

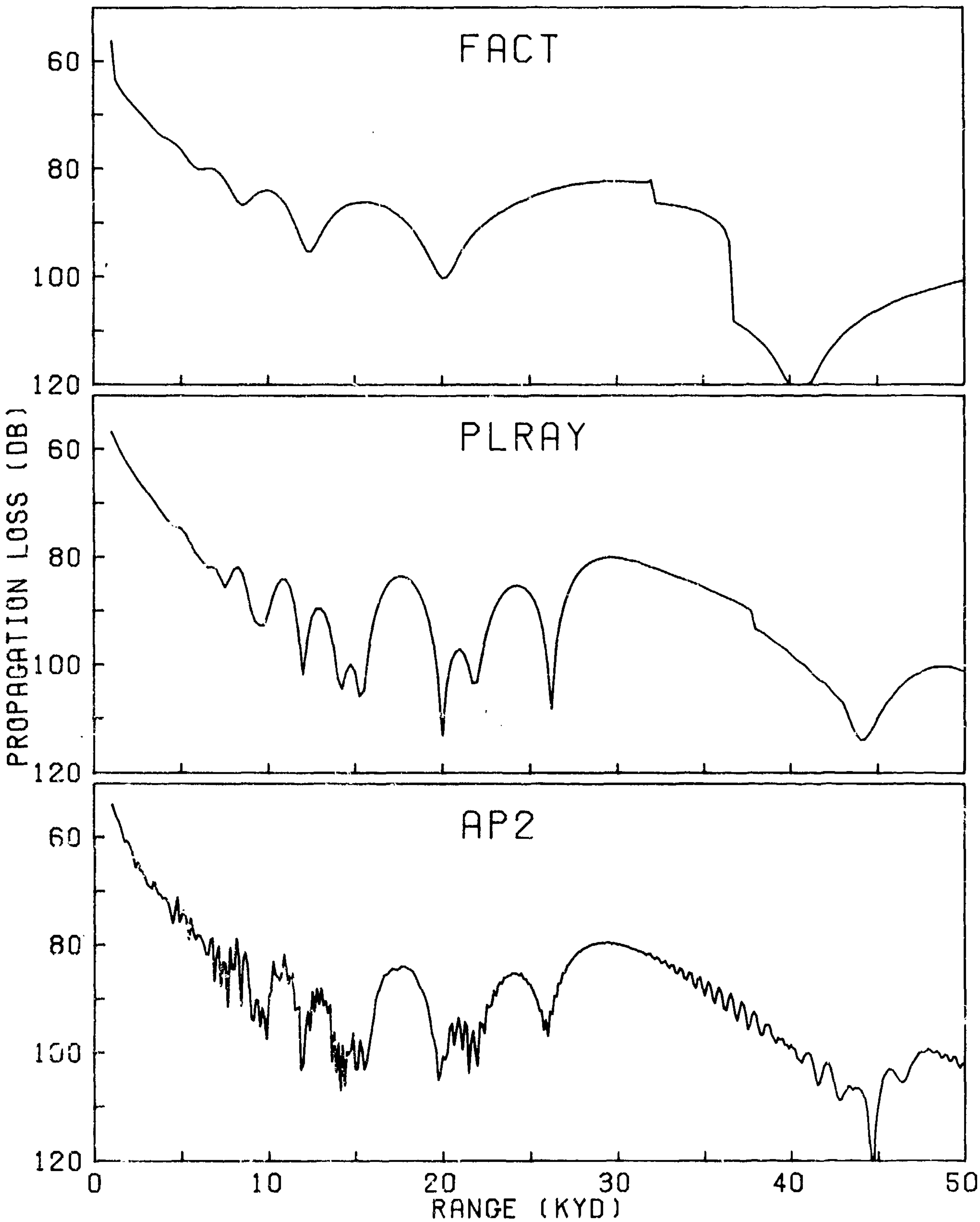

UNCLASSIFIED

(U) Figure 5-18. Propagation Loss, Example 3a.

(U) PLRAY on the other hand contains an algorithm which computes the instantaneous number of points per cycle from an analytic formula at each range. Application of the algorithm leads to the amplitude variation shown in Figure 5-15. Incidentally, at about 50 kyd the number of points per cycle associated with the receiver depth pattern begins to rise into the transition region and the effect of those oscillations can be seen at the right hand edge of the PLRAY propagation loss curve.

(U) It will be noted in the FACT output that the interference pattern is quite well represented at ranges down to about 25 kyd. Reference to Figure 5-16 reveals that the number of points per cycle at that range is less than 4. This observation suggests that the figure of 6 points per cycle, where the amplitude reduction begins, may be somewhat too conservative. A figure of 4 may be adequate.

(U) One other characteristic of the FACT model is illustrated in this example. The average level of the FACT propagation loss curve in the bottom bounce region is somewhat higher than that of PLRAY. The reason for the discrepancy is that when the frequency is intermediate between the frequencies of the two adjacent bottom loss curves, PLRAY interpolates the loss linearly between the two frequencies, whereas FACT does not. The two frequencies in this case are 100 and 500 Hz and FACT uses the curve for 500 Hz.

<u>Example 3</u> (U)

(U) This example from the Caribbean Sea was originally chosen to compare the surface duct modules of FACT and PLRAY for the PLRAY report. The velocity profile (Fig. 5-17) contains a sizeable surface duct of 328 ft and two sets of runs were made, both with the source at 250 ft in the duct. In one set the receiver was also in the duct at 150 ft and in the other the receiver was below the duct at 450 ft. An FNOC Type 5 bottom was used. Here we shall consider the pair of runs made at a frequency of 100 Hz. The surprising feature of these runs was the strange behavior of FACT at the longer ranges beyond the interval of interest for the surface duct modules.

<u>Example 3a</u> (U)

(U) Let us first consider the 150-foot case. The propagation loss for FACT, PLRAY, and AP2 is shown in Figure 5-18. The agreement between PLRAY and AP2 is quite good, suggesting that both are producing results consistent with the inputs. FACT, however, shows an entirely different interference pattern.

(U) Examination of the diagnostic output revealed the surprising discovery that FACT computes only two rays to generate the entire output (except for the surface duct module which produces measurable contributions out to the dip at 12.5 kyd). Since surface duct module replaces ray computations in the duct and since the profile is bottom limited with the sound speed at the bottom less than at the source and receiver, FACT generates only one sector. In this, the outermost sector, FACT computes two rays, the first having a source angle just beyond that of the limiting ray to the bottom and the second having a bottom grazing angle 5 degrees steeper than the first.

(U) To obtain the propagation loss FACT performs the amazing feat of fitting both a parabola

$$r = a_1 + a_2x + a_3x^2$$

where

r = horizontal range

x = $\theta - \theta_1$

θ = angle at receiver

θ_1 = angle at first ray of the sector

and the steep angle formula

$$r = 1/(a_4 \tan\theta + a_5)$$

to the two range-angle and one additional bit of information regarding the behavior in the vicinity of 90 degrees. For proper behavior near the vertical the coefficient a_4 is set equal to the total vertical distance traveled by the ray between source and receiver. The coefficient a_5 is then evaluated at the second ray (r_2, θ_2). The tangent formula is used for angles steeper than θ_2. The parabola is then fitted at the points (r_1, θ_1) and (r_2, θ_2) and joins the steep angle curve at (r_2, θ_2) with continuous slope.

(U) The resulting curves are shown in Figure 5-19. There are only two of them because the FACT coherence criterion decided that coherence occurred at the 150-foot depth but not at the 250-foot depth. (This matter will be discussed below in Example 3b.) Also, it should be noted that because the sound speed is less at 150 ft than at 250 ft, FACT has interchanged the definitions of source and receiver. The receiver angle in Figure 5-19 is the angle at 250 ft. The plain curves in Figure 5-19 represent the true range vs. receiver angle and were drawn with the aid of data from the NADC Ray-Tracing Program. The curves fitted by FACT are marked with x's. These curves are all that FACT remembers about the rays it has computed. At each specified receiver range it goes to the curves to find the ray angle and the range derivative, the latter being the dominant factor in computing ray intensities. An error in the angle is usually less serious in the computation of intensitites than an error in the range derivative, but where coherence is involved it has an important bearing on the interference pattern.

(U) The parabolas* in Figure 5-19 extend out to 6.85 degrees, beyond which the steep angle formulas apply. Inspection of the curves reveals significant differences from the true curves. The parabola on the negative side, for example, actually passes through a maximum before dropping off at steeper levels. To ascertain whether the erroneous shapes of the fitted curves might be responsible for the discrepancies in the interference pattern relative to PLRAY and AP2, the following check was made: At each receiver range between 5 and 25 kyd the coherence factor was read from the diagnostic output and the angle was obtained from the fitted curves. Then the true range corresponding to this angle was obtained by interpolating along the true curve. Finally the coherence factor was plotted first against the FACT range and then against the true range. The results for both sets of curves are shown in Figure 5-20. Here it will be seen that the two patterns have a noticeably different appearance. Differences as large as 2 kyd occur. Unfortunately it is not possible to create a reconstruction to compare with the two NADC outputs because of the failure of FACT to compute coherence at the receiver (true source) end.

(U) A discussion of the effect of slope errors on the computed spreading loss will be deferred to Example 3b.

Example 3b (U)

(U) In Example 3b the receiver was at 450 ft. Since this depth has the smaller sound speed, FACT treats it as the source depth. A plot of propagation loss for this case is shown in Figure 5-21. The eye-catcher here is the total absence of an interference pattern, even though a semi-coherent run had been requested, whereas both PLRAY and AP2 clearly exhibit patterns with roughly similar features.

(U) To investigate this problem it was necessary to exercise the old NADC Ray-Tracing Program to augment the almost non-existing ray computations of FACT. The horizontal separation between the

*They are parabolic in $\sqrt{\theta - \theta_1}$ space.

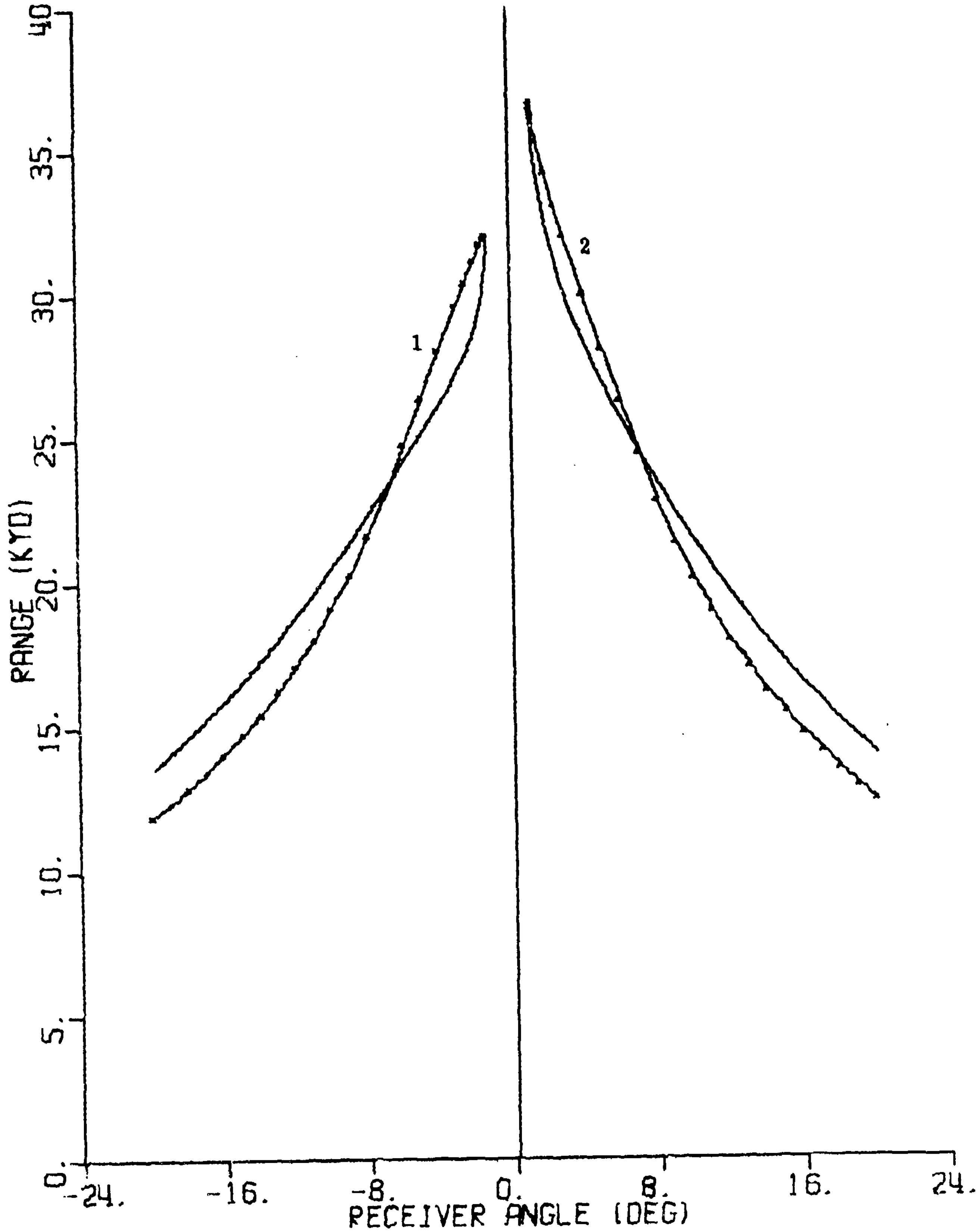

UNCLASSIFIED

(U) Figure 5-19. Range-angle Curves, Example 3a.

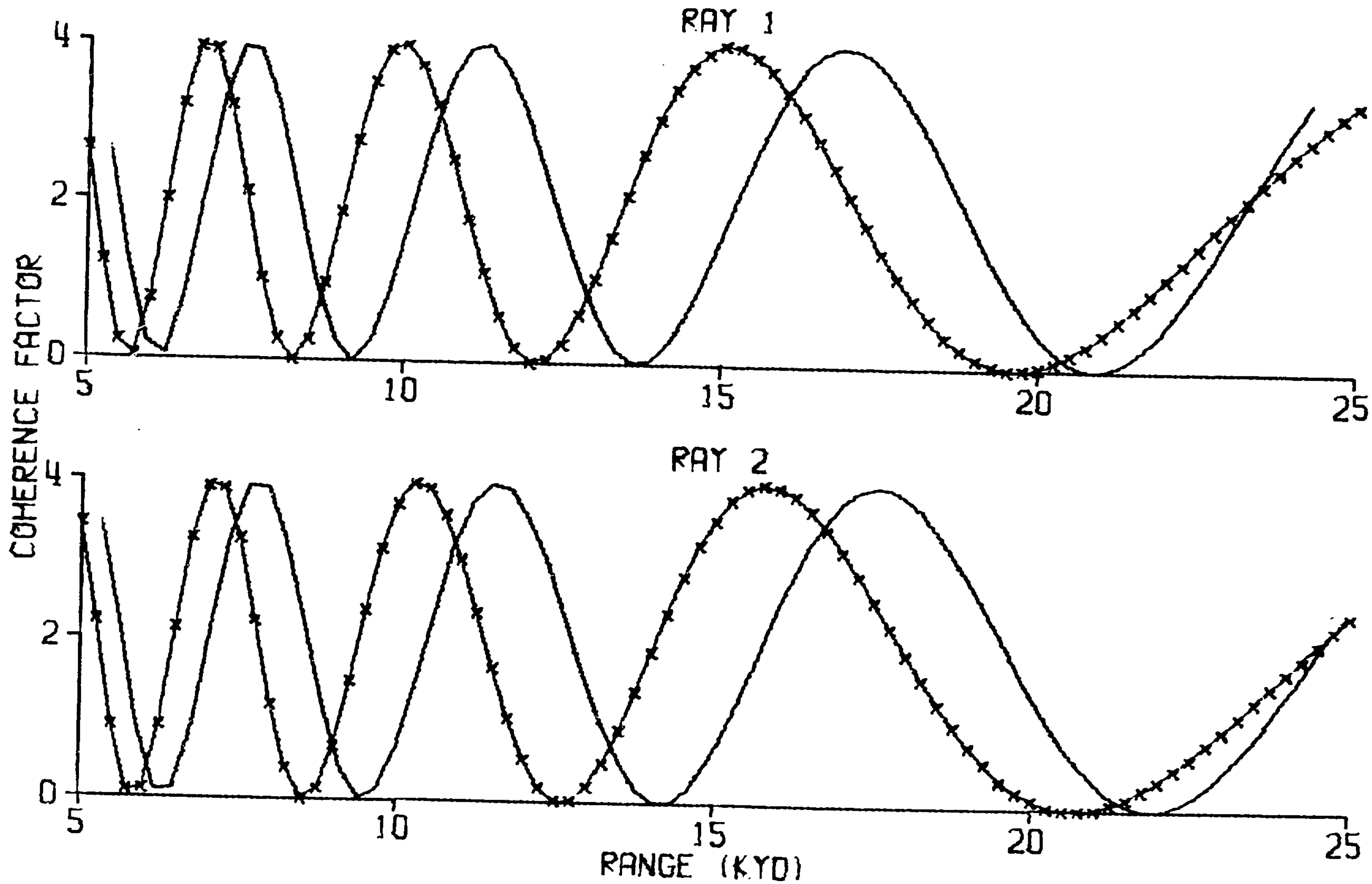

UNCLASSIFIED

(U) Figure 5-20. Interference Patterns, Example 3a.

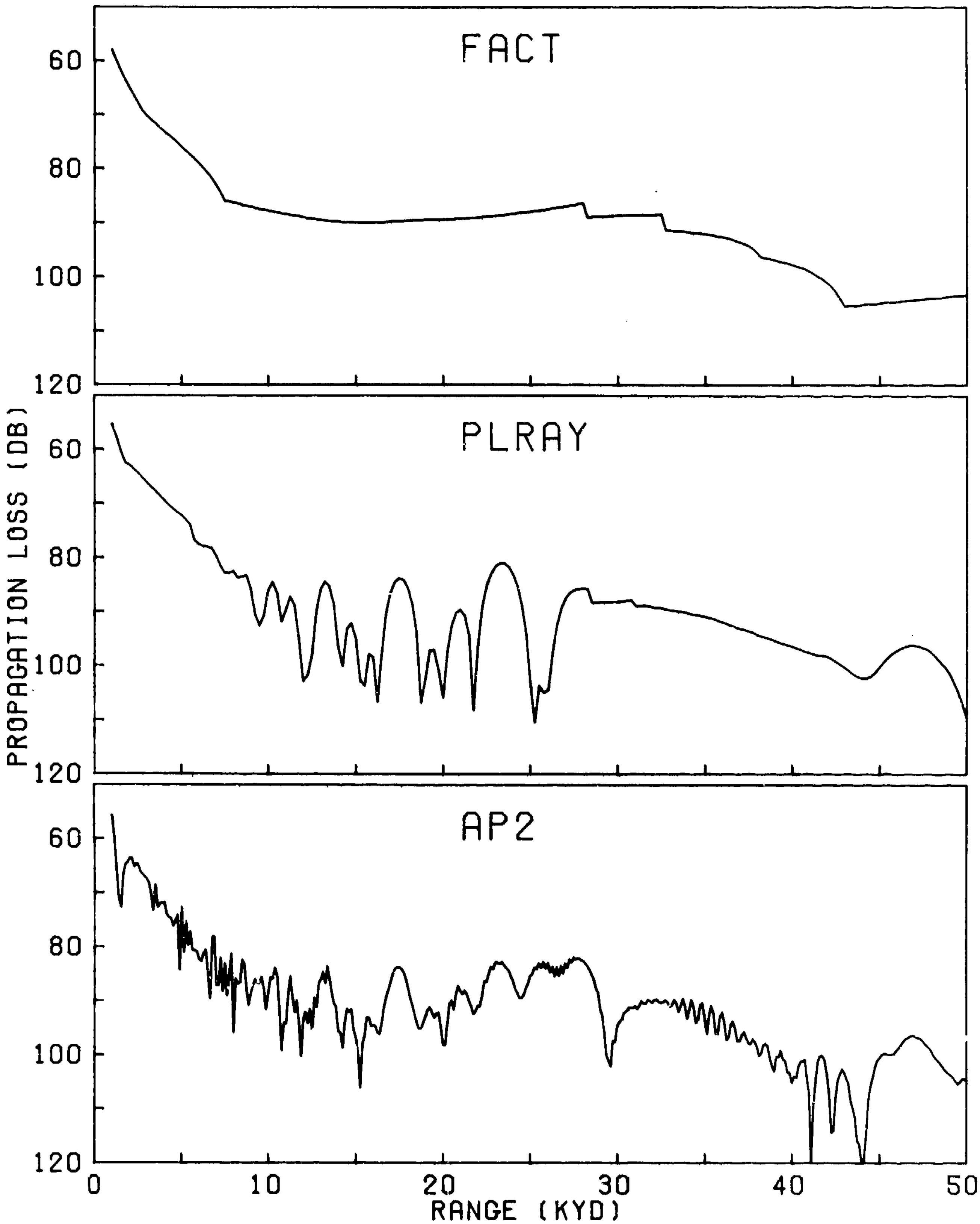

UNCLASSIFIED

(U) Figure 5-21. Propagation Loss, Example 3b.

direct (upward-going) and surface-reflected (downward-going) rays at the 250-foot depth were plotted against the average range of the four paths and are shown in Figure 5-22. The horizontal line at 12,150 ft represents the 2-mile FACT criterion. In applying its 2-mile criterion FACT tests the first and last rays of the sector and if the separation at either one exceeds the limit, coherence is not computed. In this case, as in Example 3a, there are only two rays, the first ray having the longer range. The horizontal separation of the two paths for the first ray proved to be 14,034 ft, thus exceeding the 2-mile limit. Hence coherence was suppressed. However, inspection of Figure 5-22 reveals that the horizontal separation is well under this limit over almost the entire range interval, so that suppression of coherence was a mistake.

(U) The range-angle curves for this case are plotted in Figure 5-23. The FACT fitted curves are identified by x's. Examination of these curves reveals large discrepancies as in Example 3a. Now there are four sets due to the absence of coherence. The lower set on the left side corresponds to path 1, the lower on the right to path 2, the upper on the left to path 3, and the upper on the right to path 4. The parabola for path 1 has a very pronounced maximum, indicating curvature in the wrong direction. Actually this curve predicts a maximum range caustic, but since FACT knows that caustics cannot exist in the outermost sector it does not look for one. There is also a small maximum in the parabola for path 2, though it is obscured by the x's of the plot.

(U) In this example we shall investigate the effect of the curve distortions upon the ray spreading loss. Fortunately the exact spreading loss values are available from the output of the NADC Ray-Tracing Program. Curves of spreading loss vs. range for the four paths are plotted in Figure 5-24, the FACT curves being identified by x's. Mostly the errors are of the order of 2 dB or less. However, at the longer ranges much larger errors occur. In particular the FACT curves for the first two paths fail to curve upward toward infinity. This is because of the erroneous maximum in the range-angle curves. In solving for the angle and slope corresponding to any given receiver range the FACT algorithm looks only on the outer branch of the curve where, as the limiting range is approached, the slope remains gentle whereas it should approach infinity. The effect of this behavior is visible in Figure 5-23 in the discontinuities at about 28 and 32 kyd.

Example 4 (U)

(U) This example was selected because of the absence of an interference pattern in a semi-coherent run. Also because the source and receiver were at the same depth, it provided an opportunity to investigate the behavior of the cusped caustic correction. The velocity profile (Fig. 5-25) is from the Arabian Sea. The source and receiver were at 295 ft and the run was made at 50 Hz. The bottom loss data are listed in Table 5-1. The predicted propagation loss for FACT, PLRAY, and AP2 is shown in Figure 5-26. Because PLRAY has no cusped caustic correction, the receiver was specified 10 ft away, at 305 ft.

Table 5-1. (U) Bottom Loss, Example 4

Grazing Angle (deg)	Loss (db)
0	0.8
10	0.8
20	0.9
23	1.0
35	2.4
40	4.8
90	4.8

UNCLASSIFIED

(U) The explanation for the absence of coherence in this run is the same as in Example 3. Figure 5-27 shows the horizontal separation between the direct and surface-reflected paths as a function of range. Although the curve is truncated

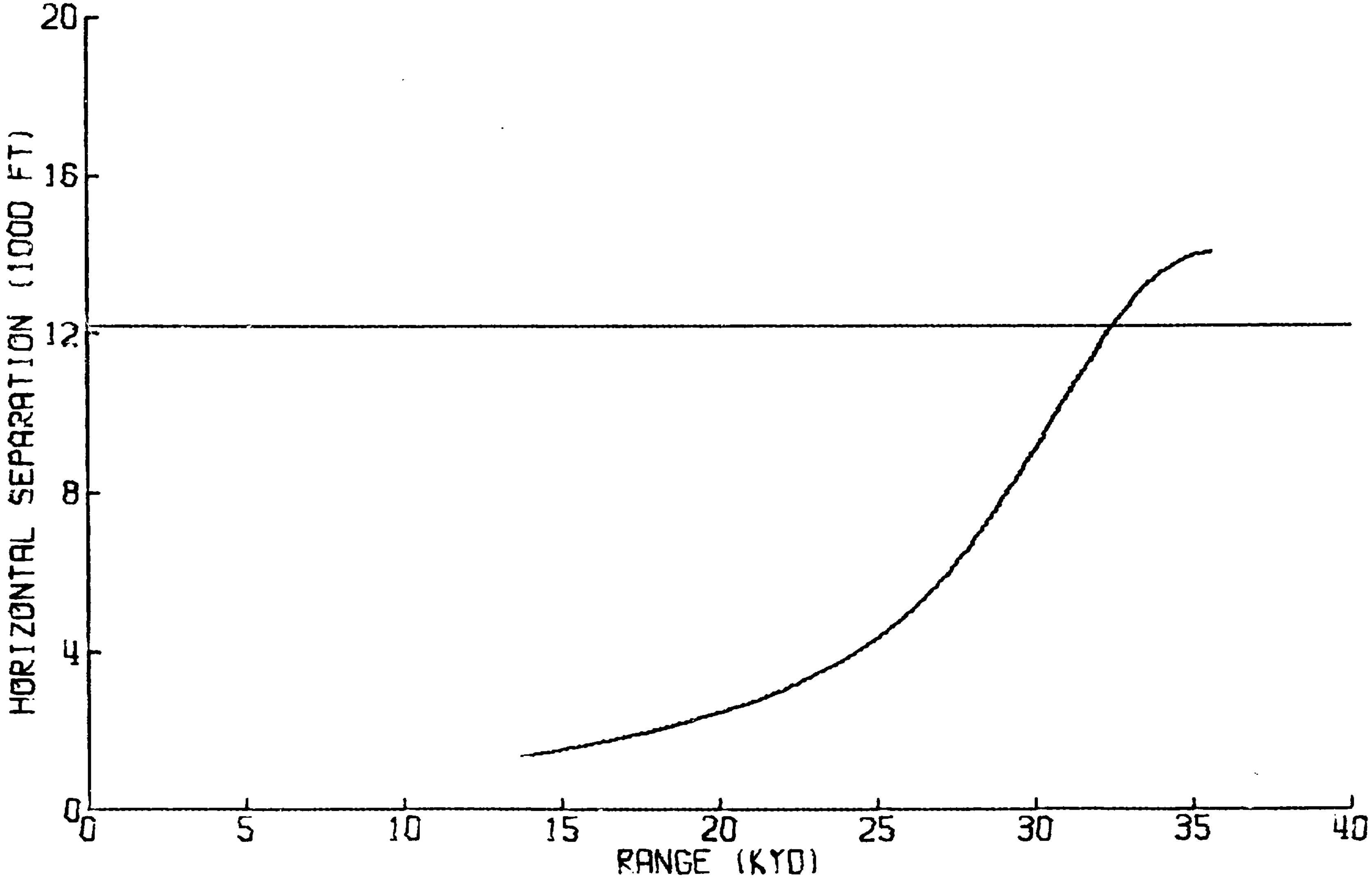

UNCLASSIFIED

(U) Figure 5-22. Horizontal Separation Between Direct and Surface-reflected Paths at 250 foot Depth, Example 3b.

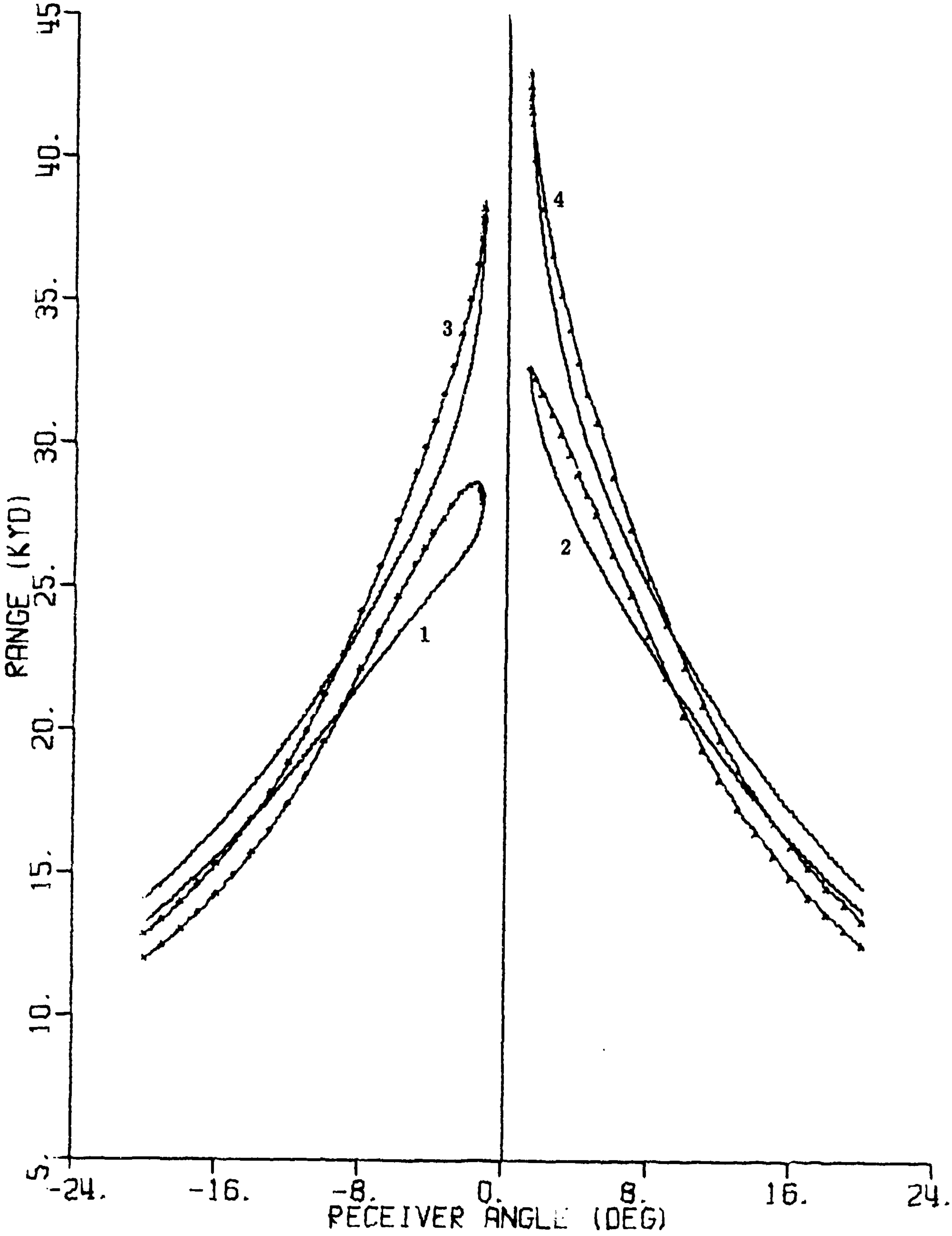

UNCLASSIFIED

(U) Figure 5-23. Range-angle Curves, Example 3b.

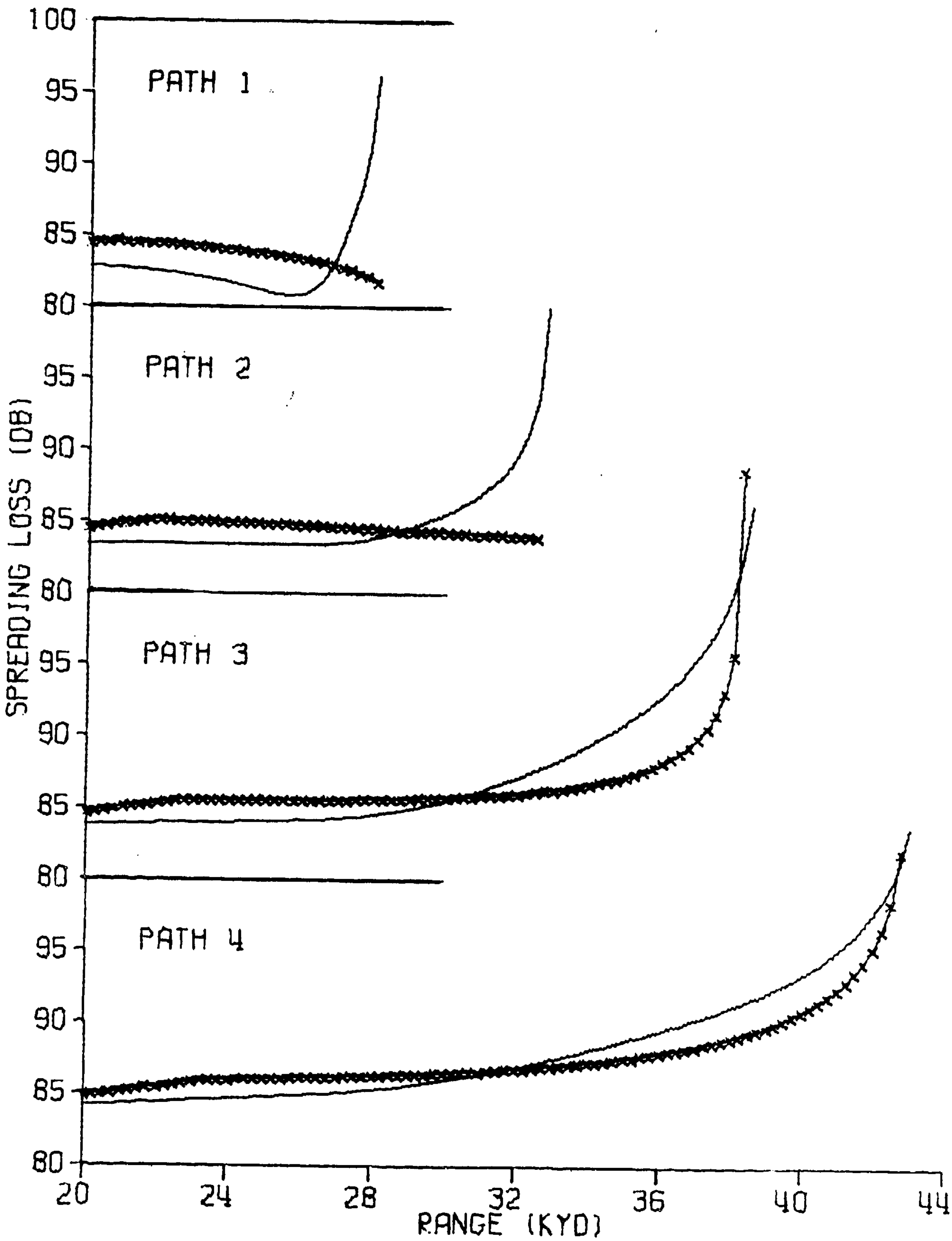

UNCLASSIFIED

(U) Figure 5-24. Spreading Loss, Example 3b.

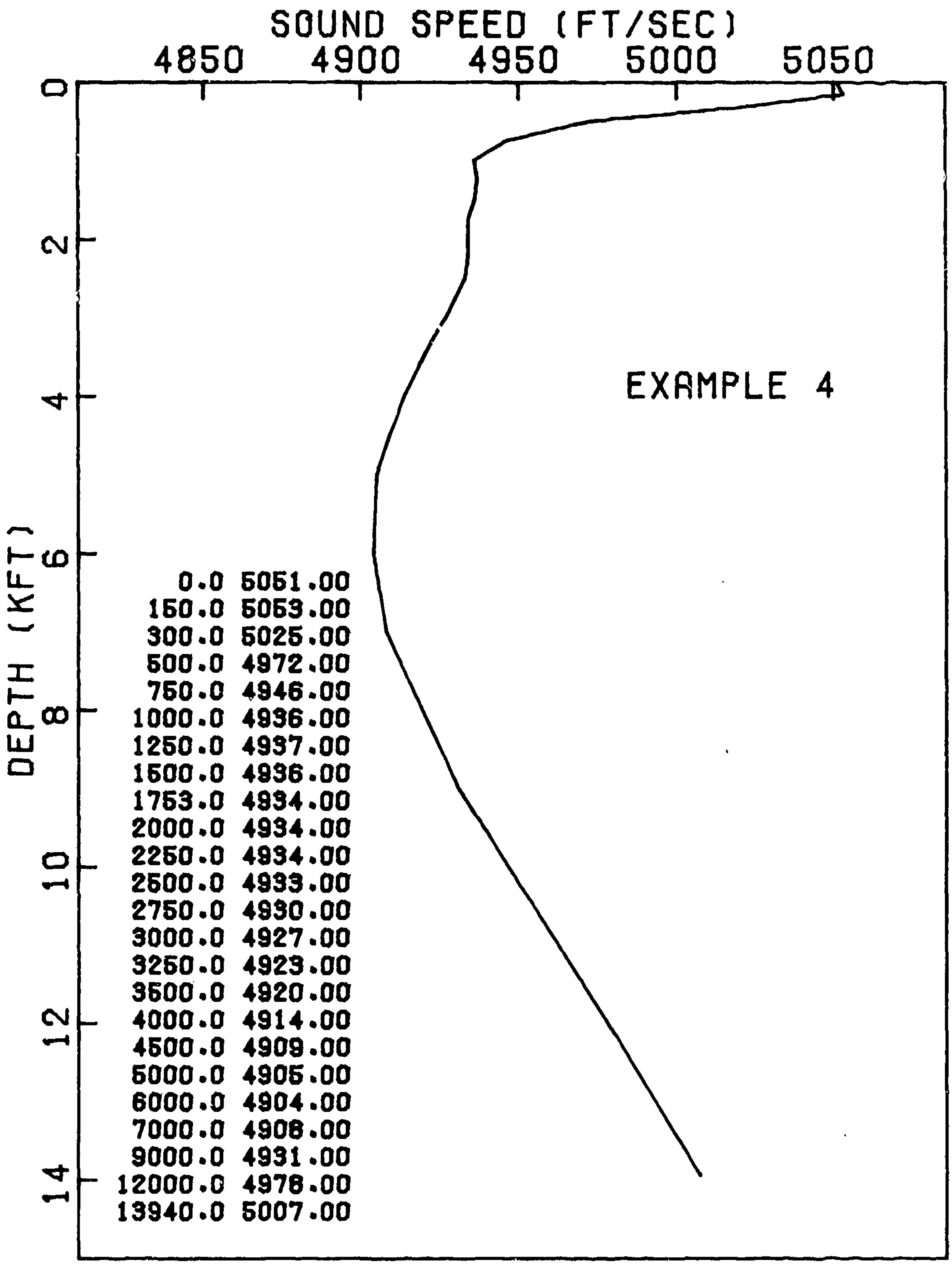

UNCLASSIFIED

(U) Figure 5-25. Sound Speed Versus Depth Profile, Example 4.

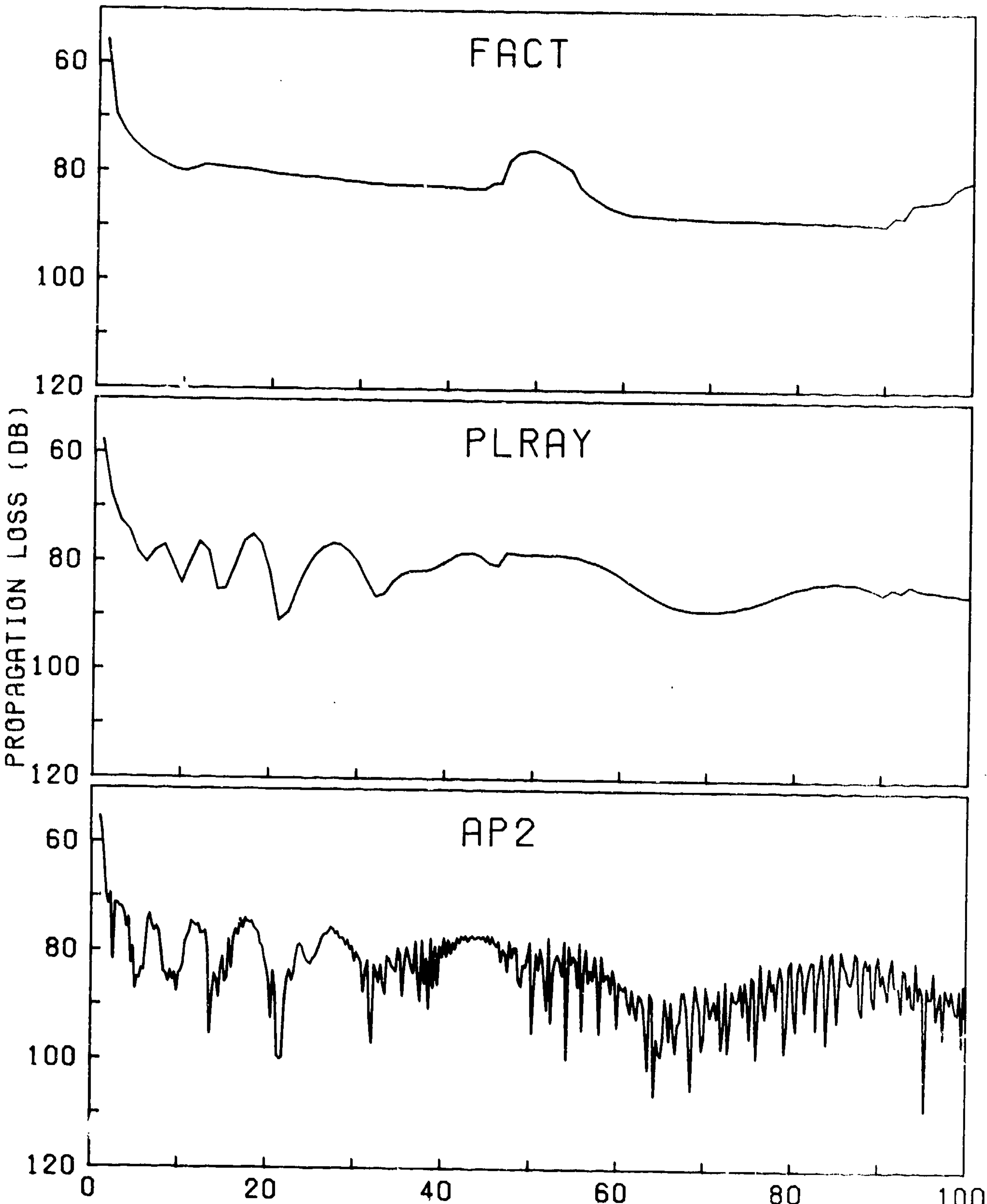

UNCLASSIFIED

(U) Figure 5-26. Propagation Loss, Example 4.

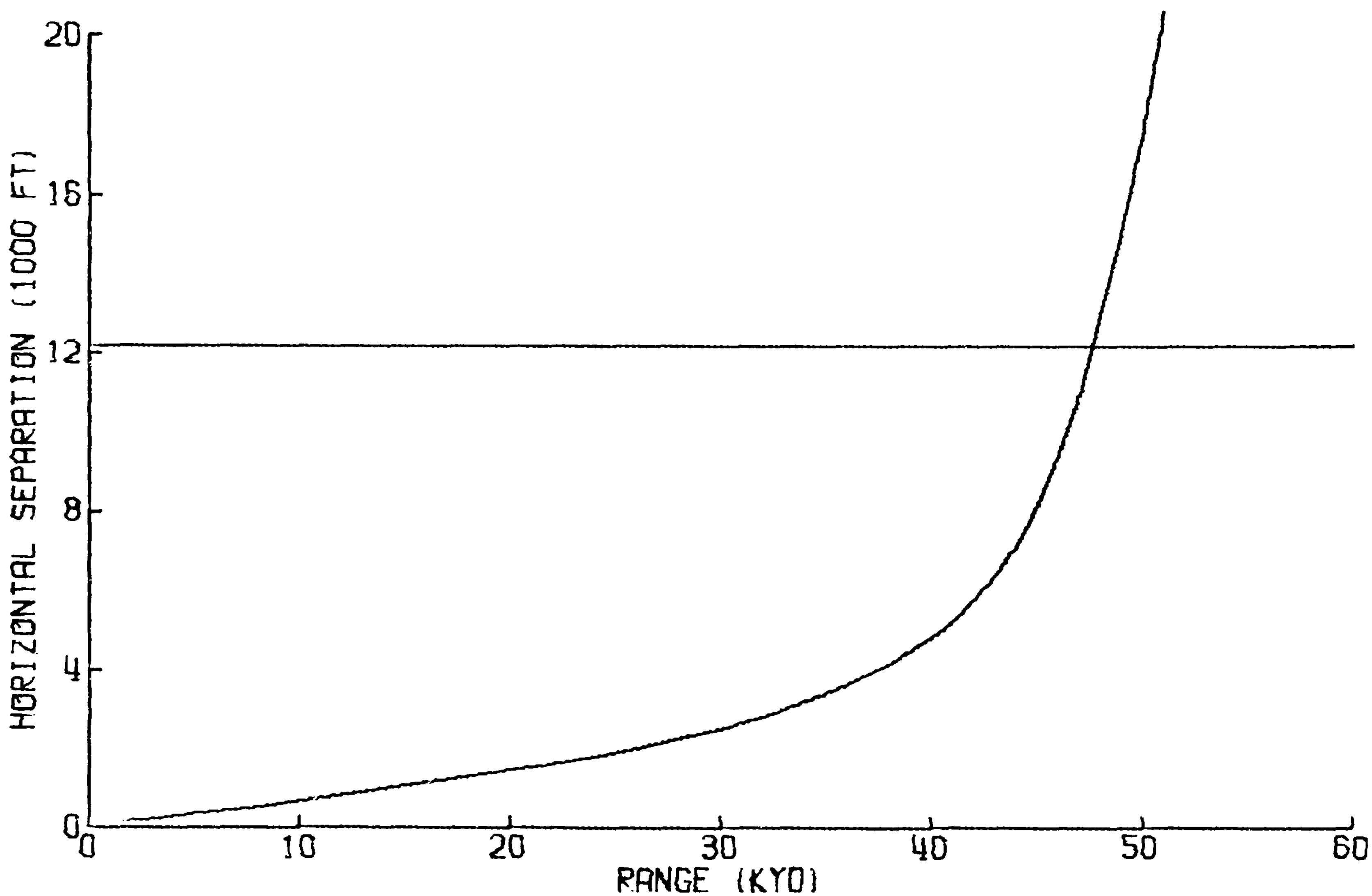

UNCLASSIFIED

(U) Figure 5-27. Horizontal Separation Between Direct and *Surface-reflected* Paths at 295 foot Depth, Example 4.

at about 20,000 ft, FACT computed a separation of over 25,000 ft for the first ray of the sector, more than twice the limiting value. However, out to 40 kyd the separation is very small, so that over the bulk of the interval the coherence criterion was met.

(U) This case offers a rather clean example of the cusped caustic correction. Although both depths were specified as 295 ft, INSERT moved the receiver depth up to 285 ft. To serve as a reference the old NADC Ray-Tracing Program was used to generate a set of range-angle curves for the case where the source and receiver are both at 295 ft. These are shown in Figure 5-28. The curves are remarkably smooth and show maximum range caustics. The cusp is at the point of intersection and an additional smooth caustic is shown nearby. The range-angle curves for the depths actually selected by FACT are plotted against receiver angle in Figure 5-29. The cusp is assumed to lie midway between the two curves at the center. The additional curve on the right which begins at the cusp is the fit for the smooth caustic and will be discussed later. The parabola for the cusped caustic fit is shown along with the true range-angle curves in Figure 5-30, plotted in source angle space. Between the two branches of the true curves is the forbidden region containing the rays which do not reach the receiver depth. The cusp parabola passes continuously through this region. It is not clear exactly how this forbidden procedure affects the results. In the present example it is the cusp correction that produces the peak at 50 kyd.

(U) Returning now to the smooth caustic, we note in the ideal picture of Figure 5-28 that it is located on branch 4 slightly above and to the right of the cusp. In the actual picture of Figure 5-29 FACT looked for a maximum range among the rays of branch 4. The maximum occurred for the second ray of the sector. FACT then fitted a parabola through three points—the end point at the right, the maximum point, and what it thought it thought was the cusp. But note that the assumed cusp is located midway between the two range-angle curves and is therefore far removed from any point on branch 4. The result is a gross distortion which moved the caustic all the way out to 55 kyd in range and 2 degrees in angle. The attempt to fit a parabola to three points when one of the three points does not lie on the original curve is a source of trouble.

(U) The velocity profile of Example 4 was used also for a brief check of the FACT limitation on the number of bottom bounces. Although special cases can be found in which more bounces may be computed, FACT normally limits the number to 4. To determine whether this limitation might lead to errors the NADC version of FACT was modified to require a minimum of 8 bottom bounces. The inputs for Example 4 were modified to call for an FNOC Type 1 bottom. A source depth of 1000 ft was selected, a receiver depth of 350 ft, a frequency of 100 Hz, and a maximum range of 200 kyd in steps of 2 kyd. Incoherent runs were made on both versions and the results were compared. The effect of the additional four bounces was found to be negligible at ranges less than about 80 kyd. Beyond this point the error gradually built up, reaching a maximum value of 1.7 dB at 118 kyd.

<u>Example 5</u> (U)

(U) This example was selected to serve as a test case for investigating the discontinuity at the bounding depth of the region in which the cusped caustic correction is applied. The velocity profile (Fig. 5-31) is from the Philippine Sea. Two semi-coherent runs were made with a receiver depth of 295 ft and a frequency of 50 Hz. In one run the source depth was set at 304.99 ft and in the other at 305.01 ft. The external bottom loss curve indicated in Table 5-2 was inserted in place of the internal curves.

(U) Since the source and receiver depths were specified less than 10 ft apart in

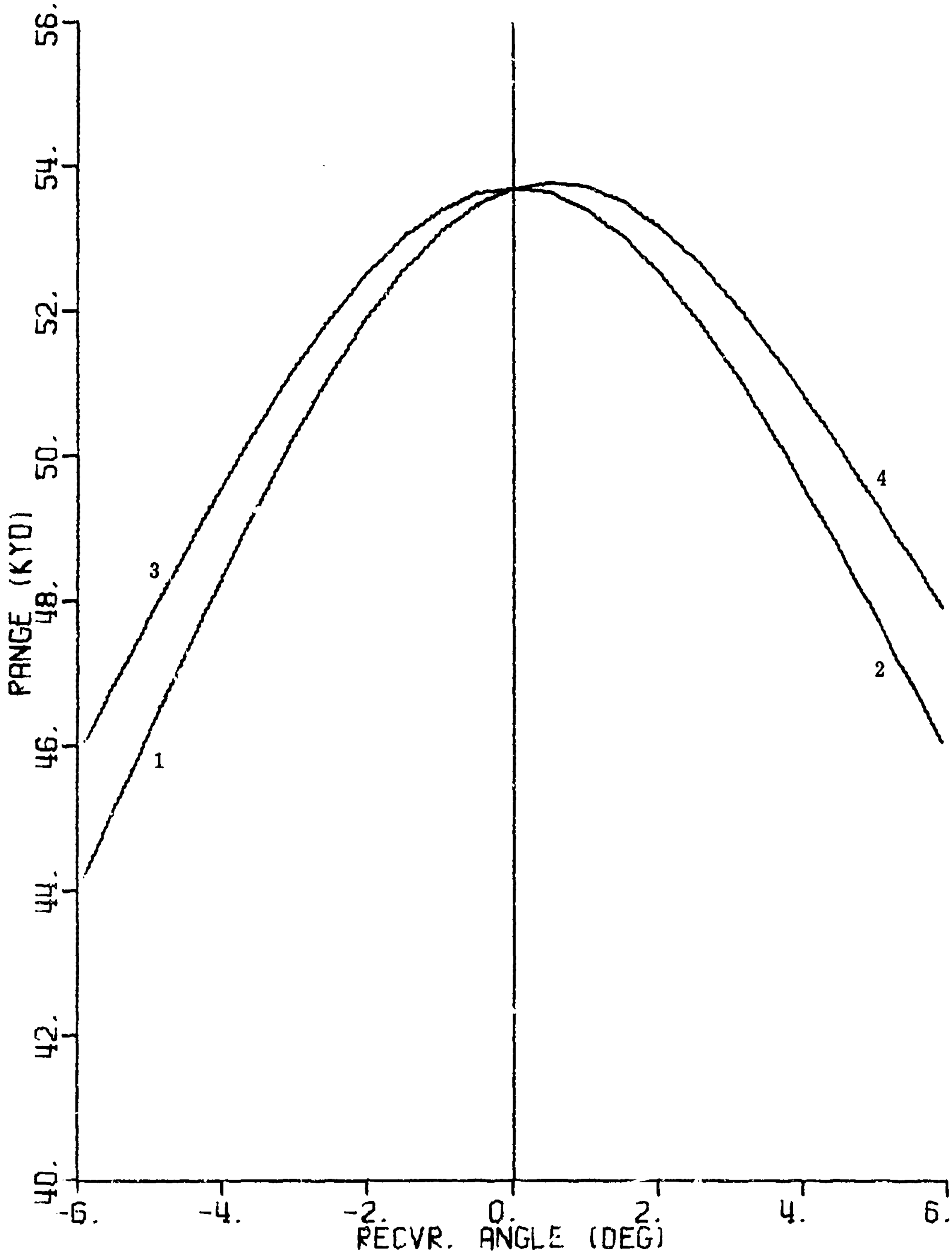

UNCLASSIFIED

(U) Figure 5-28. Ideal Range-angle Curves, Source and Receiver at 295 feet, Example 4.

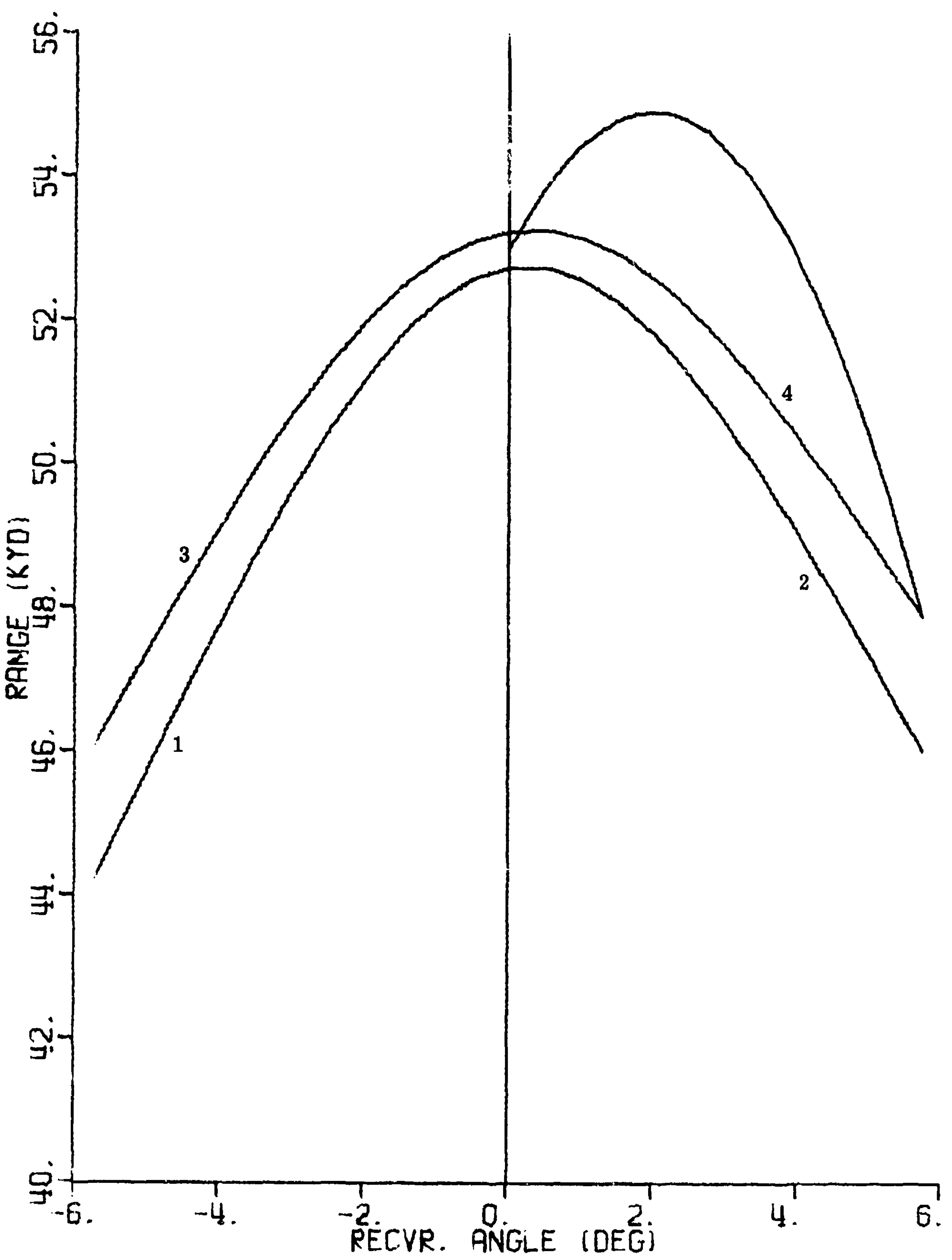

UNCLASSIFIED

(U) Figure 5-29. Range-angle Curves in Receiver Angle Space, Example 4.

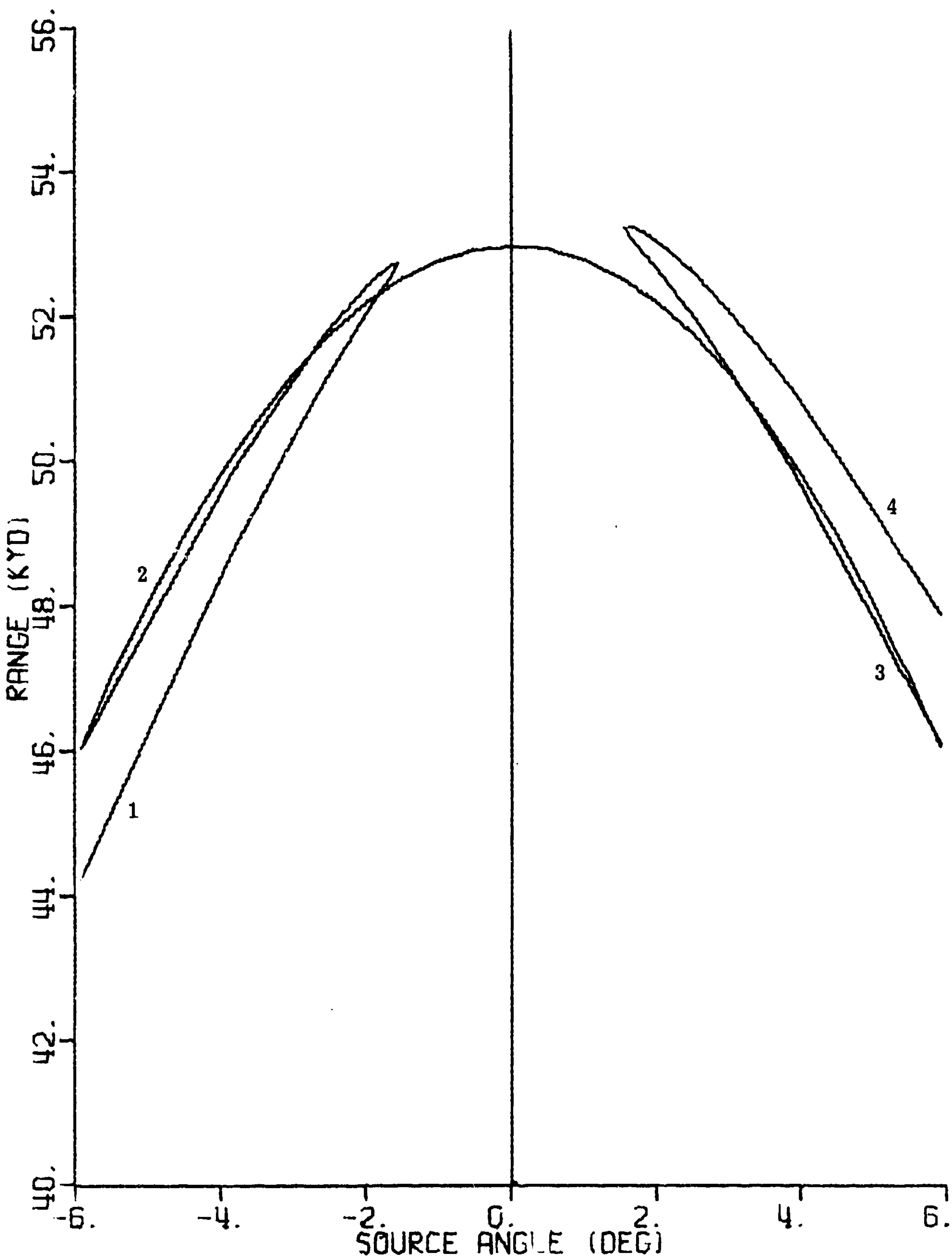

UNCLASSIFIED

(U) Figure 5-30. Range-angle Curves in Source Angle Space, Example 4.

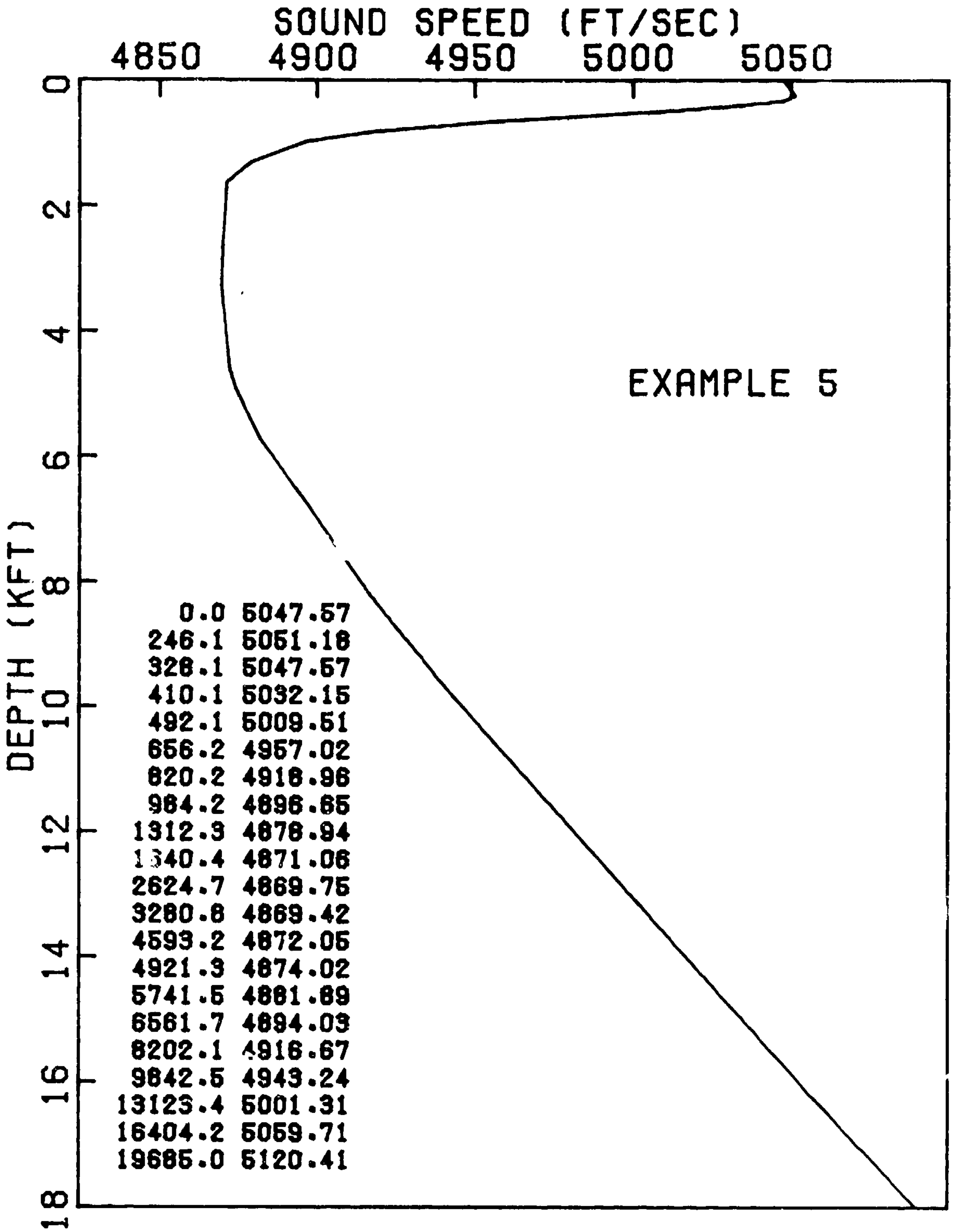

UNCLASSIFIED

(U) Figure 5-31. Sound Speed Versus Depth Profile, Example 5.

Table 5-2. (U) Bottom Loss, Example 5

Grazing Angle (deg)	Loss (dB)	Grazing Angle (deg)	Loss (dB)
0	0.05	55	8.10
8	0.05	60	8.30
10	0.36	65	8.55
15	2.00	70	8.60
20	3.30	75	8.55
30	5.50	80	8.50
40	6.70	90	8.20
50	7.20		

UNCLASSIFIED

the first run, they were moved together in INSERT, raising the source depth to 295 ft. Then after the manipulations in AXIS they were moved apart again. While one of the depths remained fixed at 295 ft, the other was moved upward to 285 ft. In the second run the depths were not moved at all because their initial separation was in excess of 10 ft.

(U) The outputs of the runs are plotted in Figure 5-32, the first run (304.99 ft) being represented by the solid line and the second run (305.01 ft) by the x's. Everywhere except in the vicinity of the peak at about 65 kyd the differences between the two curves are due solely to the difference in depth (285 instead of 305 ft). The differences between the application of the cusped caustic correction in the one run and its absence in the other occur in the vicinity of that peak.

(U) Examination of the diagnostic output for these runs revealed that by and large the program was relatively well behaved. However, one occurrence in each run is worth noting. The most dramatic event occurred in the first sector of the second run. There are two paths to be processed in the first order arrivals. The range-angle curve for the second path clearly exhibits a minimum, indicating a minimum range caustic. In theory the parameter RCUT represents the range at which the intensity on the shadow side of the caustic is to be tapered off to zero. Clearly if it is to perform this function for a minimum range caustic, its value must be less than the range to the caustic. In this case, however, for reasons not understood RCUT has been set to a value beyond the caustic. The net result is that the caustic has been wiped out. It is as though these rays had never been computed. Somewhere in the logic of INSTOR there is an error in determining RCUT.

(U) In the first run the range-angle curves from which the characteristics of the cusp are determined are sufficiently unusual that it is thought they should be displayed. Figure 5-33 is a plot of the curves in source angle space, together with the fitted parabola which spans the forbidden region.

Example 6 (U)

(U) Example 6 is what may be termed a pathological case. The velocity profile, shown in Figure 5-34, is from the Atlantic Ocean north of Bermuda and is characterized by a sub-surface channel whose axis is at a depth of 164 ft. The channel is exceedingly asymmetric with a strong negative gradient above the axis and a very weak positive gradient below. The thickness of the channel is approximately 1400 ft. The run to be described was a semi-coherent run made at a frequency of 25 Hz with the source and

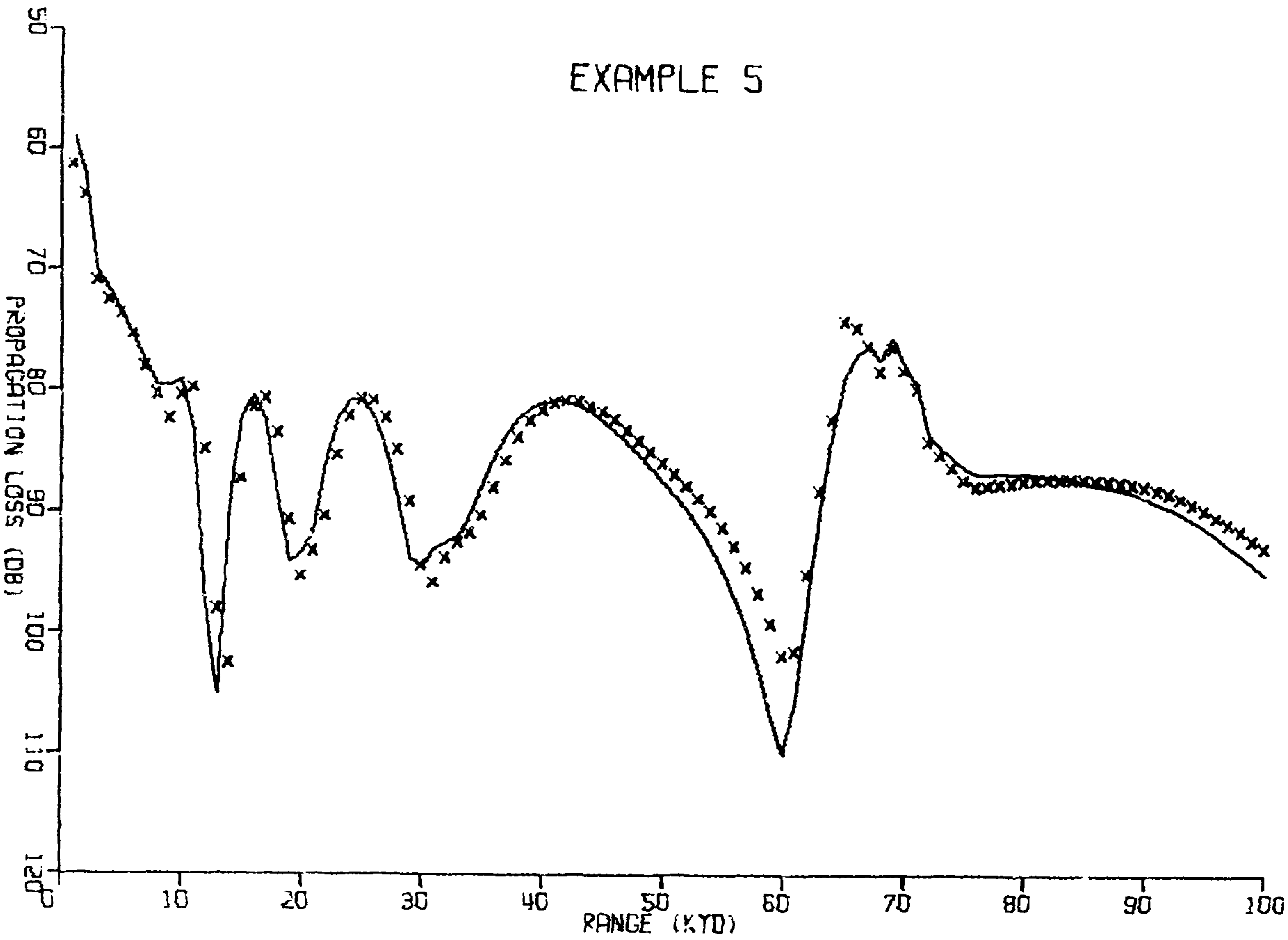

UNCLASSIFIED

(U) Figure 5-32. Propagation Loss, Example 5.
----Source Depth = 304.99 ft
xxx Source Depth = 305.01 ft
Receiver Depth = 295.00 ft

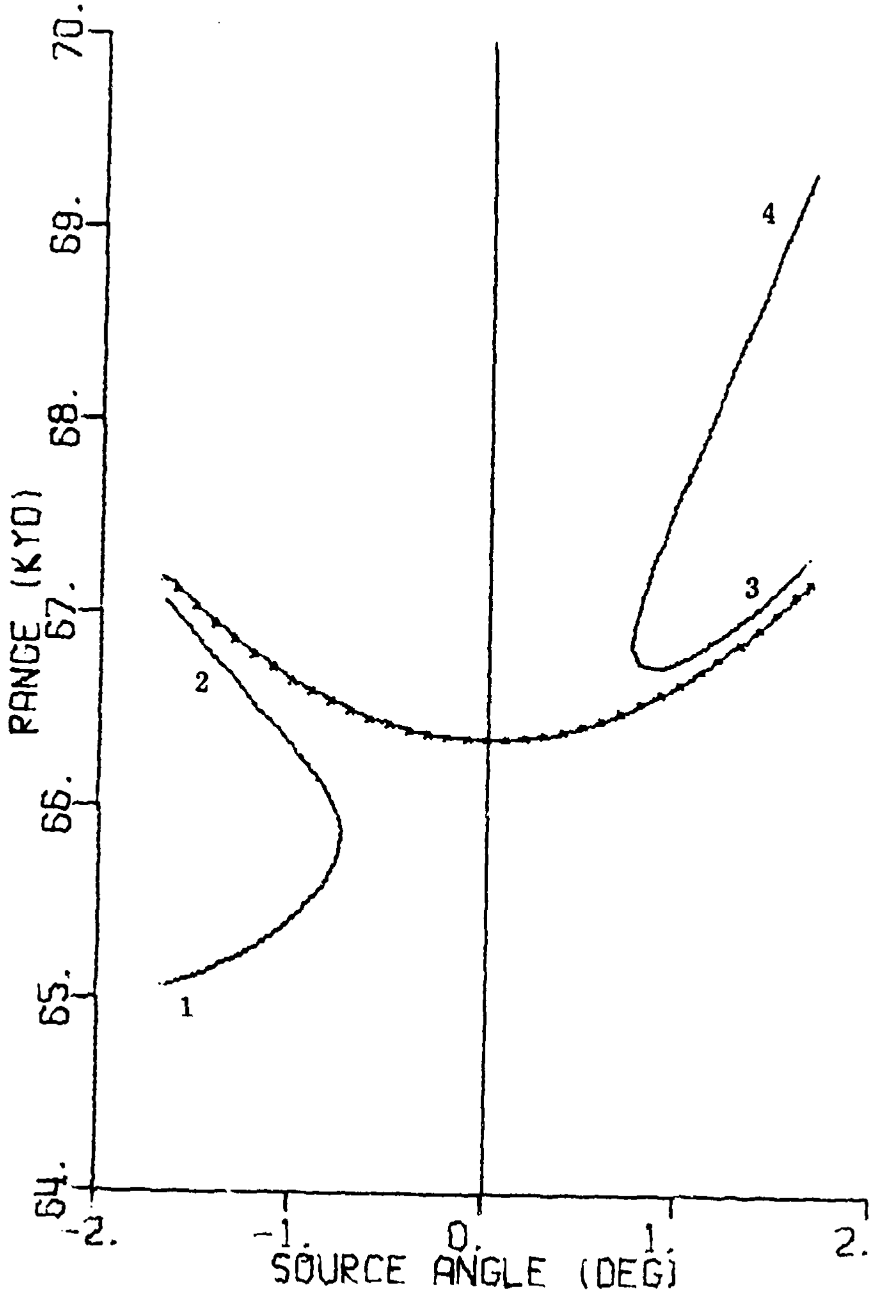

UNCLASSIFIED

(U) Figure 5-33. Range-angle Curves in Source Angle Space, Example 5.

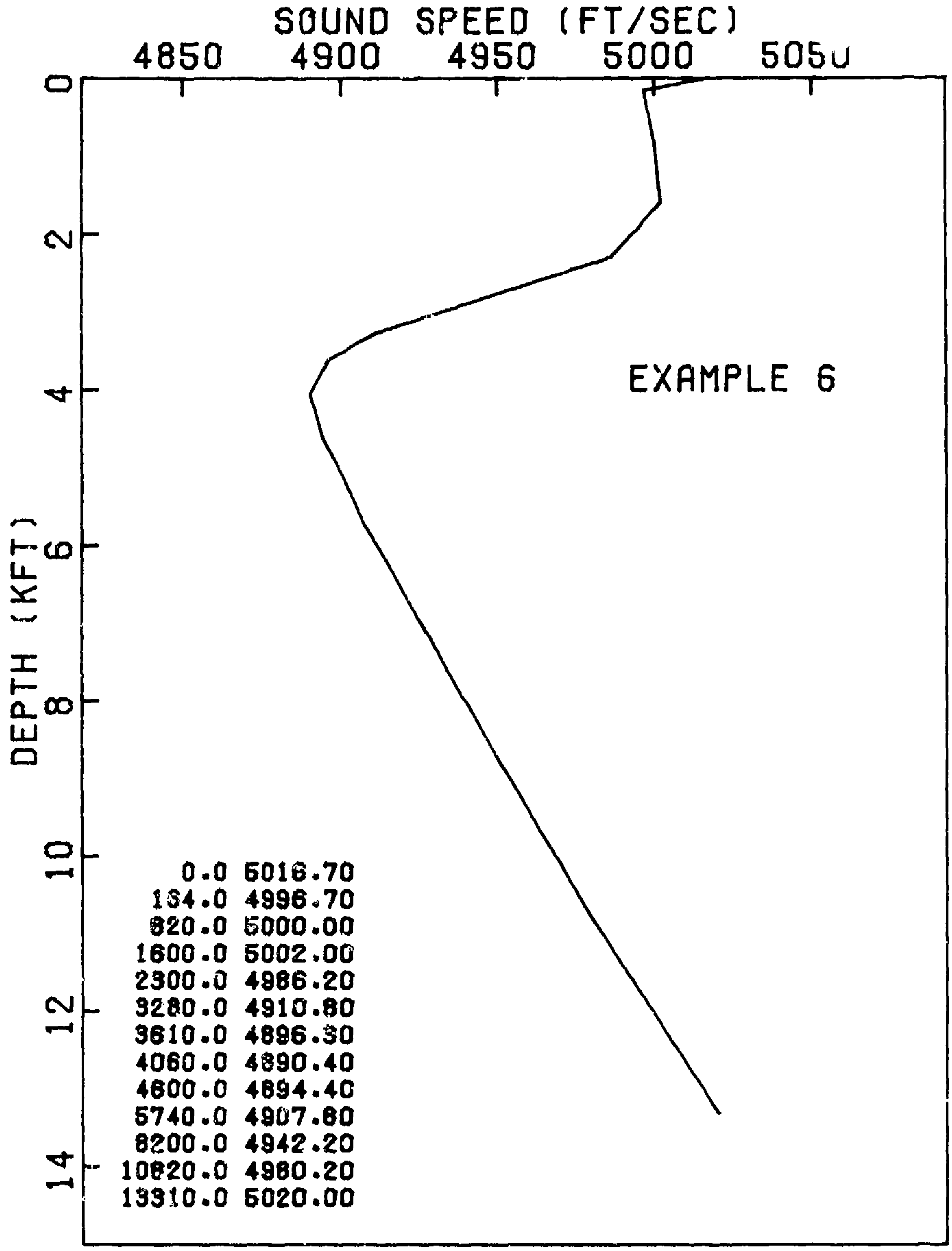

UNCLASSIFIED

(U) Figure 5-34. Sound Speed Versus Depth Profile, Example 6.

receiver both in the channel at depths of 200 and 400 ft, respectively. The bottom was an FNOC Type 5 bottom. A check run was made on the AP2 normal mode program. It had been originally intended to run this case at 50 and 100 Hz as well as 25 Hz but AP2 had difficulty finding eigenvalues at the higher frequencies because of interplay between the two families of modes generated by the double channel.* From an examination of the propagation loss outputs of the 25 Hz run, plotted in Figure 5-35, it is obvious that FACT got into trouble.

(U) The trouble began in subroutine AXIS where, after fitting semiparabolas on either side of the channel axis at 164 ft and computing the period of the zero-degree ray in the modified profile, the program found that the ray in the original profile yielding the same period extends upward to an upper vertex depth of 146.5 ft and downward to a lower vertex depth of 568.6 ft. The distance between the shallower of the source and receiver depths (200 ft) and the upper vertex depth is 53.5 ft. The distance between the deeper (400 ft) and the lower vertex depth is 168.6 ft. Comparing these two values AXIS picks the smaller and consequently moves both the source and receiver depths up to 146.5 ft. Then INSERT, finding the two depths to be equal, moves one of them (identified as the ray receiver) 10 ft farther upward. The overall result is that the originally specified depths of 200 and 400 ft have been changed to 136.5 and 146.5 ft without informing the user, and now there is a cusped caustic to correct.

(U) Next it will be noted that the lower portion of the upper channel consists of two profile segments, the lower of which has a weaker gradient than the upper. This causes ANGSCH to generate two sectors in the duct. Overall there are 5 sectors whose characteristics are listed in Table 5-3.

(U) Let us first consider sector 1, which contains the cusp. This sector is bounded on the inner edge by the limiting ray to the receiver depth and on the outer edge by the limiting ray to the 820-foot layer boundary. The source angles of these two rays are 1.264 and 1.319 degrees, respectively, so that it may be seen that sector 1 consists in source angle space of two narrow wedges of width 0.055 degree, one above the horizontal and the other below.

(U) The range-angle plot in source angle space is shown in Figure 5-36. The true curves are the two pairs of almost vertical lines at the extreme right and the

*This problem has subsequently been corrected. In running the 25 Hz case with the corrected version of AP2 it was found that 4 modes had been missed in the original run, with the result that the AP2 curve of Figure 5-35 is somewhat in error. However, the error does not affect the conclusions from this run.

Table 5-3. (U) Bottom Loss, Example 6

Sector No.	Inner Bdry.	Limiting Depth Outer Bdry.	No. Rays	Ray Type
1	Rcvr.	820 ft	4	RR, upper channel
2	820 ft	1600 ft	4	RR, upper channel
3	1600 ft	Surf.	8	RR, both channels
4	Surf.	Bottom	4	RSR
5	Bottom	(90°)	2	BB

UNCLASSIFIED

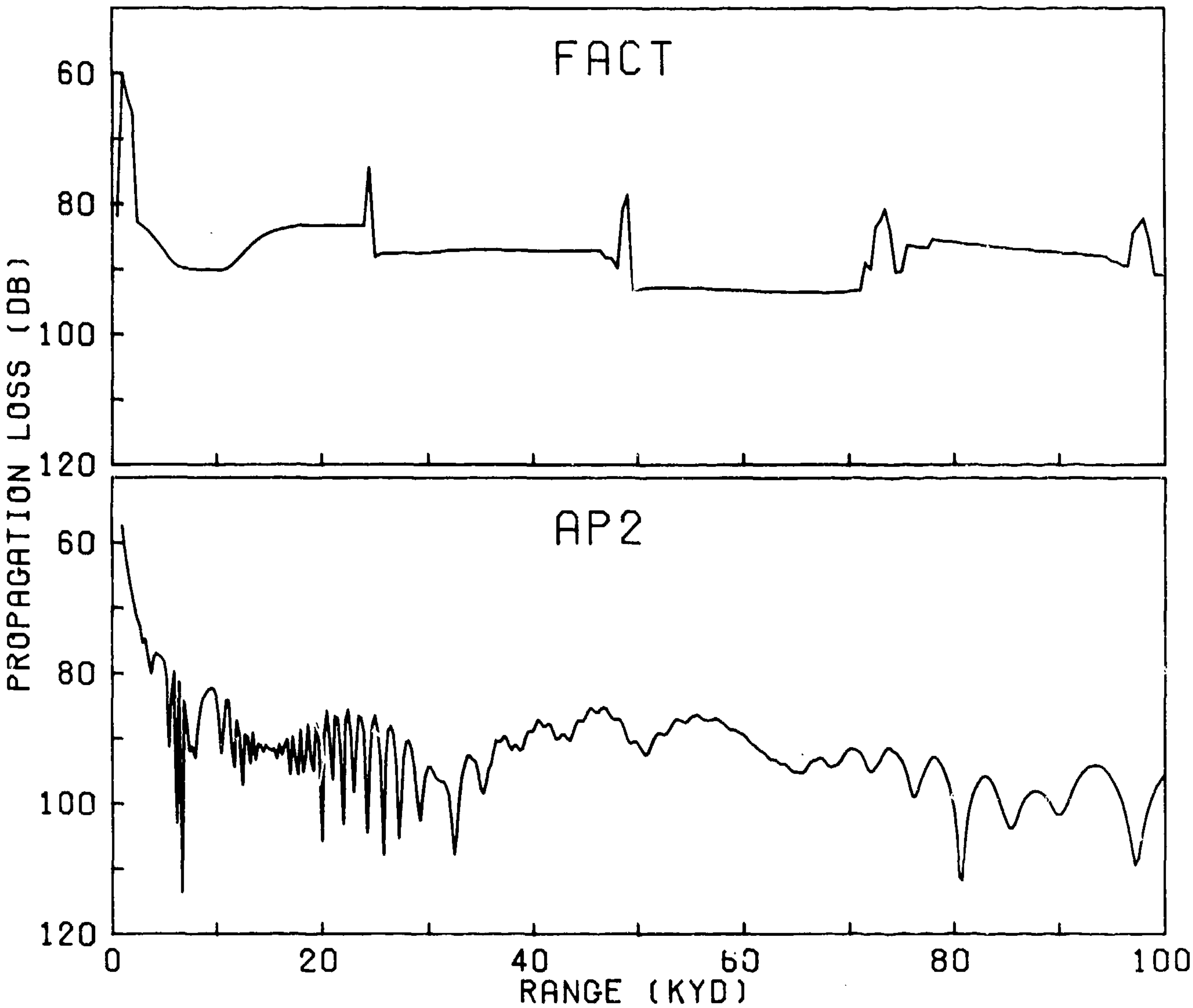

UNCLASSIFIED

(U) Figure 5-35. Propagation Loss, Example 6.

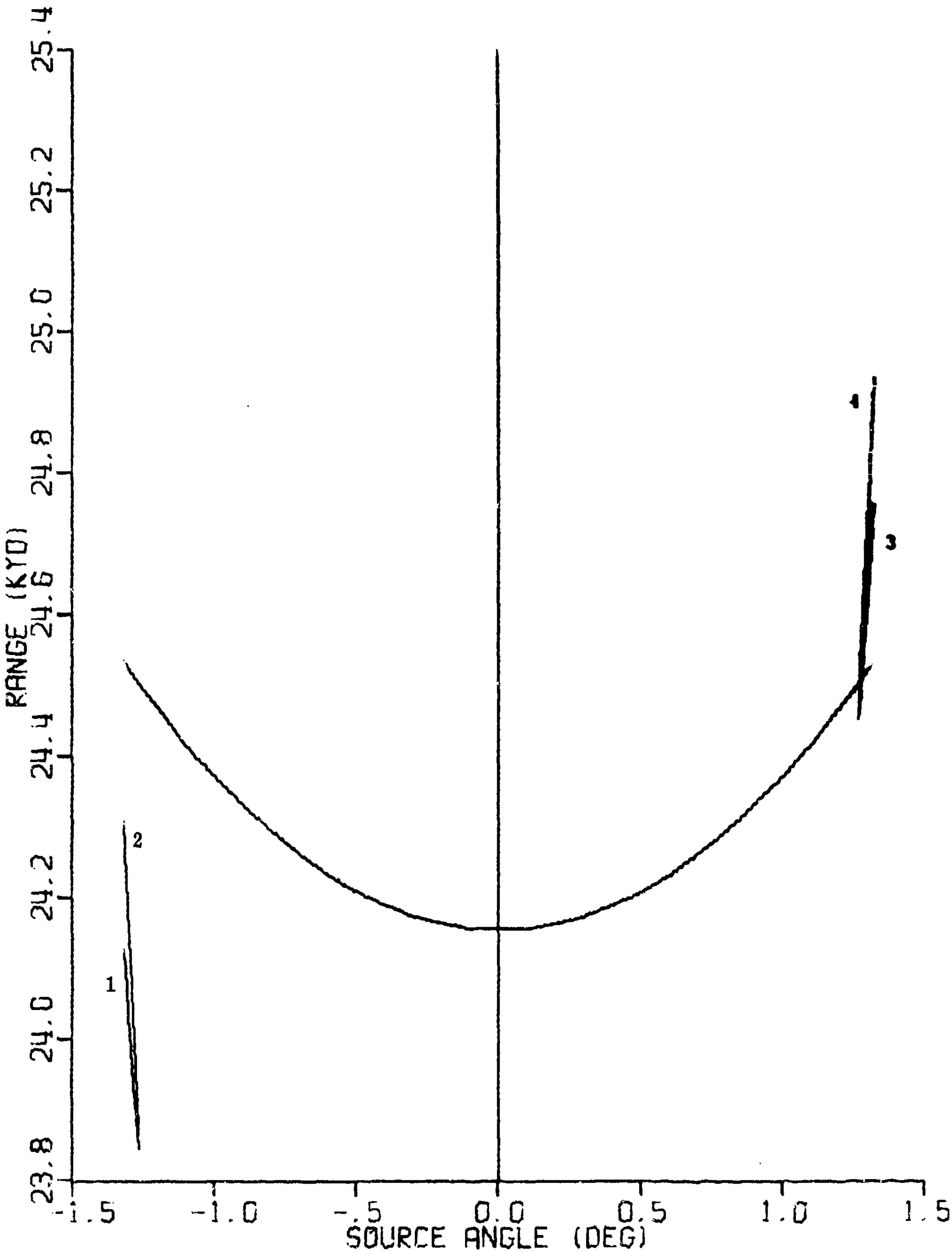

UNCLASSIFIED

(U) Figure 5-36. Range-angle Curves in Source angle Space, Example 6.

extreme left. The smooth curve extending across the forbidden region, which constitutes almost the entire plot, is the FACT parabolic fit to branches 2 and 3. This is an incredibly poor cusped caustic correction. The correction appears as a set of spikes spaced about 25 kyd apart in Figure 5-35. Successive spikes represent successive arrival orders. The spacing is the period of the zero-degree ray drawn from the modified receiver depth at 136.5 ft and bears no relation to the period which would have been obtained from the source and receiver depths actually specified in the inputs. The spikes result from the errors inherent in the parabolic fit. Obviously the parabola is grossly in error but, looking at the curves of Figure 5-36, there does not appear to be any way of guessing what the parabola should look like. More to the point, it is apparent that no attempt should be made to fit a parabola at all. The fit should be in receiver angle space. To see what the effect would be, the cusp parameter BCUSP was computed manually for a fit in receiver angle space. It was found that the recomputed value resulted in a lowering of the spikes by 5.5 dB and a spreading out in range by a factor of 2.5.

(U) When plotted against receiver angle the range-angle curves appear as in Figure 5-37. The similarity of this picture to the classical picture illustrated in Figure 1 is difficult to recognize. In Figure 5-37 the cusp C is assumed to be at an angle of 0 degrees and at a range midway between the two curves. Branches 2 and 3 are supposed to be the two halves of the curve which passes through the cusp at zero slope and branches 1 and 4 are supposed to be the two portions of the curve which passes through the cusp with finite slope. The minimum which occurs in branch 1 to the left of the zero-degree line is supposed to be the additional smooth caustic which requires correction. For this purpose it is fitted with a parabola which is normally passed through the three points corresponding to the cusp, the last ray of the sector, and the ray which produces the minimum range. In this instance the smooth caustic is close to the cusp and as a result the minimum range is generated by the first ray of the sector. Since there are now only two points available for the fit, FACT uses a slope for the third condition. In the classic picture of Figure 1 the slope of this curve is simply $2g_c/c_c$ where c_c is the sound speed at the common source/receiver depth and g_c is the gradient. Application of this technique to the distorted picture of Figure 5-37 leads to the flat parabola which begins at the computed cusp point and joins branch 1 at the edge of the sector. This is clearly a very poor fit to branch 1.

(U) The error in the curvature of the fitted parabola is manifested in an erroneous smooth caustic correction. In the first place the coefficient which relates the range scale to the argument of the Airy function is grossly in error, the error being in such a direction as to cause the intensity curve to be spread out too far in range. The scale is so large that to cover the interval from -3.5 to +1.77 of the Airy function argument would require for the first arrival order a range interval in excess of 158 kyd. The situation is worse for higher arrival orders. An error of this type tends to result in an essentially flat intensity curve over the entire correction interval. In the current example, however, another effect comes into play. In each of the caustic correction intervals to the left of the associated cusp in Figure 5-35 the argument of the Airy function is in the shadow region not far from the caustic. The value of RCUT generated for each arrival order forces a rapid decay in intensity. For the first arrival order shown in Figure 5-35 the value of RCUT is about 9.6 kyd. The dip in the curve in Figure 5-35 as the range decreases to 10 kyd is due to this effect. The effect is less noticeable in the curves for other arrival orders, partly because RCUT tends to move farther back from the cusp and partly because the effect tends

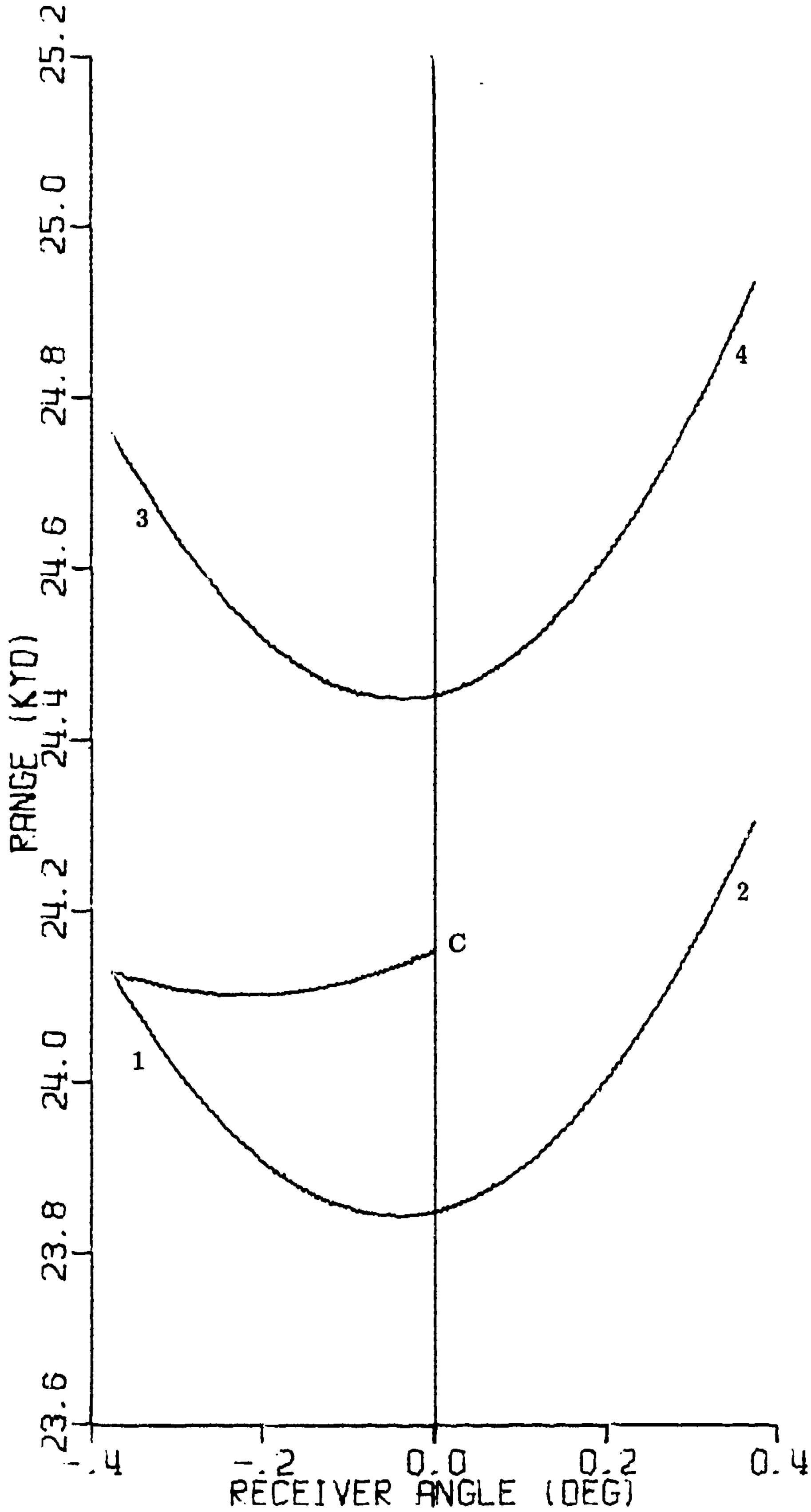

UNCLASSIFIED

(U) Figure 5-37. Range-angle Curves in Receiver Angle Space, Example 6.

to be masked by contributions from other sectors. A second consequence of the error in the curvature of the range-angle parabola is an erroneously high average level of intensity, as may be seen in Figure 5-35.

(U) If we turn to the second sector we find a new type of error. The range-angle curve fit in this sector is of the square root type rather than the tangent type. The plot for the first path (NP = 1) of the first arrival order is shown in Figure 5-38. The symbol TH refers to the angle at the receiver depth and THM is the angle of the first ray of the sector. The parabolic fit is actually very good, as may be seen from the x's which represent the rays computed by FACT. But note that the parabola passes through a minimum on the negative side of the plot. Now, a negative square root has no physical meaning in this context; it does not correspond to any physical reality in the model. But in the development of the logic in INSTOR the test which would have ruled out the negative square root was omitted. As a result the minimum of the curve meets all the requirements for a valid caustic and is treated as one. This caustic, as well as the caustic for NP = 2, shows the same kind of behavior as the smooth caustic of sector 1 - only worse. The range scale is so spread out that to cover the correction interval of x from -3.5 to +1.77 would require a range spread of over 500 kyd. As before, the computed intensity is essentially constant over the interval for each arrival order except for the tapering off due to RCUT that occurs toward the near edge. The contribution of sector 2 is thus badly in error.

(U) Sector 3 contains the RR rays that propagate through the deep ocean including both the shallow channel and the SOFAR channel. The first returns of these rays come in at about 73 kyd. It is these rays which are responsible for the higher level appearing in the 4th arrival order in Figure 5-35.

(U) The contribution of the RSR rays of sector 4 is thoroughly negligible because the sector is very narrow.

(U) Finally, sector 5 covering the bottom bounce rays appears to behave more or less normally, the only unusual observation being that the phase changes which generate the semi-coherent interference pattern are slower than usual. As a result the oscillations are very broad. It is curious that in the first arrival order, out to 25 kyd, the interference pattern of sector 5 accentuates the caustic tapering off effect of sector 1 and leads to the upswing seen in Figure 5-36. In the second order arrivals from 25 to 50 kyd the effects are less pronounced and they operate in opposing senses, one increasing while the other decreases. Almost accidentally the propagation loss curve is flat. The same situation exists in the third order arrivals. Finally, as indicated above, the fourth order arrivals are dominated by the rays of sector 3.

Example 7 (U)

(U) This example was selected for the purpose of investigating the axis-to-axis manipulations which are performed in subroutine AXIS. A Mediterranean profile from the Ionian Basin was selected and slightly modified in two ways. The first modification (Mod 1) consisted of removing two points immediately above the SOFAR axis and one point immediately below in order to provide a thick layer on either side. The profile is plotted in Figure 5-39. An incoherent run was made at a frequency of 100 Hz with the source and receiver both specified on the axis at 600 ft. An FNOC Type 2 bottom was specified. The second modification (Mod 2) was made by simply interpolating a point at a depth of 580 ft on the segment immediately above the axis. No substantive change was made in the profile. A second run was made on Mod 2, all other conditions remaining unchanged.

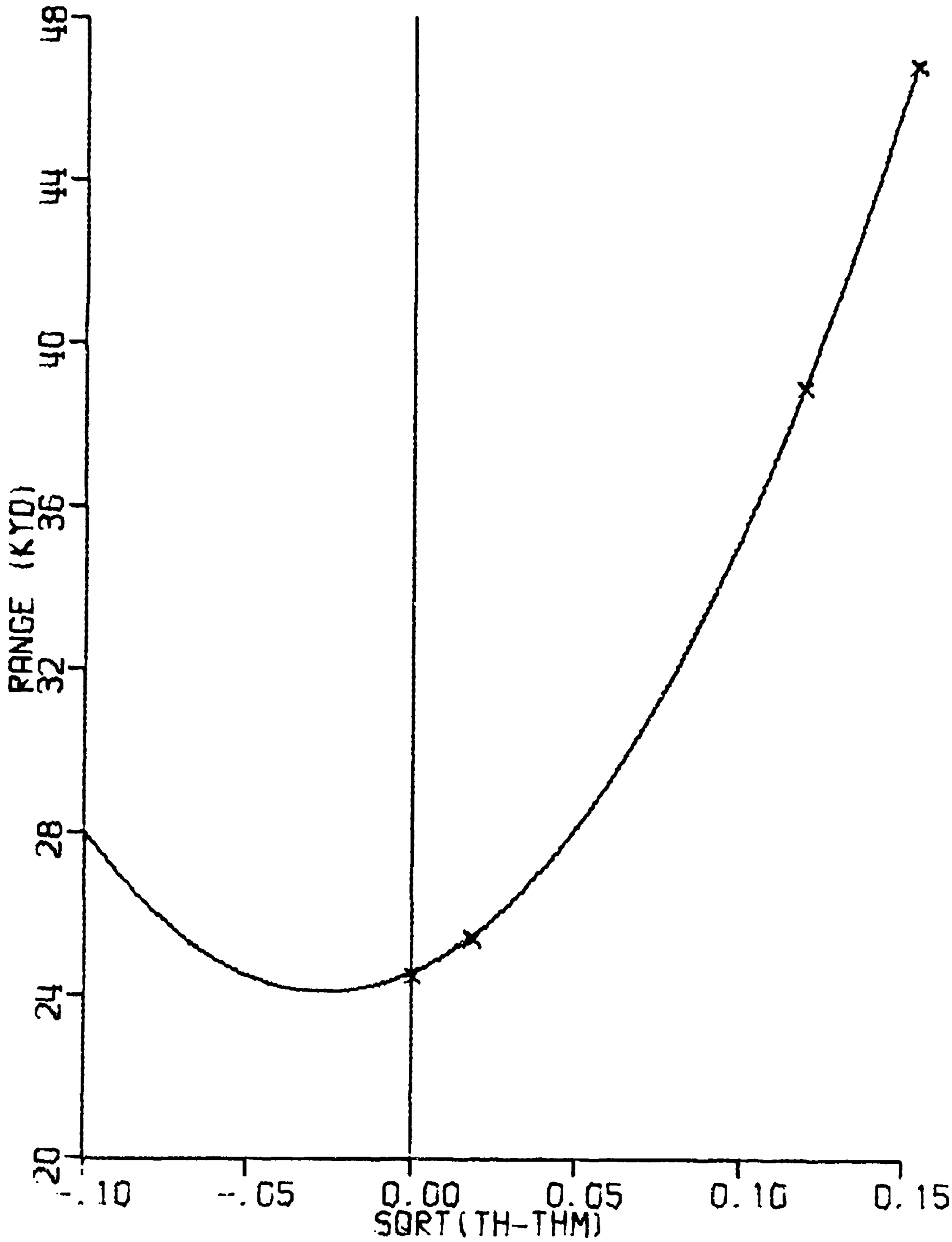

UNCLASSIFIED

(U) Figure 5-38. Erroneous Caustic Arising from Negative Square Root, Example 6.

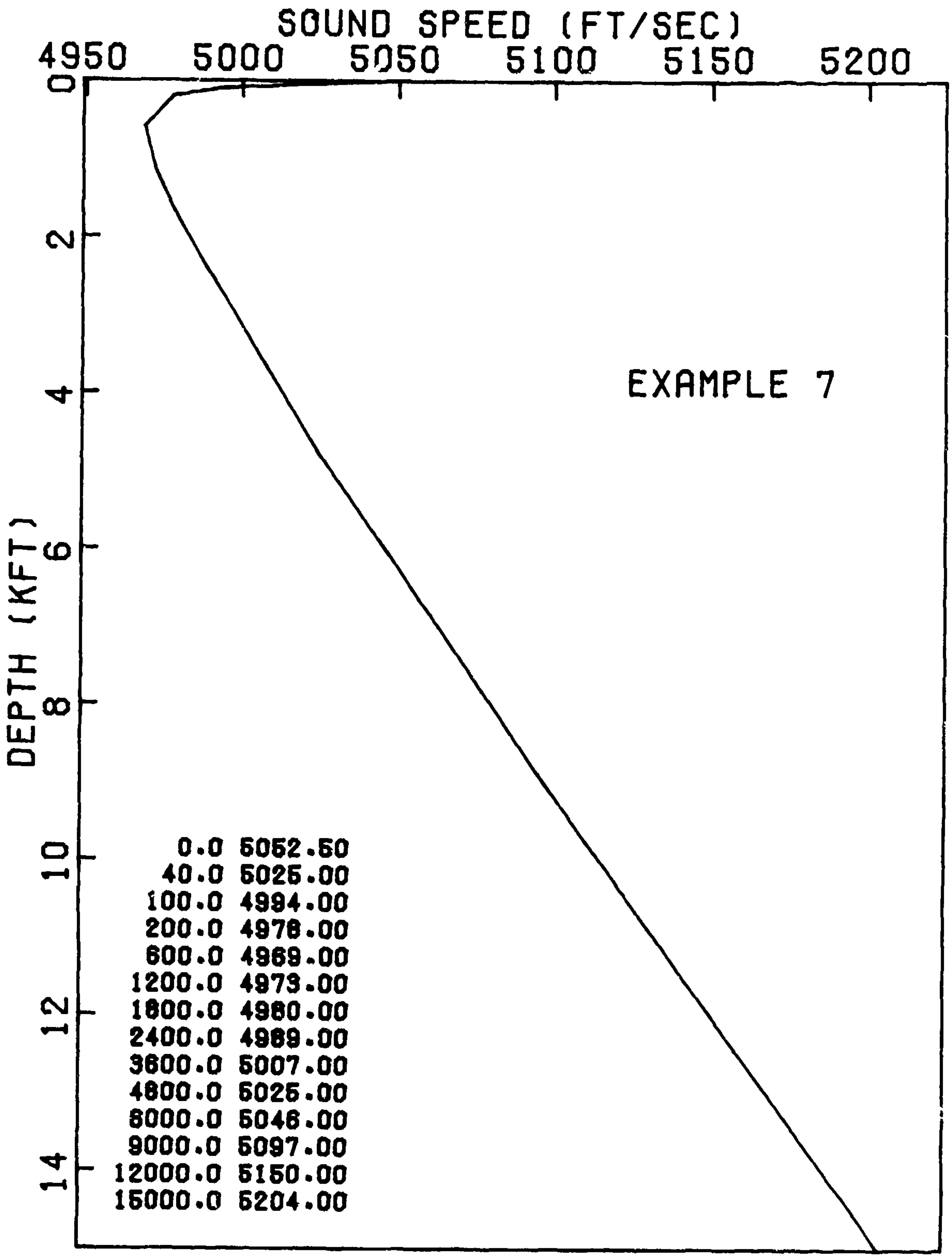

UNCLASSIFIED

(U) Figure 5-39. Sound Speed Versus Depth Profile, Example 7.

(U) The resulting propagation loss from the two runs is plotted in Figure 5-40. The solid line is the output from Mod 1 and the x's are from Mod 2. It is evident from these runs that interpolating an extra point along a linear profile segment can be a dangerous thing to do. The curves differ in two major ways: (1) the Mod 2 curve shows on the average lower loss than Mod 1 and (2) though both curves exhibit a periodicity, the periods differ. With the aid of the diagnostic print statements we shall attempt to find out what happened.

(U) Consider first Mod 1. In deciding where to fit the two half-parabolas to form the temporary smooth profile, AXIS looks above and below the axis for the next layer boundary and selects the one which has the smaller sound speed. In Mod 1 the boundary selected was the 1200-foot boundary. The half-parabolas are fitted at 1200 ft and at the corresponding point above (422 ft) where the sound speed has the same value. The period of the zero-degree ray in this smoothed profile is 20.16 kyd and the vertex depths of the ray with the same period in the original profile are 485.2 and 970 ft. Since the originally specified depth of 600 ft is closer to the upper vertex depth than to the lower, the source and receiver depths are moved to 485.2 ft, a change of 115 ft. INSERT then moved the receiver depth up another 10 ft to 475.2. With the source and receiver thus relocated the range to the cusp is found in accordance with the FACT rules to be 21.02 kyd. This is the period which is observed in the propagation loss curve.

(U) Looking now at the Mod 2 output we find that the first layer boundary encountered on either side of the axis is the boundary at 580 ft. The two half-parabolas are then fitted at 580 ft and the equi-velocity counterpart 667.5 ft. This is a quite different smoothed profile from that generated for Mod 1 and it leads to a period of only 6.61 kyd for the zero-degree ray. The vertex depths of the ray with the same period in the original profile are 587.7 and 649.8 ft. The source and receiver are therefore moved to the nearer, which is 587.7 ft. The receiver is then raised to 577.7 ft. Comparison with Mod 1 shows that interpolating the extra data point has caused the Mod 2 run to begin its ray computations in a significantly different environment. The range to the cusp in Mod 2 is 8.9 kyd, thus accounting for the periodicity observed in Figure 5-40. This period is only about 42% of that observed in Mod 1.

(U) The problem here arises from the manner in which the "smoothed" profile is constructed. In looking for the point at which to fit the half-parabolas the program merely looks for the next layer boundaries and asks no questions about their physical significance. This means that the results depend not only upon the physical characteristics of the velocity profile but also upon the manner in which the profile is formulated.

(U) Before leaving this example a few additional observations may be made. The range-angle curves for the first sector of Mod 2 are particularly interesting. The curves are plotted in receiver angle space in Figure 5-41. The true range-angle curves are the irregular lines containing many caustics. Plotted on the same graph is the cusp parabola. (Properly this should be plotted in source angle space but the difference in sound speed between source and receiver in this case is small enough to render the present plot meaningful.) Examination of these curves suggests that drawing a single parabola over the whole sector results in gross oversmoothing. In the vicinity of the cusp the curvature of the parabola bears no relation to the curvature of the true curves. For this reason virtually no confidence can be placed in the accuracy of the cusped caustic correction.

(U) When we come to the smooth caustic the situation is immeasurably worse. The caustic is formed by the little dip just to the left of 0 degrees on branch 1.

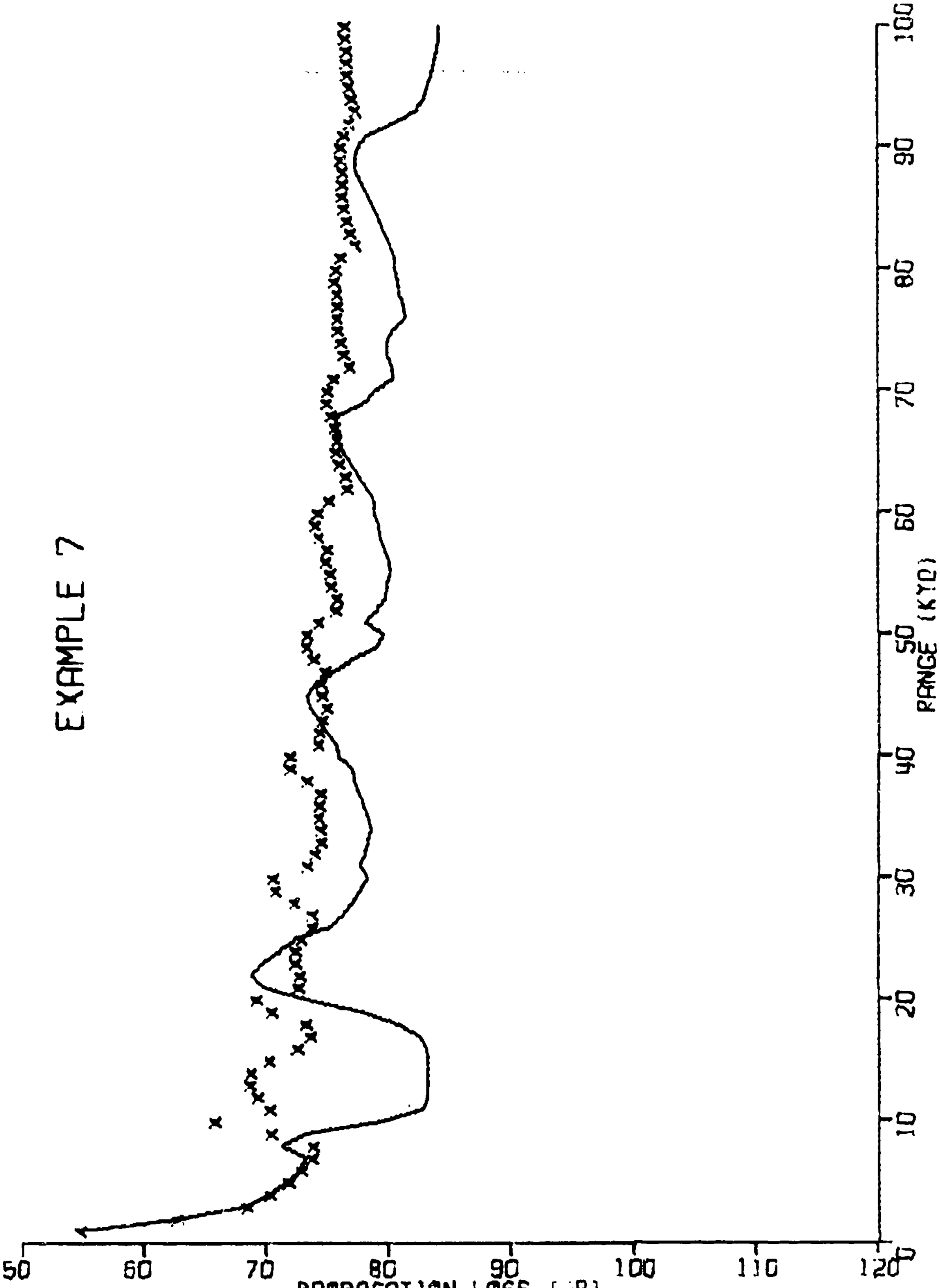

UNCLASSIFIED

(U) Figure 5-40. Propagation Loss, Example 7.

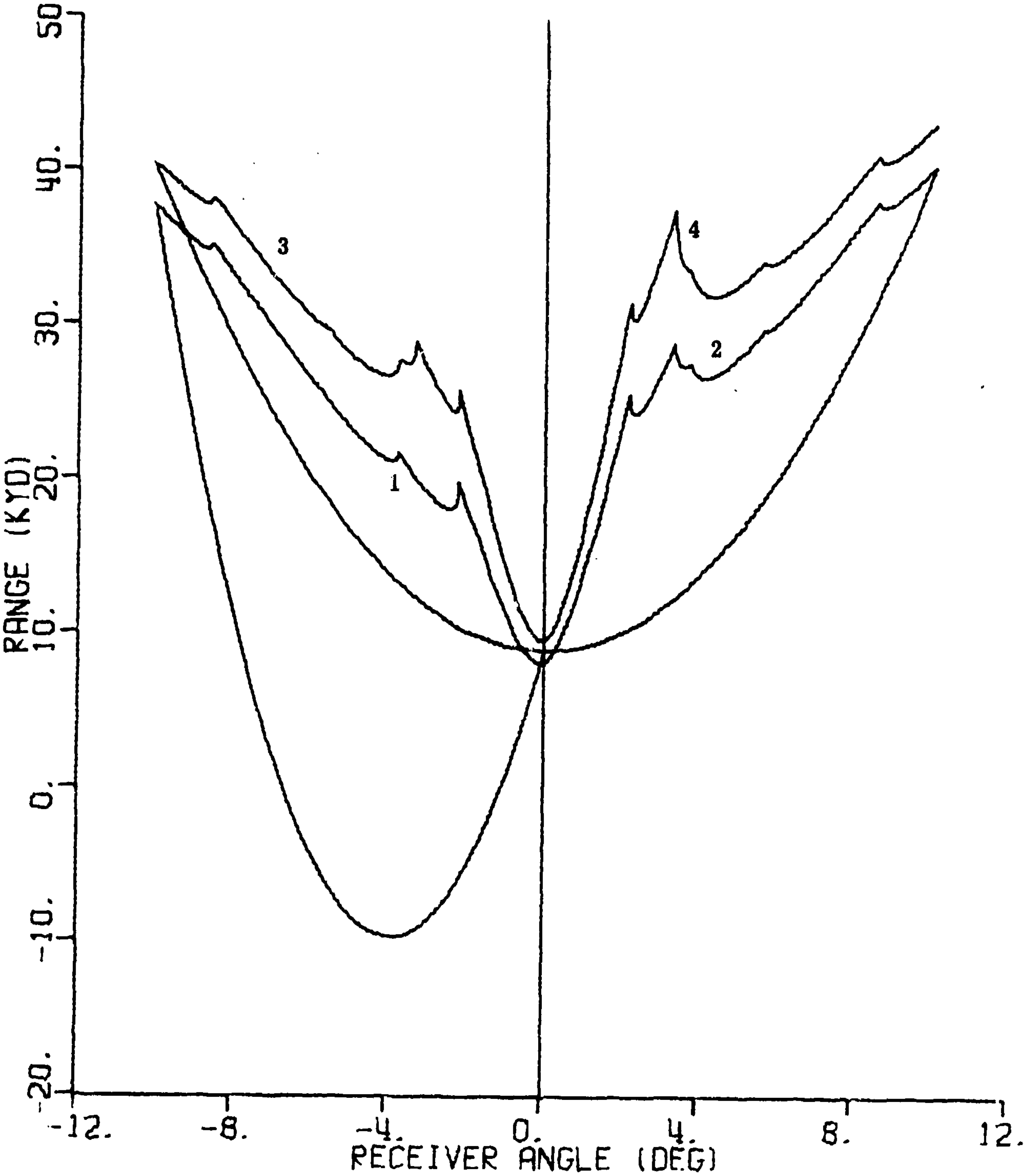

UNCLASSIFIED

(U) Figure 5-41. Range-angle Curves, Example 7.

The three points for the parabolic fit consist of the assumed cusp location, the second ray of the sector (which generated the minimum range), and the last ray of the sector. As has been stated previously, the assumed cusp location does not lie on the curve FACT is trying to fit. The situation is so bad in this case that the parabola dips far below zero in range, yielding an error of about 20 kyd in the location of the caustic. Furthermore whenever a minimum occurs in a parabola, FACT checks on the location of the minimum. If it lies outside the angular limits of the sector or if the range to the caustic is negative, the caustic is ignored. In this case FACT started off in subroutine CUSP knowing that a caustic existed. It therefore called INSTOR to process the caustic. But INSTOR made such a poor fit of the parabola that it had to conclude that there was no caustic after all. Instead it calculated ordinary ray intensities from the erroneous slope of the parabola.

(U) A bit of interesting information was also gleaned from the Mod 1 diagnostic output. This information concerns the low frequency cut-off effects. The critical angle CRITANX in this case is 2.15 degrees. Examination of the processing of the smooth caustic associated with one of the cusps (first sector, second arrival order) reveals that the ray angle evaluated at the axis depth falls below the critical angle and is therefore capable of yielding information to be checked against Figure 5-5. From information available in the diagnostic output the curves of Figure 5-42 were plotted. The upper graph shows the angle at the receiver depth and the angle at the axis depth as a function of range. As the angle at the receiver drops to zero the angle at the axis manages to fall just slightly below the critical angle. In the bottom graph is plotted the intensity correction factor, also as a function of range. In agreement with Figure 5-5 it can be seen that for the angles involved, the low frequency cut-off actually resulted in an amplification.

Example 8 (U)

(U) This example was encountered accidentally in the course of a series of routine predictions with the FACT model. The velocity profile, shown in Figure 5-43, is from the Indian Ocean. The external bottom loss curves inserted for this area are listed in Table 5-4.

Table 5-4. (U) Bottom Loss, Example 8

25 Hz		50 Hz		100 Hz	
Graz. Ang. (deg)	Loss (dB)	Graz. Ang. (deg)	Loss (dB)	Graz. Ang. (deg)	Loss (dB)
0.0	0.3	0.0	0.8	0.0	1.5
7.8	0.3	7.8	0.8	7.8	1.5
12.5	0.6	13.0	1.1	12.8	1.3
20.0	0.45	18.0	0.95	20.0	1.77
22.5	0.4	22.5	1.1	22.5	1.8
30.0	1.4	30.0	2.0	30.0	3.25
32.6	1.8	32.3	2.25	32.6	3.9
38.0	3.5	37.5	4.0	38.0	6.5
48.0	10.0	42.6	9.0	42.5	10.0
90.0	10.0	47.5	12.0	90.0	12.0
		90.0	12.0		

UNCLASSIFIED

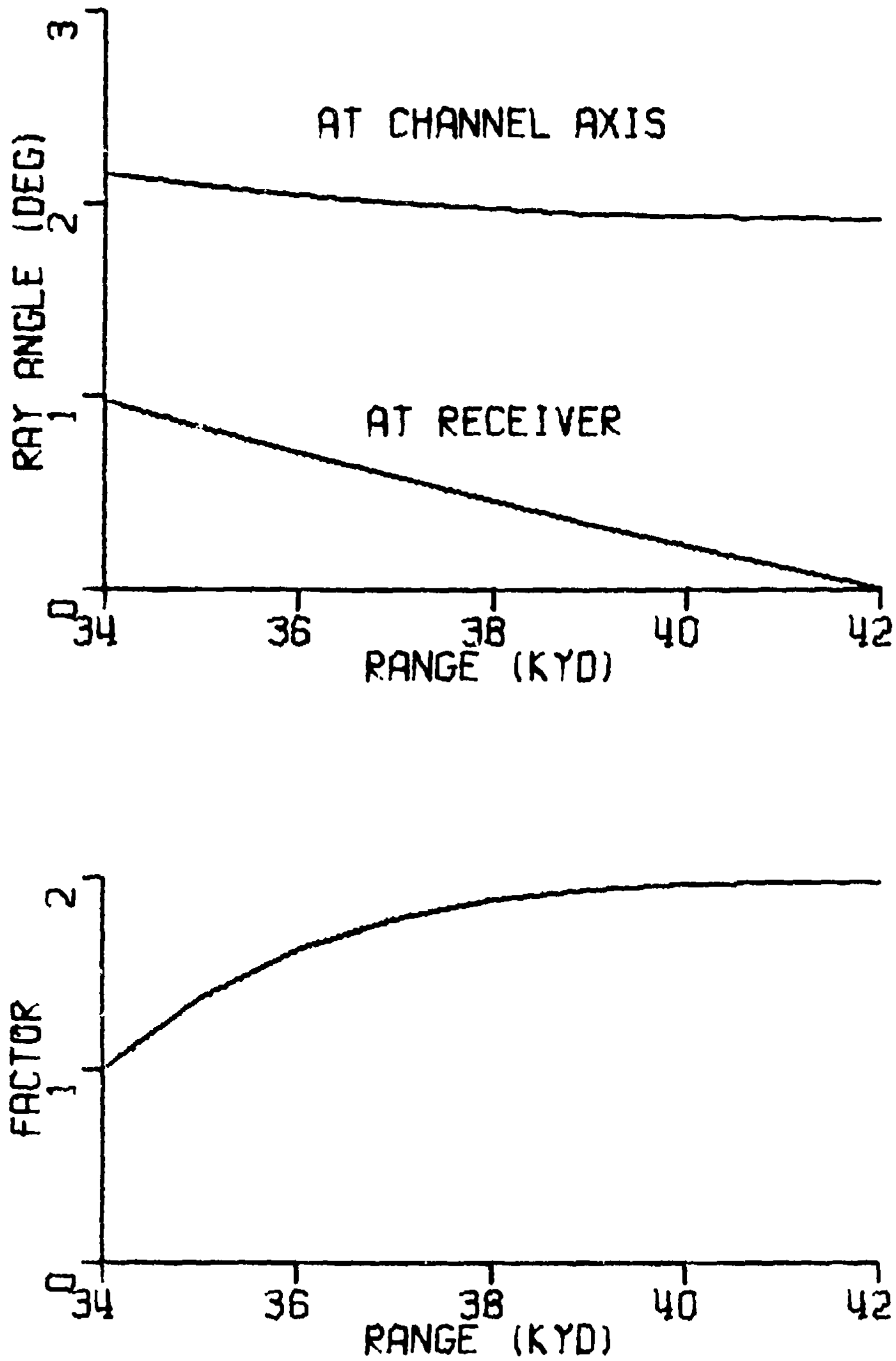

UNCLASSIFIED

(U) Figure 5-42. Low Frequency Cut-off Effects, Example 7.

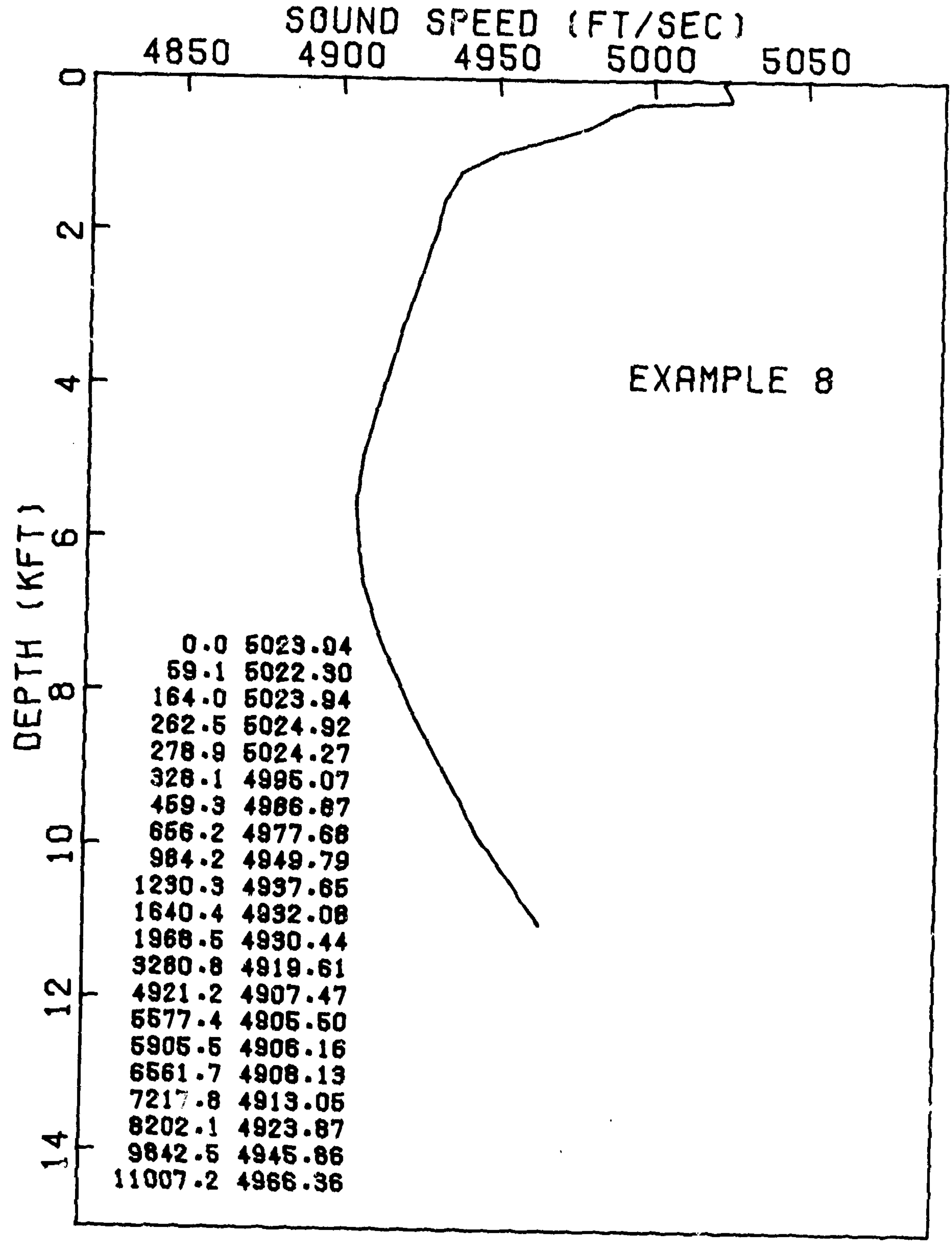

UNCLASSIFIED

(U) Figure 5-43. Sound Speed Versus Depth Profile, Example 8.

In the NADC version of FACT, when the frequency specified for the propagation loss predictions is intermediate between adjacent frequencies of the externally supplied bottom loss curves, the bottom loss at the desired frequency is obtained by linear interpolation.

(U) The unusual feature of the velocity profile used in this example is the presence of a sound channel just below the surface. This is not a typical isothermal surface duct, but rather a genuine submerged channel with a minimum velocity axis at a depth of 18 m (59.1 ft). The question arises: should this duct be treated as a genuine submerged channel, or should the concavity in the profile be ignored and the duct treated as an ordinary surface duct? It was felt that the best way to answer this question would be to make runs both ways and compare the results. Consequently two semi-coherent runs were made, one with the parameter IL set to 1 (genuine submerged channel) and the other with IL set to 4 (surface duct module replacing ray computations in the channel). The runs were made at frequencies of 30 and 90 Hz with the source at 25 ft and the receiver at 90 ft.

(U) The results of the two runs differed so greatly that it was decided to repeat them on the diagnostic version of FACT. After an examination of the diagnostic output it was decided to replace the original runs with a new set of runs with altered source and receiver depths. Accordingly, two pairs of runs were made with the source at 50 ft, one pair with the receiver at 94.9 ft and the other pair with the receiver at 95.0 ft. The reason for the changes will become evident shortly.

(U) The propagation loss curves at 30 Hz for the four runs are plotted in the top graph of Figure 5-44. The identification of the curves, labeled 1 to 4, is as follows:

Curve	IL	ZR (ft)
1	1	94.9
2	4	94.9
3	1	95.0
4	4	95.0

In view of the incredibly large disagreement among these curves, the question logically arises: Which, if any, is correct? In an attempt to answer this question, runs were made for the same inputs (receiver depth = 95.0 ft) on the AP2 normal mode program and on PLRAY. A plot of the AP2 output is shown in the center graph of Figure 5-44. To aid in averaging the extremely large oscillations of the fully coherent AP2 output, a smoothed curve, obtained from a 13-point weighted sliding window, is plotted on the same graph. The semi-coherent PLRAY output is shown at the bottom of Figure 5-44. The excellent agreement between PLRAY and the smoothed AP2 output makes it appear likely that these models are yielding correct results. If this is so, then all of the FACT curves are rather badly in error. Incidentally, PLRAY automatically treats the upper channel as an ordinary surface duct.

(U) The purpose of the alteration of the source and receiver depths was to check out a portion of the FACT model which has not thus far been tested. In the original runs an examination of the diagnostic output revealed that the period of the zero-degree ray in the "smoothed" profile was 19,945 ft and that the ray with the same period in the original profile experienced an upper vertex at a depth of 22.63 ft and a lower vertex at a depth of 122.28 ft. Since the originally specified source and receiver depths of 25 and 90 ft lay between these values, they had to be moved. The separation between the upper vertex and the shallower of these two depths (25 ft) was found to be 2.37 ft while the separation between the deeper (90 ft) and the lower vertex was found to be 32.28 ft. The algorithm in subroutine AXIS moves both the source and

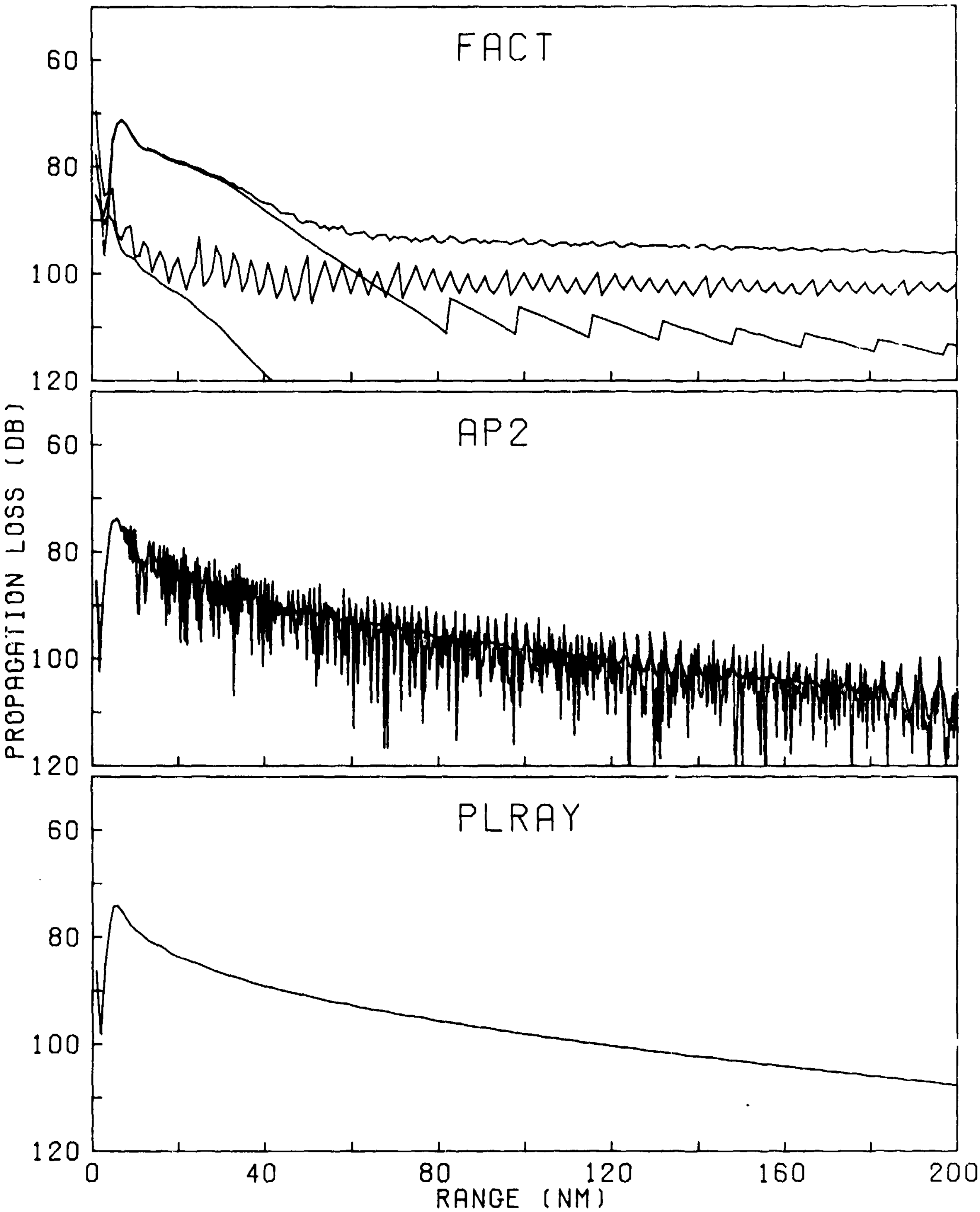

UNCLASSIFIED

(U) Figure 5-44. Propagation Loss, Example 8.

receiver to whichever vertex depth results in the smaller separation. Therefore in this instance they were both moved upward to 22.63 ft. Subsequently in subroutine INSERT one of them was moved 10 ft farther upward, resulting in depths of 12.63 and 22.63 ft in lieu of 25 and 90.

(U) With this information available it was decided to observe how much difference in output would result from moving the depths downward instead of upward. Selection of a source depth of 50 ft and a receiver depth of 94.9 ft resulted in a separation of 27.37 ft at the upper vertex and 27.38 ft, thereby causing the depths to be moved downward to 122.28 ft, followed by a subsequent raising of one of the depths to 112.28 ft. The differences between curves 1 and 3 as well as the differences between curves 2 and 4 are produced by this change in the source and receiver depths.

(U) Let us now investigate the behavior of the individual FACT curves. Consider first runs 2 and 4 which the channel was treated as a normal surface duct (IL = 4). In these runs the surface duct module, which replaces ray computations, predicts an extremely high range attenuation, so high, in fact, that the effects of the duct are visible only in the first three miles. Beyond three miles the ducted energy is completely masked by other arrivals.

(U) Like Example 3, the present profile is bottom-limited, with the maximum sound speed occurring at the bottom of the surface duct. Subroutine ANGSCH therefore defines only one sector (NGRPS = 1) and computes only two rays. As in Example 3, the entire propagation loss output, apart from the surface duct contribution in the first three miles, is generated from these two rays.

(U) After an initial oscillation resembling that of AP2 and PLRAY, curve 4 shows a steady increase in loss out to a range of about 80 nm, beyond which it continues in a series of saw teeth of steadily diminishing amplitude. Although not visible in Figure 5-44 because of the high loss, curve 2 exhibits a similar sawtooth behavior with loss values about 33 dB greater than those of curve 4. The large increase in loss in both curves with increasing range is due to the surface imaging phenomenon involved in the coherent ray summation. If coherence occurs at both ends of the ray path, as is the case in the current run, only one of the four paths is computed for each arrival order and the resultant intensity is obtained by multiplying the intensity of this one arrival by the coherence factor

$$F = 16 \sin^2\phi_S \sin^2\phi_R$$

where ϕ_S and ϕ_R are the phase angles at the source and receiver ends

$$\phi_S = 2\pi f z_S \sin\theta_S/c_S$$

$$\phi_R = 2\pi f z_R \sin\theta_R/c_R$$

and f is the frequency and z_S and z_R are the source and receiver depths. The use of the angle θ_S and θ_R and sound speeds c_S and c_R is an approximation, since the coherence computation is based on the assumption that θ and c remain constant all the way from the source and receiver depths to the surface.

(U) Considering first curve 4, for which the source and receiver depths were 112 and 122 ft, it is found that for ray angles less than about 30 degrees the phase angles ϕ_S and ϕ_R are below 90 degrees. Hence, as the range increases and the ray angles become smaller, the coherence factor steadily decreases and the propagation loss curve exhibits its steady drop.

(U) The saw teeth are explained in terms of the bottom bounce computations. The first arrival order extends from 1 to 23 m, the second from 1 to 48 m, the third from 1 to 72 m, and the fourth from 1 to 96 m. Only the first four arrival orders include propagation at steep angles out

to 90 degrees (i.e., ranges down to 1 m). The fifth order extends from 83 to 120 m, the sixth from 100 to 145 m, the seventh from 116 to 169 m, etc. As the maximum range of any given arrival order is approached, destructive interference due to the shallow angle at the surface causes the intensity to fall rapidly toward zero. Continuity of the propagation loss curve at these points is provided by contributions of higher order arrivals. However, at ranges less than 83 miles there is no fifth or subsequent arrival order to take up the slack. When the fifth order begins to appear at 83 m, the fourth order has already become so weak that a large discontinuity of about 7 dB occurs. Next, at 100 m the appearance of the sixth order creates a similar though slightly smaller discontinuity. It is in this manner that the sawtooth pattern is generated.

(U) Curve 2, if the propagation loss scale were suitably extended, would show a similar sawtooth pattern, generated in the same way. The 33 dB difference in levels between the two curves is readily accounted for. In the sawtooth region the phase angles ϕ_S and ϕ_R are so small that their sines may be replaced by the angles themselves with negligible error. The contribution of the coherence factor in dB may therefore be written

$$10 \log F = 20 \log (16\pi^2 f^2 z_S z_R \sin \theta_S \sin \theta_R / c_S c_R)$$

In comparing the coherence factors of curves 2 and 4 for the same range we note that the dominant effect comes from the difference in source and receiver depths z_S and z_R. Alteration of these depths (from 112.28 and 122.28 ft to 12.63 and 22.63 ft) will produce small changes in c_S and c_R as well as in the angles θ_S and θ_R, but to a first approximation they may be assumed to remain fixed.

With this assumption, the difference in dB level between the two curves would be expected to be

$$20 \log (112.28 * 122.28/12.63 * 22.63) = 33.6 \text{ dB}$$

When compared with the user-specified depths of 50 and 95 ft, curve 4 is 9.2 dB too high (too low loss) and curve 2 is 24.4 dB too low (too high loss). Unfortunately it can be seen that in the sawtooth region curve 4 already exhibits too high a loss when compared with AP?. Lowering it by 9.2 dB would make matters worse. The reason for this discrepancy is the failure of FACT to include steep-angle propagation in any of the bottom bounce arrival orders beyond the fourth. As may be seen in FACT curve 4 of Figure 5-2, no contributions from the fifth arrival order are included at ranges less than 83 nm. If these contributions had been included, the curve would have continued to rise instead of dropping to form the sawtooth. It appears quite likely that if the contributions from all the arrival orders had been extended inward in range instead of being terminated to form the saw teeth, the above discrepancy would be accounted for. However, even if this error were corrected, it would still be true that the moving of the source and receiver depths away from the locations specified by the user creates unacceptably large errors in the output propagation loss.

(U) Let us now turn to curves 1 and 3, corresponding to the case (IL = 1) in which the upper channel is treated as a genuine sub-surface duct, in strict accordance with the input velocity profile data. Considering first curve 1, which corresponds to the originally specified receiver depth of 94.9 ft, we find that in moving both depths to 22.63 ft, subroutine AXIS has generated a cusped caustic. There are now four sectors. The first sector is bounded on its outer edge by the limiting ray to the surface. It consists of RR rays in the upper channel and includes the cusp. The second sector is bounded by the ray to the

164-foot depth. This sector makes no appreciable contribution to the resultant intensity. The third sector is bounded by the limiting ray to the bottom of the upper channel; it contains RSR rays. The fourth sector consists of the two bottom bounce rays and is identical to the single sector of the IL = 4 case.

(U) Because of the shallowness of the sub-surface channel, the period of the ray to the cusp is slightly less than 4 nm. The dominant contribution to the resultant intensity comes from the cusped caustics, which are responsible for the sawtooth pattern, each tooth representing a different arrival order.

(U) Examination of the details of the diagnostic output reveals many of the same problems observed in previous examples. Figure 5-45 shows the range-angle curves for the first arrival order in the first sector. These curves are plotted in source angle space and show the fitted parabola which spans a forbidden zone covering the bulk of the sector. It is doubtful that such a curve can lead to reliable results. Figure 5-46 shows the curves in receiver angle space and includes the fitted parabola which is intended to represent the associated smooth caustic. Clearly the curvature of this parabola is radically different from the curvature of the true range-angle curve.

(U) In the third sector the parabolic fit is of the square root type. Figure 5-47 is a plot of range vs. $\sqrt{\theta - \theta_1}$. Here we find the same problem as we observed in Example 6, namely, a minimum occurring at a negative value of the square root. This minimum is erroneously interpreted as a caustic. Actually it has little or no bearing on the resultant propagation loss because the rays in this sector are treated coherently and the resulting destructive interference is so nearly complete as to render the contribution from sector 3 negligible. In fact, after the first few miles the contributions from all three of the outer sectors are throughly negligible in comparison with the cusped caustic contribution of sector 1.

(U) The situation with regard to curve 3 is much the same as that for curve 1, but with one major difference. First of all, it should be noted that the cusped caustic correction is about the same. Secondly, the same problem with the false caustic arises in the third sector. It appears that the occurrence of this error is sufficiently widespread as to render its correction mandatory.

(U) The major difference in this case is that, because of the increased source and receiver depths, the 2-mile criterion for the maximum horizontal separation of the direct and surface-reflected rays is not met. Therefore the rays in sector 3 (involving the erroneous caustic) are treated incoherently. Under the present conditions of extreme destructive interference the difference between coherent and incoherent addition is tremendous. As a result the contribution from the rays of sector 3 is now the dominant contribution to the overall intensity, thus accounting for the difference both in detailed structure and in average level between curves 1 and 3.

(U) The results of the 30 Hz runs rather than the 90 Hz runs have been presented in this report because the discrepancies are more dramatic than those observed at 90 Hz. However, even at 90 Hz the discrepancies are serious enough to render the results unacceptable.

(U) The characteristics of all four FACT curves can thus be accounted for in terms of the manner in which the model operates. However, all four curves are incorrect. It appears that the FACT model cannot be used to make low frequency predictions in this environment.

(U) A final comment concerning this example is in order. In the runs in which the surface duct module was used in lieu of ray computations (IL = 4) there is no need to move the source and

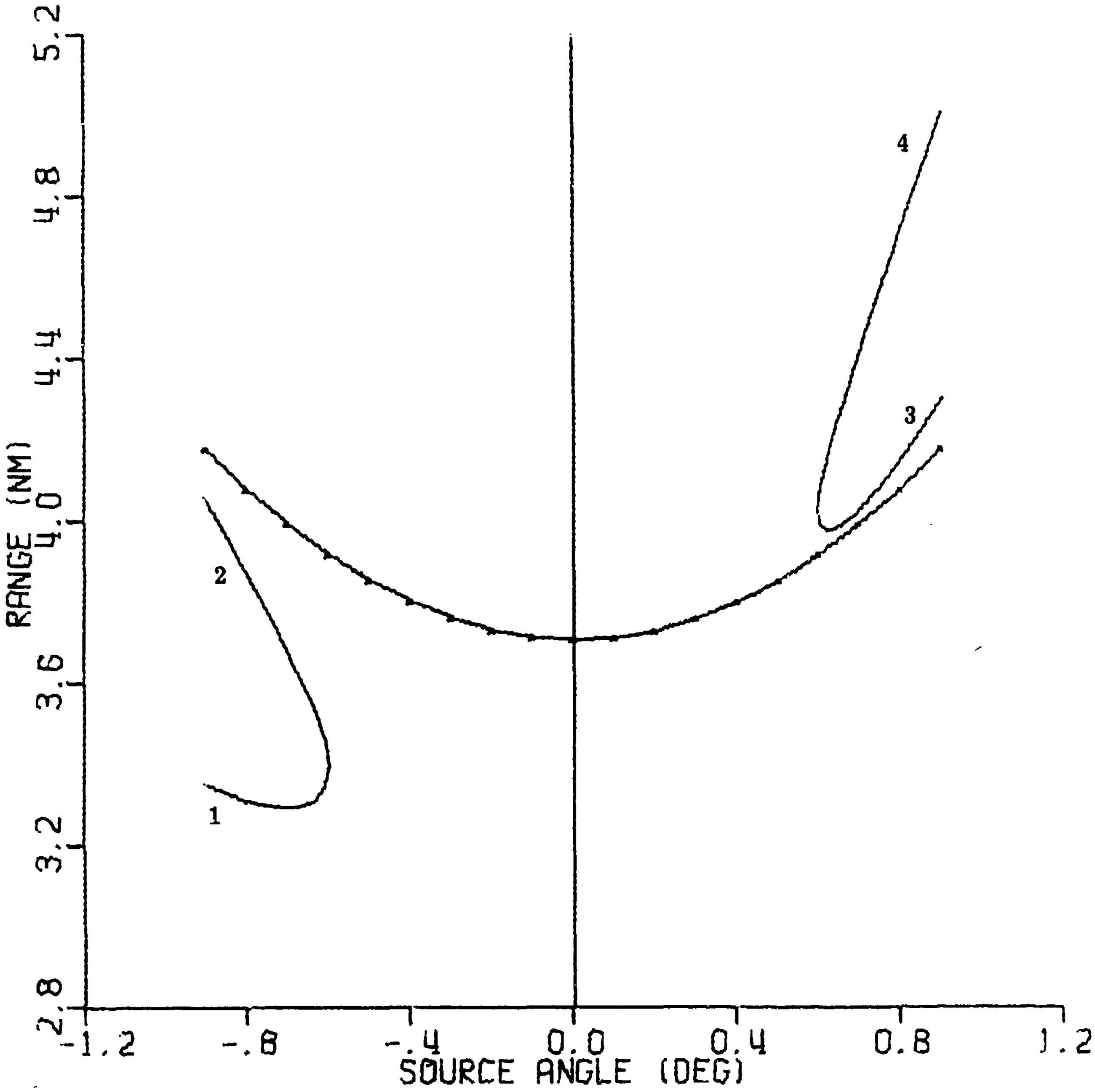

UNCLASSIFIED

(U) Figure 5-45. Range-angle Curves in Source Angle Space, Example 8.

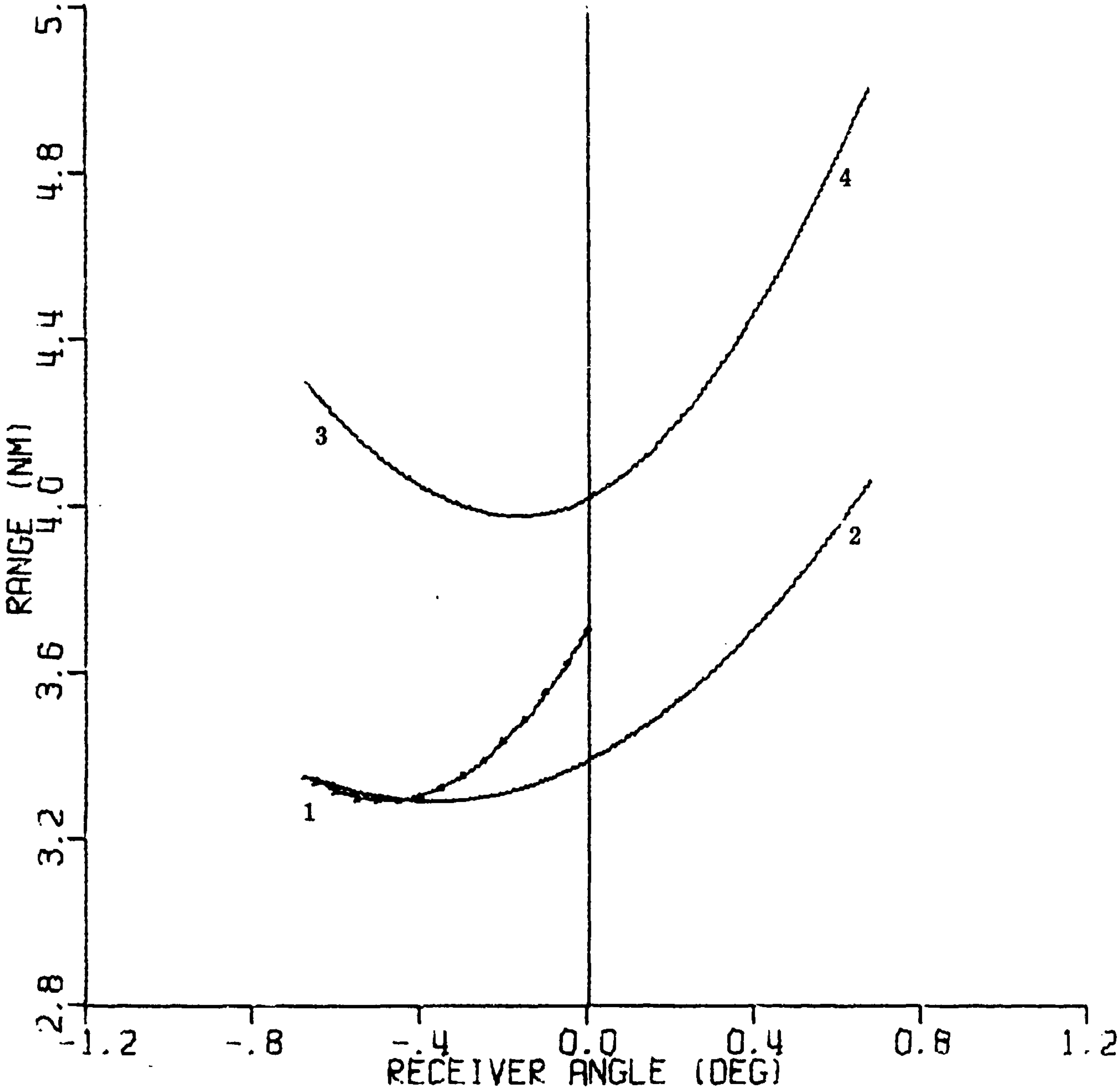

UNCLASSIFIED

(U) Figure 5-46. Range-angle Curves in Receiver-angle Space, Example 8.

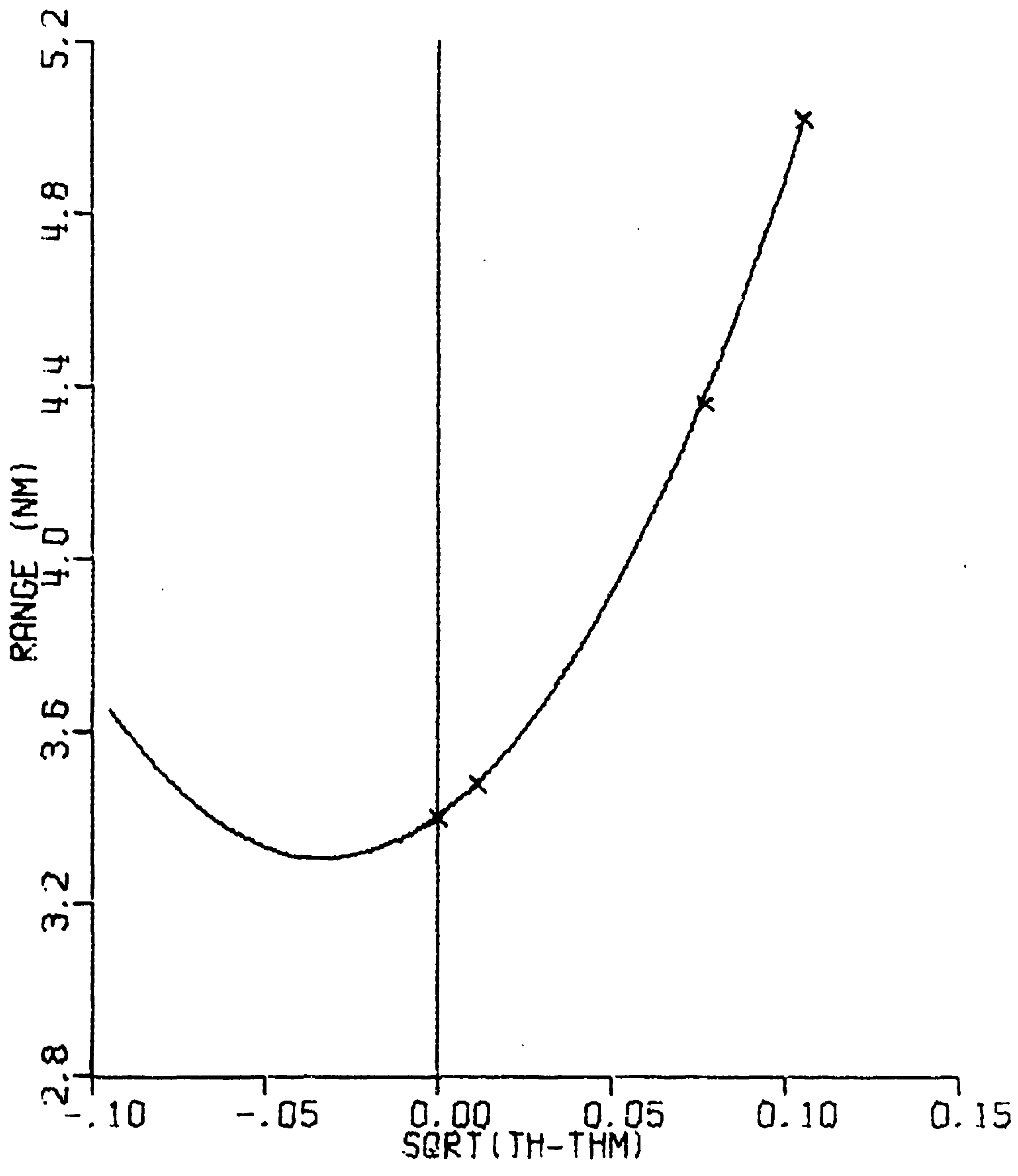

UNCLASSIFIED

(U) Figure 5-47. Erroneous Caustic Arising from Negative Square Root, Example 8.

receiver depths. Since no ray computations are made in the duct, there can be no problems from cusped caustics or near-axial ray propagation. There is thus nothing whatever to be gained but much to be lost by moving these depths.

Example 9 (U)

(U) This example was selected to investigate the effect of frequency variation on propagation in a sub-surface duct. A velocity profile from the western Atlantic Ocean was found which exhibits a prominent channel 91 m (298 ft) thick with its axis at a depth of 74 m (244 ft). The profile was modified slightly, reducing the number of layers but retaining the essential features. The modified profile is listed in Table 5-5. In order to prevent bottom returns from obscuring the effects of the channel, a very poorly reflecting bottom was arbitrarily assumed. For the AP2 normal mode program the bottom was specified in terms of geophysical parameters. It consisted of a semi-infinite homogeneous

Table 5-5. (U) Velocity Profile, Example 9

Depth (m)	Sound Speed (m/sec)
0.00	1529.30
29.39	1518.58
64.75	1491.46
74.35	1490.85
150.14	1495.71
303.83	1483.06
351.72	1480.88
472.60	1478.69
1345.10	1486.63
2529.84	1508.41

UNCLASSIFIED

non-elastic medium with a density ratio of 1.1 relative to sea water, a sound speed ratio of 0.99999 relative to the water immediately adjacent to the bottom, and a volume attenuation coefficient of 0.001 dB/ft (0.00328 dB/m) at 1000 Hz, assumed to vary linearly with frequency. For use with FACT the bottom loss as a function of grazing angle was computed from an auxiliary computer program and is listed in Table 5-6. It will be noted that for such a geophysical model the bottom loss is independent of frequency.

Table 5-6. (U) Bottom Loss, Example 9

Graz. Ang. (deg)	Loss (dB)	Graz. Ang. (deg)	Loss (dB)
0.0	0.0	4.0	20.5
0.5	2.8	5.0	23.0
1.0	5.6	6.0	24.4
1.5	8.6	8.0	26.1
2.5	14.2	15.0	26.4
3.0	16.7	90.0	26.4
3.5	18.8	UNCLASSIFIED	

(U) Runs were made on both FACT and AP2 at frequencies of 10, 30, 100, and 300 Hz with the source and receiver both in the channel at depths of 270 and 220 ft (82.3 and 67.1 m) respectively. An additional set of runs was made with the receiver well above the channel at a depth of 100 ft (30.5 m).

(U) The results of the first set of runs are shown in Figures 5-48 to 5-51 inclusive. On these plots the FACT curves are identified by x's, while the AP2 curves are plotted as plain lines. Looking first at the AP2 curves, we see that at 10 Hz the duct has virtually no effect; the energy has leaked out in the first three kiloyards. Beyond this point the curve proceeds outward in range in a series of large scallops with a period of about 40 kyd. The first scallop exhibits a set of rapid oscillations indicative of a multipath bottom interaction. These oscillations die out at longer ranges because of the high bottom loss. The peaks at about 40 and 80 kyd are actually convergence zones, although the zones are not well developed at 10 Hz. Turning now to the 30 Hz curve, Figure 5-49, we see that the leakage out of the duct is somewhat less rapid. It now takes about 6 kyd to dissipate the energy. Also the convergence zone peaks have sharpened up and have risen by about 20 dB. At 100 Hz, Figure 5-50, the

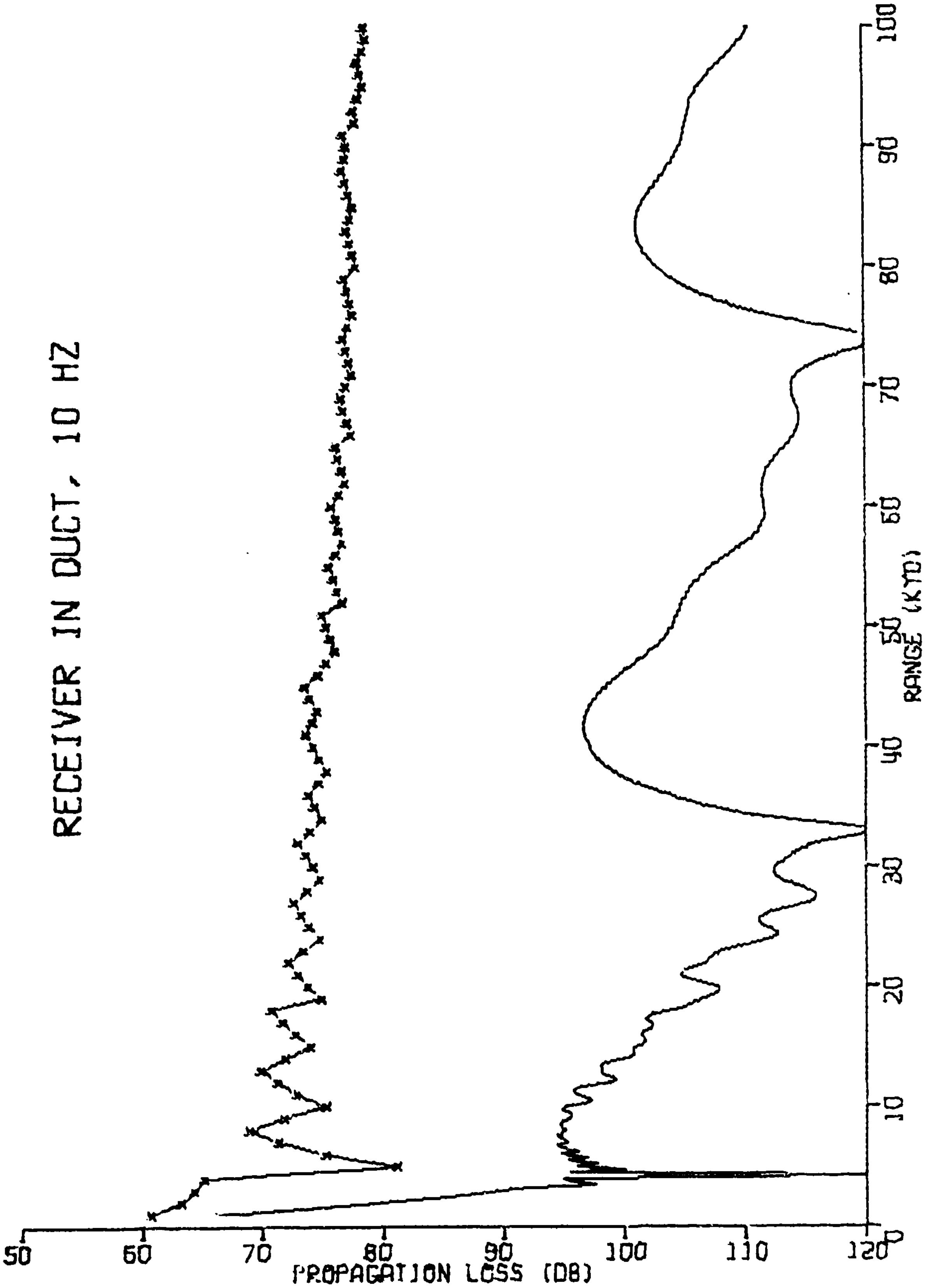

UNCLASSIFIED

(U) Figure 5-48. Propagation Loss at 10 Hertz, Example 9. Receiver in Channel.

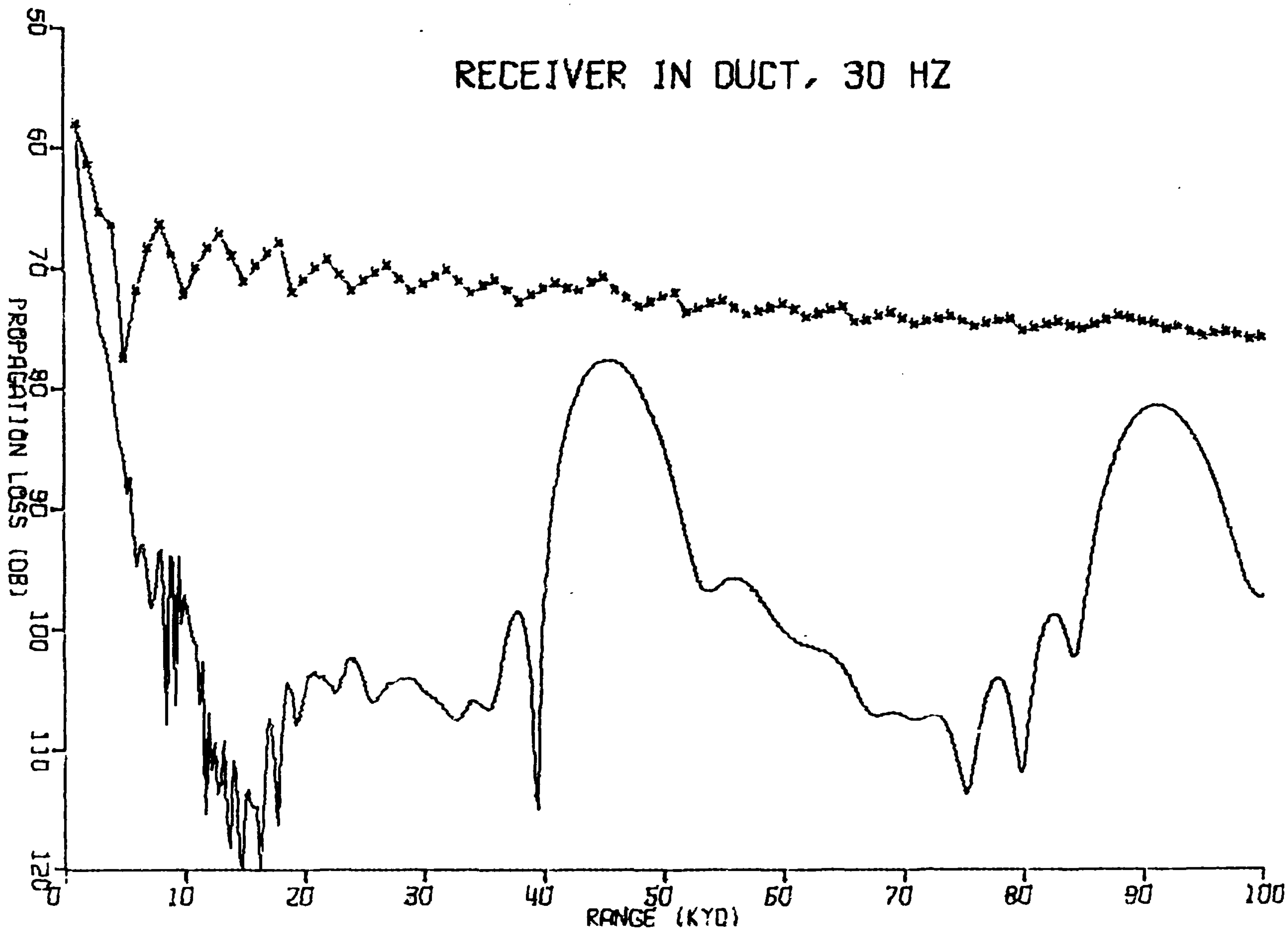

UNCLASSIFIED

(U) Figure 5-49. Propagation Loss at 30 Hertz, Example 9. Receiver in Channel.

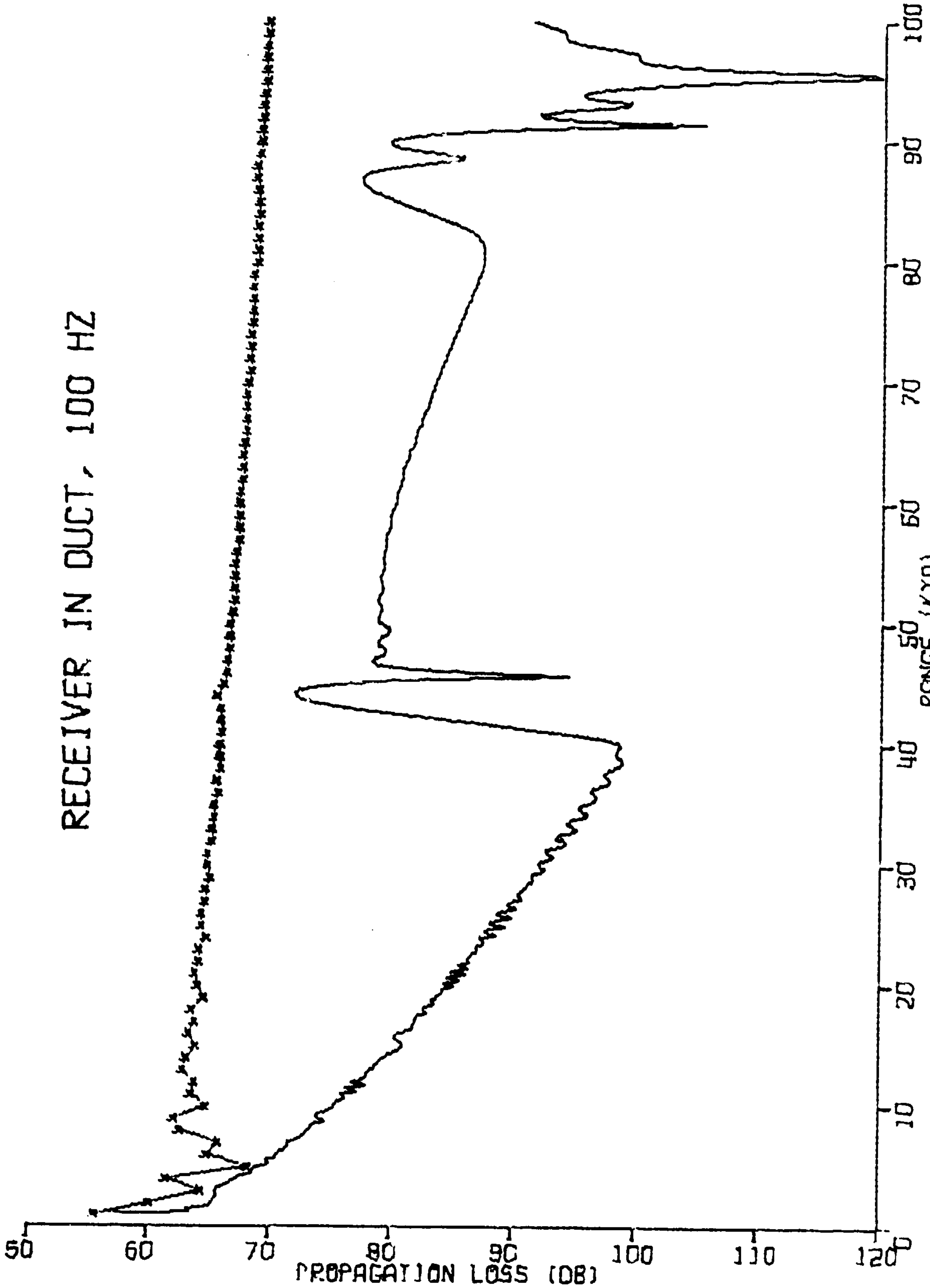

UNCLASSIFIED

(U) Figure 5-50. Propagation Loss at 100 Hertz, Example 9. Receiver in Channel.

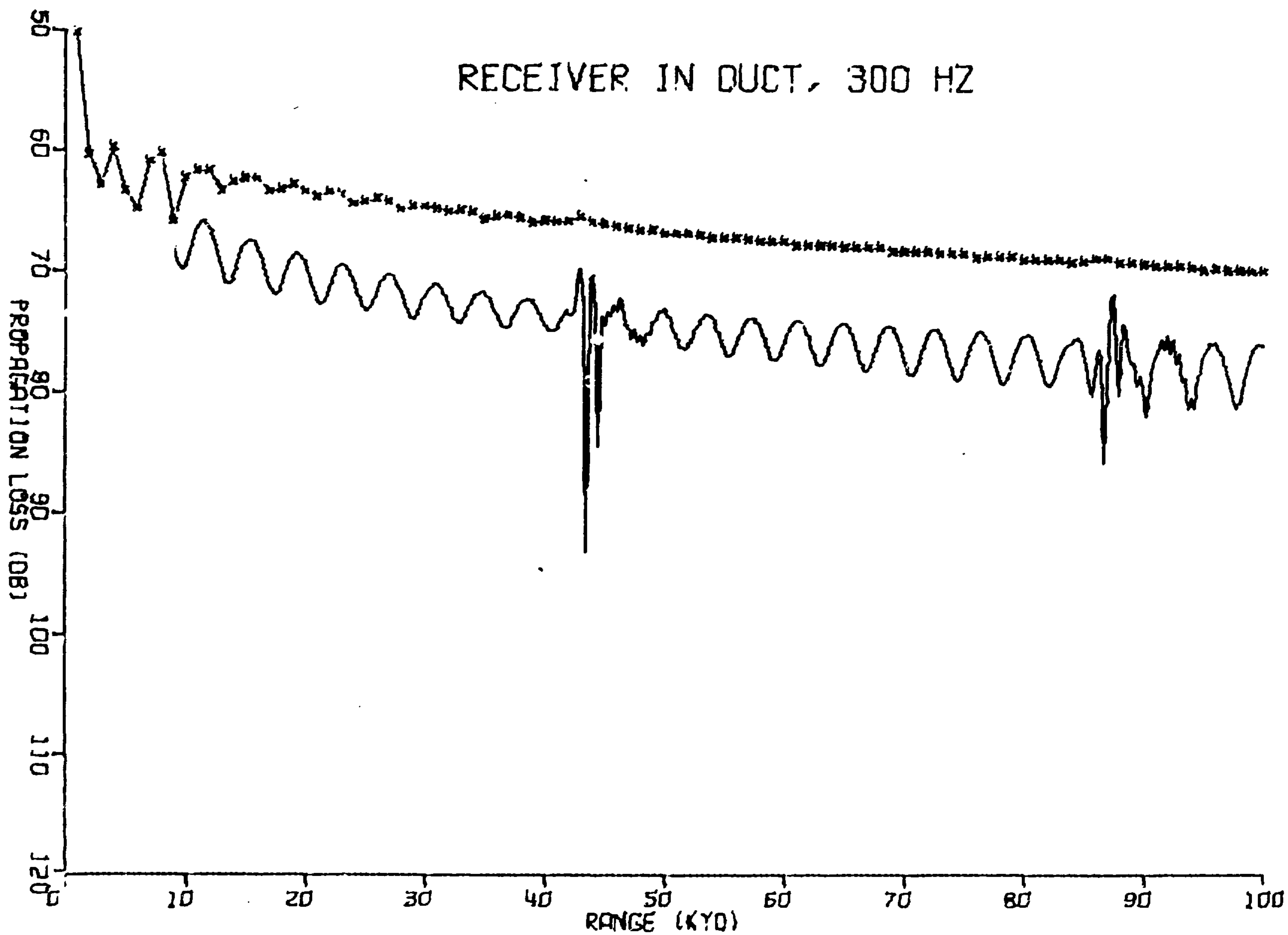

UNCLASSIFIED

(U) Figure 5-51. Propagation Loss at 300 Hertz, Example 9. Receiver in Channel.

duct has improved significantly. The energy has not all leaked out even at 40 kyd, where the first convergence zone begins. The zone peaks are now quite sharp and are about 5 dB higher than at 30 Hz. The rather high level between the convergence zones suggests appreciable trapping of energy in the duct at the first zone. Finally, at 300 Hz* the modes are so highly trapped in the duct that virtually no energy leaks out. As a result, the convergence zones are almost completely obscured by the ducted energy. They are observable only by the rapid oscillations that occur at ranges slightly beyond 40 and 80 kyd.

(U) Looking now at the FACT curves, we see that the leakage of energy out of the duct is not accounted for at any of the frequencies. As a result, all the features described above for the AP2 results are swamped by the ducted energy, though faint traces of the convergence zones can be discerned at 100 and 300 Hz. At frequencies of 100 Hz and below, the FACT output is grossly in error. Even at 300 Hz, although the FACT and AP2 curves exhibit the same trend, FACT produces an average level about 7 dB too high.

(U) It must be emphasized that the errors at 100 Hz and below, even though they are so large as to render the predictions useless, are not the result of some "bug" in the FACT Model. They are inherent in ray theory. When runs were made on PLRAY, essentially the same errors were obtained.

(U) The runs made with the receiver above the duct serve as an interesting and instructive check on the previous runs. In the 10 Hz run (Fig. 5-52) the AP2 curve is almost identical to the corresponding curve for the receiver in the duct except that the loss is about 7 dB higher. What makes this result somewhat surprising is the fact that the same convergence zone peaks show up although, with the receiver at 100 ft, ray theory predicts that there are no convergence zones--the propagation is bottom limited. This result, together with the similar slopes of the two curves at short ranges, suggests that a continuous energy leakage out of the channel occurs such that the intensity at the 100-foot receiver depth is about 1/5 the value at 220 ft at all ranges.

(U) Examination of the FACT curve shows that the leakage of energy out of the duct is not predicted by ray theory. At short ranges the finite slope associated with the leakage is replaced with a precipitous drop. The portion of the curve between about 5 and 25 kyd is produced chiefly by single bottom bounce rays. It is interesting to note that the agreement with AP2 in this interval is quite good. The strange rise in the FACT curve between 25 and 30 kyd is due to a family of RBR rays which reflect off the bottom but do not reach the surface. These rays apparently dissipate by diffraction at very low frequencies, since no equivalent contribution is apparent in the 10 Hz AP2 curve. Beyond 30 kyd the propagation loss predicted by FACT is everywhere greater than 120 dB. The energy leakage which accounts for the peaks in the AP2 curve near 40 and 80 kyd is not predicted by ray theory.

(U) Looking at the 30 Hz curves (Fig. 5-53), we again see a strong similarity between the AP2 curve for this case and the corresponding curve for the receiver at 220 ft. Most of the same comments apply here as at 10 Hz except that the contribution of the RBR rays can now be seen in the AP2 output.

(U) At 100 Hz (Fig. 5-54) the AP2 curve shows fair agreement with that of the other run (Fig. 5-50) if the curves are displaced by about 15 to 18 dB. The much larger displacement is consistent with the fact that much less energy leaks out of the duct at 100 Hz than at 30 or

*The 300 Hz AP2 output is not accurate at ranges less than about 9 kyd because of a limitation in the number of modes available (500).

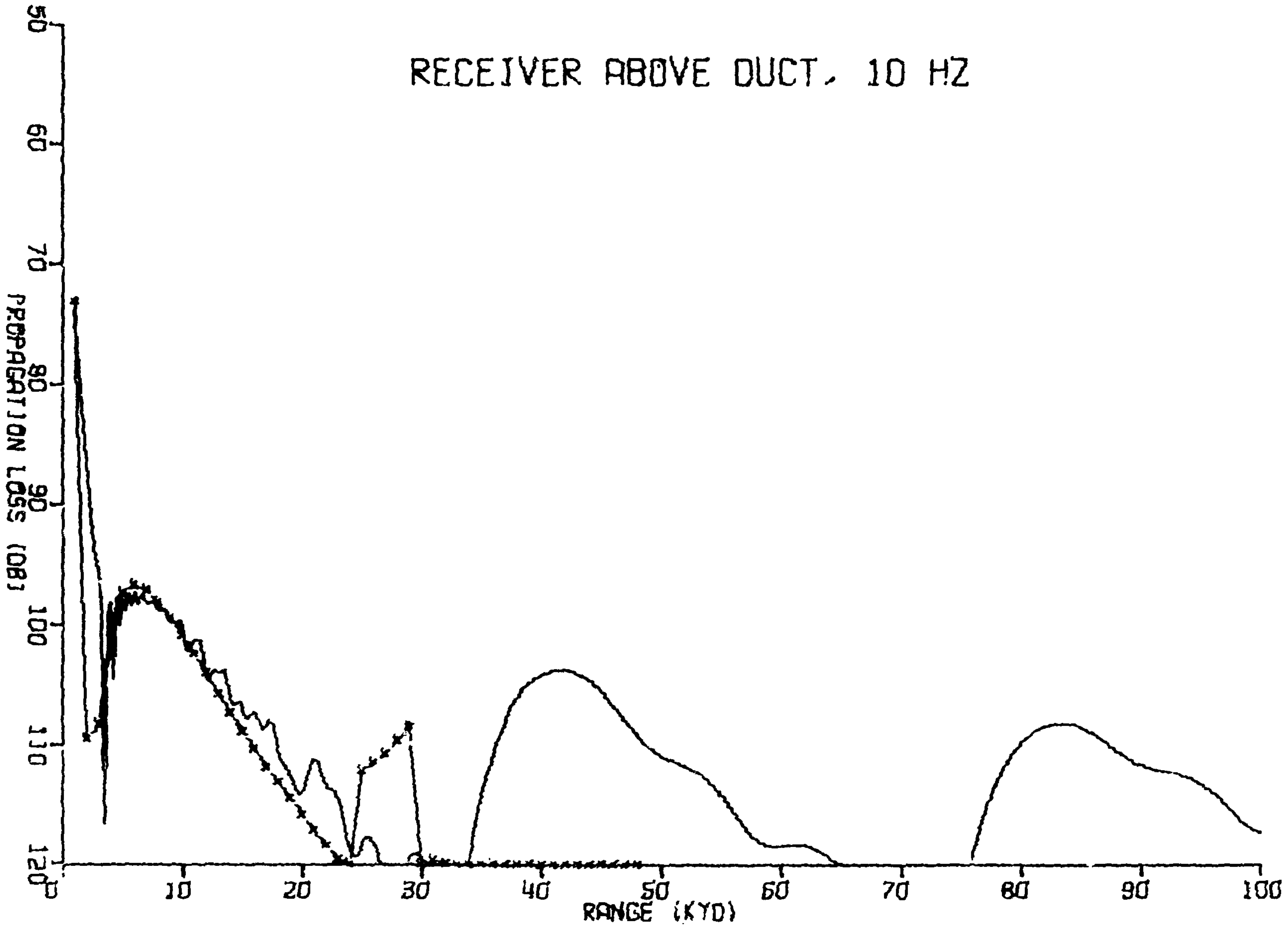

UNCLASSIFIED

(U) Figure 5-52. Propagation Loss at 10 Hertz, Example 9. Receiver Above Channel.

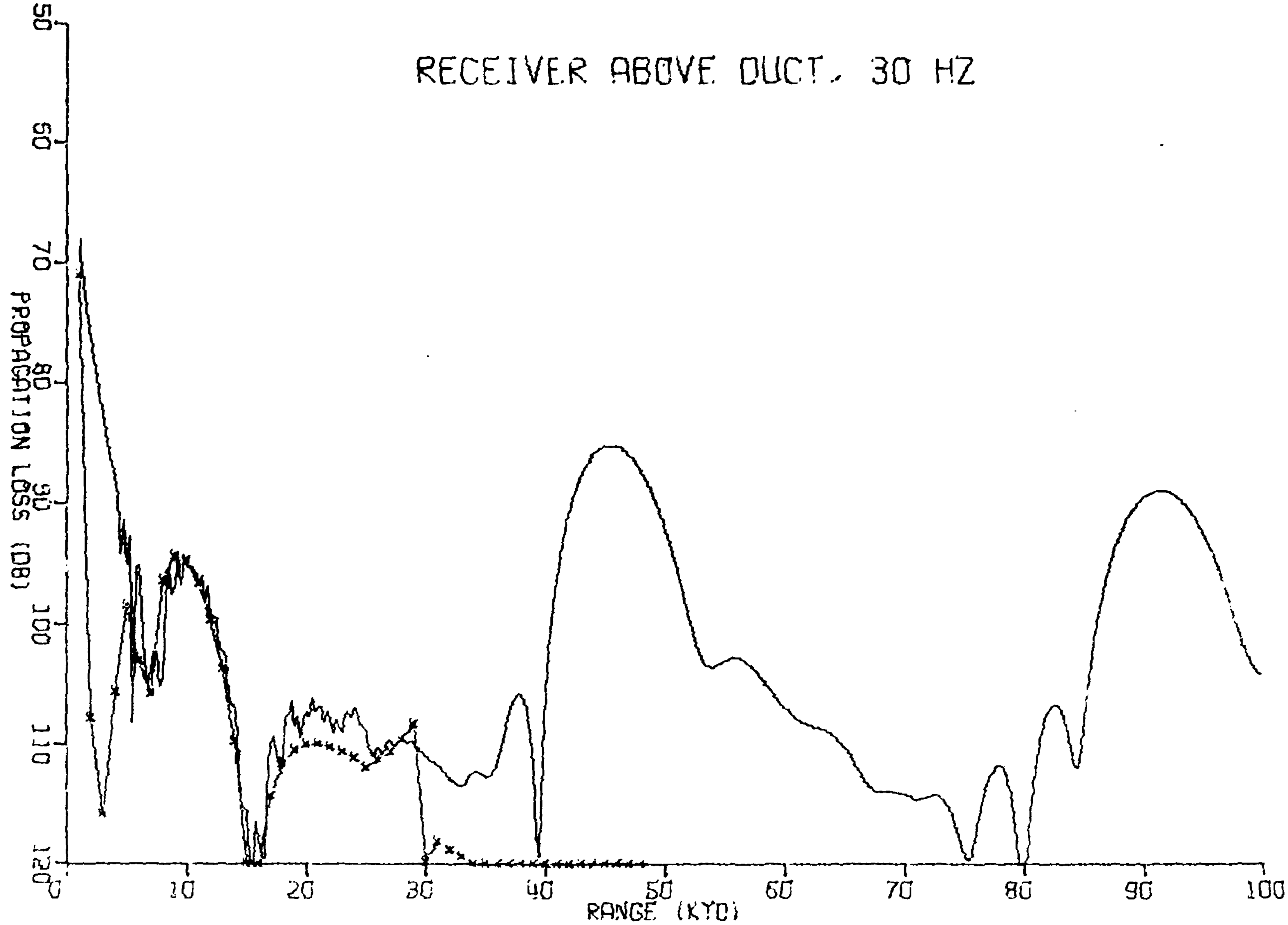

UNCLASSIFIED

(U) Figure 5-53. Propagation Loss at 30 Hertz, Example 9. Receiver Above Channel

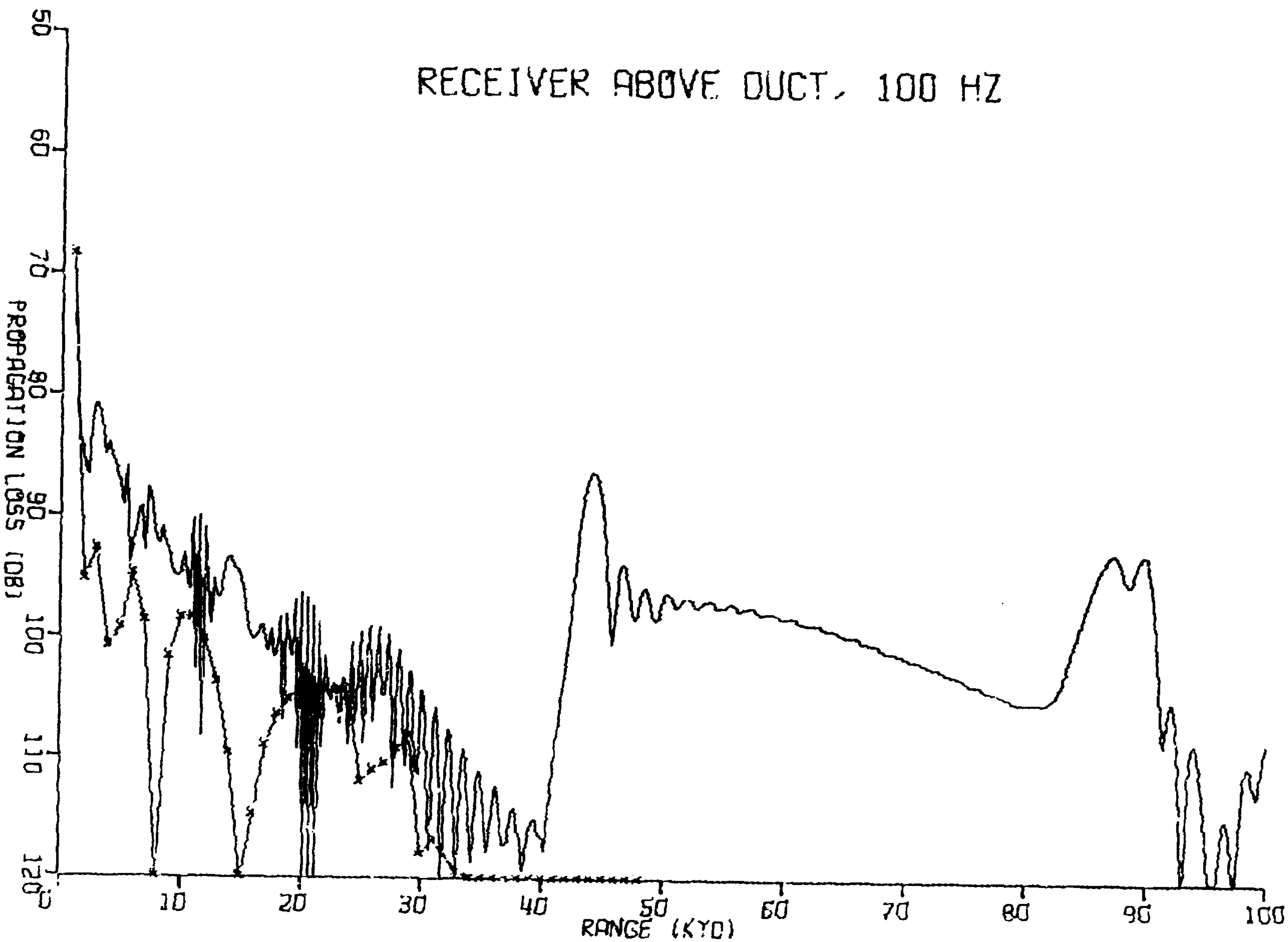

UNCLASSIFIED

(U) Figure 5-54. Propagation Loss at 100 Hertz, Example 9. Receiver Above Channel.

10 Hz. The agreement between FACT and AP2 at ranges less than 25 to 30 kyd is no longer evident at 100 Hz. The reason for the disagreement is that the principal contribution to the normal mode output in this range interval comes from leakage out of the duct, which is ignored by ray thoery.

(U) Between 100 Hz and 300 Hz (Fig. 5-55) the normal mode output suffers a drastic drop in intensity. The reason appears to be that at 300 Hz the duct is so efficient at trapping energy that very little leaks out of the 100-foot receiver level. At ranges below 30 kyd the agreement between FACT and AP2 (if sufficiently smoothed) is now very good. The convergence zone peaks in the AP2 curve are still missing from the FACT output, but the disagreement is far less serious because the intensity of those peaks is now very weak; if a bottom of average reflecting characteristics had been assumed, the disagreement would have been masked by the bottom returns.

(U) In general, as is to be expected from theory, the presence of the subsurface channel in this example introduces extremely serious errors in FACT (and other ray models) at very low frequencies. As the frequency increases, the severity of the errors decreases. In the present example the minimum frequency for acceptable results appears to be somewhere in the vicinity of 300 Hz.

Example 10 (U)

(U) This example is one of two cases reported by G. Jacobs of Ocean Data Systems, Inc. [7] The case is identified as NAVOCEANO Test Case 7. The problem reported is that when a run was made with two frequencies, 300 and 700 Hz, the results at 700 Hz were not the same as were obtained from a run at 700 Hz to alone. The two runs were repeated on the NADC version to verify that both versions of FACT led to the same results. They did. Diagnostic runs were then made to determine the cause of the discrepancy.

(U) The cause of the disagreement proved to be a difference in the number of bottom bounces computed. To understand the reason for the difference it is necessary to consider the logic employed by FACT in terminating the ray computations in the last sector. One of the criteria for stopping is based on the intensity of the arrivals. As each path of a given arrival order is processed in INSTOR, the maximum intensity among the arrivals at all ranges is determined. If this maximum intensity is less than 10^{-15} (corresponding to a loss of 140.5 dB), the sign of the parameter IGTYPP is reversed. When the sign reversal is detected upon the return to FACTTL, the processing of that path is terminated. If a similar result is obtained for all the other paths involved in the current arrival order, the entire run is terminated. In the runs of Example 10 the coherence was such that the number of paths was 1.

(U) A second criterion for stopping involves both the number of bottom bounces and the ray ranges. Assuming the intensity does not fall below the 10^{-15} minimum, computations are automatically continued through the fourth bounce. After the fourth bounce continuation is contingent upon the computed ray ranges. Additional arrival orders are processed until the minimum ray range exceeds the maximum range specified by the user. Since the minimum ray range is generated by the ray which hits the bottom at the critical angle of the bottom loss curve, it appears that this last requirement is intended to guarantee that there will be at least four bottom bounces at angles greater than critical at all receiver ranges covered by the sector.

(U) In the single frequency run of Example 10 it was found that the intensity criterion was met on the fourth bottom bounce and so the run was terminated at this point. As a result of the termination, 4 bottom bounces were computed at ranges out to 10.5 nm, 3 bounces from 11 to 22 nm, 2 bounces from 22.5 to 33.5 nm, one bounce from 34 to

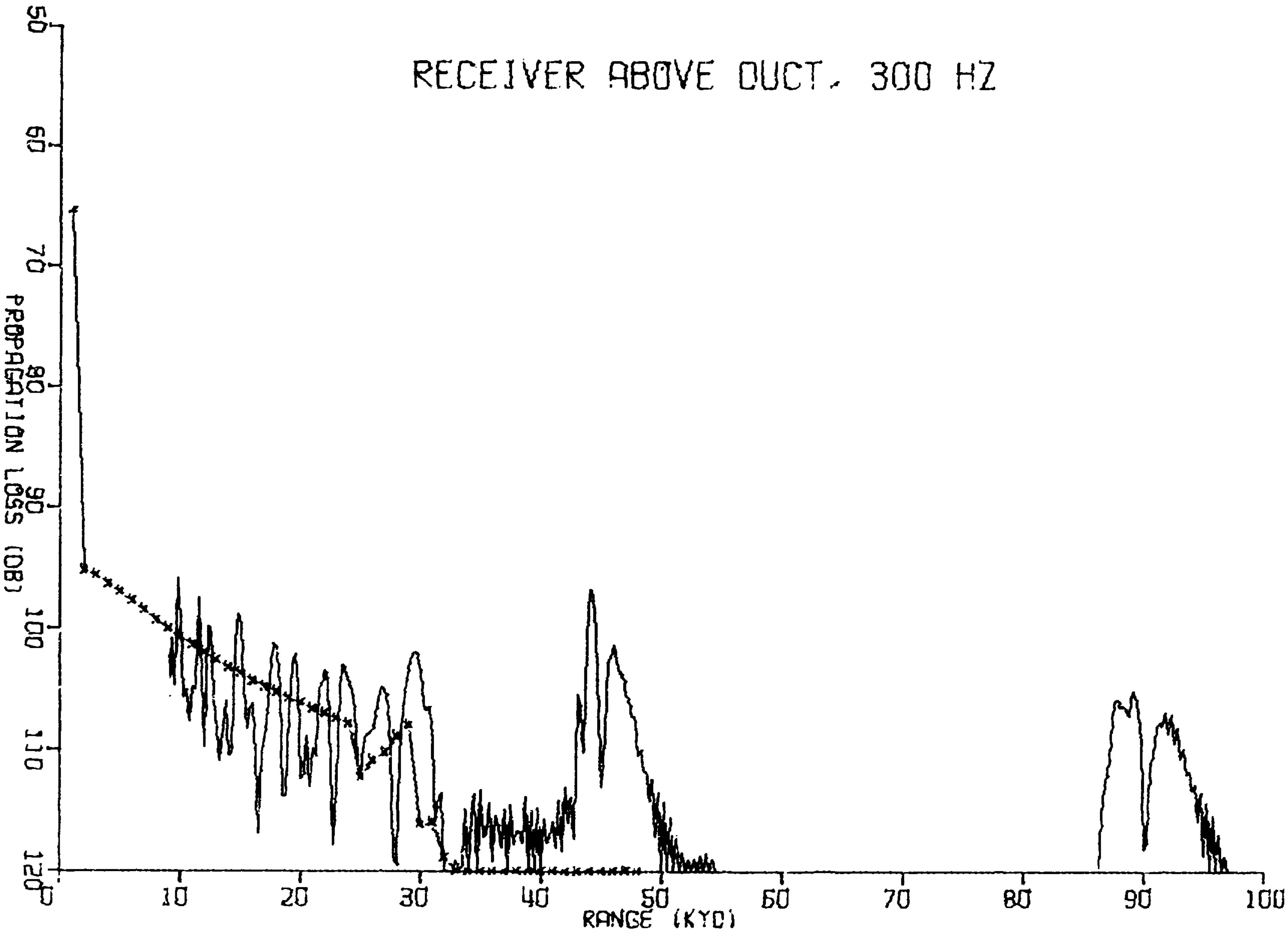

UNCLASSIFIED

(U) Figure 5-55. Propagation Loss at 300 Hertz, Example 9. Receiver Above Channel.

45.5 nm, and none from 46 to the maximum range of 60 nm.

(U) In the two-frequency run the losses at 300 Hz were less than those at 700 Hz. The higher intensity of the 300 Hz arrivals prevented the intensity criterion from operating on the fourth bottom bounce. Since the computed ranges were considerably smaller than the maximum range of 60 nm, the computations were continued into the fifth arrival order, which covered the range interval from 32.5 to 57 nm. On this passage through INSTOR the intensity criterion was met and the computations were terminated. The presence of the additional 300 Hz frequency therefore resulted in the computation of 4 bottom bounces from 0 to 10.5 nm, 3 bounces from 11 to 22 nm, 2 bounces from 22.5 to 32 nm, 3 bounces from 32.5 to 33.5 nm, 2 bounces from 34 to 45.5 nm, one bounce from 46 to 57 nm and no bounces from 57.5 to 60 nm.

(U) The largest discrepancy between the two runs occurred in the interval from 51.5 to 57 nm, where there are no intensity contributions at all in the single frequency run. (The default value of the loss is 180 dB plus the attenuation loss.) In the two-frequency run there is one bottom bounce contribution from the fifth arrival order.

(U) The nature of this error is such that it can occur only at points where the propagation loss is already exceedingly high. It does not appear to be anything to worry about.

Summary and Conclusions (U)

(U) An investigation has been made into the physics of the FACT model. Since FACT has been in wide use for several years and its characteristics and capabilities are well known, the present study has been concerned largely with an investigation of problem areas. After a review of the FORTRAN coding, the method adopted for the study was to select a set of test cases, referred to as examples, and to document in detail the operation of the model as it executed the test cases. To aid in the documentation an extensive set of diagnostic print statements was incorporated into the PL9D version of FACT resident at NADC. The examples provided concrete illustrations of a number of features which were only dimly understood from a study of the FORTRAN coding and the FACT technical reports. Among the findings are the following:

(1) The scheme for moving the source and receiver depth away from the axis of a sound channel to eliminate the computation of near-axial rays is unsatisfactory. The extent of displacement depends not only upon the physical characteristics of the velocity profile but also upon the manner in which the input data table is set up. In one example merely interpolating one extra point in a linear profile segment caused a major change in the propagation loss output. In another example the procedure led to a shift of over 250 ft in the receiver depth, which is felt to be far in excess of a tolerable limit. No indication of these changes is given in the program output.

(2) Not enough rays are computed in the outermost source angle sector (NG = NGRPS). FACT currently computes only two rays. The first of the two is immediately beyond the limiting ray to the bottom and the second ray either strikes the bottom at a grazing angle equal to the critical angle of the bottom loss curve or else is 5 degrees steeper than the first, whichever results in the larger angle. The examples have shown that when the second ray is only 5 degrees beyond the first, as is the case with a FNOC Type 5 bottom, the resulting range-angle curve-fitting may be unacceptably poor, leading to erroneous ray intensities and distorted surface-imaging interference patterns.

(3) The procedure employed for replacing range-angle curves with parabolas needs further study. Examples have been found where oversmoothing by the parabolas

leads to serious errors in caustic corrections. Also, through an oversight in the logic of the program it is possible to generate a false caustic when fitting a parabola to $\theta - \theta_1$ as the independent variable. The false caustic can have serious and unfortunate consequences.

(4) The cusped caustic correction procedure has several shortcomings. The fact that the theory being implemented assumes the source and receiver to be at the same depth, whereas in the actual operation of the FACT model they are separated, leads at the least to confusion and at the worst to errors in output. All range-angle curves throughout the program are plotted against receiver angle except the parabola for the cusped caustic corrections. Plotting this curve against source angle is a serious mistake and should be corrected. Also, the method employed to fit a parabola to a smooth caustic associated with a cusp is faulty and usually leads to a poor fit since one of the three fitting points usually does not lie on the curve to which the parabola is being fitted.

(5) In view of the manner in which it is implemented in the FACT model there is a serious question whether the cusped caustic correction is necessary.

(6) In FACT the decision whether or not to compute coherence is made by testing the horizontal separation between the direct and surface-reflected paths. If the separation for either the first or the last ray computed in a given source angle sector exceeds a preset limit, the entire sector is treated incoherently. In two of the examples cases have been found where FACT generates an incoherent output over the whole sector whereas if the decision had been made on a ray-by-ray basis virtually the whole sector would have been treated coherently.

(7) A similar consideration applies to the amplitude reduction applied to the interference pattern in cases of inadequate range sampling. FACT computes an average number of points per cycle over the entire range interval. Actually in the first bottom bounce region, where the interference pattern assumes its greatest importance, the number of points per cycle varies strongly with range, with the possible result that the FACT propagation loss curve may be undersampled at short ranges, whereas the amplitude may be unduly attenuated at long ranges.

(8) There is an error somewhere in the logic determining the parameter RCUT which is used in some applications to accelerate the attenuation of the sound field in the shadow zone of a smooth caustic. In one example an erroneous value of RCUT completely wiped out the contribution of a family of rays containing a caustic.

(9) The failure of FACT to interpolate in frequency between adjacent FNOC bottom loss curves results in undesirable discontinuities in the propagation loss output. Also the use of a single bottom type parameter for all frequencies covers both sets of internal bottom loss curves.

References (U)

1. C. W. Spofford. The FACT Model, Volume I. Acoustic Environmental Support Detachment, Maury Center Report 109, November 1974.

2. C. L. Baker and C. W. Spofford. The FACT Model, Volume II. Acoustic Environmental Support Detachment, AESD Technical Note TN-74-04, December 1974

3. C. L. Bartberger. PLRAY - A Ray Propagation Loss Program, Naval Air Development Center Report No. NADC-77296-30, 26 October 1978.

4. S. Payne and K. Focke. Reply to NORDA questionnaire on FACT, 14 August 1979.

5. H. Weinberg. Generic FACT, NUSC Technical Report 5635, 1 June 1977.

6. C. L. Bartberger and T. L. Stover. The NADC Ray-Tracing Program, Naval Air Development Center Report No. NADC-SD-6833, 4 November 1968.

7. G. Jacobs. FACT Investigations, Ocean Data Systems, Inc., memorandum to NORDA, Code 320, 26 July 1979.

6.0 (U) FACT PL9D Program Flow

(U) The following is extracted from the FACT Handout contained in section 5 of the FACT Model, Vol. II (Baker and Spofford, 1974), and is also included in the program listing as part of the FACT PL9D distribution package.

FACT MODEL PROGRAM FLOW

THIS SECTION DESCRIBES THE PROGRAM FLOW IN THE TRANSMISSION LOSS MODULE (SUBROUTINE FACTTL). THE OTHER DECKS, TLOSS, ETC. ARE MERELY DRIVER PROGRAMS TO CALL FACTTL.

FACTTL -

- INITIALIZATION OF VARIABLES AND ARRAYS
- CALL INSERT
  - MAKES SPHERICAL EARTH CORRECTIONS ON PROFILE AND SOURCE AND RECEIVER
  - COMPUTES MIXED LAYER AND THERMOCLINE GRADIENTS FOR SURFACE DUCT CALCULATION (IF APPLICABLE)
  - CALL AXIS
    - COMPUTES PERIOD OF ZERO-DEGREE RAY ALONG AXIS OF SMOOTHED EQUIVALENT PROFILE AND MOVES SOURCE AND RECEIVER (IF NECESSARY) TO SIMULATE AXIS-TO-AXIS TRANSMISSION.
    - COMPUTES LIMITING ANGLE FOR SUBSEQUENT PHASE INTEGRAL CALCULATIONS.
    - INSERTS SOURCE AND RECEIVER INTO PROFILE MOVING THEM SLIGHTLY OR CHANGING SOUND SPEEDS SLIGHTLY TO PREVENT THEM FROM HAVING THE SAME SOUND SPEED.
    - COMPUTES INFORMATION NEEDED FOR SUBSEQUENT LOCATION OF THE CUSPS FROM WHICH SMOOTH CAUSTICS IN THE FIRST FAMILY OF RAYS ORIGINATE.
    - COMPUTATION OF FREQUENCY-DEPENDENT FACTOR FOR COHERENCE, ABSORPTION, AND SURFACE DUCTS.
- CALL TABTH2
  - TABULATES THE RAY ANGLE AT THE BOTTOM IN TERMS OF THE ANGLE AT EITHER THE SOURCE OR RECEIVER DEPTH (WHICHEVER HAS A HIGHER SOUND SPEED).
- CALL CRITA
  - COMPUTES WKB PHASE FACTORS FOR LOW-FREQUENCY CUT-OFF EFFECTS.
- CALL ANGSCH
  - DETERMINES RAYS TO BE TRACED AND DEFINES RAY FAMILIES WITHIN WHICH INTERPOLATIONS ARE VALID IN A SMOOTHED ANGLE VERSUS RANGE CURVE.

UNCLASSIFIED

- LOOP ON EACH FAMILY
  - CALL RANGER FOR EACH RAY IN FAMILY
    - COMPUTES PERIOD AND RANGES OF FIRST AND SECOND ARRIVALS OF UPGOING RAY.
  - COMPUTE SEMI-COHERENT PHASE FACTORS FOR THIS FAMILY.
  - GROUP ARRIVALS FOR COHERENT COMBINATION OR IF CLOSE ENOUGH IN RANGE TO BE CONSIDERED IDENTICAL. THE NUMBER OF ARRIVALS IN A SINGLE ORDER MAY THEN BE REDUCED FROM THE USUAL FOUR TO TWO OR ONE WITH CORRESPONDING CHANGES IN AMPLITUDE.
  - PROCESS EACH REMAINING ARRIVAL IN SUCCESIVE ARRIVAL ORDERS UNTIL THE FAMILY (AND ITS CAUSTIC SHADOW ZONE FIELDS) HAS EXCEEDED THE MAXIMUM RANGE OF INTEREST.
  - FOR STEEPEST RAY FAMILY (BOTTOM-REFLECTED SURFACE-REFLECTED) CALL FITBOT
    - COMPUTES PARAMETERS OF FIVE COEFFICIENT FIT TO R(THETA) USING MINIMUM RAY, RAY AT CRITICAL ANGLE OF LOW FREQUENCY BOTTOM-REFLECTION COEFFICIENT, AND IMPLICITELY 90-DEGREE RAY.
  - FOR SHALLOWER FAMILIES CALL FINDFT
    - FITS A QUADRATIC IN EITHER TAN(THETA) OF SQRT (THETA-THETAMIN) FOR R(THETA) THROUGH BOUNDING ANGLES OF FAMILY AND MIN (OR MAX) RANGE POINT IN FAMILY .
  - CALL INSTOR IF FAMILY DOES NOT CONTAIN CUSPED CAUSTICS
    - COMPUTES THE INTENSITY CONTRIBUTION FROM THE FAMILY AT EACH RANGE POINT.
    - CAUSTIC PARAMETERS AND FIELDS ARE COMPUTES AS WELL AS ALL SEMI-COHERENT FACTORS AND BOTTOM-REFLECTION LOSSES.
  - CALL CUSP FOR FAMILIES WITH CUSPED CAUSTICS
    - COMPUTES FAMILY PARAMETERS AND CUSPED CAUSTIC CORRECTIONS.
    - CALLS XICUSP TO COMPUTE CUSPED CAUSTIC FIELDS.
    - ADDS IN BOTTOM REFLECTION LOSS IF ANY.
    - FOR FOUR RAY SYSTEMS CALLS INSTOR TO COMPUTE SMOOTH CAUSTIC CONTRIBUTION.
- END PROCESSING OF A FAMILY, GO TO NEXT FAMILY
  - ADD IN HALF-CHANNEL NON BOTTOM-REFLECTED CONTRIBUTION (FOR ASRAP III HALF CHANNEL CASES ONLY))
  - ADD IN DUCTED CONTRIBUTION
  - CONVERT TO TLOSS(R,F) (INCLUDING VOLUME ABSORPTION)

  RETURN

THE FACT PACKAGE PROGRAM LIBRARY CONTAINS ALL FORTRAN ROUTINES REQUIRED TO IMPLEMENT THE FACT ACOUSTIC MODEL. THE PROGRAM LIBRARY COMPONENTS ARE AS FOLLOWS....

MAINPROGRAM TLOSS-- READS CARD INPUTS, COMPUTES LOSSES THRU SUBROUTINE CALLS, AND PRINTS AND/OR PLOTS (ON THE LINE PRINTER) THE RESULTS.

```
     SUBROUTINE FACTTL--THE FACT RAY TRACING MODEL
     SUBROUTINE SHALTL--A SIMPLIFIED MODEL FOR SHALLOW WATER,
                        CALLED INSTEAD OF FACTTL BY AUTOTL
                        UNDER CERTAIN CONDITIONS.
     SUBROUTINE HFCHTL--A SIMPLIED HALF-CHANNEL MODEL, USED BY FACTTL
                        FOR ASRAP CASES.


THE FACT MODEL SUBROUTINE FACTTL REQUIRES
THE FOLLOWING ADDITIONAL ROUTINES....
     13 COMPUTATIONAL SUBROUTINES...     INSERT     AXIS       TABTH2
                                         CRITA      RAYT       ANGSCH
                                         RANGER     FITBOT     FINOFT
                                         FITQ       INSTOR     CUSP
                                         QUAD

      8 FUNCTIONAL SUBROUTINES....       SPEED      SETSNR     FAIRY
                                         XICUSP     PE28       THBOT
                                         BOTTOM     BTMLCS

FOR INPUT AND OUTPUT PROGRAM TLOSS REQUIRES....
      3 INPUT-OUTPUT SUBROUTINES....     RDPROF     TLHEAD     PLOTTL


TO MAKE AN OBJECT PROGRAM FOR THE CARD INPUT PROGRAM TLOSS,
ALL COMPONENTS WITH THE EXCEPTION OF AUTOTL AND SHALTL SHOULD
BE COMPILED. THE RESULTING PROGRAM OCCUPIES APPROXIMATELY
44000 (OCTAL) WORDS ON THE CDC 6600.

IN THE (CDC 6600) FACT PACKAGE PROGRAM LIBRARY,
THE FOLLOWING CONVENTIONS HAVE BEEN FOLLOWED....

     EACH DECK IS A SINGLE PROGRAM, ROUTINE, OR FUNCTION.
     THE DECK NAME IS IDENTICAL TO THE ROUTINE NAME.
     ALL DECKS ARE SEQUENCED WITHOUT CORRECTIONS.
```

UNCLASSIFIED

7.0 (U) FACT PL9D Inputs

(U) The following is extracted from the FACT Handout contained in section 5 of the FACT Model, Vol. II (Baker and Spofford, 1974), and is also included in the program listing as part of the FACT PL9D distribution package.

```
THE CARD INPUTS TO TLOSS ARE DETAILED IN THE COMMENTS WITHIN
THAT PROGRAM, AND REPEATED HERE FOR REFERENCE PURPOSES.


CARD                DATA                     FORMAT
----                ----                     ------
  1                 TITLE                    8A10
          (EOF ENDS RUN)
  2                 N,IL,IB,IW,IPL,IAR       6I5
 3A,B,...           Z(I),C(I)   (I=1,N)      8F10.2
                 OR D(I),T(I),S(I)           3(F8.2,F6.2,F6.2)
  4                 NR,DRNMI                 I5,5X,F10.2
  5                 F(I)   (I=1,6)           6F10.2
  6                 S,R,JC(I)   (I=1,6)      2F10.2,6I5
          (EOF ENDS RUN)
          (S.GE. 10E6 GOES BACK TO READ CARD 1)

          FACTTL CALLED TO COMPUTE LOSSES
          LOSSES PRINTED AND/OR PLOTTED

          (GOES TO READ CARD 6)
- - - - - - - - - - - - - - - - - - - - - - - - - - - - - - - - -
```

UNCLASSIFIED

N IS NO. OF PROFILE POINTS 2.LE.(ABS(N)).LE. 90

*FOR N POSITIVE, PROFILE IS INPUT DIRECTLY IN DEPTH, VELOCITY PAIRS, 4/CARD. A VELOCITY .LT. 3000 IS USED AS AN INDICATOR OF METRIC INPUT (M,M PER S) BOTH DEPTHS + VELOCITIES ARE CONVERTED TO ENGLISH UNITS (FT,FT PER SEC).

*FOR N NEGATIVE, PROFILE IS INPUT AS DEPTH, TEMP., SALINITY TRIPLETS, 3/CARD. METRIC UNITS ARE ASSUMED (M,CENT,PPT). WILSONS FORMULA IS USED TO COMPUTE VELOCITIES, DEPTHS + VELOCITIES ARE THEN CONVERTED TO ENGLISH UNITS.

*THE INPUT PROFILE IS ALWAYS PRINTED, IF CALCULATIONS + CONVERSIONS ARE REQUIRED, THE RESULTING VALUES ARE ALSO PRINTED.

*THE BOTTOM DEPTH IS ALWAYS Z(N)

IL IS THE INDEX OF THE MIXED LAYER DEPTH IN THE INPUT PROFILE (SEPARAT COMPUTATIONS ARE THEN PERFORMED FOR A SURFACE DUCT OF THIS DIMENSION AND NO RAYS ARE TRACED IN THE DUCT). EITHER 1 OR 0 CAN BE USED TO INDICATE THAT NO LAYER IS PRESENT. 0 .LE. IL .LE. (ABS(N)). IL = (ABS(N)) INDICATES THAT A HALF-CHANNEL CONDITION IS PRESENT AND THAT THE ROUTINE HFCHTL (NORMALLY USED ONLY FOR ASRAP) SHOULD BE USED.

IB IS THE BOTTOM TYPE
A NEGATIVE VALUE INDICATES THAT THE USER WILL SUPPLY A BOTTOM LOS FUNCTION, AND MODIFY FUNCTION BOTTOM TO CALL THE REPLACEMENT FOR THE DEFAULT FUNCTION BTMLOS.
1-9 INDICATES FNWC BOTTOM LOSS FUNCTIONS

IW IS THE WAVE HEIGHT IN FEET

IPL IS THE PRINT/PLOT INDICATOR
0.. PRINT ONLY (DB. LOSS VS. RANGE)
1.. PAGE PLOT ONLY (DB. LOSS VS. RANGE, 1 PAGE/FREQUENCY)
2.. PRINT AND PLOT (=0 PLUS 1)
-1.. PAGE PLOT ONLY (DB. LOSS VS. RANGE, ALL FREQS. ON SAME PLOT)
-2.. PRINT AND PLOT (=0 PLUS -1)

IAR IS THE ARRIVAL CALCULATION INDICATOR
0.. NO ARRIVALS
1.. ARRIVAL ANGLES VS. RANGE CALCULATED AND PLOTTED

NR IS THE NUMBER OF RANGE POINTS 1 .LE. NR .LE. 250

DR IS THE INCREMENTAL (AND FIRST) RANGE IN N.MI.

F(I) ARE THE FREQUENCIES - UP TO SIX - IN HERTZ.

S IS THE SOURCE DEPTH IN FEET.

R THE RECEIVER DEPTH IN FEET.

*IF EITHER SOURCE OR RECEIVER DEPTH IS OUTSIDE THE PROFILE LIMITS (LESS THAN ZERO OR GREATER THAN Z(N)) THE SOURCE OR RECEIVER IS BOTTOMED.

JC(I) ARE THE COHERENCY INDICATORS, AND CORRESPOND TO THE F(I)'S 1-TO-1
0 = SEMI-COHERENCE
1 = INCOHERENCE
2 = FULL COHERENCE

*THE VALUES OF JC(I) ARE NORMALLY LEFT BLANK TO INDICATE THAT SEMI-COHERENCE IS TO BE USED FOR ALL FREQUENCIES.

A MACROSCOPIC LOOK AT DECK CONSTRUCTION

```
    /-------------------------------------------------------------------------*
   /            EITHER 7-8-9 (END OF RECORD) OR YS .GE. 10E6 (NEW RUN)        *
  /                LAST CARD OF SOURCE-RECEIVER DEPTH DECK                    *
 * /------------------------------------------------------------------------*
 *//-------------------------------------------------------------------------*
 ///-------------------------------------------------------------------------*
 ///------------------------SOURCE AND RECEIVER DATA-------------------------*
 ///-------------------------------------------------------------------------*
 ///-------------------------------------------------------------------------*
 ///-------------------------------------------------------------------------*
 //  YS        YR      XXXXXXXXXXXXXXXXXXXXXXXXXXXXXXXXXXXXXXXXXXXXXXXXXXXXXXXXX*
 /                 TYPE 6 CARD--SOURCE AND RECEIVER DATA                     *
 * /------------------------------------------------------------------------*
 */  F1        F2         F3         F4         F5        F6    XXXXXXXXXXXXXXXXXX*
 /                   TYPE 5 CARD--FREQUENCY INFORMATION                      *
 * /------------------------------------------------------------------------*
 */NR XXXXX  DRNMI     XXXXXXXXXXXXXXXXXXXXXXXXXXXXXXXXXXXXXXXXXXXXXXXXXXXXXXXXX*
 /                     TYPE 4 CARD--RANGE INFORMATION                        *
 * /------------------------------------------------------------------------*
 *//-------------------------------------------------------------------------*
 ///-------------------------------------------------------------------------*
 ///------------------------------TYPE 3 CARDS------------------------------*
 ///----------------------------DEPTH, VELOCITY-----------------------------*
 ///--------------------------------OR--------------------------------------*
 ///----------------------DEPTH, TEMPERATURE, SALINITY----------------------*
 ///-------------------------------------------------------------------------*
 ///-------------------------------------------------------------------------*
 //Z(1)   T(1)  S(1)   Z(2)   T(2)  S(2)   Z(3)   T(3)  S(3) XXXXXXXXXXXXXXXXXX*
 /                         TYPE 3 CARD--DATA SET                             *
 * /------------------------------------------------------------------------*
 */NP   IL   IB   IW   IPL IAPXXXXXXXXXXXXXXXXXXXXXXXXXXXXXXXXXXXXXXXXXXXXXXXXXX*
 /                       TYPE 2 CARD--PARAMETERS                             *
 * /------------------------------------------------------------------------*
 */                          THIS IS THE TITLE                               *
 /                           TYPE 1 CARD--TITLE                              *
 *                                                                           *
 *                                                                           *
 *                                                                           *
 *                                                                           *
 *                                                                           *
 *                                                                           *
 *                                                                           *
 *                                                                           *
 *                                                                           *
 *                                                                           *
 *                                                                           *
 *---------------------------------------------------------------------------*
```

UNCLASSIFIED

7.1 (U) FACT PL9D Outputs

(U) The following is extracted from the FACT Handout contained in section 5 of the FACT Model, Vol. II (Baker and Spofford, 1974), which includes FACT Sample Run No. 1 (both data input cards and output), and is also included in the FACT PL9D program listing as part of the FACT distribution package.

DATA INPUT CARDS FOR SAMPLE FACT RUNS

```
COL.                                                                COL.
1        11        21        31        41        51        61        71        80
---------------------------------------------------------------------------------
!         !         !         !         !         !         !         !         !
```

THE RESULTING FACT OUTPUT APPEARS ON THE FOLLOWING PAGES

UNCLASSIFIED

FACT OUTPUT

FACT SAMPLE RUN NO. 1 -- PRESSURE GRADIENT PROFILE, ARRIVAL STRUCTURE COMPUTED.

2 0 4 0

0.00000 4776.00000

12000.00000 4992.00000

120 1.00

25.00 100.00

FACT SAMPLE RUN NO. 1 -- PRESSURE GRADIENT PROFILE,
ARRIVAL STRUCTURE COMPUTED. 10.49.47 09/27/76

SOURCE DEPTH = 60.0 FT, RECEIVER DEPTH = 7200.0 FT

TRANSMISSION LOSS (DB RE 1 YD)

RANGE (N MI)	25 HZ, SCOH	100 HZ, SCOH
1.00	63.4	66.4
2.00	68.4	70.1
3.00	72.9	73.0
4.00	76.1	75.0
5.00	77.5	75.8
6.00	79.5	76.3
7.00	80.9	77.3
8.00	81.7	78.2
9.00	82.5	79.0
10.00	83.3	79.7
11.00	84.1	80.5
12.00	84.9	81.3
13.00	85.5	82.1
14.00	86.0	82.9
15.00	86.5	83.6
16.00	87.0	84.3
17.00	87.4	85.0
18.00	87.9	85.7
19.00	88.4	86.5
20.00	88.8	87.3
21.00	89.3	88.1
22.00	92.7	94.0
23.00	93.1	95.0
24.00	93.5	95.2
25.00	93.9	95.6
26.00	94.4	96.1
27.00	94.3	96.7
28.00	90.6	91.6
29.00	85.4	76.8
30.00	85.5	82.6
31.00	88.7	84.1
32.00	91.9	86.6
33.00	92.4	87.3
34.00	92.9	88.0
35.00	93.3	88.6
36.00	93.6	89.1
37.00	93.9	89.6
38.00	94.2	90.1
39.00	94.5	90.6
40.00	94.7	91.1
41.00	95.0	91.6
42.00	95.3	92.1
43.00	95.5	92.6
44.00	95.7	93.0
45.00	95.9	93.5
46.00	96.1	94.0
47.00	96.1	94.5
48.00	99.3	101.7
49.00	96.9	92.0
50.00	91.3	81.0
51.00	89.2	85.2
52.00	89.9	86.7
53.00	93.1	87.7
54.00	93.7	88.6
55.00	94.1	89.3
56.00	94.5	90.0
57.00	94.9	90.6
58.00	97.0	92.7
59.00	98.0	93.2
60.00	98.2	93.6
61.00	98.5	94.0
62.00	98.7	94.4
63.00	98.9	94.7
64.00	99.1	95.1
65.00	99.2	95.5
66.00	99.3	95.8
67.00	99.2	96.2
68.00	98.6	96.5
69.00	97.2	95.6
70.00	95.3	89.4
71.00	93.4	84.0
72.00	92.0	87.5
73.00	91.8	88.6
74.00	93.4	89.5
75.00	96.2	90.6
76.00	96.7	91.3
77.00	97.0	91.8
78.00	97.3	92.3
79.00	97.6	92.8
80.00	97.9	93.3
81.00	98.1	93.7
82.00	98.3	94.1
83.00	98.5	94.5
84.00	101.4	96.7
85.00	101.5	97.0
86.00	101.5	97.3
87.00	101.3	97.6
88.00	100.7	97.9
89.00	99.7	97.4
90.00	98.2	93.9
91.00	96.7	88.5
92.00	95.2	85.8
93.00	94.2	89.6
94.00	93.9	90.5
95.00	94.6	91.2
96.00	96.9	91.8
97.00	97.5	92.3
98.00	97.8	92.7
99.00	98.1	93.2
100.00	98.3	93.6
101.00	99.7	94.7
102.00	100.0	95.0
103.00	100.2	95.4
104.00	100.3	95.7
105.00	100.4	96.1
106.00	100.5	96.4
107.00	100.4	96.7
108.00	100.2	96.9
109.00	99.7	96.9
110.00	98.9	95.4
111.00	99.1	92.2
112.00	97.8	88.5
113.00	96.7	87.6
114.00	96.8	91.3
115.00	95.7	92.1
116.00	96.6	92.7
117.00	97.2	93.2
118.00	99.1	93.6
119.00	99.4	94.0
120.00	99.6	94.4

UNCLASSIFIED

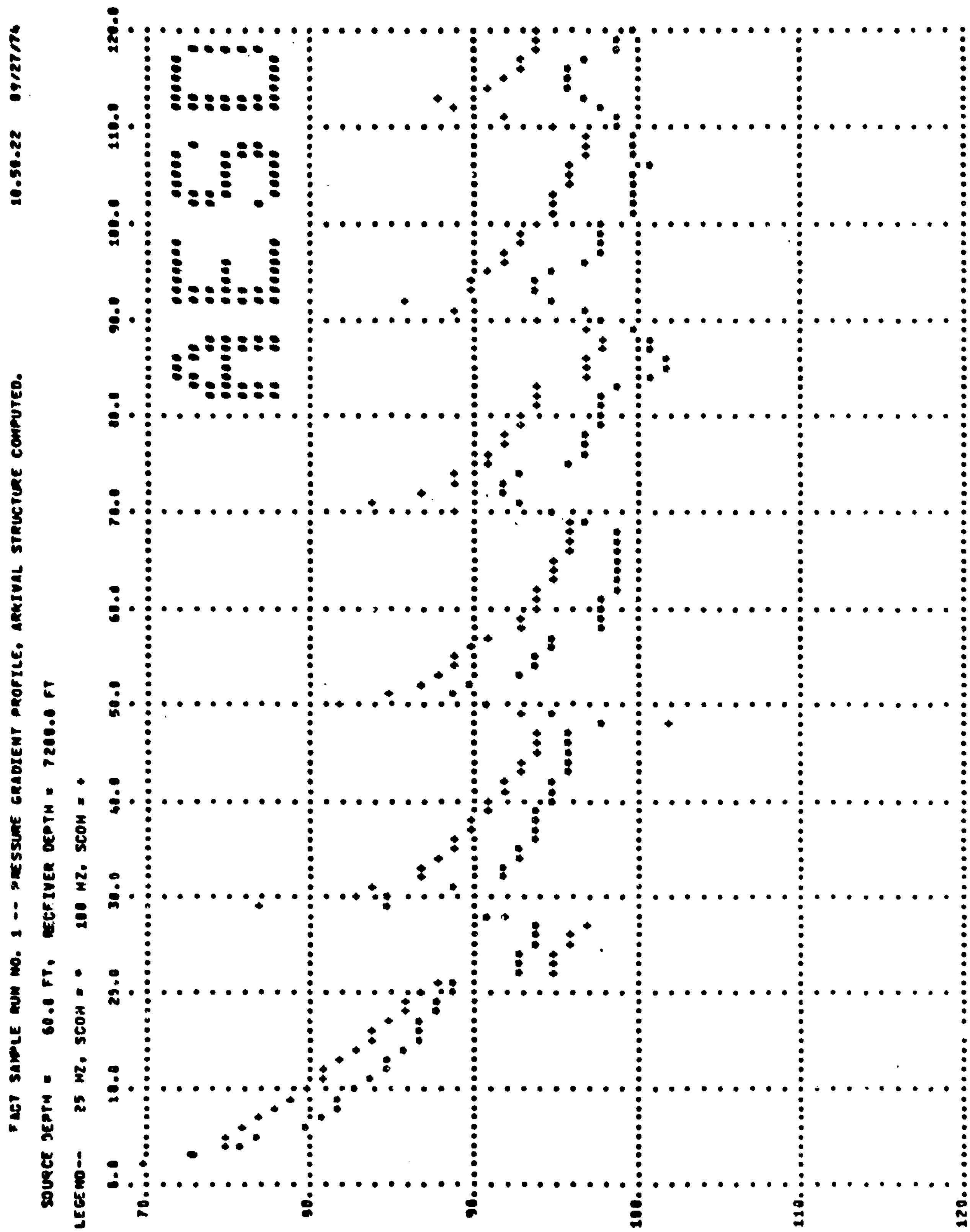

UNCLASSIFIED

FAST SAMPLE RUN NO. 1 -- PRESSURE GRADIENT PROFILE, ARRIVAL STRUCTURE COMPUTED. 10.50.29 09/27/74

SOURCE DEPTH = 60.0 FT, RECEIVER DEPTH = 7200.0 FT

ARRIVAL STRUCTURE -- ANGLE VS. RANGE

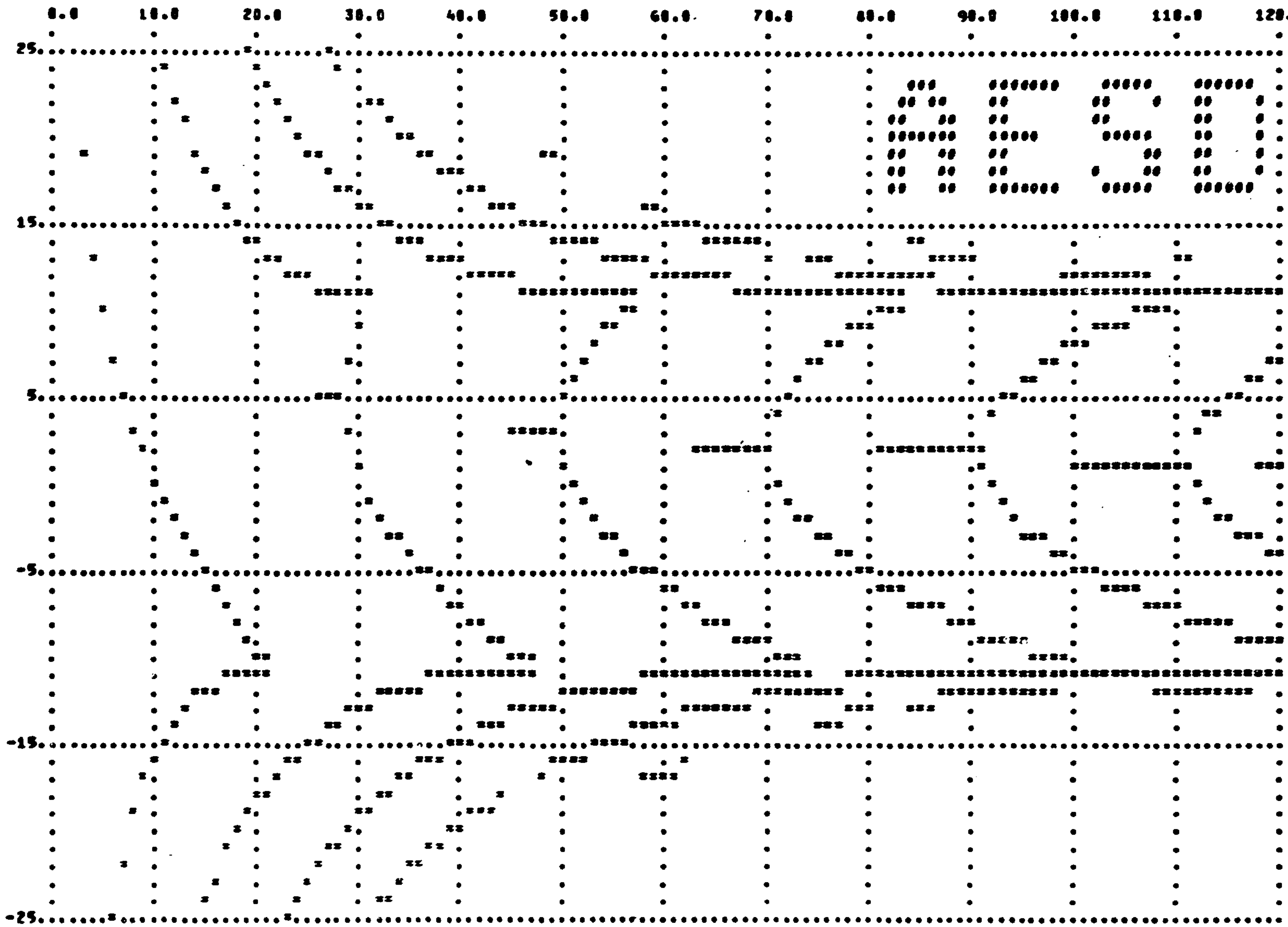

UNCLASSIFIED

FAST SAMPLE RUN NO. 1 -- PRESSURE GRADIENT PROFILE,
ARRIVAL STRUCTURE COMPUTED. 10.50.29 09/27/74
SOURCE DEPTH = 7200.0 FT, RECEIVER DEPTH = 7200.0 FT

TRANSMISSION LOSS (DB RE 1 YD)

RANGE (N MI)	25 HZ, SCOM	100 HZ, SCOM
1.00	64.6	64.6
2.00	70.1	70.1
3.00	73.0	73.0
4.00	75.0	75.0
5.00	76.5	76.5
6.00	77.6	77.6
7.00	78.7	78.7
8.00	79.7	79.7
9.00	80.6	80.6
10.00	81.8	81.8
11.00	82.1	82.1
12.00	82.3	82.3
13.00	82.4	82.4
14.00	82.5	82.5
15.00	82.5	82.6
16.00	82.4	82.4
17.00	82.5	82.5
18.00	81.5	81.5
19.00	80.6	79.7
20.00	79.0	77.0
21.00	77.2	73.2
22.00	75.9	76.8
23.00	76.5	79.8
24.00	80.4	80.5
25.00	81.6	81.6
26.00	82.6	82.6
27.00	87.2	87.2
28.00	87.8	87.8
29.00	88.3	88.4
30.00	88.9	89.9
31.00	89.4	89.4
32.00	89.8	89.8
33.00	90.2	90.3
34.00	90.3	90.7
35.00	86.2	87.6
36.00	84.4	86.3
37.00	86.1	86.2
38.00	85.3	85.3
39.00	84.8	83.8
40.00	83.7	82.0
41.00	82.5	79.3
42.00	81.2	77.2
43.00	80.3	80.8
44.00	80.4	82.9
45.00	82.3	84.1
46.00	85.0	85.1
47.00	85.8	85.9
48.00	86.5	86.6
49.00	87.1	87.2
50.00	87.7	87.8
51.00	88.2	88.3
52.00	88.7	88.8
53.00	93.2	93.2
54.00	93.5	93.6
55.00	93.8	93.9
56.00	93.8	94.3
57.00	89.4	91.4
58.00	85.3	82.2
59.00	84.3	85.5
60.00	85.9	84.6
61.00	85.2	87.7
62.00	86.2	88.6
63.00	83.5	79.8
64.00	82.9	83.9
65.00	82.8	85.2
66.00	84.8	86.2
67.00	87.0	87.0
68.00	87.7	87.7
69.00	88.2	88.3
70.00	89.2	89.3
71.00	89.7	89.8
72.00	90.2	90.2
73.00	90.6	90.7
74.00	91.0	91.1
75.00	91.4	91.5
76.00	91.5	91.8
77.00	91.2	92.1
78.00	89.7	91.5
79.00	86.6	85.0
80.00	85.8	86.3
81.00	85.5	85.8
82.00	86.4	83.3
83.00	85.6	81.8
84.00	84.9	82.8
85.00	86.5	85.8
86.00	84.5	86.9
87.00	85.5	87.7
88.00	88.3	88.4
89.00	89.2	89.3
90.00	89.8	89.9
91.00	90.3	90.4
92.00	90.7	90.8
93.00	91.1	91.2
94.00	91.5	91.6
95.00	91.8	92.0
96.00	92.1	92.3
97.00	92.5	93.2
98.00	91.8	93.4
99.00	90.1	91.4
100.00	87.5	85.6
101.00	86.4	85.3
102.00	85.0	84.8
103.00	86.0	83.6
104.00	86.3	82.8
105.00	85.8	84.1
106.00	85.8	87.5
107.00	86.8	88.4
108.00	86.8	89.1
109.00	89.2	89.7
110.00	90.2	90.3
111.00	90.7	90.8
112.00	91.1	91.2
113.00	91.5	91.6
114.00	91.9	92.0
115.00	92.2	92.4
116.00	92.8	93.1
117.00	92.9	93.6
118.00	92.5	93.7
119.00	91.5	93.3
120.00	90.0	90.0

UNCLASSIFIED

FAST SAMPLE RUN NO. 1 -- PRESSURE GRADIENT PROFILE, ARRIVAL STRUCTURE COMPUTED. 10.50.40 09/27/74

SOURCE DEPTH = 7200.0 FT, RECEIVER DEPTH = 7200.0 FT

L, ID-- 25 HZ, SCOH = * 130 HZ, SCOH = +

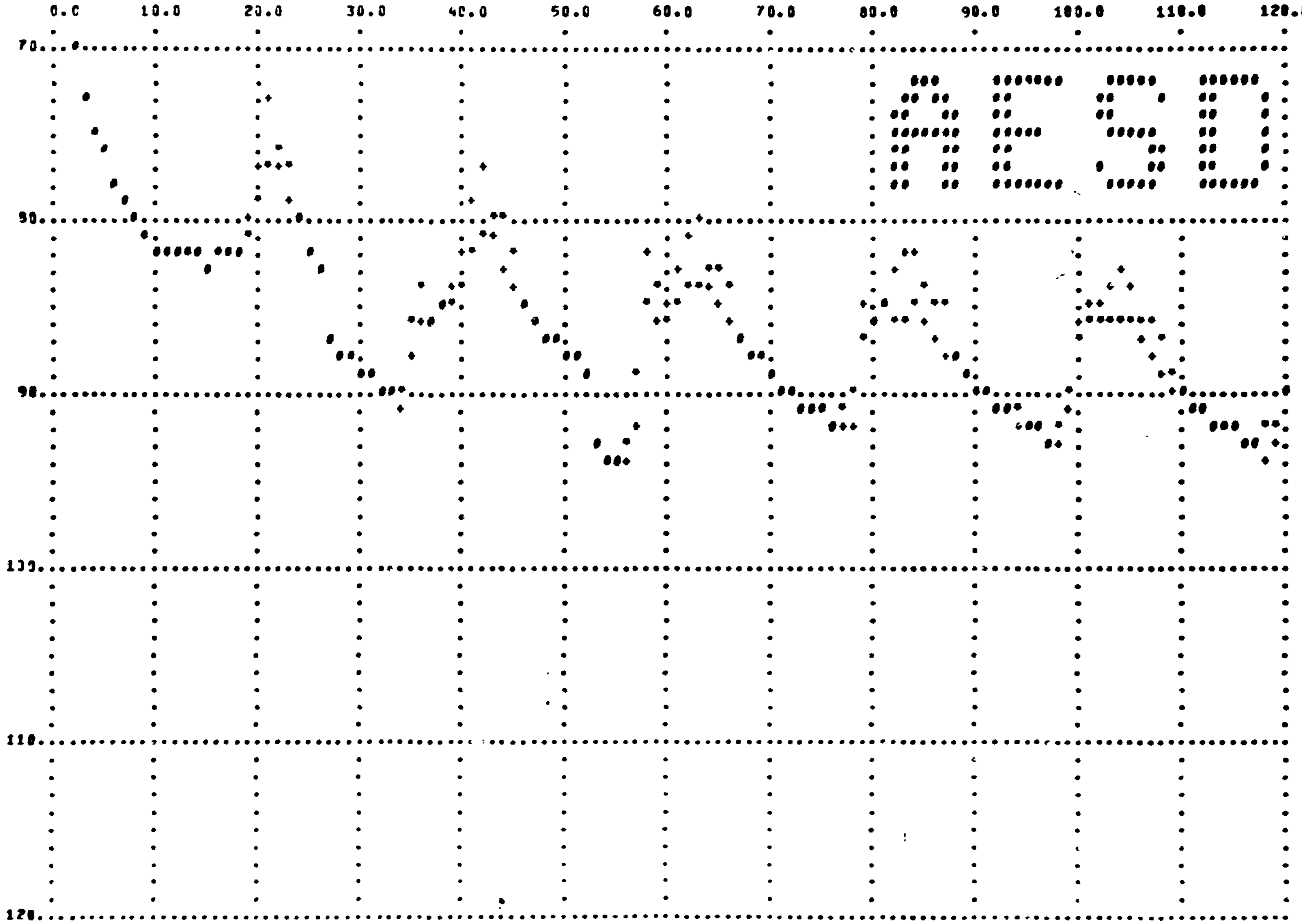

UNCLASSIFIED

FACT SAMPLE RUN NO. 1 -- PRESSURE GRADIENT PROFILE, ARRIVAL STRUCTURE COMPUTED. 10.50.58 09/27/74

SOURCE DEPTH = 7200.0 FT, RECEIVER DEPTH = 7200.0 FT

ARRIVAL STRUCTURE -- ANGLE VS. RANGE

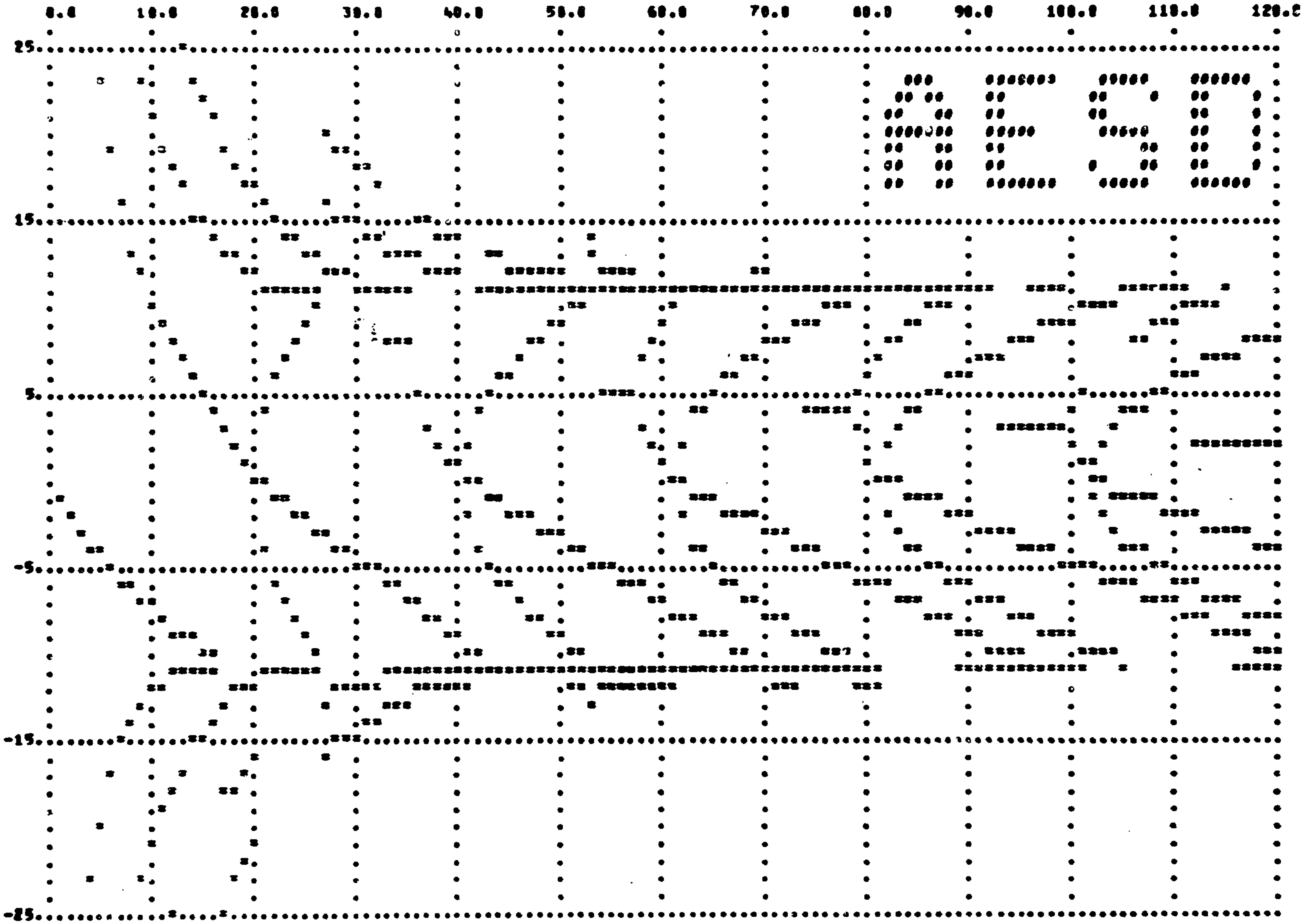

UNCLASSIFIED

8.0 (U) Organizational Responsibility for FACT PL9D

(U) The responsibility for FACT PL9D configuration control, upgrading, maintenance and distribution is held by

Naval Ocean Research and Development Activity
Code 323
NSTL Station, MS 39529
Tel. (601) 688-5434
Autovon 485-5434

9.0 (U) Test Cases for Implementation on a New Computer

(U) As part of a task funded by the Naval Oceanographic Office (NOO) in support of the ICAPS project, 77 FACT input test cases (Jacobs, 1979) were devised which exercise every line of code and every possible branch in the FACT-9D model. These cases do not, in general, represent physically realizable environments. They are not intended to establish that FACT is giving correct answers, but rather that the version under test agrees with the FACT PL9D model as run on the CDC 6600.

(U) Section 5 of Baker and Spofford (1974) is the FACT Handout, a computer-maintained document which is an integral part of the FACT package. Included in that section are three test cases that include inputs as shown below and the resulting FACT output (an example is shown in Section 7.1).

9.1 (U) Computer Systems on Which FACT Versions are Running

Computer	Operating System	Command/Company
CDC 3400	AUTEC Test Data Processing	NUSC/West Palm Beach Detachment
CDC 6400	COLETA	Santa Barbara Analysis Planning Corp.
CDC 6500	--	Planning Systems, Inc.
CDC 6600	KRONOS	NADC
CDC 6600	--	NORDA (at Eglin AFB)
CDC 6600	--	Singer Co., Simulation Products Div.
CDC 6600	BOS	Honeywell, Inc., Training Control Systems Center
CDC 6700	NOS/BE	NSRDC
CDC 6700	Scope 3.4	EG&G, Washington Analytical Services Center, Inc.
CDC 7600	--	AAI Corp.
CDC 7600	--	Arete Associates
CYBER 171	NOS 1.3	ARL/UT
CDC 7600	--	TRW, Inc.
CYBER 174	--	TRW, Inc.
CYBER 174	--	TRW, Inc.
UNIVAC 1108	EXEC 8	Naval Underwater Weapons Engineering Station
UNIVAC 1108	EXEC 8	NAVOCEANO
UNIVAC 1108	EXEC 8	Naval Underwater Systems Center
UNIVAC 1108	EXEC 8	Tracor, Inc.
UNIVAC 1108	EXEC 8	Bell Telephone Laboratories
UNIVAC 1108	--	Naval Ocean Systems Center
VAX-11/780	VAX/VMS	Sanders Associates, Ocean Systems Division
Xerox Sigma 7	RBM, CPV	Defence Research Establishment Pacific, Victoria, B. C., Canada
AN/UYK 7	CMS-2	Singer Co., Simulation Products Division
Burroughs 6750	Version 3	Center for Naval Analyses
Burroughs 5700	MCP MKXVI.0	Naval Coastal Systems Center
Data General Eclipse S230	AOS	MAR, Inc.
DEC TOPS-20	TENEX	Bolt, Beranak and Newman, Inc.
GE 635	GECOS	General Electric Company
HARRIS/6	07A	Rohr Marine, Inc.
IBM 360	--	Naval Postgraduate School, Dept. of Oceanography
IBM 360	--	Naval Hydrographic Office of the Gov't of India
IBM 360/91	OS/MVT runwith ASP	Colombia Univ., Lamont-Doherty Geological Observatory
IBM 370	--	Bell Telephone Laboratories
IBM 370/168	VMOS	IBM . FSD Manassas
IBM 3033-D	OS/VS2 MVS JCL-JES 2	Lockheed-California Co.
ICL 1903A	George 2	Fleet Oceanographic Center, RAF Northwood, U.K.
NOVA	--	Naval Ocean Systems Center
NOVA 800	XDOS (XEBEC)	NAVOCEANO
PDP-10	TOPS-10(6.03)	Sanders Associates/Ocean Systems Division
PDP-11/34A	RSX11-M	Institute de Acustica Laboratories de Hidroacustica, Madrid, Spain
PDP-11/34	RSX11-M	Tetra Tech
PRIME 400	Revision 15	ORI, Inc.
SEL 32/75	RTM Version 7.1	Cubic Corporation
ICAPS FACT SEL 32/75	RTM Version 7	Naval Air Test Center (AT-41)
TI - ASC	'SL	Naval Research Laboratory
UNIVAC 1110	--	Naval Ocean Systems Center
UNIVAC 1110	--	Ocean Data Systems, Inc.
UNIVAC 1108/82	EXEC 8	Sperry-Rand Corp., Sperry Gyroscope Division

UNCLASSIFIED

10.0 (U) FACT Versions

(U) This report examines only one version of the FACT model, FACT PL9D, in detail. Several other versions of FACT exist and are in use. The following material describes these versions in terms of their physical basis, inputs and outputs and particularly emphasizes differences between a given version and FACT PL9D.

10.1 (U) SHALFACT: A Shallow Water Transmission Loss Model

(U) The following information on SHALFACT is extracted from Garon, 1976:

(U) SHALFACT is a modification to the standard FACT model designed specifically to describe the gross features of propagation within a limited shallow-water environment.

(U) The environment in SHALFACT is limited to the same inputs as the standard FACT model (i.e., single sound speed profile, single FNOC/NOO bottom class, etc.) with the exception that a single bottom slope β, expressed in degrees, may be introduced referenced to the receiver.

(U) The propagation problem in SHALFACT is principally controlled by a single parameter: the range dependent ray angle at the bottom, $\emptyset$ (R) where $\emptyset$ (R) is related to the actual bottom grazing angle, ψ, of the ray by

$$\psi = \theta(R) - \beta.$$

(U) The period of the ray, in conjunction with the ray angle $\emptyset$ (R) dictates the approach by which energy is transferred from one range interval to another. In SHALFACT upslope rays are eliminated if they are about to turn around. FACT is run for waterborne (i.e., RR and RSR) paths and when β=0, FACT is also run for the RBR family. For β=0, the bottom angle provides the key to a table look-up whereby a new ray period, phase integral, and upper turning point are determined, linearly interpolating in both angle and range. The intensity of the ray fan bundle is computed, accounting for the effects of surface-image interference and low-frequency cut-off at both the source and receiver and the total sustained bottom loss. The resulting intensity is then added to the intensities already accumulated (by running FACT for the waterborne paths) at the appropriate range. The bottom bounce ray bundle is marched out in range until either the loss becomes excessive (180 dB), the ray turns around ($\theta > \pi/2$), maximum range is reached, or there is no hope of the ray ever reaching the source depth (i.e., the ray's upper turning point is below the source). This process is continued until all rays within the fan have been treated.

(U) The input requirements and output options to SHALFACT are exactly equivalent to the standard FACT model with the exception that the user must also specify a bottom slope and bottom depth at the receiver. Card 2 of the FACT input stream is modified as follows:

FORMAT	PARAMETER	DESCRIPTION
(6I5, 2F10.2)	N	Standard FACT Input
	IL	" " "
	IB	" " "
	IW	" " "
	IPL	" " "
	IAR	" " "
	Z∅	=Bottom depth in feet at receiver
	BETA	=Bottom slope in degrees (+downslope, -upslope)

UNCLASSIFIED

(U) Several additional notes are in order. The user should attempt to input a profile such that the greatest depth of the profile is deeper than the greatest bottom depth (Z(R=0) or Z ($R=R_{max}$)). If the user does not specify a bottom depth at the receiver then the program defaults to a normal FACT run. Additionally, when the arrival angle flag (IAR) is set and the program

is in the SHALFACT mode of operation, only the arrival angles of the water-borne paths will be displayed.

10.2 (U) Minifact

(U) The following is extracted from Folke and Ohlendorf (1977):

(U) MINIFACT is a version of FACT PL9D implemented on the NOVA 800 minicomputer. The MINIFACT module is implemented as two overlays and is written entirely in FORTRAN IV. The maximum amount of core required to load the module is approximately 20,480 decimal (50,000 octal) words on the NOVA 800 system running under the XDOS operating system.

(U) Several options available with FACT have been deleted from MINIFACT. For the purposes of MINIFACT the arrival structure is not needed and is therefore no longer calculated. As with FACT, a combination of two or more ray paths within a family may be computed using a semicoherent summation; the coherent and incoherent summation options, however, are not available. MINIFACT has been designed for deep water problems; as yet, the shallow water option available in FACT has not been implemented in MINIFACT. The run time in shallow water with low loss bottoms will therefore increase because of a large number of surface-reflected, bottom-reflected ray paths.

(U) Subroutine HFCHTL is designed to approximate the results of a complete MINIFACT solution for half-channel transmission while significantly reducing run time. As in FACT PL9D this option should be used only for ASRAP frequencies and source-receiver depth combinations.

MINIFACT Inputs: (U)

SOUND SPEED PROFILE: Speed of sound in feet/sec, depth in feet, maximum of 48 points.

SURFACE CONDITIONS: Wave height in feet.

BOTTOM CONDITIONS: FNOC merged (i.e., low (<1000 Hz) and high frequency) bottom classes.

SOURCE AND RECEIVER POSITIONS: Depths in feet.

FREQUENCY INFORMATION: Frequencies in hertz (maximum of five frequencies)

RANGE INFORMATION: Number of range points (maximum of 250) and range point spacing (nautical miles)

MINIFACT Outputs: (U)

(U) The primary output from the MINIFACT module is an array, ITL of dimension 250 x 5, giving (semi-coherent) transmission loss (in dB x 10 re 1 yd) at each of the range points and frequencies specified as input parameters. If the ray selection process results in either too many ranges (>100) or too many families (>20), the ITL array will contain zeros at the specified ranges and frequencies.

(U) The documentation includes a description of each of the components of the MINIFACT package, the main computational routines and auxiliary subroutines and functions. For each of these, the following material is included: (1) a brief description of the function of the component in the model; (2) equations used by the component when these are not immediately evident from the function of the component or the program listing; (3) parametric and common input and output variables; (4) flow charts, expressed in physical terms to the greatest extent possible for the major programs and routines of the model; and (5) additional material, as applicable, to present the details of the program logic not included in the flow charts for the routine. Finally, the document includes test cases as follows:

1. Source depth 60 ft
   Receiver depth 7200 ft
   Merged FNWC bottom 64
   Wave Height 0 ft
   Sound speed profile:
   Z=0 ft c=4776 ft/sec
   Z=12,000 ft c=4992 ft/sec

Number of range points 250
Range increment 1 naut. mi.
Frequencies 25, 100 Hz
Index of surface layer in profile: IL=0

II. Same as Case I except that source depth 7200 ft

III. Source depth 500 ft
Receiver depth - 300 ft
Index of surface layer in profile: IL=2
Wave Height 0 ft
Merged FNWC bottom 64
Sound speed profile:

Z=0 ft	c=5026.57 ft/ ft/sec
219.98	5028.87
250.00	5018.70
.	.
2379.89	4859.25
.	.
17472.02	5078.09

Number of points 250
Range increment 1 naut. mi.
Frequencies 100, 300 Hz

IV. Same as case III except that Receiver depth = 10,800 ft

UNCLASSIFIED

10.3 (U) ICAPS Version of FACT

(U) The Integrated Command ASW Prediction System (ICAPS) relies heavily on the FACT model as illustrated in Figure 10-3.1 taken from NOO RP-24 (1979). The modules depending on FACT outputs are:

- LATRAN -- yeilds passive lateral range predictions
- ADEPS -- computes detection probabilities for 12 sonobuoy patterns
- TAPS -- provides detection coverage for surface unit towed array systems
- TASDA -- predicts passive sonobuoy field detection
- COMPASS -- aids in planning search options

Sample ICAPS tabular and graphic displays in Figures 10-3.2 - 10-3.6.

(U) The locations and associated computers on which ICAPS is operational (and hence, the ICAPS version of FACT) are given by Floyd (1980):

<u>NOVA 800/820</u>

<u>NAVOCEANO</u>

VP-ASWOC
- Bermuda
- Lajes, Azores
- Moffett Field, Calif.
- Keflavik, Iceland
- Sigonella, Italy

SUB
- CTF-69 Naples, Italy

TRAINING
- Fleet Combat Training Center, Atlantic
- *ASWOC, North Island
- **Cecil Field, FL (VS)

CV-ASWM
- USS AMERICA
- USS SARATOGA
- USS INDEPENDENCE
- USS NIMITZ
- USS FORRESTAL
- USS EISENHOWER
- USS RANGER
- USS CONSTELLATION

*Additional CVs
- USS KITTY HAWK,
- USS J. F. KENNEDY
- USS ENTERPRISE

* Installations to be completed by summer of 1980.
**To be completed at a later date.

UNCLASSIFIED

Other Computers (U)

WWMCCS (H6000)
Naval Air Development Center (CDC 6600)
Air Test and Evaluation Squadron One (SEL 32)
SUBDEVRON 12 (BURROUGHS)
SACLANTCEN (UNIVAC 1106)
Canadian Maritime Command (Honeywell 415)
Pending
- Additional VP (10 sites)
- NATO (6 sites)

(U) The following ICAPS FACT program description and input decription with comments is extracted from NOO RP-24 (1979).

<u>File Name</u>: FACT

<u>Function</u>: Fast Asymptotic Coherent Transmission is a passive propagation-loss program designed for a single profile, flat bottomed environment. Propagation losses are computed at one kiloyard intervals for up to three specified source-receiver pairs and up to four frequencies for a given bottom province, wave height, maximum range, and sonic layer depth.

<u>Input</u>: The program reads the intermediate work file, Z999ICAP:IM, containing

the PROFGEN input parameters, the computed sound-velocity profile, and sonic layer depths in both English and metric units. The console input includes sonic layer option, maximum range, wave height, bottom province option, desired frequencies and total number, and desired source and receiver depths and total number. Also, the operator selects the desired output displays.

Output: The work file, Z999ICAP:IM, now containing the PROFGEN input, the FACT parameters, and propagation-loss computations for all frequencies and source-receiver pairs. The operator may choose to output any of the following on the display screen:

1. A table of the FACT input parameters.
2. All the propagation-loss tables for 1 kiloyard intervals.
3. The sound-velocity profile.
4. The source-receiver pair ray-trace graphs for 100- or 200-kiloyard ranges.
5. All the propagation-loss-versus-range graphs with optional decibel range override on one-page graphics.

Classification: Output displays coupling geographic location with bottom type are classified CONFIDENTIAL. Hard copies of these displays should be marked and handled in accordance with OPNAVINST 5510.1F, Naval Security Regulations.

Operator Interface: By following the conversational format of the program, the operator loads the work file. Table 10.3-1 describes the interchange of information between the operator and the CRT keyboard under normal working conditions.

Execution Time: 45 seconds to 20 minutes, depending on the number of source receiver pairs and frequencies selected.

(U) A description of outputs would be incomplete without the following, extracted in toto from ICAPS-ON-SCENE (April 1980):

FACT Model Upgraded to 9F Version
by Paul J. Banas (U)

(U) The Fast Asymptotic Coherent Transmission (FACT) passive propagation loss model used in the ICAPS has been recently upgraded and validated to the PL9F or "9F" level. The 9F version requires no additional execution time and the updates have not altered the operation of the program. The updates may be described under two categories-accuracy and bottom loss.

(U) The accuracy of the FACT model has been upgraded in two ways. First, the changes associated with the transition from 9D to the 9F level improved the model. Secondly, precision increased (doubled) in many of the FACT subroutines and functions. Validation of these updates began by selecting benchmark test cases from the Computer Program Performance Specification (CPPS) for the FACT model. Numerous FACT runs were made, and the output compared favorably (to within ± 0.1 dB) with the CPPS reference standard predictions. These test cases were designed to execute all possible branches of the FACT model, whether environmentally realistic or not.

(U) A revised bottom loss subroutine incorporated into FACT 9F utilizes a smoothing (interpolation) function for the transition between bottom loss curves. Bottom loss curves depict acoustic energy loss per bottom bounce as a function of grazing angle. Two sets of curves exist, the low frequency (Bassett Wolff) bottom loss curves and the high frequency (NAVOCEANO) bottom loss curves. Each set of curves is applicable to frequencies within a particular frequency band. For any given prop loss prediction, the frequency and acoustic bottom type determine the appropriate curve to be used by the model.

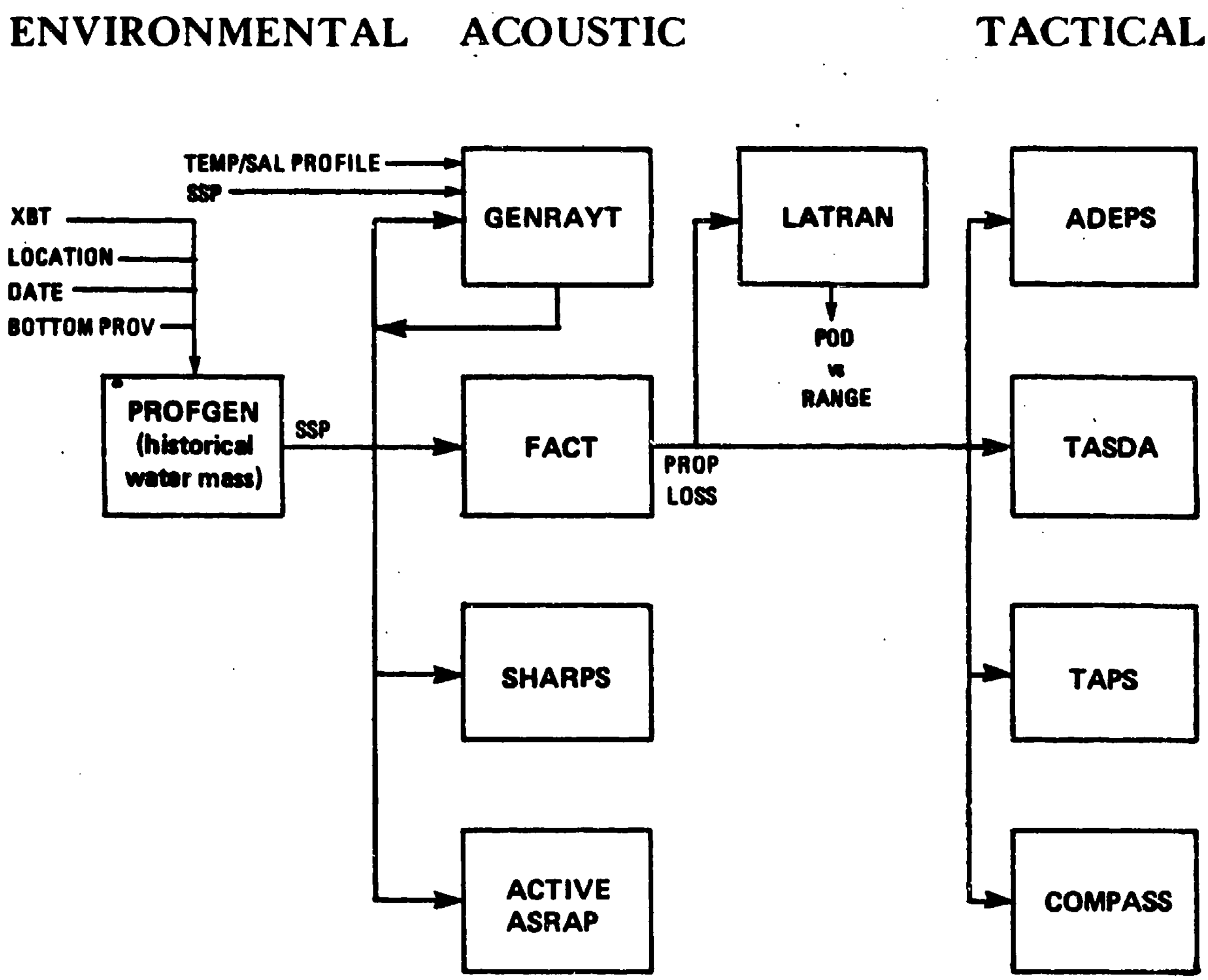

UNCLASSIFIED

Figure 10-3.1. (U) Configuration of ICAPS programs

```
***** FACT (ICAPS) *****
USER RUN IDENTIFIER=TEST
BOTTOM PROVINCE (FREQ. LESS THAN 1000 HZ) =         0
DO YOU WISH TO CHANGE ? (1=YES,0=NO)     1
BOTTOM PROVINCE (1,3, OR 4) = 3
BOTTOM PROVINCE (FREQ. GREATER OR EQUAL TO 1000 HZ) =
DO YOU WISH TO CHANGE ? (1=YES,0=NO)     1
BOTTOM PROVINCE (1-8) = 7
BOTTOM DEPTH =     17000 FT
SONIC LAYER DEPTH =       450 FT
DO YOU WISH TO CHANGE ? (1=YES,0=NO)        0
MAXIMUM RANGE IN KILOYARDS (0-200,DEFAULT=100) = 200
WAVE HEIGHT IN FEET (0-50) = 5
NUMBER OF FREQUENCIES (1-4) = 4
FREQUENCY IN HERTZ = 50
FREQUENCY IN HERTZ = 150
FREQUENCY IN HERTZ = 300
FREQUENCY IN HERTZ = 1000
NUMBER OF SOURCE-RECEIVER DEPTH PAIRS (1-3) = 3
SOURCE DEPTH IN FEET (0-BOTTOM) = 60
RECEIVER DEPTH IN FEET (0-BOTTOM) = 60
SOURCE DEPTH IN FEET (0-BOTTOM) = 500
RECEIVER DEPTH IN FEET (0-BOTTOM) = 60
SOURCE DEPTH IN FEET (0-BOTTOM) = 500
RECEIVER DEPTH IN FEET (0-BOTTOM) = 1000
```

UNCLASSIFIED

Figure 10-3-2. (U) FACT input display

PROPAGATION-LOSS VALUES

DATE = 4 / 15 / 79 LAT = 3710 N LONG = 4851 W

WAVE HEIGHT........ 5 FT SOURCE DEPTH... 60 FT
SONIC LAYER DEPTH.. 459 FT RECEIVER DEPTH. 60 FT
FREQUENCY...... 150 HZ

RANGE (KYDS)	1	2	3	4	5	6	7	8	9	10
1	64.1	67.9	70.4	72.4	74.2	75.7	77.1	78.3	79.4	80.4
11	81.3	82.0	82.7	83.3	83.8	84.3	84.6	84.9	85.1	85.3
21	85.5	85.6	85.7	85.8	85.9	85.9	86.0	86.0	86.0	86.0
31	86.0	86.0	86.0	86.0	86.0	86.0	86.0	86.1	86.2	86.3
41	86.6	86.8	87.1	87.4	87.6	87.9	88.2	88.4	88.7	88.9
51	89.2	89.4	89.7	90.0	90.2	90.4	90.7	90.9	91.2	91.4
61	91.6	91.9	92.1	92.2	81.1	68.6	74.9	77.7	83.1	84.6
71	85.9	87.0	87.9	88.7	89.3	89.8	90.3	90.6	90.9	91.3
81	91.7	92.0	92.3	92.6	92.8	92.9	93.0	93.1	93.2	93.3
91	93.3	93.4	93.5	93.6	93.7	93.7	93.8	93.8	93.9	94.0
101	94.0	94.0	94.1	94.1	94.2	94.2	94.2	94.2	94.3	94.3
111	94.3	94.3	94.3	94.3	94.3	94.4	94.4	94.4	94.5	94.6
121	94.7	94.8	95.0	95.1	95.2	95.3	95.5	95.6	95.6	89.5
131	76.4	78.1	79.6	81.2	82.5	83.8	85.0	86.0	88.8	90.4
141	91.0	91.6	92.0	92.5	92.9	93.3	93.6	93.9	94.2	94.4
151	94.6	94.9	95.0	95.2	95.4	95.5	95.6	95.7	95.9	96.1
161	96.3	96.5	96.6	96.8	97.0	97.2	97.3	97.5	97.7	97.9
171	98.0	98.1	[illegible]	98.3	98.4	98.5	98.6	98.8	98.9	99.0
181	90.1	[illegible]	[illegible]	99.5	99.6	99.7	99.9	97.9	97.9	97.9
191	[illegible]	[illegible]	[illegible]	96.0	96.6	95.8	77.1	80.8	82.4	83.6

UNCLASSIFIED

Figure 10-3.3. (U) [illegible]CT tabular propagation loss vs. range

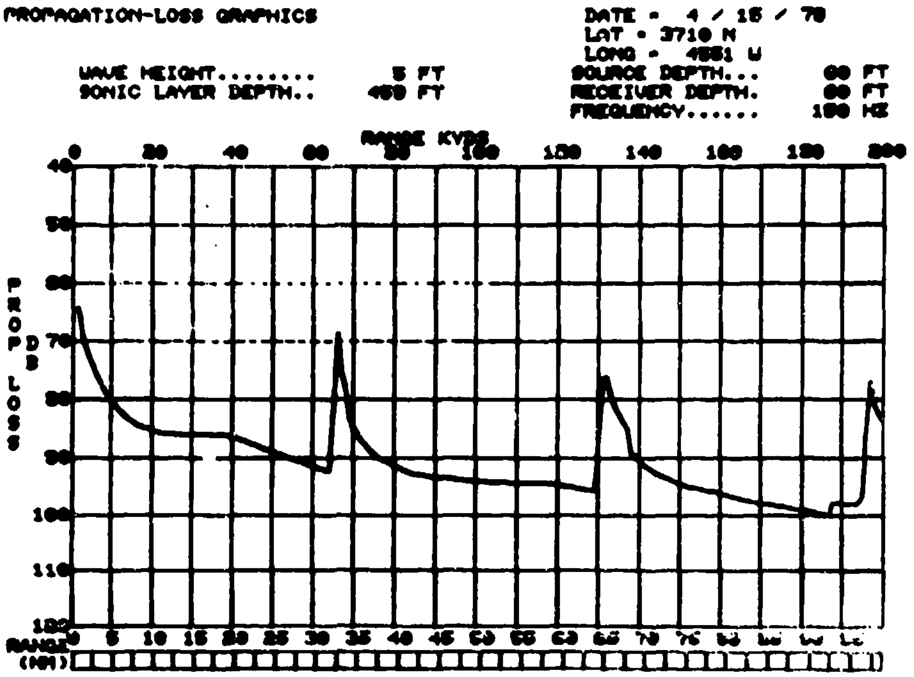

UNCLASSIFIED

Figure 10-3.4. (U) FACT graphic propagation loss display

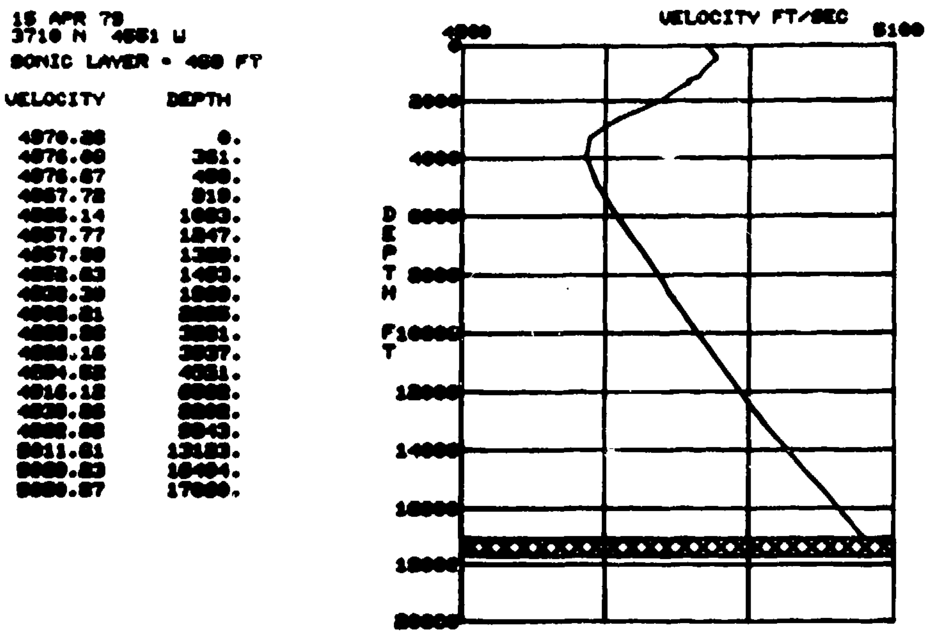

UNCLASSIFIED

Figure 10-3.5. (U) FACT sound speed profile

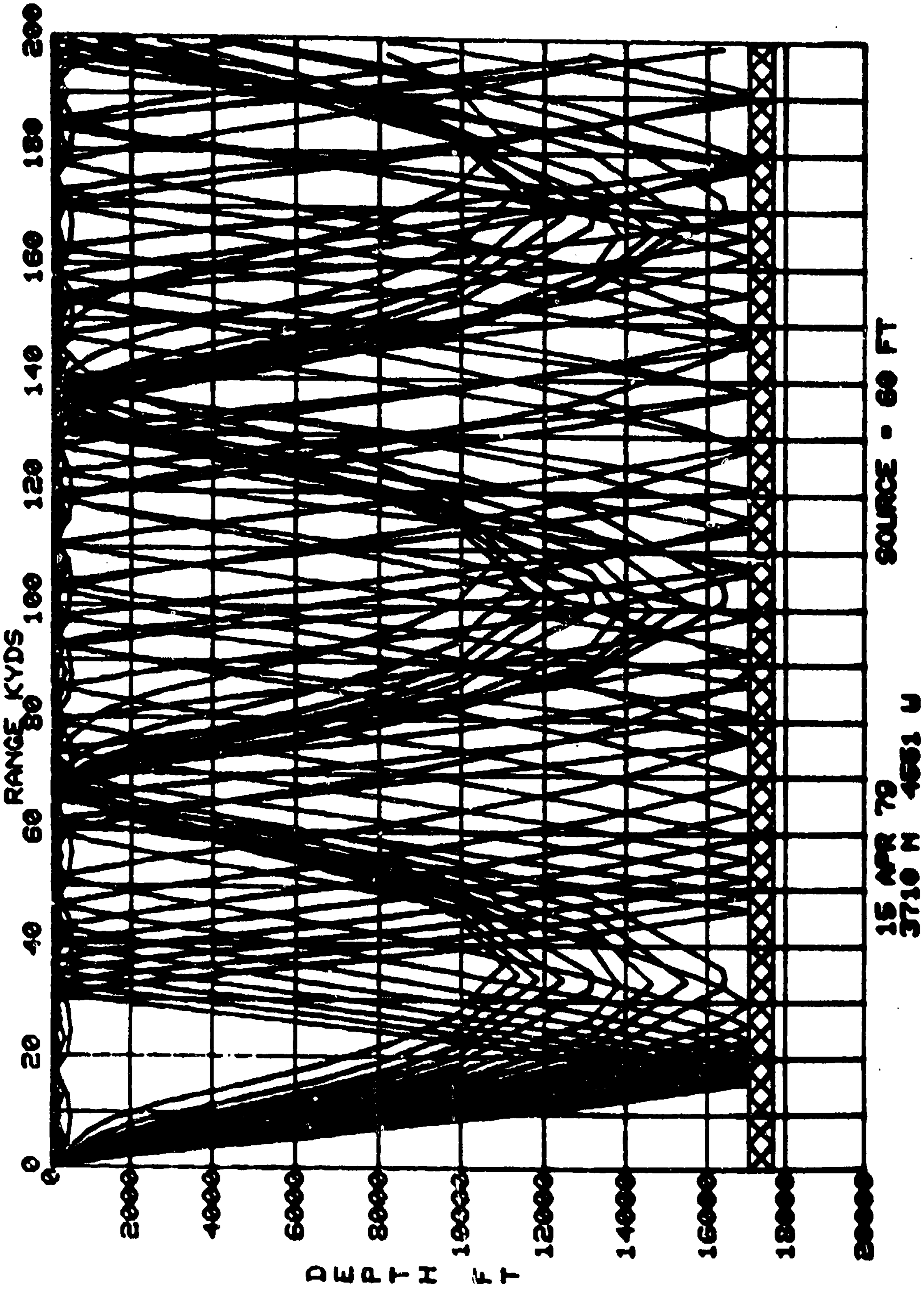

UNCLASSIFIED

Figure 10-3.6. (U) FACT raytrace display

Table 10-3.1. (U) FACT program

Event	Source	Statement/Operator Action	Comment
1	OPR	R FACT	Initiates program FACT.
2	CRT	***FACT (ICAPS)*** USER RUN IDENTIFIER =	An identifying label, maximum of 10 characters, may be entered.
	OPR	Enter label, press RETURN key	
3	CRT	BOTTOM PROVINCE (FREQ. LESS THAN 1000 Hz) = X DO YOU WISH TO CHANGE? (1 = YES, 0 = NO)	Program displays BP in slot X selected in PROFGEN.
	OPR	Enter 1 or 0 and RETURN	If 0, processing continues at event #5.
4	CRT	BOTTOM PROVINCE (1, 3, or 4) =	For a description of low frequency bottom types, see Volume II.
	OPR	Enter 1, 3, or 4 and RETURN	1, 3, 4 only acceptable entries
5	CRT	BOTTOM PROVINCE (FREQ. GREATER OR EQUAL TO 1000 Hz) = X DO YOU WISH TO CHANGE? (1 = YES, 0 = NO)	Program displays BP in slot X selected in PROFGEN
	OPR	Enter 1 or 0 and RETURN	If 0, processing continues at event #7.
6	CRT	BOTTOM PROVINCE (1-9) =	For a description of high frequency bottom types, see Volume II.
	OPR	Enter 1-9 and RETURN	1-9 only acceptable entries.
7	CRT	BOTTOM DEPTH = XXXX FT	Bottom depth appears in slot XXXX (selected or default in PROFGEN).

UNCLASSIFIED

Table 10-3.1. (U) FACT program (continued)

Event	Source	Statement/Operator Action	Comment
8	CRT	SONIC LAYER DEPTH = XXX FT DO YOU WISH TO CHANGE? (1 = YES, 0 = NO)	SLD from PROFGEN appears.
	OPR	Enter 1 or 0 ana RETURN	If 0, processing continues at event #10.
9	CRT	SONIC LAYER DEPTH IN FEET (0 - BOTTOM) =	Alter SLD as desired, in units of feet.
	OPR	Enter SLD in feet and RETURN	
10	CRT	MAXIMUM RANGE IN KILOYARDS (1-200, DEFAULT = 100) =	Enter 0 for default. Entry of a negative value causes the program to use the absolute of that value.
	OPR	Enter maximum range in kiloyards and RETURN	
11	CRT	WAVE HEIGHT IN FEET (0 - 99) =	
	OPR	Enter wave height and RETURN	
12	CRT	NUMBER OF FREQUENCIES (1-4) =	Event 13 is repeated 1-4 times, depending on response.
	OPR	Enter number of frequencies to be specified and RETURN	
13	CRT	FREQUENCY IN HERTZ =	Enter first frequency only; event repeats for additional frequencies.
	OPR	Enter first frequency in hertz and RETURN	

UNCLASSIFIED

Table 10-3.1. (U) FACT program (continued)

Event	Source	Statement/Operator Action	Comment
14	CRT	NUMBER OF SOURCE-RECEIVER DEPTH PAIRS (1-3) =	Event #15 is repeated 1-3 times, depending on response.
	OPR	Enter number of S/R depth pairs and RETURN	
15	CRT	SOURCE DEPTH IN FEET (0-BOTTOM) = RECEIVER DEPTH IN FEET (0-BOTTOM) =	Upon completion program begins to execute. Depending on number of frequencies and S/R pairs, run time is 45 seconds to 20 minutes.
	OPR	Enter source depth, RETURN, receiver depth, RETURN, for each pair specified in event #14	
16	CRT	ASRAP NORMAL END	Calculations now complete. Program halts, bell rings. (FACT = Passive ASRAP)
	OPR	If hard copy desired, press LF; to continue, press RETURN	
17	CRT	DO YOU WISH TO DISPLAY THE FACT INPUT PARAMETERS? (0 = NO, 1 = YES)	Regardless of input in events 17-20 continue synchronously. Data appear in event #24.
	OPR	Enter 0 or 1 and RETURN	
18	CRT	DO YOU WISH TO DISPLAY THE PROPAGATION-LOSS VALUES AS CALCULATED IN FACT? (0 = NO, 1 = YES)	
	OPR	Enter 0 or 1 and RETURN	
19	CRT	DO YOU WISH TO DISPLAY THE SOUND-VELOCITY PROFILE? (0 = NO, 1 = YES)	
	OPR	Enter 0 or 1 and RETURN	

UNCLASSIFIED

Table 10-3.1. (U) FACT program (continued)

Event	Source	Statement/Operator Action	Comment
20	CRT	DO YOU WISH TO DISPLAY THE RAYTRACE GRAPHICS? (0 = NO, 1 = YES WITH 0-100 KYD RANGE, 2 = YES WITH 0-200 KYD RANGE)	
	OPR	Enter 0, 1, or 2 and RETURN	
21	CRT	DO YOU WISH TO DISPLAY THE PROPAGATION-LOSS GRAPHICS? (0 = NO, 1 = YES, ONE PER PAGE, 2 = YES, TWO PER PAGE)	Choice of 0 or 2 forfeits dB override option; processing continues at event #24.
	OPR	Enter 0, 1, or 2 and RETURN	
22	CRT	DO YOU WISH TO OVERRIDE 40-120 DB RANGE? (0 = NO, 1 = YES)	If 0, processing continues at event #24.
	OPR	Enter 0 or 1 and RETURN	
23	CRT	INPUT LOWER AND UPPER DB VALUES	Enter lower and upper range boundaries separated by a comma.
	OPR	Enter number,number and RETURN	
24			Desired graphics appear as requested; when bell rings copies can be made.
	OPR	If hard copy desired, press LF To continue, press RETURN	
NOTE	OPR	If interest is for graphics only, type: R FACTGRAF:OL and RETURN	Processing begins at event #17.

UNCLASSIFIED

However, transition between frequency bands and/or bottom types was previously a potential source of disparity in the selection of a bottom loss curve and the resultant calculations. The revised subroutine eliminates any computation discontinuity between bottom loss values assigned by the different sets of curves at such transition zones via a frequency interpolation weighting scheme. To the user, this translates into elimination of unreasonable predictions in bottom bounce ranges when crossing discontinuous steps between the curves. The 9F version will soon be implemented at all ICAPS fleet sites. A final note is that low frequency (i.e., Bassett-Wolf) bottom type information has been added to the ICAPS historical atlases. Both high and low frequency bottom types are automatically accessed per geographic area. With an updated software package, the operator need not specify either frequency bottom type number unless he wishes to alter the retrieved value.

(U) [Editor's Note: The transition from 9D to 9F does not necessarily improve accuracy as claimed, but does, as also claimed remove discontinuties with respect to frequency. The claim to increased accuracy must await validation of the bottom loss curves used in the model by comparison with experimental data.]

(U) The out s available from the ICAPS version of FACT are given on the next few pages, taken from Floyd (1980). We note that this version of FACT does not have arrival angle versus range information as an output option, but does have a raytrace capability in contrast to FACT PL9D where the situation is reversed.

(U) The ICAPS version further produces propagation loss results every 1 kiloyard (not a variable range interval as in PL9D) out to a maximum range of 200 kiloyards implying points (compared to a 250 points maximum for PL9D). There are no coherence options in the ICAPS version; all results are semi-coherent.

Examples of available outputs follow: Further information on ICAPS, including of course, information on the ICAPS version of FACT, may be obtained by contacting:

Naval Oceanographic Office
Code 9200
NSTL Station, MS 39522

10.4 (U) Generic Fact

(U) From Weinberg (1980): The Generic Sonar Model is a computer program designed to provide sonar system developers and technologists with a comprehensive modeling capability for evaluating the performance of sonar systems, and investigating the ocean environment in which they operate. Recent improvements to the Generic Sonar Model have been in support of projects including sonar operational trainers, thin line arrays, and mission effectiveness models.

(U) The program is written in UNIVAC FORTRAN V and is run on the NUSC UNIVAC 1108 computer, which has a 41K word limit. The model is based on a batch mode model that can be executed from remote terminals if the run time is under five minutes. The ocean environment modeled is both range and time independent.

(U) The Generic Sonar Model contains five eigenray models, of which one is Generic FACT, a modularization of the FACT PL9D model. Generic FACT has much broader capabilities than FACT PL9D. These capabilities include the option of source and receiver beampatterns, selection of several bottom loss inputs, printing and plotting of a large number of outputs which include eigenray information (which further includes a plot of eigenray pressure (in dB//μ Pa) vs. range), propagation loss vs. range of frequency at a given range, LOFAR plots, broadband correlation coefficient at fired range, surface, volume, bottom reverberation vs. time of frequency, signal excess vs. range of frequency,

and range and bearing errors vs. range. These products rely on the eigenray results.

(U) The two sections directly based on FACT PL9D are the FACT OCEAN SOUND SPEED MODEL and the FACT EIGENRAY MODEL (note: full understanding of these sections requires background material from the reference, which is not given here) and are as follows:

FACT Ocean Sound Speed Model (U)

(U) The FACT ocean sound speed model is a constant gradient method that must be used with the FACT eigenray model. Unlike the other ocean sound speed models above, this version requires the bottom, source, and target depths as input. In order to avoid certain cases that are not correctly processed by the FACT eigenray model, ocean depths and sound speeds may be modified during the curve fitting procedure. Additional information can be found in reference 6.015 under Subroutine INSERT.

(U) Required input data statements for the FACT ocean sound speed model are

```
OCEAN SOUND SPEED MODEL = FACT
BOTTOM DEPTH = btmdpt
SOURCE DEPTH = srcdpt
TARGET DEPTH = trgdpt
RADIUS OF CURVATURE = radcrv
OCEAN SOUND SPEED TABLE
ADDITIONAL INFORMATION = addinf
```

(U) The FORTRAN references for the FACT ocean sound speed curve fit model, inverse sound speed squared model, and ray tracing subroutine are

```
CALL  FITSS5

vi = ISSSQ2( zi, gi )

CALL  RAY2
```

respectively. FITSS5 adds the three single precision arrays, Z(MAXNDX), C(MAXMDX), and G(MAXMDX), to the common block SQRISS.

FACT Eigenray Model (U)

(U) The FACT eigenray model uses the modified ray theory from reference 6.242 to solve the reduced wave equation. This Generic version includes travel times, whereas the original computer program did not. FACT is the most widely used propagation model, and is extremely fast.

(U) Please note that the semi-coherent option for adding FACT eigenrays is allowed during a compute eigenray command. FACT eigenrays may not be added semi-coherently during a compute pressure command.

(U) The required input data statements for the FACT eigenray model are

```
EIGENRAY MODEL = FACT
EIGENRAY FILE = eignam
PRESSURE FILE = prsnam
RANGE MINIMUM = rngmin
RANGE MAXIMUM = rngmax
RANGE INCREMENT = rngdel
FREQUENCY MINIMUM = frqmin
FREQUENCY MAXIMUM = frqmax
FREQUENCY INCREMENT = frqdel
FREQUENCY FACTOR = frqgam
BOTTOM DEPTH = btmdpt
SOURCE DEPTH = srcdpt
TARGET DEPTH = trgdpt
RADIUS OF CURVATURE = radcrv
WAVE HEIGHT = wavhit
BOTTOM PROVINCE = btmprv
RANGE REFERENCE = rngrfr
I/O ROUTINE = filior
ADDITIONAL INFORMATION = addinf
COHERENCE = icoher
OCEAN SOUND SPEED MODEL (must be
set to FACT)
BOTTOM REFLECTION COEFFICIENT MODEL
VOLUME ATTENUATION MODEL
```

(U) The FORTRAN reference for the FACT eigenray model is

```
CALL  CMPEI2
```

10.5 (U) Interactive FACT PL9D (As described by Jacobs, 21 Aug 1979):

(U) A preliminary interactive version of FACT 9D has been prepared and is presently operational at Eglin AFB and NSRDC. The version permits the inputting of data via an interactive terminal (e.g., Tektronix terminal, 200 UT, teletype) instead of cards and, as user option, permits the display of the output on the CRT (or teletype) or on the line-printer. The turnaround time for an execution of this program is on the order of 5 seconds during periods of non-peak system usage. Thus, an analyst can generate and review a large set of FACT outputs in a relatively short time. Also, non-NORDA organizations will be able to execute FACT-9D with a minimal amount of computer hardware resources.

FACTEX (U)

I. (U) Background and General Description

(U) FACTEX (Fact Extended), developed by the Acoustic Environmental Support Detachment (AESD*), is essentially an extension of the basic FACT model that provides a limited capability for prediction in range-variable acoustic environments. The model was originally designed for the purpose of prediction of long range propagation from surface ships. Many of the basic computational techniques employed by FACTEX are identical to those contained in FACT. Model documentation is provided in Spofford, Cavanaugh, et al. (1974).

II. (U) Modeling the Environment

(U) The ocean bottom is represented in FACTEX by a number of discrete flat-bottom regions connected by discontinuous depth jumps; i.e., the model bathymetry is stepped. Variations in sound speed structure and surface/bottom reflection characteristics are allowed to occur from one region to the next, but, over the range interval corresponding to a given depth step, the acoustic environment is assumed to be range-invariant as in FACT. Remarks contained in the FACT summary pertaining to the modeling of sound speed structure and ocean boundary reflection characteristics are applicable to FACTEX (within each discrete depth regions) with the exception of those concerning the surface duct module, which is not included in FACTEX. Volume absorption is determined as in FACT.

III. (U) Modeling Acoustic Propagation

(U) As in FACT the initial step in the prediction process is the identification of ray families for processing. This analysis is performed for the first depth region; i.e., the region containing the receiver. Then in each succeeding subregime, "equivalent" families of rays are identified based on the ray phase integral requirement imposed by the adiabatic approximation. These are modified by (1) the requirement that all rays within a given family be able to reach the receiver and (2) the introduction of the bottom. Rays belonging to refracted (RR or RSR) families in the vicinity of the receiver, but encountering the bottom at range, are deleted. The energy associated with deleted rays is added to that associated with the shallow-angled bottom-bounce paths. In proceeding from region to region (increasing source-to-receiver range), the available ray families for a given depth region constitute a nonincreasing subset of the original families. That is, once a family is deleted, it may not reappear at some greater range.

(U) In general, the techniques involved in the determination of intensity levels are the same as those employed in FACT. Semi-coherent and incoherent intensity summing options are available.

*Now resident at NORDA Code 320, NSTL Station, Mississippi 39529

IV. (U) Computer Implementation (NORDA 320)

(U) The FACTEX program was written in FORTRAN IV and is operational at NORDA 320 on a CDC 6000 series computer. The nominal execution time for an 800 nm run on a CDC 6600 computer, including line printer outputs, is on the order of 80 seconds.

V. (U) Output Presentation

(See FACT PL9D Output Description, Sec. 7.1)

VI. (U) Model Performance

(U) FACTEX is not applicable to propagation situations in which acoustic transmission changes from bottom limited (at the receiver) to refracted with increasing source-receiver range. Also, the model does not predict the effects on propagation of steeply sloping bottoms; e.g., upslope enhancement and downslope conversion.

10.6 (U) PLRAY (Bartberger and Stover, 1968)

(U) PLRAY is basically similar to FACT incorporating many features from FACT into an already existing Naval Air Development Center ray theory model. It processes only one source-receiver depth combination at a time. Each new source and/or receiver depth requires a separate set of ray computations; however, up to eight receiver depths may be specified in the input data deck for a run. On the other hand, up to six different frequencies may be processed simultaneously. There is a limit on the number of ranges at which the propagation loss may be computed. The limit is 250. Core storage is 20,480 words (50,000 octal). PLRAY is run on the CDC 6600 computer.

(U) The coherence feature for multipath propagation is essentially the same as in the FACT model. The user is provided with three options by means of a parameter (JCOH) in the input deck. The default value is the semicoherence feature. However, if this parameter is assigned the proper value, incoherent phase addition results. The third option is complete coherence (not recommended for normal use).

(U) PLRAY differs from FACT principally in the following respects:

1. The sound speed profile is fitted with curvilinear segments instead of straight lines. In each segment the square of the index of refraction varies quadratically with depth.

2. Ray intensity is computed from exact analytical formulas, whereas in FACT it is computed from the slope of a parabola which serves as an approximation to the relationship between the range and the ray source angle.

3. PLRAY contains wave corrections for only one type of caustic, the so-called smooth caustic. This is the most common type and covers most cases of interest. Correction for cusped caustics, which is contained in the FACT model, has not yet been incorporated into the new PLRAY program. This tends to lead to erroneous results when the source and receiver are both at the same depth.

4. PLRAY contains a locally generated surface duct model which is used whenever the source is in the duct and the receiver is at a depth less than 1.8 times the duct depth. When a surface duct exists and the source and receiver depths meet the above conditions, ray computations in the duct are suppressed and the special model is used instead.

5. PLRAY does not contain wave corrections for propagation in a depressed sound channel when the source and receiver are near the channel axis.

However, the need for such a correction is considerably reduced by the use of the curvilinear profile segments in lieu of the straight-line segments of FACT.

6. PLRAY contains a provision for the user to insert his own bottom loss

curves in lieu of the internally contained FNOC curves.

7. PLRAY contains a provision for inserting a beam pattern at the ray source.

Comment (U)

(U) Experience with PLRAY and FACT has shown that the two programs tend in general to yield quite similar results. Comparison with normal mode predictions has led to the conclusion that PLRAY tends to yield somewhat more accurate results than FACT in those regions where caustics are not involved, whereas the caustic corrections of FACT tend to be more reliable than those of PLRAY. The explanation of the latter conclusion is that the theory of the smooth caustic correction is based on the assumption that the ray range in the vicinity of the caustic varies quadratically with the ray source angle. In PLRAY the curves generated by real-world sound speed profiles frequently exhibit irregular shapes which deviate significantly from parabolas. The procedure employed by FACT, whereby the actual curves are arbitrarily replaced by parabolas, tends to result in better caustic corrections. On the other hand, where it is necessary to compute ray ranges and intensities by straight ray theory, the forced fit of the parabola sometimes leads to inferior results in FACT.

(U) Both FACT and PLRAY incorporate an attenuation factor for the purpose of reducing the amplitude of the oscillations in semi-coherent runs when the spacing of the receiver range points is too great to permit proper sampling. The key parameter in determining the attenuation factor is the number of range points per cycle of the interference oscillations. In FACT the value of this parameter is computed as an average over the total range interval covered by the rays of the particular family under investigation. Usually the period of these oscillations varies strongly with range, so that the use of a constant value of the attenuation factor frequently results in undercorrection at one end of the range interval and over correction at the other end. In PLRAY the attenuation factor is computed from an analytic formula at each individual range point and thus varies continuously from one end of the range interval to the other. Cases have been found in which the two approaches lead to significantly different propagation loss curves.

(U) The current version of PLRAY contains provision for insertion of a beam pattern at the source. Two additional programs have been developed, using PLRAY as a basis. One is an array gain program which computes the gain in signal-to-noise ratio of an array over an omnidirectional transducer. For this purpose an ambient noise field is read into the program in the form of dB/steradian versus angle in the vertical plane. (There is no variation in azimuth.) The other is an arrival structure program which computes arrival angles and intensities versus range. It does not contain caustic corrections.

PLRAY Input Data Deck (U)

(U) The variables appearing in the input instructions are described below.

(U) Card 1 - Control Integers

NF = number of frequencies, not to exceed 6.
NREC = number of receiver depths, not to exceed 8.
NBMAX = maximum number of bottom bounces to be included in the computations. The default value is 4.
JCOH = coherence control parameter.
= 0, semi-coherent summation.
= 1, incoherent summation.
= 2, fully coherent summation.
IPROF = environmental data input control parameter.
= 1, SSP curve-fitting only; no ray computations. Omit cards

4 to 7 inclusive. Values of ISP and IBP on card 2 are immaterial.
- = 0, normal operation.
- = 1, used if an additional run is desired for the same SSP and same bottom. In this case omit card 2 and card sets 3 and 4.
- = 2, used if an additional run is desired for the same SSP but different bottom. In this case omit card set 4.
- = 3, used if an additional run is desired for the same bottom but a different SSP. In this case omit card set 3.

IUNIT = unit control parameter for BT temperatures.
- = 0, temperature if °F. (Depths must be in feet.)
- = 1, temperature in °C. (Depths must be in meters.)

IPLOT = plot control parameter.
- = 0, no plot.
- = 1, plot propagation loss versus range on plotter at AF

IPR = print control parameter
- = 0, normal operation
- = 1, print diagnostic data.
- = 2, print more diagnostic data (in addition to those of 1).

IBEAM = beam pattern control parameter
- = 0, no beam patterns
- = 1, read and use beam patterns
- = 2, do not read. Use patterns previously read in.

(U) Card 2 - Environmental data header card. Omit card 2 when IPROF = 1.

ISP = sea state.

IBP = bottom control parameter.
- = -1, infinite bottom loss (100 dB).

Note: IUNIT is required only when BT inputs are specified. When the SSP is specified directly by sound speeds, IUNIT is not required and may be left blank.

- 0, zero bottom loss.
- 1 to 5, designates FNOC bottom types.
- = 6, for input of special bottom loss data, replacing types 1 to 5. When IBP = 6 and IPROF = 0 or 2, the bottom inputs are read in card set 3. Otherwise, card set 3 is omitted.

LAT = latitude (degrees, decimal number), necessary only for computation of sound speed from specified temperature and salinity. If left blank, default value is 45°.

IDR = N (north) or S (south, used only for identification.

IDBT = run identification, up to 40 alphanumeric characters.

(U) Card Set 3 - Special bottom loss data. Applicable only when IBP = 6 and IPROF = 0 or 2.

(U) Card 3a - NFR, (FRH(J), J = 1, NFR).

NFR = number of frequencies for which bottom loss data are to be supplied, not to exceed 6.

FRH(J)= frequency of Jth set of bottom loss data (Hz).

(U) Card Pair 3b - (DB(I,6,J), I = 1, 15)

DB(I,6,J) = bottom loss inputs (in dB) for Jth frequency. The index I refers to the point number on the bottom loss versus grazing angle curve, arranged in order of increasing grazing angle. The loss at grazing (θ = 0) is not read into the program. The first data point (I = 1) must correspond to a finite grazing angle, and the loss at all angles between that point and the origin is assumed to be constant. The total number of values to be read must be 15. In the event fewer than 15 points are needed to describe the curve, the loss value of 90° is repeated until a total of 15 data points have been specified. Two cards are required.

(U) Card Pair 3c - (DG(I,6,J), I = 1, 15).

DG(I,6,J) = grazing angles corresponding to the loss values DB(I,6,J)

Note: The cards of set 3 are arranged in the following order: card 3a, card pairs 3b and 3c for the first frequency, card pairs 3b and 3c for the second frequency, and so on.

(U) Card Set 4 - Sound speed profile, ZB(NB), CB(NB), T, S, NDCD. One card is required for each data point, arranged in order of increasing depth. These cards are omitted when IPROF = 1 or 2.

ZB(NB)= depth (ft or m).
CB(NB)= sound speed (ft/sec or m/sec).
T = temperature (°F or °C).
S = salinity (PPT).
NDCD = end code; punch a 1 in column 41 or last card only.

Note: There is no code parameter to tell the machine whether the inputs are to be sound speeds or BT data, as is done in the current program. Rather, the decision is made automatically on the basis of the data provided on the first VP card. If the sound speed on that card is zero, the computer assumes the inputs are to be temperatures and salinities; otherwise sound speeds. All inputs must be in the same set of units, either English or metric.

(U) Card 5 - (F(IF), IF = 1, NF).
F(IF) = frequency (Hz). Note that frequencies are in Hz rather than kHz.

(U) Card 6 - ZSO, (ZRO(I), I = 1, NREC).
ZSO = source depth (ft). Only one source depth may be specified.
ZRO(I)= receiver depth (ft).

(U) Card 7 - Ranges (yd).
RMIN = minimum range (yd).
DR = range increment (yd).
RMAX = maximum range (yd).

Note: (RMAX - RMIN)/DR should not exceed 250. If it does, RMAX will be adjusted accordingly.

(U) Card Set 8 - Beam patterns. Omit unless IBEAM = 1
Card 8A - NBF(IF) = No. of points to specify pattern at each frequency (not to exceed 50).
Card Set 8B - Theta(I) = angle (deg), 8 values per card. Angles are positive upward.
Card Set 8C - BMLOS (I) = Beam deviation loss (dB), 8 values per card.
Note: Stack 8B and 8C for 1st freq., then 2nd freq., etc.

(U) End Card - Insert one blank card to stop. As many data sets as desired may be stacked together in sequence. The blank card is inserted at the very end, next to the 6789 card.

Miscellaneous Information (U)

Program name:	PLRAY
File Identification:	AE1275PLRAY, ID = CLB, CY = 1.
Core Requirement:	CM2300 minimum.

11.0 (U) Test Cases Used in AMEC Evaluation

(U) Test cases were chosen from experimental data sets. The experimental data sets are described in detail by Martin (1982) and constitute a Portable Test Package for model evaluation. A subset of these cases were selected for the FACT PL9D evaluation based on time and cost constraints and availability of the data during this evaluation. The experimental sets selected were SUDS, HAYS-MURPHY, PARKA II, BEARING STAKE, JOAST, LORAD, FASOR, and GULF OF ALASKA. Some general information on these data sets is given in Table 11.1. As can be read from this table, the data sets were selected to provide broad geographic and frequency coverage and coverage with redundancy of the various propagation

Table 11.1. (U) Experimental data used in FACT PL9D evaluation

DATA SETS	LOCATION	PROPAGATION MODE	Z_S/Z_R	FREQUENCY $\leq$ 1KHZ	FREQUENCY $1 \leq F \leq$ 5KHZ	NO. OF AMEC CASES
HAYES-MURPHY	MED	BB	S/S	✓		6
PARKA	PAC	BB, CZ	S/S	✓		2
SUDS	PAC	SD	S/S	✓	✓	12
GULF OF ALASKA	GULF OF ALASKA	BB MULTI CZ	D, S/S		✓	14
BEARING STAKE	IND	BB	S/S	✓		12
LORAD	PAC	MULTI CZ	S/S	✓	✓	14
FASOR	PAC & IND	CZ, SD BBM SHAL	S/S		✓	6
JOAST	MED	CZ	S/S		✓	12

BB = BOTTOM BOUNCE   S: $\leq$ 1 KFT
SD = SURFACE DUCT   D: > 1 KFT
CZ = CONVERGENCE ZONE

CONFIDENTIAL

models. Specific characteristics of the subsets selected for the FACT PL9D evaluation are given in Table 11.2A-H which include source and receiver depths, mixed layer depth and depths of sound channel axis and bottom, frequency, and maximum range of data. Sound speed profiles, bottom loss versus grazing angle curves, and the measured acoustic data are found in Appendices IIA - IIH, respectively, for the experimental sets mentioned above. The bottom loss versus grazing data is that associated with the FACT PL9D model with bottom loss determined from geographic area designator charts with the following exceptions: (1) for PARKA II and HAYS-MURPHY, Marine Geophysical Survey (MGS) bottom loss versus grazing angle curves used by the RAYMODE model (evaluated by AMEC as reported in Volume III of this series) with bottom loss being determined from MGS area designator charts was used for FACT PL9D in addition to the standard FACT inputs, (2) a constant bottom loss of 50 dB was used for all SUDS cases, effectively eliminating bottom interacting paths, since the experiment resulted from pulsed transmission and bottom reflected paths were time-gated out, and (3) bottom loss measurements from the experiment site were used for BEARING STAKE since they differed so greatly (i.e., show much less loss) than would be obtained from either MGS or FNOC (used for FACT) area designator charts and their associated curves.

11.1 (U) Results of Test Cases Used in AMEC Evaluation

(C) SUDS: (1) Regardless of source/receiver geometry with respect to the surface duct, agreement is generally lacking between FACT PL9D results and SUDS data. This is particularly notable in (2) FACT's inability to reproduce either fluctuations or interference patterns observed in the SUDS data. (3) The identical results for FACT regardless of coherence option chosen indicates a need for closely examining this aspect of the model. (4) FACT requires a new surface duct module which includes rough surface effects and leakage.

(C) HAYS-MURPHY: (1) Significant differences in mean levels were primarily responsible for pessimistic detection range predictions by the model. These differences appear to be attributable to the bottom loss inputs within the first 25 km. Beyond this range, differences are as great and unexplained but bottom loss is not a factor. It is to be noted that for this scenario, FACT's FNOC and RAYMODE's MGS bottom loss inputs led to essentially the same results. (2) Large differences in the first 25 km were caused by FACT's coherent and semi-coherent predictions of Lloyd Mirror interference patterns absent in the HAYS-MURPHY data, possibly due to broadband (i.e., one-third octave) analysis of the latter. Once again, this disparity is not felt to represent an error in the model.

(C) PARKA: (1) FACT's own FNOC bottom loss leads to better agreement with PARKA data than does use of RAYMODE's MGS bottom loss at 400 Hz (at 50 Hz the differences are negligible). (2) FACT accurately predicts the ranges of the start of PARKA's first and second convergence zones. (3) Second and third convergence zones predicted by FACT are too narrow. (4) FACT predicts optimistic coverage compared to PARKA results.

(C) BEARING STAKE: (1) FACT fails to capture, at all ranges and regardless of coherence option chosen, the basic fluctuating nature of the experimental data (all coherence options yielded the same values). This suggests a close examination of the FACT coherence logic, particularly in BEARING STAKE type environments. (2) The basic trend of the disagreements is that the differences go from positive at short range to negative at long range (the overall statistical effect being an emphasis of the negative differences). It appears that at great range, an even smaller bottom loss than that measured in the experiment area

Table 11.2A. (U) SUDS: Test case characteristics

CASE	SOURCE DEPTH(m)	RECEIVER DEPTH(m)	FREQUENCY (kHz)	MIN RANGE (km)	MAX RANGE (km)	NO. OF POINTS	LAYER DEPTH (m)	MAX SOUND SPEED DEPTH (m)	DEEP SOUND CHANNEL AXIS DEPTH (m)
I	45	17	0.4	2.0	24.5	925	68	68	900
II	45	112	0.4	2.0	17.4	625	68	68	900
III	42	43	1.0	2.0	24.4	959	68	68	900
IV	42	112	1.0	2.0	24.8	818	68	68	900
V	41	6	1.5	0.4	24.6	796	20	250	900
VI	41	59	1.5	0.4	24.8	811	20	250	900
VII	41	6	2.5	0.4	24.8	868	20	250	900
VIII	41	59	2.5	0.4	24.8	866	20	250	900
IX	45	17	3.5	0.1	35.3	1311	79	79	900
X	45	112	3.5	0.1	35.8	918	79	79	900
XI	42	17	5.0	0.1	35.5	1421	79	79	900
XII	42	112	5.0	0.1	33.8	959	79	79	900

CONFIDENTIAL

Table 11.2B. (U) HAYS-MURPHY: Test case characteristics

CASE	SOURCE DEPTH (m)	RECEIVER DEPTH (m)	FREQUENCY (Hz)	SOUND AXIS DEPTH (m)	BOTTOM DEPTH (m)
I	24.4	137.2	35.0	61	2750
II	24.4	137.2	67.5	61	2750
III	24.4	137.2	100.0	61	2750
IV	24.4	137.2	200.0	61	2750
V	24.4	106.7	35.0	61	2750
VI	24.4	106.7	100.0	61	2750

CONFIDENTIAL

Table 11.2C. (U) PARKA: Test case characteristics

CASE	FREQUENCY (#2)	SOURCE DEPTH (m)	RECEIVER DEPTH (m)	LAYER DEPTH (m)	SOUND AXIS DEPTH (m)	BOTTOM DEPTH (m)
I	50	152.4	91.4	80	1000	5500
II	400	152.4	91.4	80	1000	5500

CONFIDENTIAL

Table 11.2D. (U) BEARING STAKE: Test case characteristics

CASE	SOURCE DEPTH(m)	RECEIVER DEPTH(m)	FREQUENCY (Hz)	MIN RANGE (km)	MAX RANGE (km)	LAYER DEPTH (m)	SOUND AXIS DEPTH (m)	BOTTOM DEPTH (m)
I	91	496	25	6	288	75	1676	3353
II	91	1685	25	6	288	75	1676	3353
III	91	3320	25	6	288	75	1676	3353
IV	91	3350	25	6	288	75	1676	3353
V	18	496	140	6	288	75	1676	3353
VI	18	1685	140	6	288	75	1676	3353
VII	18	3350	140	6	288	75	1676	3353
VIII	18	3350	140	6	288	75	1676	3353
IX	18	496	290	6	288	75	1676	3353
X	18	1685	290	6	288	75	1676	3353
XI	18	3320	290	6	288	75	1676	3353
XII	18	3350	290	6	288	75	1676	3353

CONFIDENTIAL

Table 11.2E. (U) JOAST: Test case characteristics

CASE	STATION	RUN	SOURCE DEPTH(m)	RECEIVER DEPTH(m)	FREQUENCY (KHz)	LAYER DEPTH(m)	SOUND AXIS DEPTH(m)	BOTTOM DEPTH(m)
I	1	43	6.1	18.3	3.5	-	137	2816
II	1	43	6.1	79.2	3.5	-	137	2816
III	2	43	6.1	163.1	3.5	-	137	2816
IV	2	63	6.1	18.3	3.5	-	61	2725
V	2	63	6.1	79.2	3.5	-	61	2725
VI	2	63	6.1	163.1	3.5	-	61	2725
VII	3	43	6.1	18.3	3.5	-	70	3471
VIII	3	43	6.1	79.2	3.5	-	70	3471
IX	3	43	6.1	163.1	3.5	-	70	3471
X	3	103	6.1	18.3	3.5	-	70	3471
XI	3	93	6.1	163.1	3.5	-	70	3471
XII	5	43	6.1	18.3	3.5	65.5	442	2743
XIII	5	43	6.1	79.2	3.5	65.5	442	2743
XIV	5	43	6.1	304.8	3.5	65.5	442	2743

CONFIDENTIAL

Table 11.2F. (U) LORAD: Test case characteristics

Case	Run Number	Frequency (Hz)	Source Depth(m)	Receiver Region	Bottom Bounce Zone	Convergence Zone	Min Range (km)	Max Range (km)	Sound Axis Depth(m)	Bottom Depth (m)	Layer Depth (m)
IA	3S	530	15.2	30.5	First	First	2	79	750	5670	33
IB	6S	530	15.2	30.5	Second	Second	45	143	750	5670	33
IC	8S	530	15.2	30.5		Third	182	216	750	5670	33
ID	10S	530	15.2	30.5		Fourth	250	274	750	5670	33
IE	12S	530	15.2	30.5		Fifth	313	350	750	5670	33
IF	14S	530	15.2	30.5		Sixth	376	416	750	5670	33
IG	16S	530	15.2	30.5		Seventh	440	478	750	5670	33
IIA	3D	530	15.2	304.8	First	First	3	76	750	5670	33
IIB	6D	530	15.2	304.8	Second	Second	45	143	750	5670	33
IIC	8D	530	15,2	304.8		Third	182	216	750	5670	33
IID	10D	530	15.2	304.8		fourth	250	274	750	5670	33
IIE	12D	530	15.2	304.8		Fifth	313	350	750	5670	33
IIF	14D	530	15.2	304.8		Sixth	376	416	750	5670	33
IIG	16D	530	15.2	304.8		Seventh	440	478	850	5670	33

CONFIDENTIAL

Table 11.2G. (U) FASOR: Test case characteristics

CASE	STATION	RUN	SOURCE DEPTH(m)	RECEIVER DEPTH(m)	FREQUENCY (KHz)	MIN RANGE(km)	MAX RANGE(km)	LAYER DEPTH(m)	AXIS DEPTH(m)	BOTTOM DEPTH(m)
I	FIG	3	6.1	37.0	1.5	6.0	54.0	0	NA	7648
IIa	OAK	1	23.0	37.0	1.5	26.0	44.0	30	NA	120
IIb	OAK	2	23.0	37.0	1.5	12.0	24.5	30	NA	120
IIIa	THORN	1	23.0	37.0	1.5	19.5	33.5	55	NA	104
IIIb	THORN	2	23.0	37.0	1.5	12.0	25.5	55	NA	104
IV	REDWOOD	3	6.1	37.0	1.5	1.0	36.0	19	1200	3262

CONFIDENTIAL

CONFIDENTIAL

Table 11.2H. (U) GULF OF ALASKA: Test case characteristics

CASE	RUN NO.	SOURCE DEPTH(m)	RECEIVER DEPTH(m)	FREQUENCY (KHz)	MIN RANGE(km)	MAX RANGE(km)	LAYER DEPTH(m)	SOUND SPEED MIN. DEPTH(m)	BOTTOM DEPTH(m)
I	140	30.5	30.5	1.5	37.0	63.0	10	75	4078
II	140	30.5	304.8	1.5	37.0	63.0	10	75	4078
III	143	30.5	30.5	1.5	8.5	53.0	10	90	4042
IV	143	30.5	304.8	1.5	8.5	53.0	10	90	4042
V	124	30.5	30.5	1.5	2.5	11.0	10	75	4042
VI	124	30.5	304.8	1.5	2.5	11.0	10	75	4042
VII	108	1067.0	30.5	2.5	2.5	28.0	0	85	4060
VIII	108	1067.0	304.8	2.5	2.5	28.0	0	85	4060
IX	107	1067.0	30.5	2.5	30.0	67.0	10	85	4060
X	107	1067.0	304.8	2.5	30.0	67.0	10	85	4060
XI	112B	304.8	30.5	2.5	2.0	19.5	10	75	4042
XII	112B	304.8	304.8	2.5	2.0	19.5	10	75	4042
XIII	112A	304.8	30.5	2.5	15.0	58.0	10	75	4060
XIV	112A	304.8	304.8	2.5	15.0	58.0	10	75	4060

CONFIDENTIAL

would be necessary to bring the model into agreement with the BEARING STAKE data. But what of shorter ranges (typically less than 50 to 75 km) where the experimental data has less loss than the model results? The answer may lie in the treatment of coherence. (3) The FACT PL9D model gives longer continuous detection ranges (i.e., range to which detections per opportunity ratio is 100%), but because of fluctuations, the experimental data gives longer zonal coverage. The experimental data generally predicts detection at longer ranges than are predicted by FACT for a given figure of merit.

(C) LORAD: (1) Good agreement was achieved in the first bottom bounce region to about 40 km beyond which the Generic FACT model predicted less loss than was found in LORAD data until the first convergence zone was reached. The discrepancy increased with increasing range. This result was independent of receiver depth. (2) The Generic FACT incoherent prediction showed less loss than did LORAD data through the second bottom bounce region despite the use of FACTs most lossy (i.e., Type 5) bottom. This result was independent of receiver depth. (3) For the 100 foot (30.5 m) receiver: (a) the FACT CZ start always occurred at shorter range than LORAD's; (b) the slope of the CZ start was the same for all of FACT's seven CZs. The LORAD CZ slopes agreed with FACT for CZ1 and CZ2 but became increasingly gentle with additional CZs; (c) the CZ end for FACT always extended beyond that for LORAD; (d) the LORAD CZs increased in width much more slowly than did FACT CZs with increasing zone number. (4) For the 1000 foot (305 m) receiver: (a) the first two CZ are double-lobed for LORAD; all CZs are double-lobed for Generic FACT predictions; (b) the first two CZs are of approximately the same width for LORAD and FACT. Differences in zone start and end are figure of merit dependent; (c) for the third CZ and beyond, start ranges generally differ by less than 2% of the entire range; (d) the fourth through seventh CZs are generally much narrower (factor of 2 is typical) for Generic FACT incoherent than for LORAD data.

(C) JOAST: Except for the last three cases (Station 5), which involved a surface duct, the JOAST experimental data and FACT model results were in substantial agreement with respect to convergence zone start and shape of the zone with the serious exception that for Stations 2 and 3 (Cases IV--IX), the FACT results show a substantial and anomalous broadening to the zone at its end. FACT CZ results are generally masked by bottom bounce energy for figures of merit valued greater than 105-115 dB, whereas JOAST results rarely show this effect (i.e., bottom bounce interference is absent). Results for Station 5 are ambiguous in that the JOAST data has lower CZ levels than previous stations (i.e., 1, 2 and 3) but shows a reasonably shaped CZ when compared to results for other stations. FACT results for Station 5 show anomalous zone extension to long ranges and, in Case XII, where both source and receiver were in the surface duct, the convergence zone was masked by the surface duct contribution--in contradiction to the JOAST data.

(C) FASOR: (1) The FACT model yielded identical results for coherent and semicoherent phase options for Stations FIG, THORN, and REDWOOD but not OAK. This bears further examination. (2) The agreement between experimental data and model results was far better for shallow water stations OAK and THORN than for deep water Stations FIG and REDWOOD. (3) FACT exhibited an unrealistic interference pattern for Station THORN. (4) FACT was excessively optimistic with respect to FASOR data for the "high latitude: Station FIG and excessively pessimistic for the "mid-latitutde" Station REDWOOD. For Station REDWOOD, the disagreement is likely due to the high bottom loss (type 8) designated for that area.

(C) GULF OF ALASKA: For the arctic sound speed field, FACT results were

insensitive to phase options chosen over most of the range interval when the receiver was deep (305 m). (2) In many cases, the FACT interference structure had an anomalous appearance. (3) In most cases at 2.5 kHz, FACT showed less loss than GULF OF ALASKA (GOA) data to the extent that the FACT curve often provided a low-loss envelope for the GOA data. (4) In all cases, FACT showed no fluctuations at periods of less than 1 km except at ranges between 5 and 15 km. In contrast, GOA data typically possessed fluctuations of 10 dB at periods less than 1 km. (5) FACT and GOA results at 1.5 kHz showed no basic agreement in the shape of the propagation loss curve or fea- tures therein. (6) Large negative differences (i.e., GOA- FACT 0 dB) in Run 124: Source Depth = Receiver Depth = 30.5 m, Frequency = 1.5 kHz, GOA data interval = 2.5 to 11.0 km (i.e., Case V) appear to arise from an inconsistency in the FACT results (compared to FACT results for other cases) rather than in the GOA data. (7a) at 1.5 KHz, the GOA data shows better coverage than FACT in terms of percentage of the possible range interval covered at a given FOM. When both cover a given range segment, however, FACT usually has a 100% detection per opportunity ratio while GOA's percentage is both range and FOM dependent. (7b) At 2.5 kHz, the GOA data shows poorer or equal coverage to FACT in terms of percentage of the possible range interval covered at a given FOM. When both cover a given range segment, FACT usually has a 100% detection per opportunity ratio while GOA's percentage is both range and FOM dependent.

12.0 (U) Summary and Recommendations

(U) The FACT model produces propagation loss as a function of range and frequency in an environment characterized by a single sound speed profile and a horizontal ocean floor. The evaluation herein reported has been for a specific version of the FACT model which is named FACT PL9D, and all runs were performed on the UNIVAC 1108 computer. FACT was primarily designed as a low frequency model although it has been used at frequencies of tactical sonars. In this evaluation, 5 kilohertz was the highest frequency at which FACT results were compared with experiment data.

(C) Many of the design decisions, particularly the selection of the physics utilized by FACT PL9D were driven by a requirement to achieve fast running times. The UNIVAC 1108 run times for the test cases used in this evaluation generally ranged between 3 and 6 seconds and were scenario dependent. One exception to this general range was the BEARING STAKE (i.e., Indian Ocean) environment for which FACT run times varied between 10 and 21 seconds. These longer run times were due to the presence of a low loss bottom which resulted in lengthy calculations for bottom bounce paths.

(U) The computer core required by the FACT PL9D model is 17800 decimal words which includes approximately 1000 words used for plot routines. The computers on which FACT PL9D or other versions of FACT are found include a variety of CDC machines, UNIVAC 1108 and 1110, NOVA 800, PDP-11, SEL 32/75, PRIME 400, IBM 360, 370 and 3033-D, ICL 1903A, GE 635, and Burroughs 5700 and 6750. Besides FACT PL9D, other versions of FACT are SHALFACT, MINIFACT, ICAPS FACT, FNOC FACT, Generic FACT and FACTEX.

(U) The physics of the FACT PL9D model was extensively examined by Charles L. Bartberger of the Naval Air Development Station, Warminster, PA. The depth of this examination is largely attributable to the extensive documentation of the FACT model, primarily Baker and Spofford (1974) and Spofford (1974), which give both an overview of the physics and a subroutine-by-subroutine description with flowcharts. The FACT computer code has a good number of comment cards which are essential to finding one's way through the program. Overall, the external and internal documentation of the FACT model is fairly complete and of

high quality. The distribution package of the FACT program includes test cases to assure proper installation on a new computer has been achieved.

(U) Code 323 of the Naval Ocean Research and Development Activity, NSTL Station, MS 39529 (Telephone (601) 688-5434, A/V 485-5434) is the point of contact for distribution of the FACT PL9D model and should also be addressed with regard to questions or problems relating to FACT PL9D.

(U) Based upon the examination of the FACT PL9D model (section 5.0), results of a questionnaire sent to FACT PL9D users by Mr. John Cornyn of NORDA Code 321 and comparisons of FACT PL9D model results with experimental data for eight data sets (SUDS, HAYS-MURPHY, PARKA, BEARING STAKE, JOAST III, LORAD, FASOR AND GULF OF ALASKA - all described by Martin (1981), a number of deficiencies in the FACT model have been identified. Many of these bear further investigation whereas for other remedial action is simply an implementation problem. Accordingly, recommendations pertaining to FACT PL9D deficiencies follow:

(U) (1) Replace the present bottom loss tables and curves (in subroutine BTMLOS) with tables or curves which, for a given bottom type, are continuous in frequency. The present curves have significant discontinuities in frequency.

(U) (2) Separate the choice of critical angle from array THETCR from the bottom type selected by the user. From Garon (1980), critical angle is used in FACT in two ways, both of which are not related to the computation of bottom loss. These two ways are as follows.

$$\text{Let } A = \text{maximum} \begin{cases} \text{initial angle of the ray that strikes the bottom at the critical angle} \\ 5° \text{ more than the initial angle of the first ray in the last ray family (i.e., the SRBR family} \end{cases}$$

1. Rays with initial angles steeper than A are terminated after four bottom bounces, whereas rays with initial angles shallower than A are not terminated after any particular number of bounces.

2. Rays with initial angles steeper than A are fit with a curve in range-angle space that differs in form from the fit used for shallower rays (see Baker and Spofford, 1974, sec. 5.0).

(U) The usage that terminates rays after four bottom bounces could be treated by choosing a conservatively large value, thus ensuring that significant bottom bounce energy would not be neglected. This would be at a cost of slightly longer run times in some cases (which would have to be determined).

(U) Concerning the critical angle usage for curve fitting, it is not clear that the use of this parameter leads to an optimum curve fitting scheme. It is possible that a single value may be adequate in this context (especially in view of the fact that only in the lowest frequency band [i.e., that first 5 values in THETCR], (<150 Hz) is there a direct correspondence between the critical angles of the bottom loss curves and the critical angles in the THETCR array.

(U) In view of the above it seems logical to separate not only the choice from THETCT from the user choice of bottom loss class, but to further separate THETCR into two arrays (or two values), one for each function presently served.

(U) (3) Provide for external bottom loss inputs. This alteration should follow the separation of choice from the THETCR array from the choice of bottom loss class. Otherwise, four alternatives exist with regard to a choice of critical angle: (a) whenever an external bottom loss table specified, a default value for THETCR is chosen, (b) the external bottom loss table is tested for the presence of a critical angle which, if found, if used; if not, the default value is used, (c) the critical angle is specified as an input variable; if none is specified, either (a) or (b) is involved. Six bottom loss versus grazing angle curves, corresponding to six frequencies, would permit multifrequency runs (unless each curve has an associated value for critical angle, in which case single frequency runs would be advised.

(U) (4) Provide for writing FACT outputs to tape or disk files for use by other programs (including plot routines).

(U) (5) Provide for the input of source and receiver vertical beampatterns in tabular form. This capability would permit estimates of transmission loss for vertically directive systems.

(U) (6a) Provide an eigenray output option for which a table of propagation loss, source and receiver angles, and travel time versus range would be generated for eigenrays routinely selected for use within the FACT model. The travel time computation would have to be added to the program; all other information is presently calculated internally. Note: Since arrival angle information is obtained by interpolation (curve fitting) techniques, the angle at the source determined by Snell's Law is not exact. This conclusion is particularly true for low-angle rays.

(U) (6b) Provide a ray trace capability which would display the ray paths automatically selected for processing by the FACT model.

(U) (7) The cusped caustic correction procedure has several shortcomings. The fact that the theory being implemented assumes the source and receiver to be at the same depth, whereas in the actual operation of the FACT model they are separated, leads at the least to confusion and at the worst to errors in output. All range-angle curves throughout the program are plotted against receiver angle except the parabola for the cusped caustic corrections. Plotting this curve against source angle is a serious mistake and should be corrected. Also, the method employed to fit a parabola to a smooth caustic associated with a cusp is faulty and usually leads to a poor fit, since one of the three fitting points usually does not lie on the curve to which the parabola is being fitted.

(U) In view of the manner in which it is implemented in the FACT model, there is a serious question of whether the cusped caustic correction is necessary, which should be determined by further testing.

(U) (8) The scheme for moving the source and receiver depth away from the axis of a sound channel to eliminate the computation of near-axial rays is unsatisfactory. The extent of displacement depends not only upon the physical characteristics of the sound speed profile, but also upon the manner in which the input data table is set up. In one example, merely interpolating one extra point in a linear profile segment caused a major change in the propagation loss output. In another example the procedure led to a shift of over 250 ft in the receiver depth, which is felt to be far in excess of a tolerable limit.

(U) At least two actions are indicated: (a) In the short run, list both the input source and receiver depths and those used by the program after alteration. This procedure should not be limited to the "axis-to-axis" situation, but to all cases for which source or receiver are moved internal to the FACT program. Finally, instances of sound speed profile

modification should likewise be brought to the user's attention through an output listing. (b) An alternative to the present "axis-to-axis" treatment should be sought. Perhaps a coherent approach taking advantage of phase cancellation properties rather than the rms approach (leading to an infinite number of non-zero intensities) would prove viable.

(U) (9) Not enough rays are computed in the outermost source angle sector (NG= NGRPS). FACT currently computes only two rays. The first ray is immediately beyond the limiting ray to the bottom, and the second ray either strikes the bottom at a critical angle determined by user's selection of bottom loss type or else is 5° steeper than the first (see (2) above), whichever results in the larger angle. Examples have shown that when the second ray is only 5° beyond the first, as is the case with an FNOC Type 5 bottom, the resulting range-angle curve fitting may be unacceptably poor, leading to erroneous ray intensities and distorted surface-imaging interference patterns.

(U) (10) The procedure employed for replacing range-angle curves with parabolas needs further study. Examples have been found where oversmoothing by the parabola leads to serious errors in caustic corrections. Also, through an oversight in the logic of the program it is possible to generate a false caustic when fitting a parabola to $\theta-\theta_1$ (where θ_1 is the angle of the first ray of the sector) as the independent variable. The false caustic can have serious and fortunate consequences.

(U) (11) In FACT the decision whether to compute coherence is made by testing the horizontal separation between the direct and surface-reflected paths. If the separation for either the first or the last ray in an angular sector exceeds a preset limit, the entire sector is treated incoherently. Cases have been found where FACT generates an incoherent output over a whole sector, whereas if the decision has been made on a ray-by-ray basis, virtually the whole sector would have been treated coherently. The latter decision method (i.e., ray-by-ray) is recommended for implementation in FACT.

(U) (12) A similar consideration to that of (11) applies to the amplitude reduction applied to the interference pattern in cases of inadequate range sampling. FACT computes an average number of points per cycle over the entire range interval. Actually in the first bottom bounce region, where the interference pattern assumes its greatest importance, the number of points per cycle varies strongly with range, with the possible result that the FACT propagation loss curve may be undersampled at short ranges, whereas the amplitude may be unduly attenuated at long ranges. A procedure is needed which would determine the range dependence of number of points per cycle (perhaps in range intervals) and then apply corrections accordingly.

(U) (13) There is an error somewhere in the logic determining the parameter RCUT which is used in some applications to accelerate the attenuation of the sound field in the shadow zone of a smooth caustic. In one example an erroneous value of RCUT completely wiped out the contribution of a family of rays containing a caustic. Identification and correction of this error should be undertaken.

(U) (14) The FACT PL9D model assumes specular reflection at the sea surface with no losses. A rough surface module is needed which gives surface losses as a function of wave height, frequency, and grazing angle. A proposed rough surface model is described in Spofford et al. (1977).

(U) (15) The FACT surface duct module has been recognized as deficient from the onset (sec. 2.2.5 of Spofford,1974). A proposed replacement (Spofford et al., 1977) is recognized as still having deficiencies. Investigation of available surface duct modules and testing against experimental data is indicated.

(U) (16) On computers utilizing word lengths less than (e.g., the 32 bit words of the UNIVAC 1108 and 16 bit [with 32 bit floating point arithmetic] NOVA 800 series computers) the CDC 6600 for which the FACT model was developed, errors due to lack of double precision for certain variables have been observed and the appropriate corrections made for the ICAPS version of FACT and the PL9D version at the Naval Underwater Systems Center, New London Laboratory, which was used to produce the model results for this evaluation. These double precision corrections should be distributed to all users with computers using less than 32 bit words.

(U) (17) Present versions of FACT produce propagation loss in units of dB reference 1 yard at ranges in either kiloyards or nautical miles (but not both). The user should have the choice of specifying either these options or a "metric option" for which propagation loss would be given in dB reference 1 meter and range would be given in kilometers.

(U) (18) In the present version of FACT the initial range and range increment are a single variable. This precludes focusing in on a given range interval or having a high data density (or, for that matter, choice of data density) at distant ranges. Accordingly, it is recommended that initial range and range increment be independent input variables.

(U) (19) The maximum number of points per prediction in FACT PL9D is 250 (Note: The ICAPS version can produce 400 points, but at fixed intervals of 0.5 nautical miles.) This has turned out to be too small for many purposes, including this evaluation, and one is forced to decide between maximum range or data density, or produce multiple runs (which do not have identical intervals between points due to the issue of item (18). It is recommended that the maximum number of points be raised to at least 400 points. It should further be decided whether it would be wise to have an option whereby the number of points needed for adequate sampling of interference cycles would be internally determined and applied.

(U) (20) The special purpose half-channel model (HFCHTL) resident in FACT can be used for only specific ASRAP source/receiver geometries and frequencies. This should be eliminated from the basic model and offered as an option.

(U) (21) Spofford (1974) states that the smooth and cusp caustic fields are added on an rms basis, which is inappropriate for tight geometries. A two-stage correction approach is indicated: (a) Alert the user in the output that the problem has occurred and inform as to the range interval(s) affected, and (b) solve the 4-ray problem and implement in FACT (which is admittedly difficult). Please note additional comments on the treatment of cusped caustics in (7) above.

(U) (22) The approach used by FACT, as low-frequency cut-off is approached, is admittedly "speculative at best" and "wave programs should be used wherever possible for these cases." When FACT is the only model available and is used in these cases, an output message to the effect that this situation has been encountered and that reduced confidence should be placed in the output should be added to the model.

(U) (23) In test cases different results for a given scenario have been obtained, depending on whether a single or multi-frequency run was involved. These disparities were at high loss values but indicate two needs: (a) advise all FACT users to avoid multi-frequency runs unless this would cause workload or run times which are inaccessible in a system context, and (b) resolve the problem so that single- and multi-frequency runs produce identical results for the same case.

(U) In considering the above list of recommendations, one is forced to conclude that they fall into two basic categories:

- Error correction and improvement of physics.
- Addition of input/output options.

(U) This brings up a possibility that FACT exists as a basic model with several options available. The basic model would ultimately incorporate recommendations (1), (2), (7) through (16), (18), (21) through (23) and possibly (5). The options would be (3) through (6), (17), (19), (20), and (23). It would not be necessary that all options be included in a given implementation of the model, but it would be essential that the output list the options utilized, particularly if they affect the answer (e.g., an external bottom loss table input) as opposed to those that don't (e.g., write output onto tape).

(U) The variety of FACT versions available implies that different results are obtained from models all carrying the name FACT for the same environmental inputs, and this is unfortunately true. Although, as mentioned above, different options are desirable for various applications, it should nevertheless be possible to get the same answer from all versions for basic problems, i.e., the core FACT program should be the same for all implementations containing the same basic physics. It is further recommended that any change to the physics of the FACT model be well documented and undergo test and evaluation.

(C) No model evaluation can claim to be complete and such is the case here. There are some particular omissions which must be identified: (1) propagation in an environment characterized by a sound speed profile with a double deep sound channel such as found in the eastern Atlantic Ocean; (2) no analysis was performed for frequencies above 5 kHz due to a lack of experimental propagation loss data with supporting environmental data; (3) nonanalysis for shallow water scenarios, once again due to a lack of data; (4) under-ice propagation was not examined; and (5) the performance of the FACT model in range dependent environments. This final problem was not addressed due to its complexity wherein the sound speed may vary horizontally, bathymetry may vary as may bottom loss with range in an infinite number of combinations.

(U) It is of extreme importance to estimate the frequency with which a given problem occurs and under what circumstances and to limit the problem to certain geographic areas and seasons. An evaluation of this scope cannot be performed without coordinated fleet feedback of results over a long period. Certainly feedback with regard to surface and sub-surface ducts would be valuable. Future experiments should be performed with model evaluation support as one objective - this has implications for frequency coverage, source receiver geometries, data density, and supporting environmental measurements. Attention to modes of propagation (e.g., surface duct, bottom bounce, convergence zone) is most important to model evaluation to fill many scenario gaps.

13.0 (U) References

Baker, C. L. and C. W. Spofford (1974). The FACT Model, Volume II. Acoustical Environmental Support Detachment, Technical Note TN-74-04. (Reprinted July 1977 by Naval Ocean Research and Development Activity).

Bartberger, C. L. and T. L. Stover (1968). The NADC Ray-Tracing Program. Naval Air Development Center, Report No. NADC-3D-6833.

Bassett, C. G. and P. M. Wolff (1970). Fleet Numerical Weather Central Bottom Loss Values (U). FNOC Report No. 2, August (CONFIDENTIAL).

Brekhovskikh, L. M. (1960). Waves in Layered Media. Academic Press, New York, p. 484 and pp. 452-3.

Christensen, R. E., J. Frank and O. Kaufman (1972). Proposed Navy Interim Standard Bottom Loss Curves at Frequencies from 1.0 to 3.5 KHz (U), NOO-TN-9320-02-72. (CONFIDENTIAL).

Clay, C. S. (1968). Sound Transmission in a Half Channel and Surface Duct, Technical Notes on Sound Propagation. In The Sea, Vol. 2, Meteorology International, Inc., Monterey, CA.

Floyd, W. Ray III (1980). ICAPS, the Integrated Command ASW Prediction System, 4 Digest. Naval Oceanographic Office, Technical Note TN 9200-1-80.

Folke, K. C. and M. W. Ohlenclorf (1977). The MINIFACT Module. Applied Research Laboratories, The University of Texas at Austin, Technical Memorandum No. ARL-TM-77-20.

Garon, H. M. (1976). Reference 2F: Modifications to FACT for Two Bottom Classes. Science Applications, Inc., Draft.

Garon H. M. (1980). SHALFACT: A Shallow Water Transmission Loss Model. Science Applications, Inc., Informal Notes.

Holford, R. L. and C. W. Spofford (1973). Long Range Acoustic Propagation Program Final Report (U). Bell Laboratories, Contract N00014-69-C-0088. (CONFIDENTIAL), Reference 5.

ICAPS On-Scene (1980). Environmental Systems Divisions Newsletter, Naval Oceanographic Office, Vol. 2, No. 2 (Article by P. Banas, FACT Model Upgraded to 9F Version), April.

Jacobs, G. (1979). Interactive FACT 9D. Ocean Data Systems, Inc., memorandum of 21 August.

Jacobs, G. (1979). FACT Investigations. Ocean Data Systems, Inc., memorandum of 26 July.

Jacobs, G. (1980). FACT Critical Angle Usage. Ocean Data Systems, Inc., memorandum of 31 January.

LaBianca, F. M. (1972). Continuation of LRAPP (U). (CONFIDENTIAL) Reference 8, "Critique of C. S. Clay's 'Sound Transmission in a Half Channel and Surface Duct'". (UNCLASSIFIED)

Marsh, H. W. and M. Schulkin (1967). Report on the Status of Project AMOS. U.S. Naval Underwater Sound Laboratory, New London, CT.

Martin, R. L., et al. (1982). The Acoustic Model Evaluation Comittee (AMEC) Reports, Volume IA: Summary of Range Independent Environmental Acoustic Propagation Loss Data Sets (U). Naval Ocean Research and Development Activity Report, NSTL Station, Miss., NORDA Report 34. (CONFIDENTIAL)

Naval Oceanographic Office (1979). Program Operating Procedures for the Integrated Command ASW Prediction System (ICAPS), Volume I. Reference Publication NOO RRP-24.

Spofford, C. W. (1974). The FACT Model, Volume I, Acoustic Environmental Support Detachment. Maury Center for Ocean Science, Report No. MC Report 109.

Spofford, C. W., R. C. Cabanaugh, J. H. Hannda, H. Stieglitz, H. M. Garon (1974). SASS Phase B Scenario (U). Acoustic Environmental Support Detachment, February. Classification Unknown.

Spofford, C. W., R. E. Keenan, and W. W. Renner (1977). Implementation of Rough Surface, Surface Duct, and Cusped Caustic Improvements in FACT. Science Applications, Inc., Report No. SAI-78-688-WA.

Stephens, P. (1979). FACT Modification of Source/Receiver Depths and Sound Speed Profile. Ocean Data Systems, Inc., memorandum of 26 Nov.

Underwater Systems, Inc., Report (1978). Acoustic Modeling: Report on Present

Status with Recommendations for Future Development. Appendix C. Propagation Loss Model Descriptions. USI Report of March 1978.

Weinberg, H. (1977). Generic FACT. Naval Underwater Systems Center, Technical Report 5635.

Weinberg, H. (1980). Generic Sonar Model. Naval Underwater Systems Center, Technical Document 5971A.

DISTRIBUTION LIST (U)

Department of the Navy
Asst Secretary of the Navy
(Research Engineering & System)
Washington DC 20350

Department of the Navy
Chief of Naval Research
800 N. Quincy St.
ATTN: Code 102C
Arlington VA 22217

Chief of Naval Research
800 N. Quincy St.
ATTN: Code 420
Arlington VA 22217

Department of the Navy
Chief of Naval Operations
ATTN: OP 981F
Washington DC 20350

Department of the Navy
Chief of Naval Operations
ATTN: OP 952D
Washington DC 20350

Department of the Navy
Chief of Naval Operations
ATTN: OP 224
Washington DC 20350

Department of the Navy
Chief of Naval Operations
ATTN: OP 353C
Washington DC 20350

Department of the Navy
Chief of Naval Operations
ATTN: OP 551E
Washington DC 20350

Department of the Navy
Chief of Naval Operations
ATTN: OP 981F
Washington DC 20350

Department of the Navy
Chief of Naval Operations
ATTN: OP 986G
Washington DC 20350

Department of the Navy
Chief of Naval Operations
ATTN: OP 951F
Washington DC 20350

Department of the Navy
Chief of Naval Operations
ATTN: OP 095T
Washington DC 20350

Department of the Navy
Chief of Naval Material
ATTN: MAT 0724
Washington DC 20360

Commander
Naval Air Development Center
Warminster PA 18974

Commander
Naval Air Development Center
ATTN: C. L. Bartberger
Warminster PA 18974

Commander
Naval Air Systems Command
Headquarters
Washington DC 20361

Commander
Naval Air Systems Command
Headquarters
ATTN: Code 370
Washington DC 20361

Commanding Officer
Naval Coastal Systems Center
ATTN: G. McLeroy
Panama City FL 32407

Commanding Officer
Naval Coastal Systems Center
ATTN: D. P. Vasholz
Panama City FL 32407

Commander
Naval Electronic Sys Com
Headquarters
ATTN: PME 124
Washington DC 20360

Commanding Officer
Naval Environmental Prediction
Research Facility
Monterey CA 93940

Commanding Officer
Naval Research Laboratory
Washington DC 20375

Commander
Naval Oceanography Command
NSTL Station, MS 39522

Commander
Naval Ocean Systems Center
San Diego CA 92152

Commander
Naval Ocean Systems Center
ATTN: M. A. Pederson
San Diego CA 92152

Commanding Officer
Fleet Numerical Ocean Cen
Monterey CA 93940

Commanding Officer
Naval Oceanographic Office
NSTL Station MS 39522

Commander
Naval Sea System Command
Headquarters
Washington DC 20362

Commander
Naval Sea System Command
Headquarters
ATTN: Code 63D3
Washington DC 20362

Superintendent
Naval Postgraduate School
Monterey CA 93940

Project Manager
ASW Systems Project (PM-4)
Department of the Navy
Washington DC 20360

Officer in Charge
Naval Underwater Sys Cen Det
New London Laboratory
ATTN: F. R. DiNapoli
New London CT 06320

Commander
Operational Test & Eval Force
Naval Base
Norfolk VA 23511

Director, Liaison Office
Naval Ocean R&D Activity
800 N. Quincy Street
502 Ballston Tower #1
Arlington VA 22217

Commander
Submarine Dev Sqdn TWELVE
Box 70 NAVSUBASE NLNDN
Groton CT 06349

Commander
Surface Warfare Dev Group
Naval Amphibious Base,
Little Creek
Norfolk VA 23521

Director
Naval Tactical Support Activity
P. O. Box 1042
Silver Spring, MD 20910

Director
Woods Hole Oceanographic Inst
ATTN: E. Hays
Woods Hole MA 02543

Director
Marine Physical Lab
Scripps Institute of Oceanography
ATTN: V. L. Anderson
P.O. Box 6049
San Diego CA 92106

Director
University of Texas
Applied Research Lab
ATTN: K. Hawker
P. O. Box 8029
Austin TX 78712

Director
University of Washington
Applied Physics Laboratory
ATTN: C. Sienkiewicz
1013 NE 40th ST
Seattle WA 98105

Director
University of Washington
Applied Physics Laboratory
ATTN: J. B. Lilly
1013 NE 40th ST
Seattle WA 98105

Director
Pennsylvania State University
Applied Research Laboratory
ATTN: C. P. Janota
P.O. Box 30
State College PA 16801

Director
Pennsylvania State University
Applied Research Laboratory
ATTN: S. T. McDaniel
P.O. Box 30
State College PA 16801

Commanding Officer
Naval Underwater Systems Center
Newport RI 02840

CONFIDENTIAL

(This page is unclassified)

UNCLASSIFIED

SECURITY CLASSIFICATION OF THIS PAGE (When Data Entered)

REPORT DOCUMENTATION PAGE		READ INSTRUCTIONS BEFORE COMPLETING FORM
1. REPORT NUMBER NORDA REPORT 35	2. GOVT ACCESSION NO. AD-C034018L	3. RECIPIENT'S CATALOG NUMBER
4. TITLE (and Subtitle) The Acoustic Model Evaluation Committee (AMEC) Reports. Volumn 2: The Evaluation of the FACT PL9D Transmission Loss Model (U)		5. TYPE OF REPORT & PERIOD COVERED Final
		6. PERFORMING ORG. REPORT NUMBER
7. AUTHOR(s) Richard B. Lauer		8. CONTRACT OR GRANT NUMBER(s)
9. PERFORMING ORGANIZATION NAME AND ADDRESS Naval Ocean Research & Development Activity Ocean Science and Technology Laboratory NSTL Station, Mississippi 39529		10. PROGRAM ELEMENT, PROJECT, TASK AREA & WORK UNIT NUMBERS 63795N, 63708N OP-952D
11. CONTROLLING OFFICE NAME AND ADDRESS Same		12. REPORT DATE September 1980
		13. NUMBER OF PAGES 920
14. MONITORING AGENCY NAME & ADDRESS (if different from Controlling Office)		15. SECURITY CLASS. (of this report) CONFIDENTIAL
		15a. DECLASSIFICATION/DOWNGRADING SCHEDULE OADR Declassify ~~31 December 1990~~

TBE 11 APR 1984

16. DISTRIBUTION STATEMENT (of this Report)

Distribution limited to U.S. Government agencies only. Other requests for this document must be referred to the Commanding Officer, Naval Ocean Research and Development Activity, NSTL Station, Mississippi 39529

17. DISTRIBUTION STATEMENT (of the abstract entered in Block 20, if different from Report)

18. SUPPLEMENTARY NOTES

19. KEY WORDS (Continue on reverse side if necessary and identify by block number)

Model evaluation
Propagation loss models
Underwater acoustic modeling
Acoustic Model Evaluation Committee
AMEC

20. ABSTRACT (Continue on reverse side if necessary and identify by block number)

(U) The Acoustic Model Evaluation Committee (AMEC) has applied the methodology described in Volume I of this series of reports to evaluate the FACT PL9D model. The accuracy of FACT PL9D has been assessed by quantitative comparisons with eight sets of experimental data covering a broad spectrum of environmental acoustic senarios. The physics of FACT PL9D has been examined by C. Bartberger of the Naval Air Development Center with abundant use of test cases. FACT PL9D is found to run extremely fast, typically 3-6 seconds on the UNIVAC 1108 computer. The model is well documented, including comments

DD FORM 1 JAN 73 1473 **CONFIDENTIAL** IS OBSOLETE

(This page is unclassified)

UNCLASSIFIED

SECURITY CLASSIFICATION OF THIS PAGE (When Data Entered)

within the computer code. Many serious deficiencies and errors in the Physics of FACT PL9D were discovered in the surface direct module, "axis-to-axis" computations, curve fitting in range-angle space, caustic correction application, decisions regarding coherence and amplitude reduction factors, and number of rays calculated in the outermost source angle sector. Other deficiencies are lack of eigenray information, dependence of initial range and range increment for propagation loss calculations, and the lack of vertical beampatterns and external bottom loss capabilities. This evaluation was completed in September 1980.

DEPARTMENT OF THE NAVY
OFFICE OF NAVAL RESEARCH
800 NORTH QUINCY STREET
ARLINGTON, VA 22217-5660

IN REPLY REFER TO
5510/1
Ser 93/160
10 Mar 99

From: Chief of Naval Research
To: Commander, Naval Meteorology and Oceanography Command
1020 Balch Boulevard
Stennis Space Center MS 39529-5005

Subj: DECLASSIFICATION OF PARKA I AND PARKA II REPORTS

Ref: (a) CNMOC ltr 3140 Ser 5/110 of 12 Aug 97

Encl: (1) Listing of Known Classified PARKA Reports

1. In response to reference (a), the Chief of Naval Operations (N874) has reviewed a number of Pacific Acoustic Research Kaneohe-Alaska (PARKA) Experiment documents and has determined that all PARKA I and PARKA II reports may be declassified and marked as follows:

   Classification changed to UNCLASSIFIED by authority of Chief of Naval Research letter Ser 93/160, 10 Mar 99.

   DISTRIBUTION STATEMENT A: Approved for public release. Distribution is unlimited.

2. Enclosure (1) is a listing of known classified PARKA reports. The marking on those documents should be changed as noted in paragraph 1 above. When other PARKA I and PARKA II reports are identified, their markings should be changed and a copy of the title page and a notation of how many pages the document contained should be provided to Chief of Naval Research (ONR 93), 800 N. Quincy Street, Arlington, VA 22217-5660. This will enable me to maintain a master list of downgraded PARKA reports.

3. Questions may be directed to the undersigned on (703) 696-4619, DSN 426-4619.

Peggy Lambert

PEGGY LAMBERT
By direction

Copy to:
NUWC Newport Technical Library (Code 5441)
NRL Washington (Mary Templeman, Code 5227)
NRL SSC (Roger Swanton, Code 7031)
✓DTIC (Bill Bush, DTIC-OCQ)

Continuation of LRAPP Final Report, February 1972, Contract N00014-71-C-0088, Bell Telephone Labs, Unknown # of pages
(NUSC NL Accession # 057708)

PARKA II-A, The Oceanographic Measurements, February 1972, MC Report 006, Volume 2, Maury Center for Ocean Science (ONR), 89 pages
(NUSC NL Accession # 059194) (NRL SSC Accession # 85007063)

Project Pacific Sea Spider - Technology Used in Developing A Deep-Ocean Ultrastable Platform, 12 April 1974, ONR-ACR-196, 55 pages
√(DTIC # 529 945)

LRAPP Program Review at the New London Laboratory, Naval Underwater Systems Center, 24 April 1975, NUSC-TD-4943, Unknown # of pages
(NUSC NL Accession # 004943)

An Analysis of PARKA IIA Data Using the AESD Parabolic Equation Model, December 1975, AESD Technical Note TN-75-09, Acoustic Environmental Support Detachment (ONR), 53 pages
(NRL SSC Accession # 85004613)

Bottom Loss Measurements in the Eastern Pacific Ocean, 26 January 1977, NADC-76320-20, 66 pages
√(DTIC # C009 224)

PARKA I Oceanographic Data Compendium, November 1978, NORDA-TN-25, 579 pages
√(DTIC # B115 967)

Sonar Surveillance Through A North Pacific Ocean Front, June 1981, NOSC-TR-682, 18 pages
√(DTIC # C026 529)

The Acoustic Model Evaluation Committee (AMEC) Reports, Volume 1, Model Evaluation Methodology and Implementation, September 1982, NORDA-33-VOL-1, 46 pages
√(DTIC # C034 016)

The Acoustic Model Evaluation Committee (AMEC) Reports, Volume 1A, Summary of Range Independent Environment Acoustic Propagation Data Sets, September 1982, NORDA-34-VOL-1A, 482 pages
√(DTIC # C034 017)

The Acoustic Model Evaluation Committee (AMEC) Reports, Volume 2, The Evaluation of the Fact PL9D Transmission Loss Model, Book 1, September 1982, NORDA-35-VOL-2-BK-1, 179 pages
√(DTIC # C034 018)

The Acoustic Model Evaluation Committee (AMEC) Reports, Volume 2, The Evaluation of the Fact PL9D Transmission Loss Model, Book 2, Appendices A-D, September 1982, NORDA-35-VOL-2-BK-2, 318 pages
(DTIC # C034 019)